Characterisation of the Molecular Mechanisms Regulating the Signalling and Post-endocytic sorting of the Receptors for Calcitonin Gene-Related Peptide and Adsenomedullin

Roux, Benoit

Award date:
2013

Awarding institution:
University of Bath

UNIVERSITY OF BATH

Characterisation of the Molecular Mechanisms Regulating the Signalling and Post-Endocytic Sorting of the Receptors for Calcitonin Gene-Related Peptide and Adrenomedullin

Benoît Thomas Roux

Submitted for the Degree of Doctor of Philosophy (PhD)

University of Bath,
Department of Pharmacy and Pharmacology

July 2013

Abstract

Calcitonin gene-related peptide (CGRP) and adrenomedullin (ADM) receptors are heterodimeric complexes composed of the calcitonin receptor-like receptor (CLR) and a receptor activity-modifying protein (RAMP). Association with RAMP1 gives a high affinity CGRP receptor, whereas association with RAMP2 or RAMP3 gives high affinity ADM receptors. CGRP and ADM are widely distributed throughout the body and play important roles and are implicated in many diseases including migraine, heart failure and sepsis.

Recently, CGRP has been shown to promote nitric oxide (NO) production and inducible NO synthase (iNOS) expression in trigeminal ganglion glial cells via ERK activation. CGRP is known to induce iNOS/NO production in thoracic artery smooth muscle cells (TA-SMC) pretreated with interleukin-1b. However, the molecular mechanism of CGRP-induced iNOS/NO production in TA-SMC is unknown. Therefore, in order to determine if CGRP induces iNOS/NO production via ERK activation, I first investigated the exact mechanisms through which CGRP activates ERK1-2 in HEK cells. By using different inhibitors I showed that CGRP-induced ERK activation is mainly activated through two major pathways. I showed for the first time that CGRP induces ERK activation through transactivation of ErbB1 and as expected through the cAMP/PKA pathway. Then, in order to characterise a suitable model to study CGRP-induced iNOS expression, I used primary TA-SMC and I showed that CGRP induces iNOS upregulation, which is reduced when cells are incubated with U0126, a MEK inhibitor. Thus, these results suggest that CGRP induces iNOS expression via ERK activation in TA-SMC. However, further experimentation is required to determine the exact ERK pathway responsible for iNOS induction.

Compared to CLR•RAMP1 and CLR•RAMP3, little is known about the post-endocytic sorting of CLR•RAMP2. Using HEK cells stably expressing CLR•RAMP2, I investigated the molecular mechanisms regulating the ADM receptor. I first showed that, unlike CLR•RAMP1, even transient stimulation of CLR•RAMP2 with ADM promotes degradation of both CLR and RAMP2, indicating that this ADM receptor does not recycle to the cell-surface. Moreover, I showed that CLR, not RAMP2, is constitutively ubiquitinated, which was further enhanced upon ADM stimulation. In order to elucidate the role of ADM-mediated ubiquitination of CLR, I made a lysine-less mutant of CLR, named CLRD9KR. I showed that ubiquitination of CLR did not affect ADM-induced trafficking of CLR•RAMP2 to lysosomes, nor did it affect the degradation or the ERK signalling of CLR•RAMP2. However, I showed that ubiquitination of CLR regulated the rate of degradation of the receptor. Together, these results indicate that CLR•RAMP2 does not recycle and is degraded via a molecular mechanism that is accelerated by ADM-induced ubiquitination of CLR.

Acknowledgements

First, I wish to express my sincere gratitude to my supervisor Dr Graeme Cottrell for the continuous support of my Ph.D study and research, for his patience, motivation, enthusiasm and immense knowledge. His guidance helped me in all the time of research and writing of this thesis. Also I would like to thank my other advisor Professor Stephen Ward for his encouragement, insightful comments and hard questions.

I also would like to express a special thanks to all members of the PhD student office, past and present that made my time here in Bath really easy and fun. Of course not to forget all the people in the department who helped me or just share some moments with me.

I would like to thank my wife Eva, who really supported me all along and even tried to understand what was my job. Likewise, I thank my family and friends for their love and support from far away.

Finally, I thank British Heart Foundation for funding.

Abbreviations

5-HT	5-hydroxytryptamine
AC	adenylate cyclase
ACE	angiotensin-I-converting enzyme
ADAM	a disintegrin and metalloprotease
ADM	adrenomedullin
ADM2	adrenomedullin-2
Akt	protein kinase B
ALIX	apoptosis-linked gene-2-interacting protein X
Ca^{2+}	calcium
cAMP	cyclic adenosine monophosphate
ang II	angiotensin II
AP	adaptor protein family
AT_1R	AT_1 receptor (angiotensin receptor family)
AT_2R	AT_2 receptor (angiotensin receptor family)
ATP	adenosine triphosphate
α_{1B}-AR	α_{1B}-adrenoceptor
α_{2A}-AR	α_{2A}-adrenoceptor
β_1-AR	β_1-adrenoceptor
β_2-AR	β_2-adrenoceptor
B_2 receptor	bradykinin receptor family
BSA	bovine serum albumin
CalDAG-GEFI	Ca^{2+}- and diacylglycerol-regulated guanine nucleotide exchange factor I
CGRP	calcitonin gene-related peptide

CHX	cycloheximide
CLR	calcitonin receptor-like receptor
CNS	central nervous system
CSBP	cytokinin Specific Binding Protein
CT	calcitonin
CTR	CT receptor
CXCR2	chemokine receptor family
CXCR4	chemokine receptor family
DAG	diacylglycerol
DMEM	Dulbecco's Modified Eagles medium
DMSO	dimethyl sulphoxide
DNA	deoxyribonucleic acid
cDNA	complementary DNA
δOR	δ receptor (opioid receptor family)
κOR	κ receptor (opioid receptor family)
μOR	μ receptor (opioid receptor family)
DUB	de-ubiquitinating enzymes
ECE-1	endothelin-converting enzyme-1
E. coli	*Escherichia coli*
EP2 receptor	prostanoid receptor family
ER	endoplasmic reticulum
ErbB1	epidermal growth factor receptor
ERK	extracellular signal-regulated kinase
pERK	phosphorylated ERK
ES	embryonic stem
ESCRT	endosomal sorting complex required for transport

Hrs	hepatocyte growth factor-regulated tyrosine kinase substrate
GDP	guanosine diphosphate
GEF	guanine nucleotide exchange factor
cGMP	cyclic guanosine monophosphate
GnRH receptor	gonadotrophin-releasing hormone receptor family
GPCR	G protein-coupled receptor
GTP	guanosine triphosphate
GRK	GPCR kinase
IAPP	islet amyloid polypeptide
ILV	intralumenal vesicles
IP3	inositol 1,4,5-triphosphate
JNK	c-Jun N-terminal kinase
LH	luteinizing hormone
LMP	lysosomal membrane protein
LPA	lysophosphatic acid
M_1 receptor	acetylcholine receptor (muscarinic) family
M_3 receptor	acetylcholine receptor (muscarinic) family
MAPK	mitogen-activated protein kinase
MEK	MAP kinase kinase
MHC	major histocompatibility complex
MVB	multivesicular bodies
NK_1R	NK_1 receptor (tachykinin receptors family)
NO	nitric oxide
e/iNOS	endothelial/inducible NO synthase
NSF	N-ethylmaleimide-sensitive fusion protein
$P2Y_1$ receptor	P2Y receptor family

$P2Y_{12}$ receptor	P2Y receptor family
PAMP	ProADM N-terminal 20 peptide
PDGF	platelet-derived growth factor
PDZ	postsynaptic density 95/disc large/zonula occludens-1
PI3K	phosphatidylinositol 3-kinase
PKA	protein kinase A
PKC	protein kinase C
aPKC	atypical PKC
cPKC	conventional PKC
nPKC	novel PKC
PLC	phospholipase C
pM	picomole
PP2A	protein phosphatase type 2A
proADM	pro-adrenomedullin
proCT	pro-caclitonin
PTH	parathyroid hormone
PTH1 receptor	parathyroid hormone receptor family
PTH2 receptor	parathyroid hormone receptor family
PTX	pertussis toxin
PVDF	polyvinylidene difluoride
PYK2	proline-rich tyrosine kinase 2
RAMP	receptor activity-modifying protein
RCP	receptor component protein
RIPA	radioimmunoprecipitation assay
RK	reactivating kinase
RKIP	Raf kinase inhibitor protein

RNA	ribonucleic acid
RT	room temperature
RTK	receptor tyrosine kinase
S.E.	standard error
SMC	smooth muscle cells
SNX1	sorting nexin-1
SP	substance P
TA-SMC	thoracic aorta SMC
TfR	transferrin receptor
TPA	12-o-tetradecanoylphorbol-13-acetate
Tsg101	tumour susceptibility gene 101
UIM	ubiquitin-interacting motif
V_2R	V_2 receptor (vasopressin and oxytocin receptor family)
$VPAC_1$ receptor	VIP and PACAP receptor family
$VPAC_2$ receptor	VIP and PACAP receptor family
Vps4	vacuolar protein sorting 4
WT	wild type
Z-PAD	Z-Phe-Ala-diazomethylketone

Table of Contents

Table of Figures

Table of Tables

Chapter 1. Introduction

1.1 Calcitonin Peptide Family

The calcitonin peptide family includes calcitonin (CT), islet amyloid polypeptide (IAPP), calcitonin gene-related peptide (CGRP), adrenomedullin (ADM) and adrenomedullin-2 (ADM2). The mature peptides exhibit a high degree of sequence homology, particularly a highly conserved disulphide bond (**Fig. 1.1**). They exhibit similar biological properties on a wide range of tissues. All these peptides have been listed in order of discovery, although CGRP and ADM, subject of this study, are described in more detail.

1.1.1 Calcitonin

CT is a 32 amino acid peptide, discovered and purified in 1962 by Copp *et al.* (Copp et al., 1962; Copp and Cheney, 1962). Calcitonin is produced from the calcitonin-related polypeptide alpha gene *CALCA*, located on the short arm of chromosome 11 (Hoppener et al., 1984; Przepiorka et al., 1984). Alternative splicing of *CALCA* gene transcripts results in the production of two different mRNAs encoding either for proCT or for CGRP (Amara et al., 1982) (**Fig. 1.2**). ProCT is then cleaved to form CT and another 21 amino acid peptide named katacalcin (Hillyard et al., 1983). Katacalcin (also known as PDN-21) does not possess similar structure to CT or other members of the calcitonin peptide family. The biological activities of katacalcin are poorly defined, however they are believed to be similar to CT (Hillyard et al., 1983). The *CALCA* gene consists of 6 exons (reviewed in (Breimer et al., 1988)). The first three exons are common to both mRNAs. Exon IV codes for proCT, followed by a polyadenylation signal, whereas exons V and VI code for CGRP, followed by the polyadenylation signal.

CT was initially shown to be secreted by the thyroid gland (Hirsch et al., 1963) and was later more precisely identified as the secretion product of thyroidal parafollicular cells (later termed C cells) (McMillan et al., 1974; Meyer and Abdel-Bari, 1968; Wolfe et al., 1973). The name CT was given because of its hypocalcemic effect on blood Ca^{2+} (Copp and Cheney, 1962), countering the action of parathyroid hormone (PTH). CT contributes to Ca^{2+} homeostasis by direct inhibition of osteoclast-mediated bone resorption and by enhancing Ca^{2+} excretion by the kidney (Friedman and Raisz, 1965; Raisz and Niemann, 1967; Warshawsky et al., 1980). Salmon CT is currently used as therapeutic to treat osteoporosis and Paget's disease ((Overgaard et al., 1992) and is reviewed in (Hamdy and Daley, 2012; Lee and Sinko, 2000; Patel et al., 1993)).

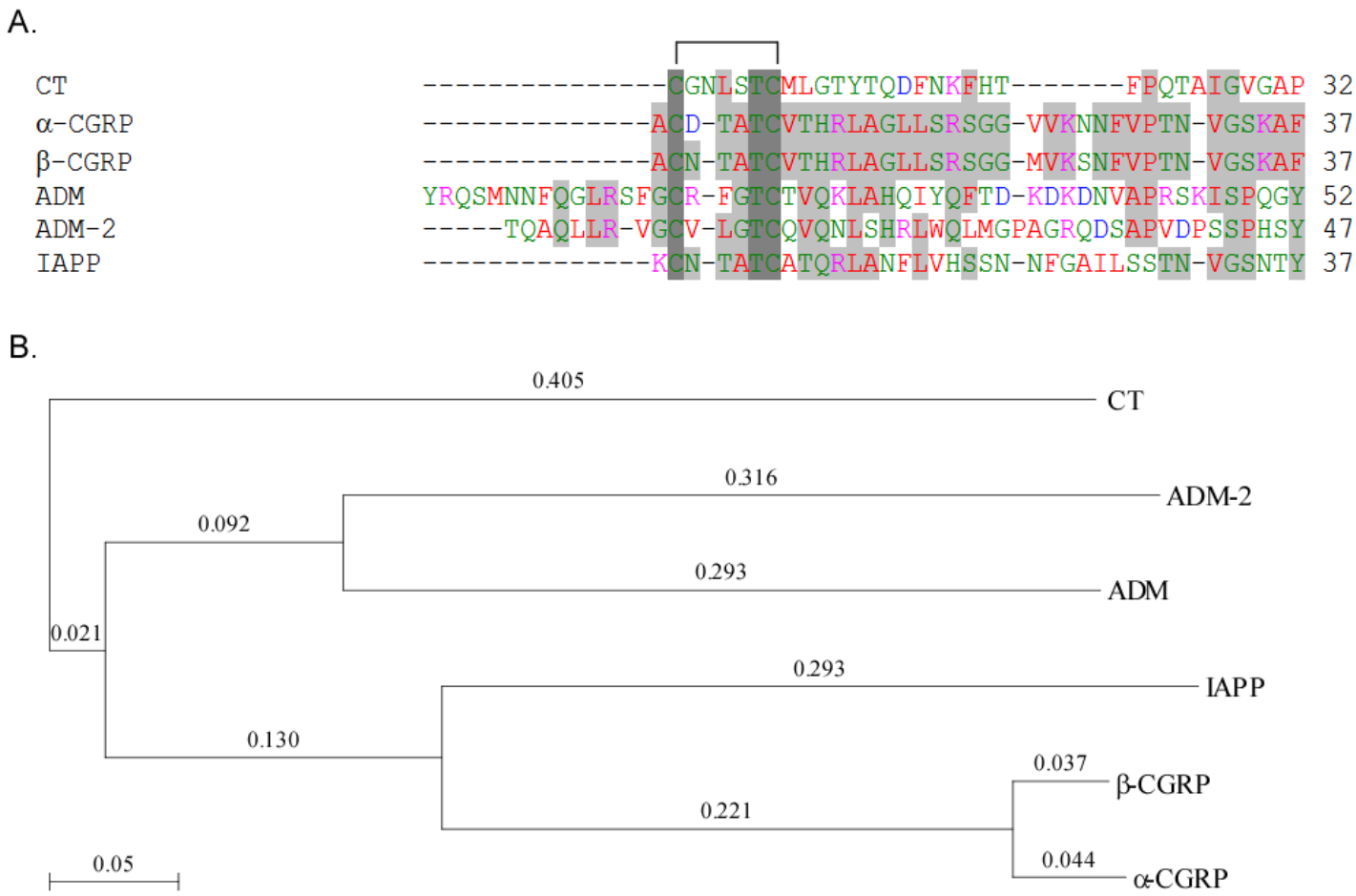

Figure 1.1 **Members of the calcitonin peptide family.** (**A**) Sequence alignment of the human calcitonin peptide family members collected from the UniProtKB/Swiss-Prot database. The sequences were aligned using the EMBL-EBI ClustalW2 software. Amino acids are colour coded according to their properties: Red=small + hydrophobic, Blue=acidic, Magenta=basic and Green=hydroxyl + amine + basic. Residues highlighted in light grey are conserved in at least two different members of the family and in dark grey are conserved in all members. Brackets represent the disulphide bridge between the cysteine residues. (**B**) Phylogenetic tree sequences were obtained from EMBL-EBI ClustalW2-Phylogeny software and drawn using the free online software Njplot (Perriere and Gouy, 1996).

CT has also been found in brain (Cooper et al., 1980; Fischer et al., 1981; Flynn et al., 1981), suggesting a role in the central nervous system (CNS). Indeed, CT has been found to inhibit food intake in rats when given by intracerebral and subcutaneous injection (Freed et al., 1979; Levine and Morley, 1981; Perlow et al., 1980). Moreover, administration of CT in humans reduces gastric emptying (Jonderko et al., 1988) and inhibits glucose-induce insulin secretion (Passariello et al., 1981).

1.1.2 Calcitonin Gene-Related Peptide

1.1.2.1 Structure and Synthesis of CGRP

CGRP is a 37 amino acid neuropeptide that was identified in 1982 (Amara et al., 1982). It was discovered from the alternative tissue-specific processing of mRNA transcripts from the *CALCA* gene. This alternative splicing results in the production of a distinct mRNA that encodes CGRP (Amara et al., 1982). CGRP exists in two forms, denoted α and β (or I and II), which differ by only three amino acids, but share similar biological activities. αCGRP is encoded by the calcitonin gene *CALCA* located on chromosome 11 (**Fig. 1.2**). The expression of mRNA splicing for CT or αCGRP is tissue-specific (Amara et al., 1982; Rosenfeld et al., 1983). For example, the expression of CT mRNA predominates in the thyroid whereas αCGRP-specific mRNA appears to predominate in the nervous system. βCGRP isoform is coded by a separate gene *CALCB*, also located on chromosome 11 and is thought to have arisen by gene duplication (Amara et al., 1985; Steenbergh et al., 1985). It is the effects of αCGRP that are discussed in this study and hereafter will be denoted CGRP.

The tertiary structure of CGRP has not been fully determined. However, in common with other members of the calcitonin family, CGRP has a disulphide bridge (Cys^2-Cys^7) in the N-terminal region. This ring structure is followed by an α-helix initially thought to exist between residues Val^8 and Arg^{18} (Breeze et al., 1991; Lynch and Kaiser, 1988), and then later confirmed between residues Val^8 and Leu^{16} (Boulanger et al., 1995), followed by a γ-turn between residues Ser^{19} and Gly^{21} (Boulanger et al., 1995).

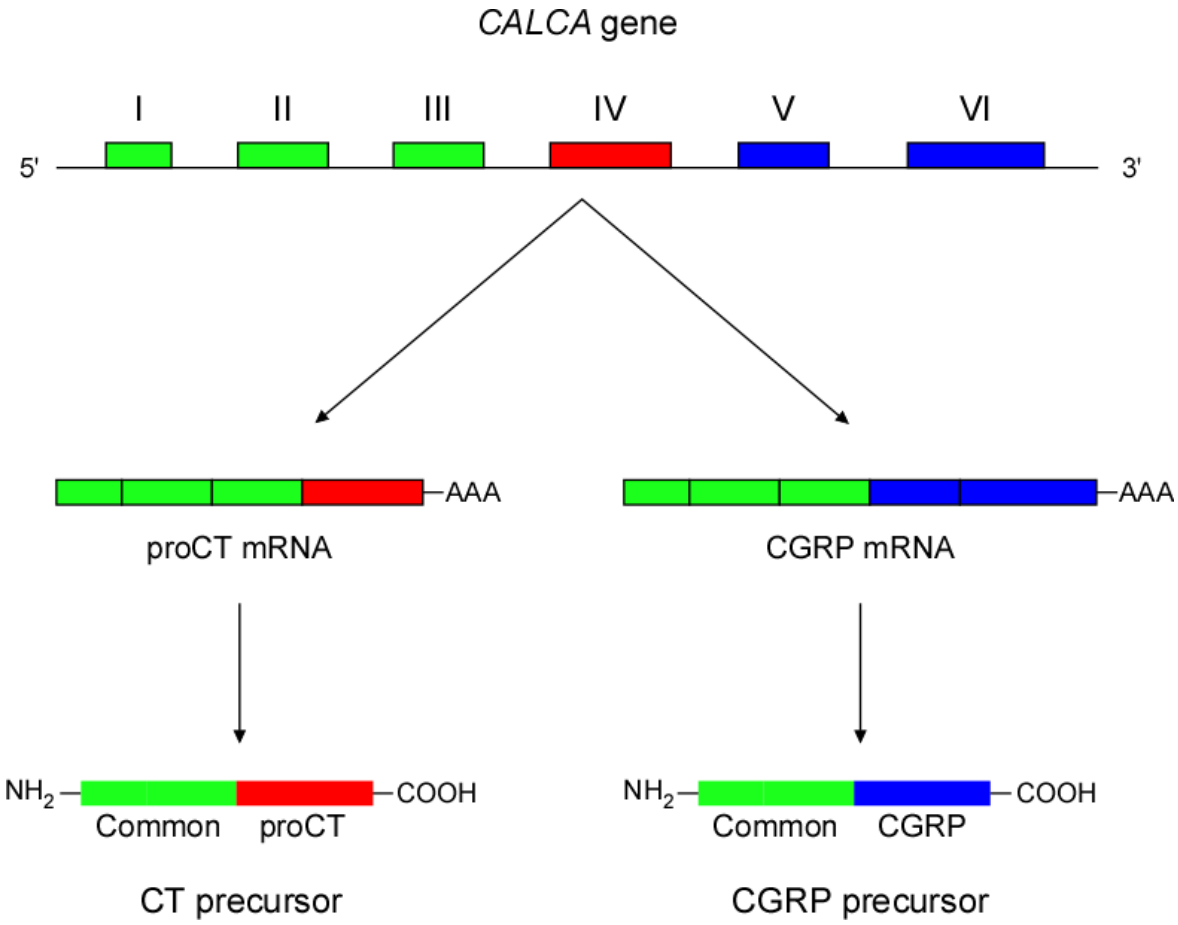

Figure 1.2 **Schematic representation of the transcription/translation of *CALCA* gene.** *CALCA* is located on the short arm of chromosome 11. Alternative splicing of the transcript of *CALCA* leads to the formation of two different mRNAs. Splicing of the exon IV yield a proCT mRNA (hightlighted in red), which is translated into the CT/KC precursor. Splicing of the exon V and VI produce a CGRP mRNA, leading to the CGRP precursor (hightlighted in blue). Exons hightlighted in green represent non-translated and precursor sequences.

1.1.2.2 Distribution of CGRP

CGRP has been shown to be concentrated in distinct areas of the peripheral and central nervous systems (Rosenfeld et al., 1983) and it has been detected in both autonomic and motor neurons. In many tissues, CGRP-containing nerves are closely associated with blood vessels (Brain and Cambridge, 1996), which alluded to its function as a vasoactive mediator. Indeed, CGRP-containing nerves innervate smaller arteries in the vascular smooth muscle layer. This allows CGRP to be released where it can act on smooth muscle cells (SMC) layer to promote arteriolar dilatation (reviewed in (Brain and Grant, 2004)). The distribution of CGRP-containing nerves has been studied in most tissues, but it most extensively been reviewed with respect to the pathophysiological function in the cerebral circulation (reviewed in (Edvinsson, 2001)). CGRP-containing nerves have a perivascular distribution and as a consequence plasma levels of CGRP in human are generally low, normally in the picomole (pM) range (Girgis et al., 1985). It is generally considered that the levels of CGRP in plasma are likely to be due to leakage after localised release rather than for a specific systemic function. However, CGRP has the ability to decrease blood pressure and increase heart rate when given by intravenous administration in human volunteers, indicating that if sufficiently high plasma levels of CGRP are reached, systemic vasoactive effects can be triggered (Gennari and Fischer, 1985). Moreover, this observation suggests that CGRP can act on endothelial cells, confirmed by the fact that certain endothelial cells express CGRP receptors (Nikitenko et al., 2006).

1.1.2.3 Biological Effects of CGRP and its Role in Disease

CGRP is distributed throughout the central and peripheral nervous systems, which suggests its involvement in various brain activities associated with gastrointestinal, sensory and cardiovascular functions (reviewed in (Maggi, 1995; van Rossum et al., 1997)).

When CGRP is given by intracerebroventricularly, it reduces food intake (Krahn et al., 1984). This observation was supported by the fact that lesions of the lateral part of the dorsal parabrachial nucleus, a region rich in CGRP-containing cell bodies (Shimada et al., 1985), induce hyperphagia (Nagai et al., 1987). Moreover, CGRP inhibits gastric acid secretion (Kraenzlin et al., 1985; Tache et al., 1984) and gastric emptying (Raybould et al., 1988).

CGRP is widely studied for its effects on the cardiovascular system, which are the subject of this study. CGRP is the most potent microvascular vasodilator identified to date. This effect was first demonstrated in skin, where femtomole-pM amounts of injected CGRP induced reddening, due to local microvascular dilation (Brain et al., 1985). In addition to its great potency, CGRP also differs from other

vasodilatory substances in that it has a particularly long duration of action. A dose of 15 pM injected into human skin produces an erythema that lasts for 5–6 h (Brain et al., 1985).

It has been identified that CGRP can promote vascular relaxation through activation of a number of different signalling pathways. These mechanisms include either nitric oxide (NO)/endothelium-dependent mechanisms or cyclic adenosine monophosphate (cAMP)-mediated/endothelium-independent pathways. The most common pathway is cAMP/endothelium-independent. CGRP acts on SMC to stimulate adenylate cyclase (AC) activity producing an increase in cAMP production. This mechanism has been shown in cultured SMC (Crossman et al., 1990), endothelium denuded arteries in cat brain vessels (Edvinsson et al., 2001) and in human intracranial arteries (Edvinsson et al., 1998). The increase in cAMP promotes activation of protein kinase A (PKA), which in turn phosphorylates and opens ATP-sensitive K^+-channels, leading to relaxation. In fact, the ATP-sensitive K^+-channel blocker, glibenclamide prevents CGRP-induced responses and hyperpolarises arterial SMC (Nelson et al., 1990; Smillie and Brain, 2011). Endothelium-dependent relaxation to CGRP occurs by a significant increase in both cAMP and cyclic guanosine monophosphate (cGMP) (Gray and Marshall, 1992). This implicates the release of NO from the endothelium, which relaxes the SMC through activation of guanylate cyclase and accumulation of cGMP. The importance of the increase in cAMP in the vascular endothelial cells remains to be determined, but it has been demonstrated that cAMP is able to stimulate endothelial NO synthase (eNOS) activity, leading to increased synthesis and release of NO (Ferro et al., 1999). The activation of eNOS via cAMP is probably mediated via PKA and protein kinase B (Akt), as a study demonstrated that PKA and Akt can phosphorylate and activate eNOS (Harris et al., 2004). CGRP also induces the production of NO via inducible NOS (iNOS) (Schini-Kerth et al., 1994; Vause and Durham, 2009). iNOS is known to produce large quantities of NO (Nathan and Xie, 1994) which is implicated in inflammatory processes. For example, in sepsis bacterial components such as lipopolysaccharide are known to induce expression of iNOS (Okamoto et al., 1998), which may lead to severe hypotension observed in sepsis (reviewed in (Hauser et al., 2005)). NO production is also implicated in the pathophysiology of migraine (Goadsby et al., 1990; Iversen and Olesen, 1996; Olesen and Jansen-Olesen, 2000) and in atherosclerosis, where it seems to be beneficial by inhibiting SMC proliferation (reviewed in (Ginnan et al., 2008)).

Since its discovery, CGRP has been implicated in the pathogenesis of migraine. Goadsby *et al.* showed that during migraine, plasma levels of CGRP but not of other neuropeptides, such as neuropeptide Y, vasoactive intestinal polypeptide and substance P (SP) were increased (Goadsby et al., 1990). For this reason, pharmaceutical companies initiated development of CGRP receptor antagonists to treat migraine. Current treatments for migraine include the selective 5-

hydroxytryptamine (5-HT, also known as serotonin) receptor 1B/1D agonists called triptans, which work by constricting cranial blood vessels and by reducing the release of CGRP and SP (Tepper et al., 2002). However, triptans can have side effects and are not effective for all patients. For example some patients may suffer from severe rebound attacks and triptans are not suitable for patients with cardiovascular disorders such as angina (Dahlof, 2002). Clinical trials have shown that some CGRP receptor antagonists have a comparable efficacy to other treatments, but with higher safety and tolerability profiles (reviewed in (Villalon and Olesen, 2009)). One of them, the non-peptide BIBN4096BS, later called olcegepant, developed by Boehringer Ingelheim (Doods, 2001) showed promising results and was delivered in phase II clinical trials (Olesen et al., 2004). However, further trials were not pursued as the drug could be delivered only intravenously. Merck Research Laboratories developed an orally bioavailable agent MK-0974, called telcagepant, which reached phase III clinical trials (Ho, 2009; Ho et al., 2008a; Ho et al., 2008b). However, the trials have been stopped as some patients showed elevated liver transaminases (Tepper and Cleves, 2009). Boehringer has developed another antagonist, BI 44370 TA that has completed the phase II trial (Diener et al., 2011). The potent antagonist BMS-846372, is orally active but show limited aqueous solubility (Luo et al., 2012b). Subsequently, a derivative was made, the BMS-927711, which is currently in phase II clinical trials (Luo et al., 2012a). The role of CGRP in migraine is yet to be more clearly defined and understanding the mechanisms that regulate CGRP receptor trafficking and signalling may help to discover new therapies to treat this and other diseases.

1.1.3 Islet Amyloid Polypeptide

Islet amyloid polypeptide (IAPP), also named amylin, is a 37 amino acid peptide purified from amyloids in pancreatic islets, characteristic of type-2 diabetes (Cooper et al., 1987; Westermark et al., 1987). The *IAPP* gene consists of 3 exons located on the short arm of chromosome 12 (Roberts et al., 1989).

IAPP is co-secreted with insulin from β-cells of the pancreatic islet of Langerhans in response to increased glucose levels (Moore and Cooper, 1991). IAPP possesses a vasodilatory activity (Brain et al., 1990), which is 100 times less potent than CGRP and is not thought to be involved in the regulation of the blood pressure. On the other hand, IAPP together with insulin plays an important role in glycaemic control. However, whereas insulin promotes storage of glucose from the blood to different tissues, IAPP prevents absorption of nutrients. Notably, IAPP acts by slowing gastric emptying (Kong et al., 1997; Young et al., 1995) and by inhibiting food intake (Chance et al., 1993; Lutz et al., 1994; Morley et al., 1994). IAPP has also been reported to inhibit glucagon secretion (glucagon counters insulin action by forcing tissue to release glucose in the blood flow), which has

been found to be beneficial in patients suffering from type-1 and 2 diabetes (Fineman et al., 2002a; Fineman et al., 2002b; Gedulin et al., 1997). Moreover, IAPP has also been shown to be increased in obese people not suffering from diabetes, reduced in the type-2 diabetes population (Enoki et al., 1992), and elevated in pancreatic cancer (Permert et al., 1994). Due to its action on the food metabolism, the IAPP receptor antagonist pramlimtinde (Kolterman et al., 1995), has been approved by the Food and Drug Administration in 2005 for the treatment of type-1 and 2 diabetes (reviewed in (Jones, 2007)).

IAPP is the main component of amyloid deposits that form in the islets of Langerhans in patients with type-2 diabetes (Cooper et al., 1987; Westermark et al., 1987), where it has been shown that those amyloid deposits are toxic for the β-cells (Lorenzo et al., 1994), which suggests that they may be the cause of the insulin-related dysfunction in type-2 diabetes.

1.1.4 Adrenomedullin

1.1.4.1 Structure and Synthesis of Adrenomedullin

Human ADM is a 52-amino acid peptide with a single disulphide bridge between cysteine residues 16 and 21 and with an amidated tyrosine at the carboxy terminus. ADM is a potent hypotensive peptide originally isolated from human pheochromocytoma cells and was identified by its ability to stimulate cAMP production in platelets (Kitamura et al., 1993a). ADM shares homology with CGRP and was therefore added to the calcitonin peptide family (Kitamura et al., 1993a). Rat ADM has 50 amino acids, with 2 deletions and 6 substitutions compared with the human peptide (Sakata et al., 1993).

ADM is first synthesised as a large precursor molecule, termed proadrenomedullin (proADM). In both rat and human this precursor consists of 185 amino acids. ProADM is cleaved between Lys^{43} and Arg^{44} to produce a 20-amino acid amidated peptide, designated proADM N-terminal 20 peptide (PAMP). ADM is produced by cleavage of the Lys^{93}-Arg^{94} and Arg^{148}-Arg^{149} bonds (Kitamura et al., 1993b; Sakata et al., 1993). The proteolytic enzymes responsible for this processing are currently unknown. PAMP is not discussed in this report but for more detail see (Samson, 1998). The gene encoding proADM has been mapped and localised to a single locus of chromosome 11. The human *ADM* gene comprises 4 exons and 3 introns, with TATA, CAAT and GC boxes in the 59-flanking region (Ishimitsu et al., 1994).

1.1.4.2 Circulating Adrenomedullin in Health and Disease

The *ADM* gene is expressed in a wide range of tissues. The initial report on the distribution of ADM mRNA, suggested that the highest levels of expression were in the adrenal medulla, ventricle, kidney, and lung (Kitamura et al., 1993b). However, it is now known that ADM is more highly expressed in endothelial cells (Sugo et al., 1994) and vascular SMC (Sugo et al., 1995) than in the adrenal medulla and that ADM has come to be regarded as a major secretory product of the vascular endothelium, together with NO and endothelin-1. An initial study reported that circulating levels of ADM in plasma were in the pM range (Kitamura et al., 1994). This was confirmed by several research groups, with a normal plasma concentration of ADM of 1-10 pM, with most values between 2-3.5 pM (reviewed in (Hinson et al., 2000)). ADM levels have been measured in a wide range of disease states (reviewed in (Hinson et al., 2000)). In many cardiovascular disorders, plasma levels of ADM are reported to be elevated, possibly released to compensate for elevated blood pressure. In general, it appears that elevated ADM is a consequence, rather than a cause of the pathology. It is unclear whether the increases in plasma ADM are due to a required hormonal function or whether it represents leakage due to excess production (reviewed in (Hinson et al., 2000)). Of all the conditions investigated, the greatest increase in plasma ADM has been observed during sepsis and septic shock (Ehlenz et al., 1997; Hirata et al., 1996). ADM plays a key role in the pathophysiology of septic shock (see below).

1.1.4.3 Biological Actions of Adrenomedullin

ADM and its receptors are expressed in several tissues and organs, including the heart, blood vessels, kidneys, lungs, gastrointestinal tract, endocrine glands and brain (reviewed in (Hinson et al., 2000)). This wide distribution suggests that ADM is involved in the regulation of several biological functions. Although the first paper on ADM described only the cardiovascular effects of this peptide (Kitamura et al., 1993a), it is now known that ADM is rather more than simply a vasodilator. ADM has been shown to have a remarkable range of actions, from regulating cellular growth and differentiation, through modulating hormone secretion, to antimicrobial effects (reviewed in (Hinson et al., 2000)). Similar to the other members of the calcitonin family, ADM has been found to reduce food intake in rats (Murphy and Samson, 1995; Taylor et al., 1996), as well as inhibiting insulin secretion (Martinez et al., 1996) and gastric emptying (Martinez et al., 1997). However, only the effects on the cardiovascular system are discussed in this report.

The mechanisms via which ADM can elicit vascular relaxation are heterogeneous with respect to both species and vascular bed. The mechanisms are incompletely understood, but relaxation predominantly occurs by the

eNOS/NO pathway and K^+-channel-dependent mechanisms (Hirata et al., 1995; Lang et al., 1997; Terata et al., 2000). Nishimastu *et al.* examined the NO-dependent relaxation to ADM in the rat aorta and identified the involvement of a phosphatidylinositol 3-kinase (PI3K)/Akt-dependent pathway in the stimulation of eNOS (Nishimatsu et al., 2001). The results showed that ADM stimulated Akt activation in aortic endothelium via a Ca^{2+}/calmodulin-dependent mechanism (Nishimatsu et al., 2001). There are therefore a variety of mechanisms by which ADM may induce vascular relaxation, and further research is required to fully understand them. However, it is clear that there is an overall similarity in the mechanisms of CGRP and ADM-induced relaxation (reviewed in (Brain and Grant, 2004)).

The vascular endothelium constitutes a cellular barrier that plays a crucial role in the maintenance of vessel integrity and controls exchange of small solutes and macromolecules between the intravascular and interstitial space. Increased endothelial permeability is a hallmark of virtually every acute inflammatory reaction. It results in extravasation of fluid and plasma molecules as well as inflammatory mediators through the activated endothelium. Two main mechanisms are involved: perturbation of adhesion structures resulting in the loss of endothelial cell-cell contacts and activation of the actin-myosin based contraction system resulting in cell retraction and subsequent intracellular gap formation (reviewed in (Temmesfeld-Wollbruck et al., 2007)). Upregulation of ADM is observed in sepsis and septic shock. Studies with three separate knockout mouse models affecting the ADM system (*ADM* gene, *CALCRL* gene (ADM receptor component) and *peptidylglycine alpha-amidating monooxygenase* gene enzyme which catalyses the COOH-terminal amidation of peptide hormones) have shown an extreme generalised oedema formation suggesting a strong barrier stabilising function for the peptide (Caron and Smithies, 2001; Czyzyk et al., 2005; Dackor et al., 2006). *In vitro* studies have shown that ADM concentration-dependently reduced the hyperpermeability induced by stimuli as diverse as hydrogen peroxidase, thrombin, *Escherichia coli* (*E. coli*) hemolysin or *Staphylococcus aureus* α-toxin (Brell et al., 2005; Hippenstiel et al., 2002; Hocke et al., 2006). ADM acts by blocking the phosphorylation of endothelial myosin light chain induced by these molecules. This, in turn, reduces the formation of F-actin stress fibres, known to be vital for force generation during actin-myosin based cell contraction in the endothelium (Brell et al., 2005; Hippenstiel et al., 2002). Thus, ADM may act as a general microfilament-relaxing peptide in endothelial cells. The tightening effect of ADM on endothelial barrier has also shown in an *ex vivo* model (Hocke et al., 2006). Overall, ADM stabilises endothelial barrier function *in vitro*, *ex vivo* and *in vivo* under several conditions simulating inflammatory reaction in various vascular beds (e.g. (Brell et al., 2005; Hippenstiel et al., 2002; Kis et al., 2001)). However, the exact mechanism of how ADM acts on endothelial cells to maintain endothelial barrier function remains unclear.

1.1.5 Adrenomedullin-2

Adrenomedullin-2 (ADM2, also known as intermedin) was simultaneously discovered by two groups using two different approaches. The first approach utilised searches of genomes from humans, other mammals and non-vertebrates (Roh et al., 2004). The second approach screened mammalian complementary DNA (cDNA) libraries for potential mammalian homologues of five orthologues of ADM which they had identified in pufferfish (Takei et al., 2004). The ADM2 gene is located on the distal arm of the chromosome 22q13 (Roh et al., 2004). It is translated as a prepro-peptide of 148 amino acids, which can be cleaved in two alternative peptides: short ADM2 (40 amino acids) and long ADM2 (47 amino acids) (Roh et al., 2004). Short ADM2 is believed to be the most important one *in vivo*. Similar to ADM, the tissue distribution of ADM2 is quite wide and is reviewed in (Hong et al., 2012). The highest peptide content is present in the kidney, hypothalamus and stomach (Roh et al., 2004; Takei et al., 2004).

ADM2 has similar biological activities to ADM and CGRP. When ADM2 is administered by intraperitoneal (Roh et al., 2004) or intravenous injection (Takei et al., 2004), it decreases blood pressure through vasodilatation. However, when it is given by intracerebroventricularly, it increases blood pressure and heart rate by activating the sympathetic nervous system (Hashimoto et al., 2007; Takahashi et al., 2011).

As ADM2 expression is high in the stomach and kidney it was not surprising to find that it regulates energetic metabolism. ADM2 inhibits food and drink intake (Roh et al., 2004; Taylor et al., 2005), gastric emptying (Roh et al., 2004) and induces anti-diuresis and anti-natriuresis (Takei et al., 2004). Moreover, ADM2 has been shown to be involved in the regulation of secretion of other peptides including prolactin and growth hormone (Taylor and Samson, 2005). Thus, it seems that ADM2 plays an important role in the regulation of the homeostasis of growth and metabolism.

1.2 G Protein-Coupled Receptors

In order to maintain homeostasis in any living organism, it is essential that cells are able to sense and respond to the external environment. To do so, cells communicate with each other through mediators released into the extracellular milieu. Therefore, they also need mechanisms that recognise and integrate these mediators. One mechanism, by which cells do this, is through the expression of cell-surface receptors. The largest family of cell-surface receptors is the superfamily of the GPCRs. This family of cell-surface receptors is characterised by its seven transmembrane spanning domains and represents the largest class of drug targets. There are more than 800 known GPCRs in the human genome, which are involved in virtually every physiological process (Fredriksson et al., 2003). In the cardiovascular system GPCRs play a pivotal role by regulating essential cardiovascular functions such as heart rate and contractility and vascular tone. GPCRs can be divided into five subfamilies: the rhodopsin (originally called A or I), secretin (B or II), glutamate (C or III), adhesion and frizzled/taste2 (Fredriksson et al., 2003). All the calcitonin peptide family exert their biological actions through activation of GPCRs that belong to the secretin family.

1.2.1 Activation and Termination of GPCR-Induced Signalling

1.2.1.1 Activation of G Proteins

GPCRs can be activated by a wide range of stimuli, such as photons of light, odorant molecules, peptides, hormones and lipid molecules (reviewed in (Kristiansen, 2004)). GPCRs transfer extracellular signals across the plasma membrane to intracellular effectors via G proteins (**Fig. 1.3**). G proteins belong to the GTPase family, enzymes able to hydrolyse guanosine triphosphate (GTP) (reviewed in (Kjeldgaard et al., 1996)). G proteins consist of three protein subunits, a guanosine diphosphate (GDP)/GTP-binding α-subunit and a β-subunit and a γ-subunit. The β- and γ-subunits form a stable dimeric complex referred as the $\beta\gamma$-subunit. The inactive form predominates when GDP is bound to the α-subunit and promotes the association with the $\beta\gamma$-subunit complex. The binding of the agonist to the receptor induces a conformational change of the GPCR allowing activation of heterotrimeric G proteins by interaction with the GPCR. Upon activation, GDP is realised from the G protein allowing GTP to bind to the α-subunit, which subsequently leads to the dissociation of the GTP-α-subunit from the $\beta\gamma$-subunit complex. Both GTP-α-subunit and the $\beta\gamma$-subunit complex are then free to activate downstream effectors (reviewed in (Cabrera-Vera et al., 2003; Kjeldgaard et al., 1996)). Gα-subunits are divided into four families based on similarity of α-subunits: Gα_s, G$\alpha_{i/o}$, G$\alpha_{q/11}$ and G$\alpha_{12/13}$. The Gα_s and G$\alpha_{i/o}$ activate or inhibit the activity of AC resulting in an increase or decrease of cAMP production, respectively. The

$G\alpha_{q/11}$ stimulates phospholipase C (PLC) leading to the formation of inositol trisphosphate (IP_3) and diacylglycerol (DAG). The $G\alpha_{12/13}$ activates small GTPases including the Rho family of GTPases e.g., RhoA. These second messengers then activate several intracellular pathways to modulate cell function (reviewed in (Cabrera-Vera et al., 2003; Hamm, 1998)).

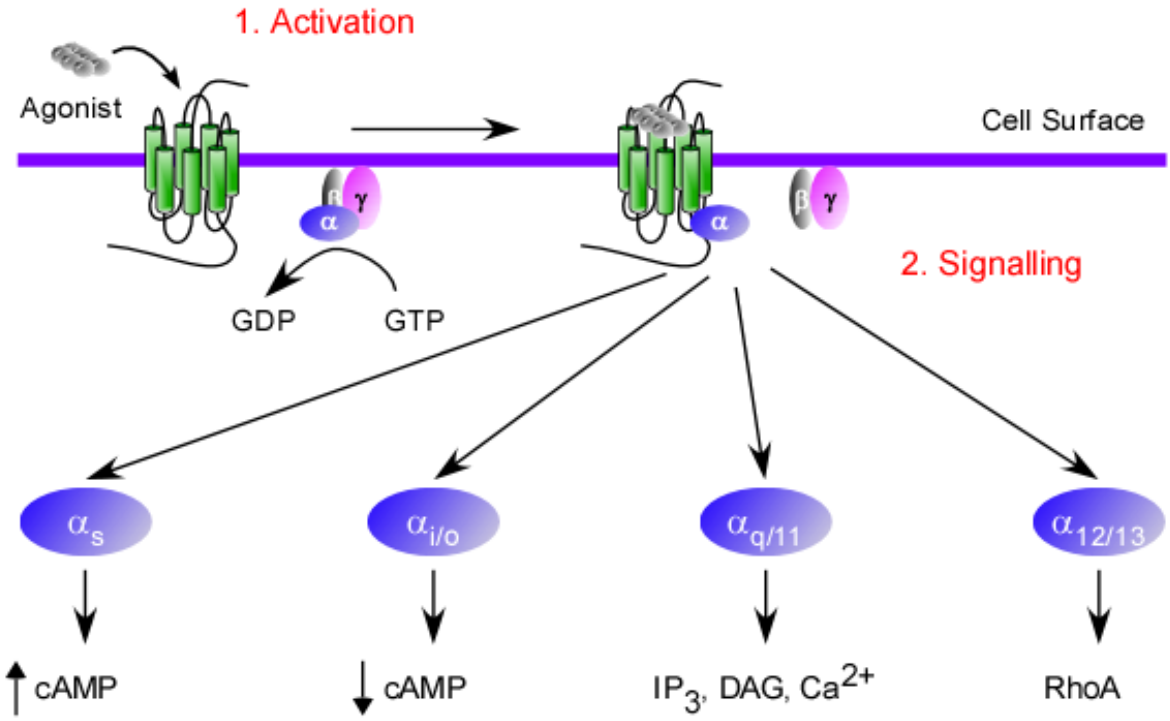

Figure 1.3 **GPCRs interact with different G protein families to initiate cell-surface signalling.** (1) Agonist binding to GPCRs promotes coupling of the receptor and the G protein. This coupling induces realised of GDP from the G protein that allows GTP to bind to the α-subunit, leading to the dissociation of the α-subunit from the $\beta\gamma$-subunits. (2) Once free, the α-subunit induces signalling of the receptor. There are four main Gα-subunit that can activate different signalling pathways. Gα_s promotes activation of AC leading to the formation of cAMP. G$\alpha_{i/o}$ inhibits AC activity resulting in a decrease of cAMP. G$\alpha_{q/11}$ promotes the activation of PLC which mediates the formation of IP_3 and DAG. IP_3 then induces mobilisation of Ca^{2+} from intracellular stores. G$\alpha_{12/13}$ promotes activation of small GTPases such as RhoA.

1.2.1.2 Desensitisation

Activation of GPCRs triggers not only activation of G proteins, but also cellular events that lead to a rapid attenuation of receptor responsiveness, a process termed desensitisation. Signalling of activated GPCRs at the cell-surface must be rapidly terminated in order to prevent uncontrolled signalling. There are two types of desensitisation: homologous and heterologous. Homologous desensitisation is the activation of one subtype of GPCR leading to the loss of responsiveness of only this subtype. For example, consider a cell that expresses receptors A and B. The cell is stimulated with the agonist of receptor A and it induces desensitisation of only receptor A, this is considered homologous desensitisation. Whereas, the activation of one subtype of GPCR that leads to the desensitisation of multiple GPCRs subtypes, independently of their agonist occupation is considered heterologous desensitisation. In other words, in our cell with receptors A and B, stimulation with the agonist A leads to the desensitisation of both receptors A and B.

The first step in desensitisation is phosphorylation of the receptor (reviewed in (Claing et al., 2002; Ferguson, 2001)), either by second messenger activated kinases, such as PKA (Benovic et al., 1985; Stadel et al., 1983) and protein kinase C (PKC) (Cho et al., 2007; Hardy et al., 2005); or by another kinase family named GPCR kinase (GRK) (Benovic et al., 1986b; Strasser et al., 1986) (**Fig. 1.4**). The second messenger-dependent phosphorylation can both act as homologous and heterologous desensitisation and was originally believed to be the principal mechanism of desensitisation. The exact mechanism of desensitisation remains poorly understood. However, it is believed that the GPCR is phosphorylated within the site required for association with G proteins and thus prevents their interaction (Benovic et al., 1985). Since their discovery, GRKs have been shown to play a central role in the desensitisation of many GPCRs (reviewed in (Premont and Gainetdinov, 2007)). This mechanism was first described in the vision system with the rhodopsin receptor. Protein kinases called rhodopsin kinases (i.e. GRK1) phosphorylate light-activated rhodopsin receptors (Kuhn, 1978), which lowers rhodopsin-mediated activity (Miller and Dratz, 1984). Another protein that was identified to bind to activated rhodopsin receptor, called 48-kDa protein, was shown to be required to promote complete desensitisation of the receptor (Wilden et al., 1986). This protein later called S-antigen or arrestin, showed to bind only to phosphorylated rhodopsin receptor. Studies with the β_2-adrenoceptor (β_2-AR, also known as β-adrenergic receptor) similarly identified kinases that only phosphorylate activated β_2-AR and thus named β-adrenergic kinase or βARK (Benovic et al., 1986a; Benovic et al., 1986b). βARK (i.e. GRK2) also induces desensitisation of β_2-AR. However, βARK phosphorylation is by itself insufficient to induce desensitisation, which can be restored by adding arrestin (Benovic et al., 1987). These results suggested that arrestin-like protein could exist in non-visual

systems. Subsequently, β-arrestin1 and β-arrestin2 were discovered and cloned (Attramadal et al., 1992; Lohse et al., 1990).

1.2.1.3 Internalisation

Another mechanism, by which uncontrolled/sustained signalling is terminated, is by removal of GPCRs from the cell-surface. This process termed endocytosis, controls and regulates the entry and exit of small and large molecules. There are two broad categories of endocytosis: phagocytosis, which is the uptake of large particles and typically restricted to certain mammalian cells; and pinocytosis, which is the uptake of fluid, solute and small particles. Four main mechanisms have been described for pinocytosis (reviewed in (Conner and Schmid, 2003; Doherty and McMahon, 2009)), but the two best-characterised mechanisms for GPCR internalisation are clathrin-mediated endocytosis and caveolae-mediated endocytosis.

The caveolae-mediated endocytosis was observed and described more than 50 years ago (Yamada, 1955) (**Fig. 1.5**). Caveolae are essentially composed of cholesterol and sphingolipids and are referred to lipid rafts (reviewed in (Harder and Simons, 1997)). The main structural member of caveolae is the caveolin protein family (Rothberg et al., 1992). They form a curved membrane invagination with wide opening and narrow-neck that can be pinch off. The dynamin family proteins are large GTPases that have been shown to be involved in endocytosis of coated pits and large invaginations (Damke et al., 1994). Notably, they have been shown to self-assemble into rings around the neck of membrane invaginations (Hinshaw and Schmid, 1995), suggesting a role in the “constriction” of the neck to release the caveolae from the plasma membrane ((Henley et al., 1998; Oh et al., 1998) and reviewed in (Schnitzer et al., 1996)). The activation of dynamin in caveolae has been shown to be regulated by the protein kinase Src (Shajahan et al., 2004). Moreover, Src has been found to phosphorylate caveolins (Li et al., 1996), which is believed to trigger internalisation of caveolae (Aoki et al., 1999; Li et al., 1996; Mastick et al., 1995; Nomura and Fujimoto, 1999; Schlegel et al., 2001).

Clathrin-mediated endocytosis was first described in 1964 (Roth and Porter, 1964) and is involved in the constitutive transport of essential nutrients, such as iron-laden transferrin that binds to transferrin receptors (TfR) (reviewed in (Mayle et al., 2012)) (**Fig. 1.5**). However, it is clear now that clathrin-mediated endocytosis is also involved in internalisation of agonist-activated receptors (reviewed in (Brodsky et al., 2001)). Clathrin was first identified in 1975 (Pearse, 1975) and later described as a three-legged structure, named triskelion, which can self-assemble to form closed polygonal “cages” (reviewed in (Brodsky et al., 2001)). The other major components of clathrin-mediated endocytosis are the adaptor

proteins family (AP), identified in 1979 (Keen et al., 1979). There are four isoforms of AP (AP1-4), each mediating vesicle formation at distinct subcellular localisations (reviewed in (Robinson and Bonifacino, 2001)). Only AP2 regulates the endocytosis at the plasma membrane. AP2 plays a central role in clathrin-mediated endocytosis as they direct the self-assembled clathrin “cage” into curved bud (reviewed in (Brodsky et al., 2001)), and also interact with different cargos to be internalised (Collins et al., 2002; Ohno et al., 1995). GPCRs cannot bind directly to AP2, instead it has been shown that β-arrestins physically link GPCRs to AP2 (Laporte et al., 1999) and clathrin (Goodman et al., 1996). These interactions are important for an efficient recruitment of the GPCR into clathrin-coated pits, but not essential, as it has been shown that disabling or deletion of either binding site in β-arrestins does not completely prevent receptor internalisation (reviewed in (Kim and Benovic, 2002)).

After internalisation, the fate of GPCRs depends on both the cell type and on the type of receptor. Typically, following agonist-induced internalisation GPCRs are efficiently recycled back to the cell-surface. However, many GPCRs are trafficked to a degradation pathway and proteolytically degraded in the lysosome, a process called down-regulation. This molecular “sorting” of GPCRs can occur at many different subcellular localisations, including the plasma membrane and the endosome.

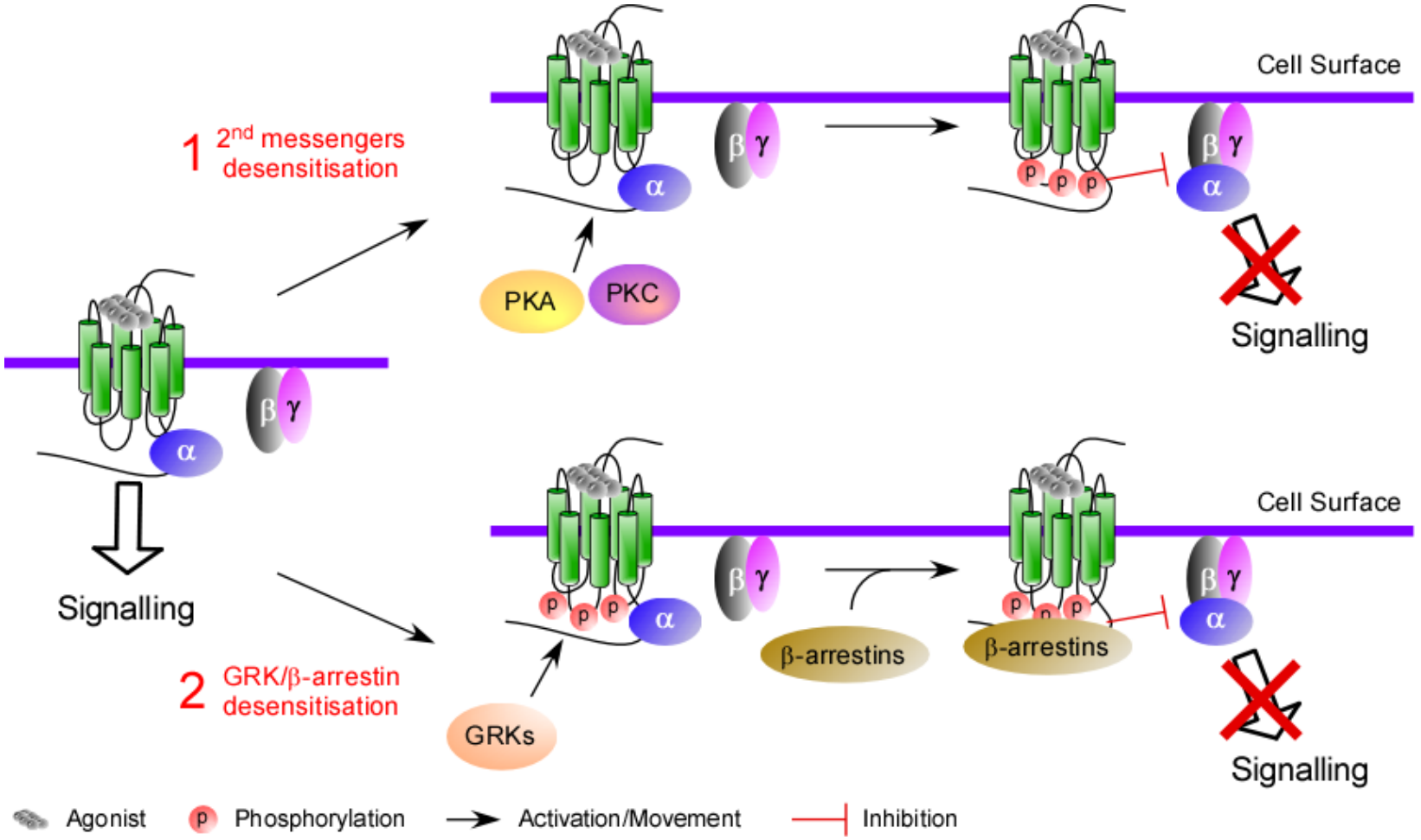

Figure 1.4 **GPCRs desensitisation.** Agonist binding to its receptor promotes cell-surface signalling. In order to stop excessive signalling, G protein-dependent signalling is rapidly block by a process called desensitisation. (1) GPCR can get phosphorylated by second messenger such as PKA and/or PKC. These phosphorylations are believed to alter Gα-dependent signalling by interfering with its association with the receptor. (2) Alternatively, GPCR are phosphorylated by a protein kinase family called GRK. These phosphorylations increase the affinity of the receptor for β-arrestins which physically uncouples the receptor from the G protein and terminates cell-surface signalling.

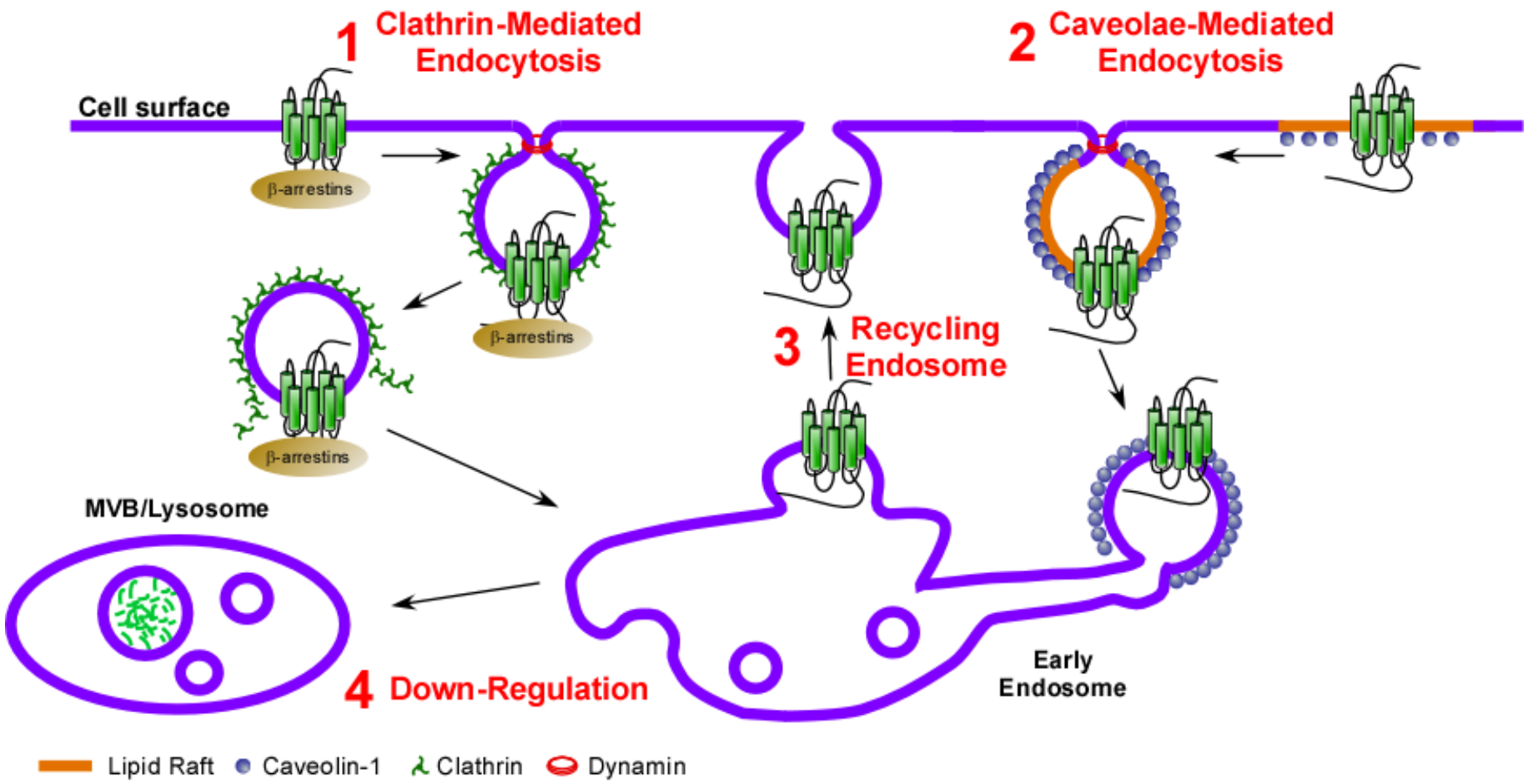

Figure 1.5 **Clathrin- and caveolae-mediated GPCRs endocytosis.** After being desensitised the receptor is internalised by two main mechanisms. (1) In the clathrin-mediated endocytosis, β-arrestin associated with the GPCR, interact with member of the clathrin pits to mediate internalisation. (2) In caveolae-mediated endocytosis, the mechanism of action is poorly understood, but the receptor is associated with lipid raft and the internalisation is then trigger by phosphorylation of caveolin-1. Both pathways lead to the traffic of the receptor into early endosome, where it can either (3) recycle back to the cell surface or (4) be targeted to lysosomes for down-regulation.

1.2.2 Molecular Mechanisms of GPCR Sorting at the Plasma Membrane

The first molecular sorting of GPCRs occurs at the plasma membrane, where agonist-activated receptors differ in their ability to undergo specific endocytosis pathways (i.e. clathrin versus caveolae endocytosis pathways). Moreover, some of these receptors are post-translationally modified to direct them through a specific molecular pathway.

1.2.2.1 Segregation of GPCRs in Microdomains of the Plasma Membrane

Before endocytosis, GPCRs can be directed into different microdomains of the membrane, which would then affect their fate. The β_2-AR has been shown to be internalised via clathrin-dependent mechanism in several cell types such as COS-1 cells (fibroblast-like cell line) (Goodman et al., 1996) and HEK cells (human embryonic kidney cell line) (Orsini and Benovic, 1998). However, other studies suggest that in A431 cells (human epidermoid carcinoma cell line), β_2-ARs undergo clathrin-independent endocytosis (Raposo et al., 1989). Cholecystokinin 1 receptor internalisation was observed to occur via both clathrin- and caveolae-mediated endocytosis in CHO cells (Chinese hamster ovary cell line) (Roettger et al., 1995). The existence of these two mechanisms may explain the two different fates of the receptor: a rapid resensitisation versus a less rapid resensitisation and down-regulation. The internalisation of the $P2Y_1$ and $P2Y_{12}$ receptors (P2Y receptor family, also known as purinergic receptors) is clathrin-mediated, however, only internalisation of $P2Y_{12}$ is β-arrestin-dependent (Mundell et al., 2006). $P2Y_{12}$ and $P2Y_1$ have been shown to segregate in distinct coated pits, which subsequently lead to their different post-endocytic fates (Mundell et al., 2006).

1.2.2.2 Interaction with β-Arrestins

β-arrestins have been shown to regulate desensitisation and internalisation of GPCRs (reviewed in (Luttrell and Gesty-Palmer, 2010)). GPCRs have different affinities for β-arrestin1 or 2, which based on this affinity has led to two classes of GPCRs (Oakley et al., 2000). GPCRs such as the β_2-AR which preferentially bind β-arrestin2, are termed class A receptors. Soon after internalisation, these receptors release β-arrestin2 and rapidly recycle to the cell-surface. Whereas class B GPCRs such as the V_2 receptor (V_2R, vasopressin and oxytocin receptor family) bind to both β-arrestin isoforms with equal affinity. Class B GPCRs receptors internalise with β-arrestins and recycle more slowly to the cell-surface (Oakley et al., 1999; Oakley et al., 2000). Moreover, when the C-terminal tails of β_2-AR and the V_2R are “swapped”, the kinetics of trafficking of these receptors is

completely reversed (Oakley et al., 1999). This result led to the discovery of a cluster of serine residues within the C-terminal tail that determines the affinity for β-arrestins, and that modification of this cluster is sufficient to alter the kinetics of GPCR trafficking (Oakley et al., 2001). Similarly, mutation of serine residues in the C-terminal tail of the CXCR4 (chemokine receptor family) showed impairment in endocytosis and down-regulation (Marchese and Benovic, 2001; Parent et al., 1999), suggesting involvement of serine phosphorylation in the pre- and post-endocytic sorting.

1.2.2.3 Ubiquitination of GPCRs

Certain GPCRs are directed to specific endocytic pathways by covalent modification of intracellular facing lysine residues by a small regulatory protein called ubiquitin. Ubiquitin is best known for its role in targeting proteins to the proteasome to be degraded (reviewed in (Glickman and Ciechanover, 2002)), including the proteasome-dependent degradation of GPCRs that may occur due to misfolding during the biosynthetic pathway (Cook et al., 2003; Petaja-Repo et al., 2001). Ubiquitin is also involved in the pre- and post-endocytic sorting of GPCRs.

The ubiquitin machinery is composed of three enzymes called E1, E2 and E3 (responsible for conjugating ubiquitin moieties to the protein) and de-ubiquitinating enzymes (DUBs) that proteolytically remove ubiquitin molecules from proteins. Ubiquitin conjugation to proteins requires three steps. Ubiquitin is first “activated” by an E1 enzyme (activating enzyme) in an ATP-dependent reaction by forming a thioester bond at its active-cysteine site with the COOH-terminus of ubiquitin. Ubiquitin is then transferred to the active site cysteine residue of an E2 enzyme (conjugating enzyme). Finally, ubiquitin is transferred to a lysine residue on the target protein by forming an isopeptide bond. This action is either mediated directly by an E3 enzyme (homologous to the E6-AP carboxyl terminus (HECT)-domain containing E3 ligases) or by the E2 enzyme with assistance from the E3 ligase (Really Interesting New Gene (RING)-finger containing E3 ligases) (Hershko et al., 1983). It is known that there is only two E1 (Ciechanover et al., 1982; Pelzer et al., 2007), several E2 and multiple families of E3, which are therefore able to provide reactions with specificity. DUBs are a large family of proteases comprised of about 90 members and specifically cleave the bond that links ubiquitin and proteins. Their main function is to remove the ubiquitin before the protein is degraded in order to maintain ubiquitin-homeostasis and recycle ubiquitin pool. This process usually occurs at the entry of the proteasome and the lysosome (reviewed in (Nijman et al., 2005)). Indeed, DUBs have been shown to also regulate the post-endocytic sorting of receptors, such as for PAR2 (protease-activated receptor) (Hasdemir et al., 2009) and CXCR4 (Berlin et al., 2010), where deubiquitination promotes lysosomal targeting and down-regulation of these receptors.

The role for ubiquitin in the endocytic sorting of GPCR was first shown for the yeast GPCR, Ste2 (**Fig. 1.6**). Ubiquitination of the C-terminal tail of the receptor is required to promote internalisation and trafficking to the vacuole (equivalent to the mammalian lysosome) (Hicke and Riezman, 1996). In contrast, PAR1 (protease-activated receptor) is constitutively ubiquitinated and deubiquitination promotes internalisation of the receptor (Wolfe et al., 2007). Studies on β_2-AR have shown that ubiquitination of β-arrestin was required for the internalisation and subsequent down-regulation of the receptor (Shenoy et al., 2001), where the time course of ubiquitination/deubiquitination of β-arrestin correlates with the time of association/dissociation with the receptor (Shenoy and Lefkowitz, 2003). Therefore, ubiquitin indirectly regulates the endocytosis of GPCRs by controlling the association of β-arrestin with the receptor.

A study of the β_2-AR (Shenoy et al., 2001) was the first one to show that mammalian GPCRs are regulated by ubiquitination. Ubiquitination of the β_2-AR promotes its trafficking to lysosomes for degradation (**Fig. 1.6**). Indeed, a mutant lacking all intracellular facing lysine residues, although able to signal and internalise normally, but was not ubiquitinated and exhibited reduced degradation (Shenoy et al., 2001). Other GPCRs such as PAR2 (Jacob et al., 2005) and the CXCR4 (Marchese and Benovic, 2001) are similarly regulated by ubiquitination. However, ubiquitination of GPCRs is not always required for downregulation. Activation of the δ receptor (δOR, opioid receptor family) promotes ubiquitination and trafficking to lysosomes (Tanowitz and Von Zastrow, 2002; Tsao and von Zastrow, 2000b). However, lysine-less δOR mutant still efficiently trafficked to lysosomes, even in the absence of ubiquitination (Tanowitz and Von Zastrow, 2002). A subsequent study showed that ubiquitination of δOR regulates the rate at which the receptor is degraded (Hislop et al., 2009).

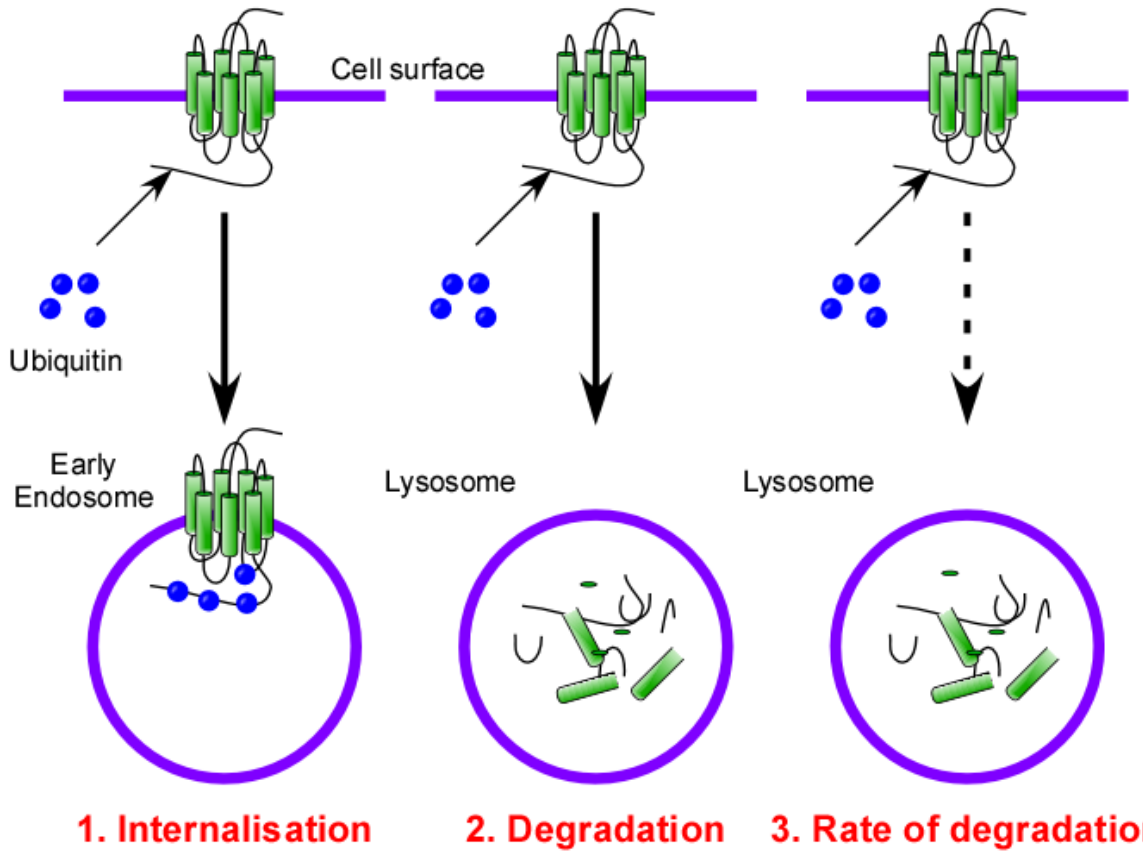

Figure 1.6 **Roles of ubiquitination in the regulation of GPCRs.** Ubiquitin is a small regulatory protein, that can be covalently attached to GPCRs to lysine residues. Ubiquitination can perform at least three known functions. (1) Ubiquitin can regulate the internalisation of GPCRs, as has been shown for Ste2 (Hicke and Riezman, 1996) or PAR1 (Wolfe et al., 2007). (2) Ubiquitin also targets the GPCR to the lysosome, where the receptor is degraded, as shown for PAR2 (Jacob et al., 2005). (3) Finaly, ubiquitination regulates the rate of degradation, as for the δOR (Hislop et al., 2009).

1.2.3 Endosomal Sorting of GPCRs

Once internalised, GPCRs traffic to early endosomes (reviewed in (Mellman, 1996)), where they are sorted into recycling pathways to return to the cell-surface or alternatively, enter the down-regulation pathway to be trafficked to lysosome.

1.2.3.1 Recycling Pathway of GPCRs

The recycling pathway was for a long time thought to occur by default. However, accumulating evidence showed the recycling pathway as a complex and active system.

Studies of the β_2-AR have shown that dephosphorylation of the receptor was required before recycling back to the cell-surface (Krueger et al., 1997; Pippig et al., 1995; Sibley et al., 1986). Dephosphorylation was mediated by the protein phosphatase type 2A (PP2A) (Pitcher et al., 1995). Similar mechanisms also regulate other GPCRs, such as the V_2R (Innamorati et al., 1998) and the NK_1 receptor (NK_1R, tachykinin receptors family, also known as neurokinin 1 receptor) (Garland et al., 1996). Subsequently, it has been shown that dephosphorylation reduces binding of β-arrestins to GPCRs (Sohlemann et al., 1995) and that the longer they are associated with β-arrestins the longer they are “sequestered” on endosomes (Oakley et al., 1999; Oakley et al., 2000). These studies suggest that β-arrestins play an important role in the sorting of the receptor by preventing its entry into the recycling pathway.

PDZ (postsynaptic density 95/disc large/zonula occludens-1) domain-containing proteins have been shown to bind to C-terminal tail of GPCRs and affect their post-endocytic sorting. A PDZ domain (Kennedy, 1995) is a motif required for protein-protein interactions that is found in the C-terminal tails of many GPCRs (reviewed in (Marchese et al., 2008)). For example, the Na^+/H^+ exchanger regulatory factor (NHERF), which contains a PDZ domain, has been found to bind β_2-AR and promote efficient recycling of the receptor (Cao et al., 1999). This PDZ domain, when inserted into the C-terminal tail of the δOR, is sufficient to induce recycling of this receptor that normally undergoes efficient down-regulation (Gage et al., 2001). The N-ethylmaleimide-sensitive fusion (NSF) protein has also been shown to bind to the C-terminal tail of the β_2-AR, and is also involved in the regulation of its recycling (Cong et al., 2001). When the binding domain of NSF was mutated, β_2-AR failed to recycle normally after agonist stimulation. However, studies with the β_2-AR showed that PDZ domain was sufficient to induce recycling of the receptor independently of NSF binding (Gage et al., 2005). GPCRs unable to bind such regulator proteins undergo down-regulation pathways and are targeted to lysosomes.

1.2.3.2 Regulation of GPCRs by the Rab GTPase Family

In humans, the GTPase Rab proteins constitute one of the biggest groups of the Ras-like protein family (reviewed in (Zerial and McBride, 2001)). They have been shown to regulate the trafficking and transportation of intracellular vesicles by regulating the budding, transport, tethering, docking and fusion of vesicles (reviewed in (Tuvim et al., 2001)). Due to their central role in intracellular traffic, Rab proteins have been shown to regulate the trafficking of GPCRs. An important aspect of the Rab family is that each member is localised in surfaces of distinct membrane-bound vesicles/organelles. For example, Rab5 is mediating the transport of vesicles from the plasma membrane to early endosome (Gorvel et al., 1991) (**Fig. 1.7**). Many GPCRs have been shown to internalise in Rab5-positive vesicles, such as the β_2-AR and the NK_1R, where the use of the dominant negative Rab5-S34N mutant inhibited agonist-induced internalisation of these receptors (Schmidlin et al., 2001; Seachrist et al., 2000). Unlike the β_2-AR, the AT_1 receptor (AT_1R, angiotensin receptor family) has been found to directly bind to Rab5 and internalise into Rab5-containing large hollow core vesicles (Seachrist et al., 2002). However, dominant negative of Rab5 did not block its internalisation, but prevented the receptor to traffic to those large vesicles. Therefore, AT_1R by binding to Rab5 seems to regulate its own trafficking into those target vesicles. Conversely Rab4 and Rab11 are involved in the recycling of cargo from early and recycling endosomes to the cell-surface. Rab4 on its own promotes rapid recycling from early endosomes (van der Sluijs et al., 1992), whereas in association with Rab11, Rab4 induces later and slower recycling from recycling endosomes to the cell-surface (Sonnichsen et al., 2000). For example, the dominant negative Rab4-N121I mutant blocks the recycling of the β_2-AR, without affecting its desensitisation and internalisation (Seachrist et al., 2000). Similarly, the dominant negative Rab11a-S25N mutant also blocks the slower recycling of CXCR2 (Fan et al., 2003).

Regarding the down-regulation pathway, Rab7 has been found to localise to late endosomes and lysosomes. In fact, Rab7 regulates the traffic of vesicles from early to late endosomes (Meresse et al., 1995) and then to lysosome (Bucci et al., 2000). Indeed, overexpression of the dominant negative Rab7-N125I and Rab7-T22N mutants prevents the degradation of κ receptor and CXCR2 (Fan et al., 2003; Li et al., 2000).

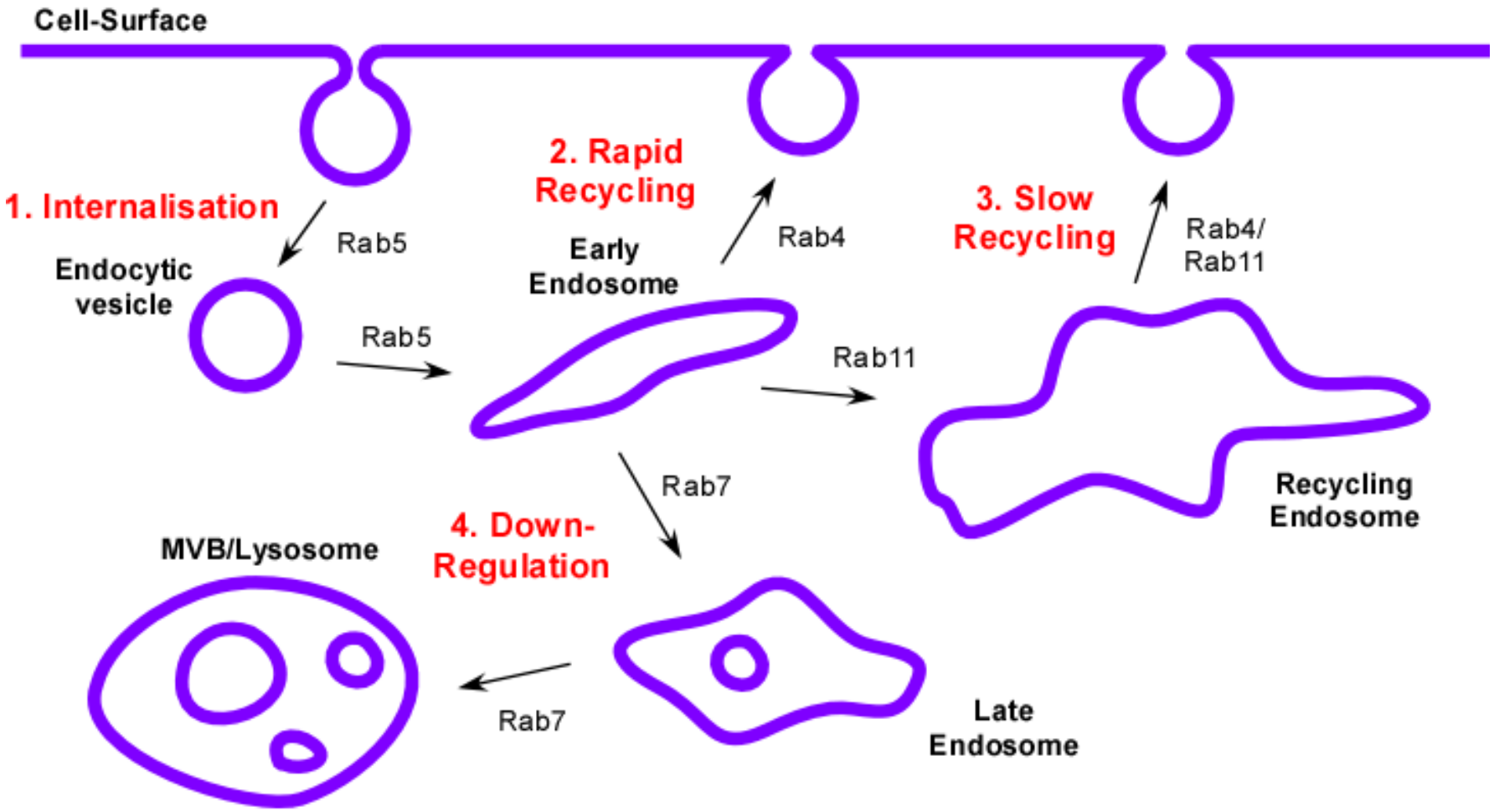

Figure 1.7 **Representation of the Rab GTPase transportation system.** The Rab GTPase protein family is responsible of regulating the budding, transport, tethering, docking and fusion of vesicles. Each member is localised in surfaces of distinct membrane-bound vesicles/organelles. For example, (1) Rab5 is responsible to regulate transport from the plasma membrane to early endosome. (2) Rab4 promotes rapid recycling of vesicle to the cell-surface, (3) whereas in association with Rab11, they induce slower recycling from recycling endosomes to the cell-surface. (4) Rab7 is involved in the transportation of vesicles to late endosomes and lysosomes.

1.2.3.3 Down-Regulation Pathways of GPCRs: the ESCRT Machinery

Persistent activation of GPCRs can promote trafficking to down-regulation pathways, an important process for signal termination. However, certain GPCRs are always directly targeted to these pathways to be degraded.

Studies in yeast (Stack et al., 1995) have revealed a set of proteins, involved in the traffic of ubiquitinated cargos from endosomes to lysosomes, that are highly conserved between species (reviewed in (Williams and Urbe, 2007)). This machinery is called the endosomal sorting complex required for transport (ESCRT) and is divided in 4 main complexes. ESCRT-0 is the complex responsible for clustering ubiquitinated-cargos, which comprises the hepatocyte growth factor-regulated tyrosine kinase substrate (Hrs) (**Fig. 1.8**). Hrs contains an ubiquitin-interacting motif (UIM) that targets ubiquitinated-cargos to the ESCRT machinery (Hofmann and Falquet, 2001; Lloyd et al., 2002). ESCRT-I and ESCRT-II are involved in the formation of intralumenal vesicles (ILVs) within the endosome and ESCRT-III is involved in the cleavage of the neck of these vesicles. Once endosomes are filled with many of these ILVs they are referred to as a multivesicular bodies (MVBs), organelles that precede lysosomes (Morales et al., 1999). The protein tumour susceptibility gene 101 (Tsg101), a component of ESCRT-I (Babst et al., 2000), has been shown to directly bind Hrs to mediate traffic of ubiquitinated-cargos to lysosome (Lu et al., 2003). The main components of ESCRT-III are the charged MVB protein (CHMP) family (Howard et al., 2001) that have been found to polymerise around the neck of ILVs and induce their scission (Hanson et al., 2008). The AAA-ATPase vacuolar protein sorting 4 (Vps4) is another protein essential for ESCRT function that disassembles and recycles ESCRT-III components (Azmi et al., 2006; Babst et al., 1998; Scheuring et al., 2001).

Many GPCRs that traffic to lysosomes have been reported to require the ESCRT machinery. CXCR4 was the first mammalian GPCR to shown to interact with components of ESCRT machinery. Down-regulation of CXCR4 has been shown to be dependent on Hrs and Vsp4 (Marchese et al., 2003). The post-endocytic sorting of PAR2 also has been reported to be Hrs-dependent (Hasdemir et al., 2007) unlike PAR1 which traffics to lysosomes independently of Hrs and Tsg101 (Gullapalli et al., 2006). However PAR1 requires interaction with CHMP4B and C and Vsp4, which is mediated by apoptosis-linked gene-2-interacting protein X (ALIX) (Dores et al., 2012). ALIX is protein regulator involved in apoptosis (Vito et al., 1999) but also recruits CHMP4/ESCRTIII complexes to facilitate MVB formation (Katoh et al., 2003). A more recent study on the ocular albinism type 1 GPCR has also shown that its degradation is dependent on several components of the ESCRT-0, –I and –III (Giordano et al., 2011). Interestingly, some GPCRs that traffic to lysosomes in an ubiquitin-independent manner have been shown to interact directly with some components of the ESCRT machinery, such as the δOR

that require Hrs and Vsp4 to traffic to lysosome (Hislop et al., 2004) and the CGRP receptor that require Hrs (Hasdemir et al., 2007).

1.2.3.4 Non-ESCRT Protein Implicated in Lysosomal Sorting of GPCRs

The GPCR-associated sorting protein (GASP) family were first identified as a binding partner of the δOR (Whistler et al., 2002). Overexpression of the last 497 residues of the C-terminal tail of GASP that act as a dominant-negative or mutation of the domain for interaction between the receptor and GASP caused recycling of the receptor. Subsequently, GASP was been found to bind to a broad spectrum of GPCRs, such as the dopamine 2 (D_2) receptor (Bartlett et al., 2005), the opioid receptors μOR and κOR, β_1-AR and the CT receptor (CTR, calcitonin receptor) (Simonin et al., 2004). GASP is widely distributed, but is predominantly expressed in the CNS (Simonin et al., 2004). Interestingly, GASP has been found to bind β_2-AR, a receptor that usually undergoes recycling. This suggests that GASP may be involved in the sorting of β_2-AR for down-regulation, observed during chronic stimulation (Whistler et al., 2002).

Sorting nexins (SNX) are another protein family involved in the endosomal sorting of GPCRs to lysosomes. These membrane-associated proteins are characterised by the presence of a PX domain (named after NADPH oxidase domains of $p40^{phox}$ and $p47^{phox}$) (reviewed in (Ponting, 1996)). They consist of approximately 100-130 amino acids and have the ability to bind various phosphatidylinositol phosphates (PIPs) (reviewed in (Ponting, 1996)). SNXs were first implicated in the sorting of the epidermal growth factor receptor (ErbB1), a receptor tyrosine kinase (RTK), where stimulation with epidermal growth factor (EGF) promotes binding of SNX-1 to the receptor and induced degradation of ErbB1. Degradation was enhanced by overexpression of SNX-1 (Kurten et al., 1996). SNX-1 was also shown to bind Hrs, promoting the sorting of ErbB1 to lysosomes (Chin et al., 2001). PAR1 was the first GPCR identified to associate with SNX-1, where overexpression of the C-terminal tail of SNX-1 that function as a dominant negative blocked agonist-mediated trafficking of PAR1 to endosomes (Wang et al., 2002). Suggesting that SNX-1 is involved in the trafficking of PAR1 to lysosomes. This was later confirmed using siRNA to deplete cells of endogenous SNX-1 (Gullapalli et al., 2006). Interestingly, as opposed to ErbB1, SNX-1-mediated PAR1 trafficking to lysosomes is Hrs- and Tsg101-independent (Gullapalli et al., 2006). SNX-1 has been shown to bind other GPCRs, including the oxytocin receptor and δOR, both of which are known to undergo lysosomal sorting (Heydorn et al., 2004). However, similarly to GASP, SNX-1 has been found to bind members of the NK_1R and acetylcholine (muscarinic) receptor family, which are known to recycle back to the cell-surface (Heydorn et al., 2004), which

again suggests a role for SNX-1 in down-regulation after chronic agonist stimulation.

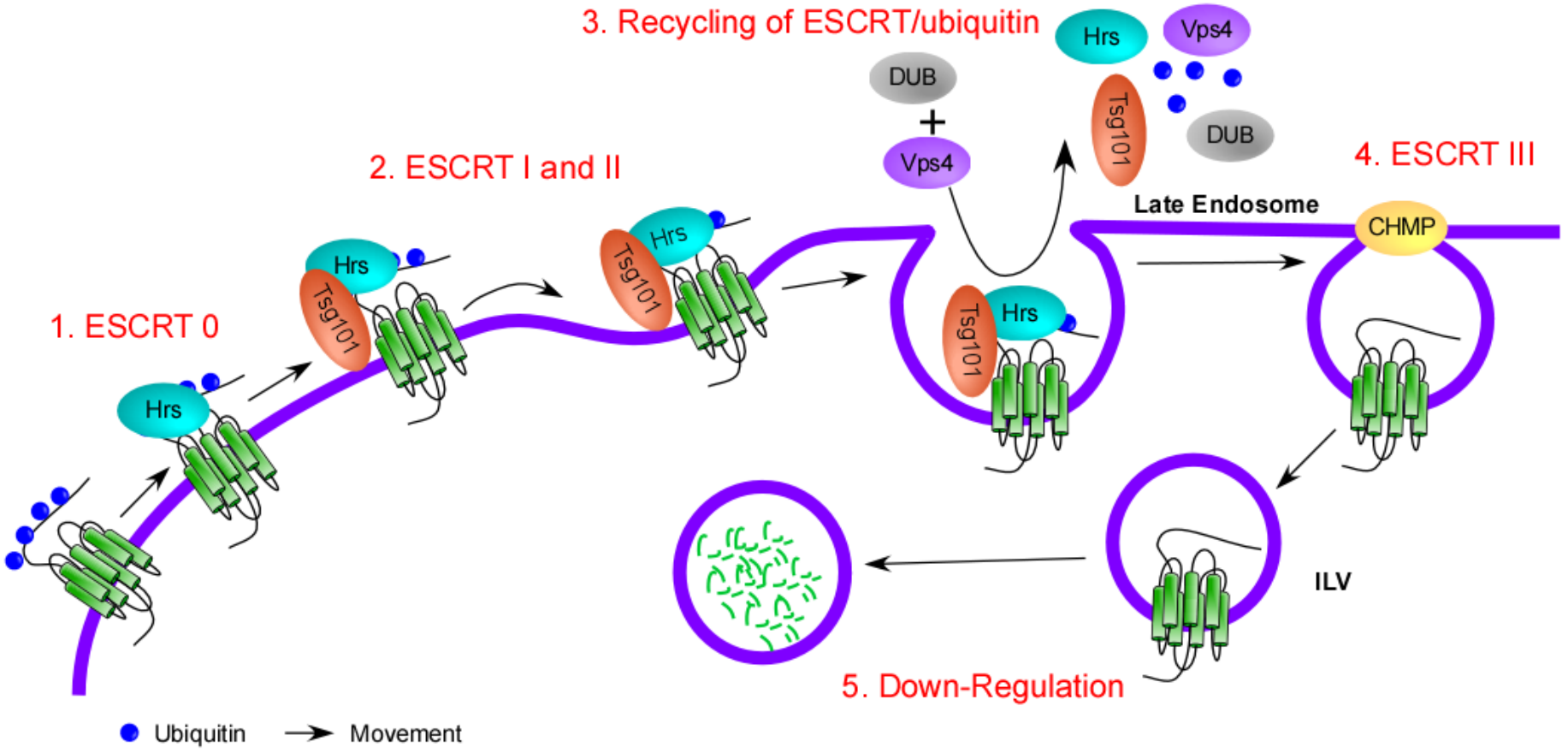

Figure 1.8 **Representation of the ESCRT machinery.** Once in late endosomes, (1) ubiquitinated GPCRs are recognised by members of the ESCRT 0 complex, such as Hrs. (2) ESCRT 0 complex then, interact with members of ESCRT I and II complexes, such as Tsg101, which promote the formation of intralumenal vesicles (ILVs). (3) Before the vesicle closes, Vps4 mediates the recycling of ESCRT 0, I and II. Similarly, DUB proteases promote the recycling of ubiquitin. (4) Members of the ESCRT III, such as the CHIMPs family proteins, are responsible of cleavage of the neck of ILVs. (5) Once the endosomes is full with ILVs, it is referred as multivesicular bodies (MVB) before it merges with the lysosome for down-regulation.

1.2.4 Down-Regulation of GPCRs

1.2.4.1 Proteasome

The proteasome is a multi-protein complex found in the cytoplasm and nuclei of all eukaryotic cells. The function of the proteasome is the degradation of abnormal/misfolded proteins and proteins involved in the regulation of cell viability and cell cycle by degrading critical regulatory protein such as cyclins and transcription factors. It also has been found to be involved in the processing and presentation of major histocompatibility complex (MHC)-class I antigens at the cell-surface (Rock et al., 1994).

The proteasome is composed of two main particles often referred to their Svedberg sedimentation coefficient (denoted S): the core particle 20S (DeMartino and Goldberg, 1979; Wilk and Orlowski, 1983) (responsible for the proteolytic activity) and the regulatory particle 19S, which is responsible for the recognition of ubiquitin-complex protein (Schmid et al., 1984; Schuldt and Kloetzel, 1985). The 20S and 19S form the complex denoted 26S and named proteasome (Arrigo et al., 1988). The proteasome is a threonine protease (Fenteany et al., 1995; Seemuller et al., 1995) that possesses three main activities: a chymotrypsin-like activity that cleaves after large hydrophobic residues; a trypsin-like activity that cleaves after basic residues; and a peptidylglutamyl-peptide hydrolysing that cleaves after acidic residues (Wilk and Orlowski, 1983). As the proteasome is found in both the cytoplasm and nucleus, its main targets are cytoplasmic and nuclear proteins. However, proteasome has been found to be involved in the regulation of misfolded GPCRs during their biosynthetic pathway, such as the δOR (Petaja-Repo et al., 2002).

1.2.4.2 Lysosome

Unlike the proteasome, many studies have shown that the degradation of GPCRs mainly occurs in lysosomes (Hanyaloglu and von Zastrow, 2008; Marchese et al., 2008; Tsao and von Zastrow, 2000a). Lysosomes were first described in the mid 1950's (De Duve et al., 1955) as new cytoplasmic membrane-enclosed organelles that contain different types of enzymes that requiring an acidic pH (~pH 5). Lysosomes constitute the primary degradative compartment of the cell and receive their substrates from endocytosis or autophagy. However, lysosomes are also involved in the presentation of MHC-class II (Collins et al., 1991) and in cell death (Trump et al., 1962).

Lysosomes are comprised of two main classes of proteins, soluble hydrolytic enzymes and lysosomal membrane proteins (LMPs). Lysosomes contain about 50 different degradative enzymes that can hydrolyse proteins, DNA, RNA,

polysaccharides and lipids (review in (Weissmann, 1964)). The proteases, which are described more precisely below, comprise aspartic, cysteine and serine protease families of hydrolytic enzymes, such as the cathepsin family. LMPs are generally contained within the lysosomal compartment and have diverse functions, including acidification of the lysosomal lumen, protein import from the cytosol, membrane fusion and transport of degradation products to the cytoplasm (reviewed in (Callahan et al., 2009)). Among them, lysosome-associated membrane proteins (LAMPs) are one of the most abundant, however their roles remain poorly understood.

1.2.5 Regulation by Proteases

Proteases are enzymes that catalyse proteolysis, which consists of the hydrolytic breakdown of peptide bond. Proteases are classified into six groups according to their active site: serine proteases, cysteine proteases, threonine proteases, aspartic proteases, glutamic proteases and metalloproteases (Rawlings et al., 2012). Beyond their proteolytic role in digestion in the stomach and the down-regulation of protein in lysosomes, proteases have been found to be involved in the regulation of GPCRs, by acting on the activation of receptors, promoting transactivation of receptor tyrosine kinases or controlling the post-endocytic sorting of GPCRs.

Proteases can control the availability of extracellular bioactive components, which mediate GPCRs' activation. For example, angiotensin I-converting enzyme (ACE) is a zinc metalloprotease that cleaves angiotensin I, an inactive precursor, into the active angiotensin II (ang II) (Skeggs et al., 1956). Ang II can then promote its actions (e.g. vasoconstriction) through the activation of AT_1R and AT_2R receptors (reviewed in (de Gasparo et al., 2000)). Additionally, ACE has been found to degrade bradykinin (Grafe et al., 1993; Jaspard et al., 1993) and then prevent the vasodilatatory activity of this peptide. Therefore, ACE regulates blood pressure by increasing the levels of ang II and degrading bradykinin. Alternatively, some proteases such as thrombin and trypsin have been found to directly stimulate PAR receptors by cleaving the N-terminus and to expose a new N-terminus, which acts as a tethered ligand (Nystedt et al., 1994; Vu et al., 1991). Conversely, other proteases such as the cathepsin G have been found to prevent activation of PARs by proteolytically removing the tethered ligand (Dulon et al., 2003).

The transactivation of ErbB1 by GPCRs was first described by Daub *et al.* in 1996 (Daub et al., 1996). The mechanism by which GPCRs induce ErbB1 transactivation is still unclear and can depend on receptor and cell type. However, many mechanisms involve the release of precursor forms of the ErbB1 type ligands, such as the heparin binding-EGF, transforming growth factor-α, and

amphiregulin. These ligands are generated by the activation of zinc-dependent metalloproteases from the a disintegrin and metalloprotease (ADAM) family. ErbB1 transactivation promotes activation of extracellular signal-regulated kinase (ERK) and PI3K/Akt pathways to regulate cell proliferation and migration (Prenzel et al., 1999; Schafer et al., 2004a; Schafer et al., 2004b).

Finally, proteases are also involved in the sorting of certain GPCRs. For example, DUBs cleave ubiquitin-protein bonds allowing GPCRs to be trafficked for degradation (**see 1.2.2.3**). Endosomal proteolysis of GPCR ligands can also regulate GPCR signalling, trafficking and resensitisation. Endothelin-converting enzyme-1 (ECE-1) is present in early endosomes and regulates many GPCRs. Following activation, GPCRs, together with the ligand and β-arrestin internalise to early endosomes. β-arrestin must be released for GPCRs to recycle back to the cell-surface (Oakley et al., 1999) and until recently the mechanism triggering the release of β-arrestins was unknown. Studies on the post-endocytic sorting of NK_1R and CGRP receptor revealed that ECE-1 degrades SP and CGRP at endosomal pH, destabilising the GPCR/ligand/β-arrestin complex and promoting recycling of receptors back to the cell-surface (Padilla et al., 2007; Roosterman et al., 2007).

1.3 Receptors of the Calcitonin Peptide Family

1.3.1 Heterodimeric Receptors

Receptors of the calcitonin peptide family are GPCRs belonging to the secretin family (class II). Based on their ability to bind both β-arrestin isoforms they are sometimes termed class B receptors. The CTR was first cloned in 1991 (Lin et al., 1991) and consists of 482 amino acids. The calcitonin receptor-like receptor (CLR), was cloned shortly after, based on sequence homology with CTR (~55% homology between the receptors) and consists of 461 amino acids (Fluhmann et al., 1995; Njuki et al., 1993). However, CLR was consider as orphan until Aiyar *et al.* observed evidence of CGRP binding and CGRP-dependent cAMP activation in HEK cells transfected with CLR (Aiyar et al., 1996). A major breakthrough was achieved two years later when McLatchie *et al.* (McLatchie et al., 1998) showed that a family of single transmembrane proteins called receptor activity-modifying proteins (RAMPs) were necessary to confer receptor function to CLR. Unlike CLR, CTR possesses receptor function when expressed alone (Lin et al., 1991). The RAMP family consists of three proteins named RAMP1-3. When CLR associates with RAMP1 (CLR•RAMP1), it forms a high affinity CGRP receptor. Alternatively, when CLR associates with RAMP2 or 3 (CLR•RAMP2 and CLR•RAMP3), they form high affinity receptor for ADM (McLatchie et al., 1998) (**Fig. 1.9**). RAMPs not only confer specificity of ligand but also are necessary to promote terminal glycosylation of CLR and to promote its transit from the ER/Golgi to the cell-surface (Fraser et al., 1999; Hilairet et al., 2001b; McLatchie et al., 1998).

Similarly to CLR, RAMPs have been shown to interact with CTR (Christopoulos et al., 1999; Muff et al., 1999), where association with RAMPs forms IAPP receptors. A specific receptor for ADM2 has not yet been clearly defined, however, ADM2 can activate CGRP and ADM receptors, as well as IAPP receptors. Although, the highest affinity receptor observed for ADM2 is CLR•RAMP3 (Roh et al., 2004). The redundancy of CTR, CLR and RAMPs combinations has shown a certain degree of cross reactivity between the different peptide of the family, which could also explain the similarity of biological functions of these peptides (Christopoulos et al., 1999). It certainly suggests that these receptors must be tightly regulated in order to present the correct cellular phenotype. Moreover, RAMPs also bind other members of the secretin GPCR family, such as the PTH1 and PTH2 receptors (parathyroid hormone receptor family) and the $VPAC_1$ and $VPAC_2$ receptors (VIP and PACAP receptor family) (Christopoulos et al., 2003).

CTRs are often coupled to $G\alpha_s$ and $G\alpha_q$ mediating accumulation of cAMP and activation of PLC, respectively (Chabre et al., 1992; Force et al., 1992). For example, CT induces inhibition of bone resorption by rat osteoclasts in a cAMP- and PKC-dependent manner (Su et al., 1992). Interestingly, CTR has been found to couple to $G\alpha_s$, $G\alpha_i$ and $G\alpha_q$ in LLC-PK1 (kidney tubule cell line) in a cell cycle

dependent manner (Chakraborty et al., 1991). Regarding CLR, it is generally accepted that receptors predominantly signal via $G\alpha_s$-mediated activation of AC to increase intracellular cAMP and activate PKA (Aiyar et al., 1999; Poyner et al., 1992; Van Valen et al., 1990; Withers et al., 1996). However, similarly to CTR, CLR has been found to also stimulate activation of PLC by coupling with $G\alpha_{q/11}$ (Drissi et al., 1998) and also to be sensitive to pertussis toxin (PTX, a toxin that specifically inhibits $G\alpha_i$) (Main et al., 1998; Mittra and Bourreau, 2006).

1.3.2 Receptor Component Protein

There is evidence of another protein that associates with CGRP and ADM receptors, the receptor component protein (RCP). RCP was first identified in 1996 by its ability to promote the CGRP-mediated responses in *Xenopus laevis* oocytes (Luebke et al., 1996). RCP was specific for CLR•RAMP1 and CLR•RAMP2, as it had no effect on the signalling of receptors for CT, IAPP, neuropeptide Y, vasoactive intestinal peptide and β-endorphin (Luebke et al., 1996; Prado et al., 2001). RCP was shown to be highly conserved in mice, rabbit and human (~82% of homology at the protein level) (Naghashpour et al., 1997; Rosenblatt et al., 2000). In parallel, the cloning and expression of CLR in HEK cells showed evidence of CGRP binding and CGRP-induced cAMP production (Aiyar et al., 1996), but not in COS-7 cells (fibroblast-like cell line) (Han et al., 1997), suggesting the presence of a component in HEK cells that makes CLR a functional receptor. However, when CLR was transfected with RAMPs only in COS-7 cells, it yields a functional receptor (Buhlmann et al., 1999). Later studies showed that in fact RCP was endogenously found in COS-7 cells (Evans et al., 2000). Additionally, the distribution of the expressed RCP in the central and peripheral nervous system in rat correlates with that of CGRP receptors (Ma et al., 2003). The use of an RCP antisense construct transfected in NIH 3T3 cells (mouse embryonic fibroblast cell line) has been shown to reduce ADM-induced activation, but did not affect ADM binding to the receptor or receptor expression at the cell-surface (Evans et al., 2000; Prado et al., 2001), suggesting that RCP does not act as a chaperone to target CLR to the cell-surface, but rather to facilitates efficient coupling of the receptor to the cellular signalling pathways. However, the real implication of RCP in a functional complex receptor remain to be determine as a study in yeast strongly suggest that RAMP itself is sufficient to confer functional activity of CGRP and ADM receptor (Miret et al., 2002).

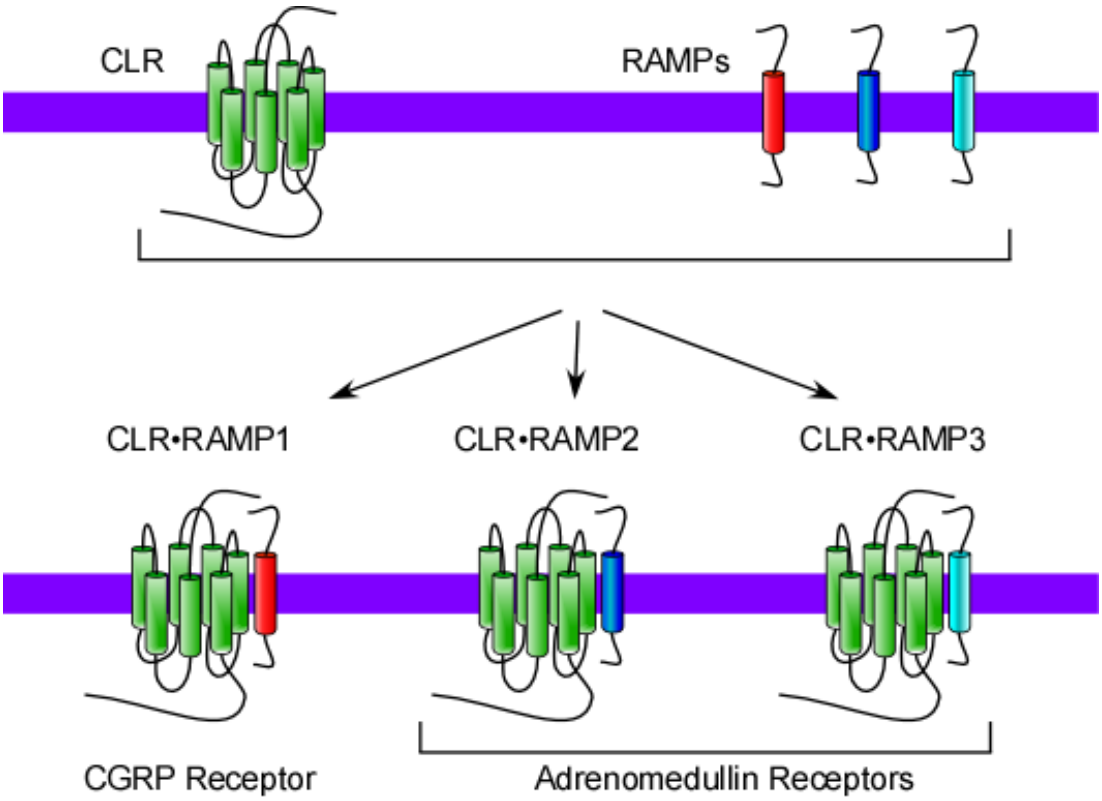

Figure 1.9 **CGRP and ADM receptors.** The GPCR CLR that belongs to the secretin family and bind both β-arrestins (class B), can bind with the different members of the RAMPs transmembrane proteins. When CLR associates with RAMP1 (CLR•RAMP1), it forms a high affinity CGRP receptor, however when CLR associates with RAMP2 or 3 (CLR•RAMP2 and CLR•RAMP3), high affinity ADM receptors are formed.

1.3.3 CGRP and ADM Receptor Regulation

Like many of GPCRs, CGRP and ADM receptors internalise after agonist-induced stimulation (Hilairet et al., 2001a; Kuwasako et al., 2000). Once internalised the fate of CLR•RAMP1 depends on the duration of the exposure to CGRP (Cottrell et al., 2007). Transient stimulation of CLR•RAMP1 with CGRP allows recycling of CLR•RAMP1, whereas continuous stimulation causes trafficking of CLR•RAMP1 to lysosomes where it is degraded (Cottrell et al., 2007). As mentioned previously, it has been shown that the recycling of CLR•RAMP1 is regulated by the metalloprotease, ECE-1 (Padilla et al., 2007). Another study looking at the post-endocytic sorting of CLR•RAMP3 has shown that the C-terminal tail of RAMP3, but not RAMP1 or 2, contains a PDZ type I domain. They showed that NSF binds to this PDZ domain and promotes recycling of CLR•RAMP3 back to the cell-surface (Bomberger et al., 2005). Unlike CLR•RAMP1 and CLR•RAMP3, very little is known about the trafficking and post-endocytic sorting of CLR•RAMP2 (Kuwasako et al., 2000).

1.4 G Protein-Coupled Receptor Signalling: Activation of Mitogenic Signalling Pathways

The mitogen-activated protein kinases (MAPK) are enzymes involved in the regulation of critical cell functions such as proliferation, gene expression, differentiation, mitosis, cell survival and apoptosis. The traditional notion that only RTKs are able to mediate activation of MAPK is no longer adequate. It is now well established that GPCRs can promote activation of mitogenic pathways in many different cell types (reviewed in (Luttrell, 2003; Rozengurt, 2007)). Therefore, the elucidation of the intracellular signalling pathways activated by GPCRs is of great importance, as these studies could establish new potential targets or strategies for the treatment of human disease. This study is focused on GPCR-induced pathways that activate ERK1 and 2. These have been separated in four main pathways: 1) cAMP/PKA, 2) PLC/PKC/Ca^{2+}, 3) ErbB1 transactivation and 4) β-arrestin-dependent endosomal signalling.

1.4.1 Overview of the MAPK Pathways

The first MAPK to be identified was ERK2, defined by its molecular weight around 42 kD. Three independent studies observed this protein, which they named p42, to be phosphorylated on tyrosine residues following stimulation with different mitogenic agents such as EGF, platelet-derived growth factor (PDGF) and 12-o-tetradecanoylphorbol-13-acetate (TPA) (Bishop et al., 1983; Gilmore and Martin, 1983; Nakamura et al., 1983). p42 itself was later found to be a serine/threonine protein kinase (Rossomando et al., 1989). The first MAPK to be cloned was p44 and named ERK1 for extracellular signal-regulated protein kinase 1, because of the wide variety of extracellular signals that activate it (Boulton et al., 1990). Shortly after, ERK2 and 3 were cloned (Boulton et al., 1991) suggesting the existence of an ERK family. ERK1 and 2 have ~85% sequence identity. Other MAPKs have since been identified such as the c-Jun N-terminal kinases (JNK) (Derijard et al., 1994; Hibi et al., 1993; Kyriakis et al., 1994) and p38 (also known as Cytokinin Specific Binding Protein (CSBP) or reactivating kinase (RK)) (Han et al., 1994; Lee et al., 1994; Rouse et al., 1994). They show some regulation similarities with ERK1 and 2 but are activated by different mitogenic agents.

Generally, MAPKs are activated by a cascade of phosphorylation and by other protein kinases. The cascade usually consists of at least three distinct kinases, from upstream to downstream: MAPK kinase kinase (MAP3K), MAPK kinase (MAP2K) and MAPK, which then promote cellular responses (**Fig. 1.10**) (reviewed in (Pearson et al., 2001; Seger and Krebs, 1995)). MAP3K are generally activated by small GTPases. For example, the ERK1-2 module generally consists of

activation of Ras a small GTPase, Raf kinase (MAP3K), MEK1-2 (MAP2K) and finally ERK1-2 (MAPK) (reviewed in (Robinson and Cobb, 1997)).

There are two important aspects of MAPK pathways. First is the existence of cross talk, where intermediates can regulate activation or inhibition of other signalling pathways (Corbit et al., 1999; Frost et al., 1997). Second is the formation of complexes between scaffolding proteins and the different members of signalling cascades that facilitate signal transduction (Choi et al., 1994; Yasuda et al., 1999). One such scaffolding protein is β-arrestin (Lefkowitz and Shenoy, 2005).

The functions of ERK1 and 2 are similar and difficult to distinguish from each other. A study from Yao et al. showed that genetic deletion of *erk2* gene resulted in embryonic lethality in mice. The mice exhibited disrupted mesoderm formation with an increase in apoptosis and defects in cellular differentiation. The same group also created an *erk2* null embryonic stem (ES) cell line for *in vitro* studies. Interestingly, although *erk2* null cells exhibit a reduction in total ERK activation upon stimulation, with an augmentation of ERK1 phosphorylation, there is no significant difference in ES cells proliferation. This result suggests that ERK1 is able to compensate the loss of ERK2. However, the mutant *erk2* embryos possessed no ERK1-2 phosphorylation, suggesting that ERK1 activity was not present to compensate the loss of ERK2 (Yao et al., 2003). In contrast, *erk1* deficient mice are viable, fertile, and of normal size. However, these mice show a deficit in the maturation of thymocytes leading to severe reduction of proliferation of T cells (Pages et al., 1999). These results show that ERK2 is able to compensate ERK1, even if the findings from the study of thymocytes were controversial (Nekrasova et al., 2005).

Analysis of zebrafish embryogenesis using expression knockdown techniques revealed that ERK1 and 2 can promote expression of both common and distinct sets of genes (Krens et al., 2008). ERK1 induced transcription of genes regulating dorsal-ventral patterning development and subsequent embryonic cell migration, whereas ERK2 induced transcription of genes involved in cell migration, mesendoderm differentiation and patterning (Krens et al., 2008). Together, these observations suggest that ERK1 and ERK2 are not entirely functionally redundant and have similar yet distinct functions. ERK2 seems to play a more critical role than ERK1, as loss of the latter can be compensated by ERK2, whereas the opposite is not always true. As the effects of ERK1 and 2 are difficult to distinguish, this pathway is usually referred to as the ERK1-2 pathway.

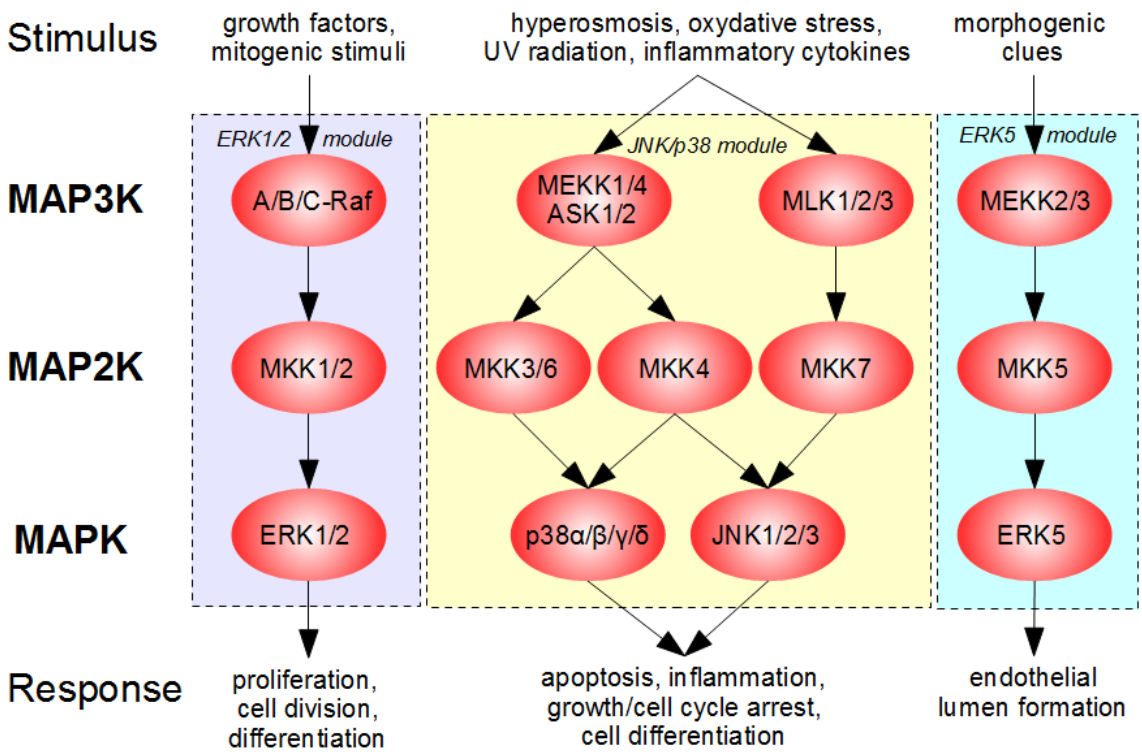

Figure 1.10 **Simplified Overview of Mammalian MAPK Cascades.** Schematic representation of the organisation of MAPK cascades. Extracellular stimulus can promote activation of MAP3K that phosphorylate and activate MAP2K, which then phosphorylate and activate MAPK and lead to cellular responses. Three main MAPK modules are listed with their different cellular outcomes. Image was taken from Wikipedia website file: MAPK-pathway-mammalian.png http://en.wikipedia.org/wiki/Mitogen-activated_protein_kinase.

1.4.2 The cAMP/PKA Pathway

GPCRs coupled to $G\alpha_s$ stimulate the activation of AC to promote the increase of intracellular cAMP levels (reviewed in (Gilman, 1984a; Gilman, 1984b)) that subsequently activates PKA (Brostrom et al., 1970; Gill and Garren, 1971; Tao et al., 1970). The PKA pathway regulates several MAPK pathways, including activation of p38 (Zheng et al., 2000) or inhibition of ERK5 (Pearson et al., 2006). GPCRs that activate $G\alpha_s$ proteins have also been shown to regulate the ERK1-2 module (**Fig. 1.11**).

1.4.2.1 Activation of the ERK1-2 Module

The first evidence that the cAMP/PKA pathway can stimulate ERK1-2 came from a study where a constitutively active $G\alpha_s$ subunit mutant was shown to promote ERK1 phosphorylation in COS-7 cells (Faure et al., 1994). This observation was later confirmed by another study examining the β_2-AR in wild type (WT) or mutant S49 lymphoma cell lines lacking $G\alpha_s$ or PKA. When the β_2-AR was expressed in WT cells, isoproterenol stimulation induced ERK1-2 activation, whereas when β_2-AR was expressed in the mutant cell lines, it was unable to promote ERK1-2 activation following stimulation (Wan and Huang, 1998). Further analyses have shown that the small GTPase, Rap-1 and the protein kinase, B-Raf (MAP3K) were also involved in this pathway (Vossler et al., 1997; Wan and Huang, 1998). Rap-1 activation is mediated by PKA and promotes association with B-Raf, which then triggers B-Raf activation. Additional studies have shown that in fact PKA promotes phosphorylation of Src (Obara et al., 2004; Schmitt and Stork, 2002) which recruits a Rap-1 guanine nucleotide exchange factor (GEF), Crk SH3 domain-binding guanine nucleotide-releasing factor (C3G) (Schmitt and Stork, 2000; Schmitt and Stork, 2002). This complex Src-C3G then activates Rap-1 by replacing its GDP by GTP and promoting activation of the ERK1-2 module. In contrast, studies have also shown that the activation of Rap-1 was mediated in a cAMP-dependent but PKA-independent manner (Laroche-Joubert et al., 2002; Weissman et al., 2004). This mechanism involves EPAC (exchange protein directly activated by cAMP), another Rap-1 GEF that is directly activated by cAMP. The activation of EPAC then promotes activation of Rap-1 (Laroche-Joubert et al., 2002). However, the use of an EPAC-specific analogue that activates EPAC but not PKA, has shown that Rap-1 activation failed to promote ERK1-2 phosphorylation (Enserink et al., 2002), suggesting that Rap-1 and ERK1-2 are independently regulated. In fact, it was subsequently shown that it was the subcellular localisation of EPAC that was responsible for the lack of activation of ERK1-2 (Wang et al., 2006). Indeed, this study showed that EPAC was normally localised to the periphery of the nucleus, which lead to activation of Rap-1 but not

ERK1-2. In contrast, an EPAC mutant that contains a CAAX membrane-targeting motif was able to activate Rap-1 and ERK1-2 (Wang et al., 2006).

1.4.2.2 Inhibition of the ERK1-2 Module

Activation of $G\alpha_s$-mediated cAMP/PKA pathway can also lead to inhibition of ERK1-2 module (Cook and McCormick, 1993; Graves et al., 1993; Wu et al., 1993). Activation of cAMP/PKA pathway lead to the inhibition of PDGF- and EGF-mediated ERK1/2 activation, through inhibition of Raf-1 (also known as C-Raf, MAP3K), another member of the Raf family (Cook and McCormick, 1993; Wu et al., 1993). Raf-1 is phosphorylated *in vitro* and *in vivo* in a cAMP/PKA dependent manner (Hafner et al., 1994; Mischak et al., 1996; Wu et al., 1993). The PKA-mediated phosphorylation of Raf-1 first leads to a reduction in its association with Ras (a small GTPase that activates Raf-1) and therefore attenuates the activation of Raf-1 by Ras (Dhillon et al., 2002). Additionally, $G\alpha_s$-mediated inhibition of ERK1-2 has also been shown to involve Rap-1 (Schmitt and Stork, 2001). Indeed, activation of cAMP/PKA-mediated Rap-1 leads to the sequestration of Raf-1 and prevents its activation by Ras.

1.4.3 The PLC/PKC/Ca^{2+} Pathway

Similarly to $G\alpha_s$, activation of $G\alpha_{q/11}$ leads to the activation of ERK1-2, JNK and p38 MAPK modules. $G\alpha_{q/11}$ activates the activation of PLCβ isoforms (Smrcka et al., 1991; Taylor et al., 1991; Taylor et al., 1990), which in turn catalyses the hydrolysis of phosphatidylinositol 4,5-biphosphate into two second messengers: IP_3 and DAG. IP_3 induces mobilisation of Ca^{2+} from endoplasmic reticulum (ER) (Putney, 1986). DAG and intracellular Ca^{2+} then act in synergy or individually to promote ERK1-2 activation via PKC-dependent or –independent mechanisms. There are many members of the PKC family and they are divided into three main groups: the conventional PKC isoforms (cPKC) that are activated by both Ca^{2+} and DAG; novel PKC isoforms (nPKC) that are activated only by DAG; and the atypical PKC isoforms (aPKC) that are activated by neither Ca^{2+} or DAG, but rather by other second messengers such as small GTPases (reviewed in (Webb et al., 2000)). Interestingly, the $\beta\gamma$ subunits activated by GPCRs has been found to also promote PLCβ isoforms activation (Camps et al., 1992; Della Rocca et al., 1997; Katz et al., 1992) leading to the ERK1-2 activation.

1.4.3.1 PKC-Dependent Pathways

Early experimentation showed that members of the three groups of PKCs where able to promote TPA-mediated ERK1-2 activation (Kolch et al., 1993; Schonwasser et al., 1998; Ueda et al., 1996). The cPKC- and nPKC-mediated mechanisms require the activation of Raf-1, notably PKCα that has been found to directly phosphorylate Raf-1 (Kolch et al., 1993) (**Fig. 1.12**). For example, this mechanism has been observed for the AT_1R (Arai and Escobedo, 1996), the B_2 receptor (bradykinin receptor family) (Adomeit et al., 1999) and the 5-HT_2 receptor (Hershenson et al., 1995). Another mechanism has been described for PKC-mediated ERK1-2 activation. In unstimulated cells, Raf kinase inhibitor protein (RKIP) sequesters Raf-1 and prevents its activation. However, when stimulated with TPA or EGF, PKC phosphorylates RIKP which leads to the dissociation of the RKIP/Raf-1 complex and Raf-1 is thereby free to be activated and promote activation of MEK and ERK1-2 (Corbit et al., 2003). Additionally, RKIP has been found to also bind and inhibit GRK-2 when it is released from Raf-1, thus preventing desensitisation and sustain ERK1-2 activation of α_{1B}-AR (adrenoceptor), PTH receptor and β_2-AR (Lorenz et al., 2003). However, more experimental evidence is needed to define this mechanism of GPCR regulation. It is also interesting to note that, the B_2 receptor, the M_1 and M_3 receptors (acetylcholine receptors (muscarinic) family) and the β_2-ARs that can activate both $G\alpha_i$ and $G\alpha_{q/11}$, have been shown to activate ERK1-2 via a cooperation of $G\alpha_{q/11}$-mediated PKC and of $G\alpha_i$-induced Ras activation (Blaukat et al., 2000). Similar observations were seen for the α_{1B}-AR and α_{2A}-AR (Della Rocca et al., 1997).

1.4.3.2 PKC-Independent Pathways

An alternative $G\alpha_{q/11}$-mediated activation of ERK1-2 involves the protein kinase proline-rich tyrosine kinase 2 (PYK2), which belongs to the focal adhesion kinase family (Lev et al., 1995) (**Fig. 1.12**). It has been shown that bradykinin, which promotes $G\alpha_{q/11}$-mediated increase of intracellular Ca^{2+}, leads to PYK2 phosphorylation independently of PKC (Lev et al., 1995). In turn, phosphorylated PYK2 induces ERK1-2 activation. Furthermore, bradykinin-induced PYK2 phosphorylation leads to its association with and activation of Src to promote ERK1-2 activation in a Ras-dependent manner (Dikic et al., 1996). Another study, observed that α_{1B}-AR dependent activation of $G\alpha_{q/11}$, promoted activation of Ca^{2+}-calmodulin, which directly and indirectly regulated PYK2 phosphorylation and thus ERK1-2 activation (Della Rocca et al., 1997). A more recent study has revealed that activation of WFB cells (rat fibroblast cell line) with vasopressin, endothelin or PDGF induced Ca^{2+}-calmodulin to directly bind to PYK2 and leads to its activation (Kohno et al., 2008). Additionally, $G\alpha_{q/11}$-mediated activation of M_1 receptor promotes ERK1-2 activation in a Rap-1/B-Raf-dependent manner (Guo et al.,

2001). Similarly to the $G\alpha_s$-mediated activation of Rap-1, this mechanism requires the activation of a Rap-1 GEF, namely Ca^{2+}- and DAG-regulated GEF I (CalDAG-GEFI) that in turn activates Rap-1 independently of PKC (Guo et al., 2001).

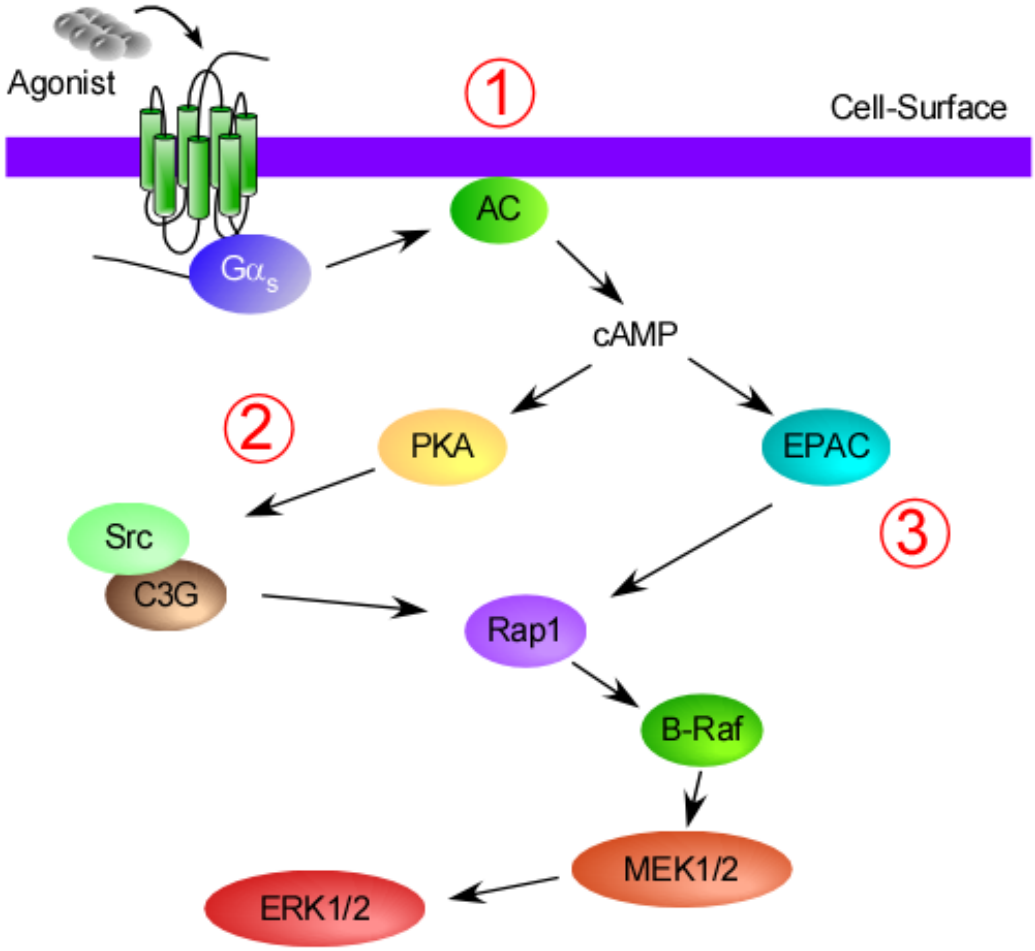

Figure 1.11 **The cAMP/PKA-mediated ERK1-2 activation.** (1) Stimulation of $G\alpha_s$ leads to AC activation and production of cAMP. (2) cAMP promotes activation of PKA that induces phosphorylation by Src of C3G, a Rap-1 GEF and lead to activation of Rap-1 and in turn to ERK1-2 pathway via B-Raf. (3) Alternatively, cAMP can directly activate another Rap-1 GEF, EPAC that also induce Rap-1 activation and ERK1-2 independently of PKA.

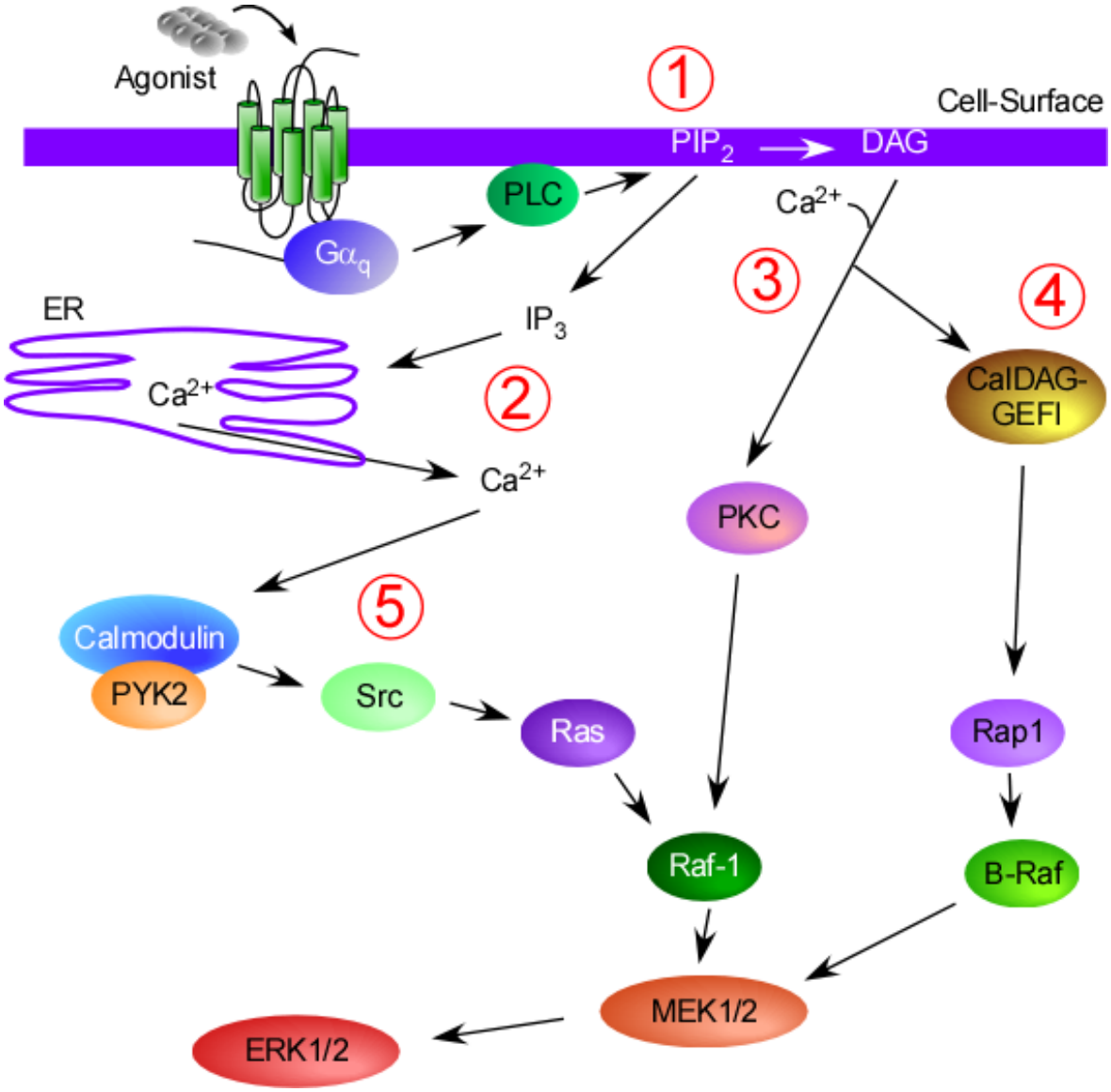

Figure 1.12 **The PLC/PKC/Ca^{2+}-mediated ERK1-2 activation.** (1) Stimulation of $G\alpha_q$ leads to activation of PLC that promotes hydrolyse of PIP_2 and formation of IP_3 and DAG. (2) IP_3 then induces release of Ca^{2+} from intracellular storage (e.g. endoplasmic reticulum, ER). (3) Ca^{2+} and DAG promotes activation of PKC that induces phosphorylation of Raf-1 and in turn lead to ERK1-2 activation. (4) Alternatively, Ca^{2+} and DAG can directly activate the Rap1 GEF CalDAG-GEFI to promotes activation of ERK1-2, independently of PKC. (5) Finaly, Ca^{2+} alone can induce the activation of the complex calmodulin/PYK2 that phosphorylates Src and lead to ERK1-2 activation through Ras/Raf-1, independently of PKC.

1.4.4 Transactivation of ErbB1

As previously mentioned, activation of certain GPCRs can lead to transactivation of ErbB1 (Daub et al., 1996). Other members of the RTK family are also transactivated by GPCRs including the insulin growth factor receptor (Rao et al., 1995) and the PDGF receptor (Linseman et al., 1995). However, ErbB1 transactivation remains the best characterised, even if the mechanisms are not fully understood. ErbB1 transactivation occurs in many different cell types, is mediated by many different GPCRs and occurs through many different mechanisms.

Daub and colleagues first identified ErbB1 transactivation in Rat-1 cells (fibroblasts cell line) using endothelin-1, lysophosphatic acid (LPA) and thrombin that involve $G\alpha_{q/11}$- and $G\alpha_i$-mediated responses (Daub et al., 1996) and in HaCaT (human keratinocytes cell line), primary mouse astrocytes and COS-7 cells, using LPA (Daub et al., 1997). In these studies, they described a mechanism that required Src in order to induce ERK1-2 activation but downstream of ErbB1 activation (**Fig. 1.13**). Whereas ang II-induced ErbB1 transactivation in primary rat thoracic aorta SMC (TA-SMC) showed that Src phosphorylation is required to activate ErbB1 (Eguchi et al., 1998). Other studies have also identified that increases in intracellular Ca^{2+}, most likely through PLC activation, were required to induce ErbB1 transactivation, leading to ERK1-2 activation via Ras activation, such as the bradykinin receptor (Zwick et al., 1997) and AT_1R (Eguchi et al., 1998; Murasawa et al., 1998). Moreover, the studies of AT_1R showed that ErbB1 transactivation was mediated through activation of the calmodulin/PYK2 complex (Eguchi et al., 1998; Murasawa et al., 1998).

All these pathways appear to converge on GPCR-mediated release of soluble EGF-like ligand, which then activates ErbB1 receptor (reviewed in (Ohtsu et al., 2006)) (**Fig. 1.13**). EGF-like ligands, such as the heparin binding-EGF (Prenzel et al., 1999), transforming growth factor-α (Pai et al., 2002) and/or amphiregulin (Gschwind et al., 2003), are released by proteolytic cleavage by member of the ADAMs metalloprotease family (Gschwind et al., 2003; Prenzel et al., 1999; Schafer et al., 2004a; Schafer et al., 2004b). In this mechanism, Src activation is required upstream of the metalloprotease to induce ErbB1 activation (Buteau et al., 2003), downstream of ErbB1 to mediate ERK1-2 activation (McCole et al., 2002) or for both (Pierce et al., 2001).

It should be noted that these mechanisms are mediated by GPCRs coupled to both $G\alpha_{q/11}$ and $G\alpha_i$ proteins. Studies have shown that forskolin-induced increases cAMP production promote transactivation of ErbB1 and subsequent ERK1-2 activation (Bertelsen et al., 2004; Piiper et al., 2002; Piiper et al., 2003). This mechanism involves activation of PKA that promotes ErbB1 phosphorylation directly and/or indirectly (Bertelsen et al., 2004; Piiper et al., 2003). To date, only a

few $G\alpha_s$-mediated ErbB1 transactivation events leading to ERK1-2 activation have been described. One such event is activation of the EP_2 receptor (prostanoid receptor family, known as prostaglandin E2 receptor), where cAMP/PKA/Src activation mediates ErbB1 transactivation (Sales et al., 2004). The GnRH receptor (gonadotrophin-releasing hormone receptor family, also known as luteinizing hormone (LH) receptor) (Carbajal et al., 2011; Evaul and Hammes, 2008; Panigone et al., 2008) and the MC_2 receptor (melanocortin receptor, also known as adrenocorticotropic hormone (ACTH) receptor) (Carbajal et al., 2011) also induce ErbB1 transactivation in a cAMP/PKA-dependent manner in cells issued from the three major steroidogenic tissues: the testes, the ovary, and the adrenal gland. However, LH-, but not ACTH-induced transactivation has been shown to be both metalloprotease-dependent (Carbajal et al., 2011; Panigone et al., 2008) and metalloprotease-independent (Carbajal et al., 2011; Evaul and Hammes, 2008), depending on tissue.

1.4.5 The β-Arrestin-Dependent Pathway

As previously mentioned, activation of a specific MAPK module feature two important aspects, first is the existence of cross talk between these pathways (Corbit et al., 1999; Frost et al., 1997) and second is the formation of complexes between scaffold proteins and the different member of a MAPK module to facilitate signal transduction (Choi et al., 1994; Yasuda et al., 1999). One of this scaffold protein identified is β-arrestin (Lefkowitz and Shenoy, 2005).

The role of β-arrestins as promoter of GPCR desensitisation and internalisation has already been described. However, β-arrestins also facilitate mitogenic signalling due to their ability to act as a scaffold for signalling proteins (reviewed in (Luttrell and Gesty-Palmer, 2010)). This role was first described for the β_2-AR, where β_2-AR associated with β-arrestin1 binds to activated Src and promotes a G protein-independent ERK1-2 activation (Luttrell et al., 1999) (**Fig. 1.14**). Activation of PAR2 (DeFea et al., 2000) and AT_1R (Luttrell et al., 2001) induces association of the receptors with β-arrestins and internalisation of the receptor/β-arrestins complex, where Raf-1, MEK1 and ERK1-2 were found in this complex. The formation of this receptor/β-arrestins complex was shown to induce ERK1-2 activation. Similarly, β-arrestins have been shown to bind members of the JNK MAPK module, such as JNK3 and apoptosis signal–regulating kinase 1 (activator of JNK), when AT_1R was activated (McDonald et al., 2000). Additionally, this β-arrestin-dependent signalling takes place not only at the plasma membrane, but also in the endosomal system, where certain GPCRs can be sequestered for long periods. Stimulation of AT_1R promotes internalisation of the receptor together with β-arrestin2 leading to a subcellular distribution of ERK1-2 activation in endosome

(Luttrell et al., 2001). This β-arrestin-dependent pathway, also referred as endosomal signalling, has been described to have slower and more sustain kinetics, compared to the cell-surface G protein-dependent ERK activation (Ahn et al., 2004). Moreover, it has been shown that β-arrestin-activation of ERK module does not induce translocation of phosphorylated ERK1-2 into the nucleus, which fails to elicit a transcriptional response or stimulate cell proliferation (DeFea et al., 2000; Tohgo et al., 2002). These results suggest that endosomal signalling is involved in the cytosolic responses that require slower but persistent activation of ERK1-2. Additionally, when a NK_1R fused to β-arrestin1 was expressed in HEK cells, the receptor was constitutively desensitised, uncoupled from G proteins and sequestered in endosomes. This mutant receptor did not respond to neurokinin A stimulation, however, it promoted a robust, constitutive activation of ERK1-2. Immunoprecipitation of the receptor revealed presence of Raf-1, MEK1 and ERK1-2. These results suggested that stable association between β-arrestin and the receptor formed a stable “signalosome” able to promote MAPK activation (Jafri et al., 2006).

Similarly, NK_1R, which internalises with β-arrestin in endosomes following SP stimulation, has been shown to sustain ERK1-2 activation when the complex NK_1R/β-arrestin is sequestered in endosomes (Cottrell et al., 2009). Indeed, it has been previously shown that the dissociation of this complex was promoted by the degradation of SP in endosomes by the metalloprotease ECE-1 (Roosterman et al., 2007). Inhibition of ECE-1 leads to the retention of the complex NK_1R/β-arrestin. Altogether, all these results show β-arrestins acting as a scaffold protein able to bind members from ERK1-2 modules and promoting their activation. This G protein-independent signalling takes place from the cell-surface to endosomes and lead to more sustain but less robust ERK1-2 activation compare to G protein-mediated ERK1-2 activation.

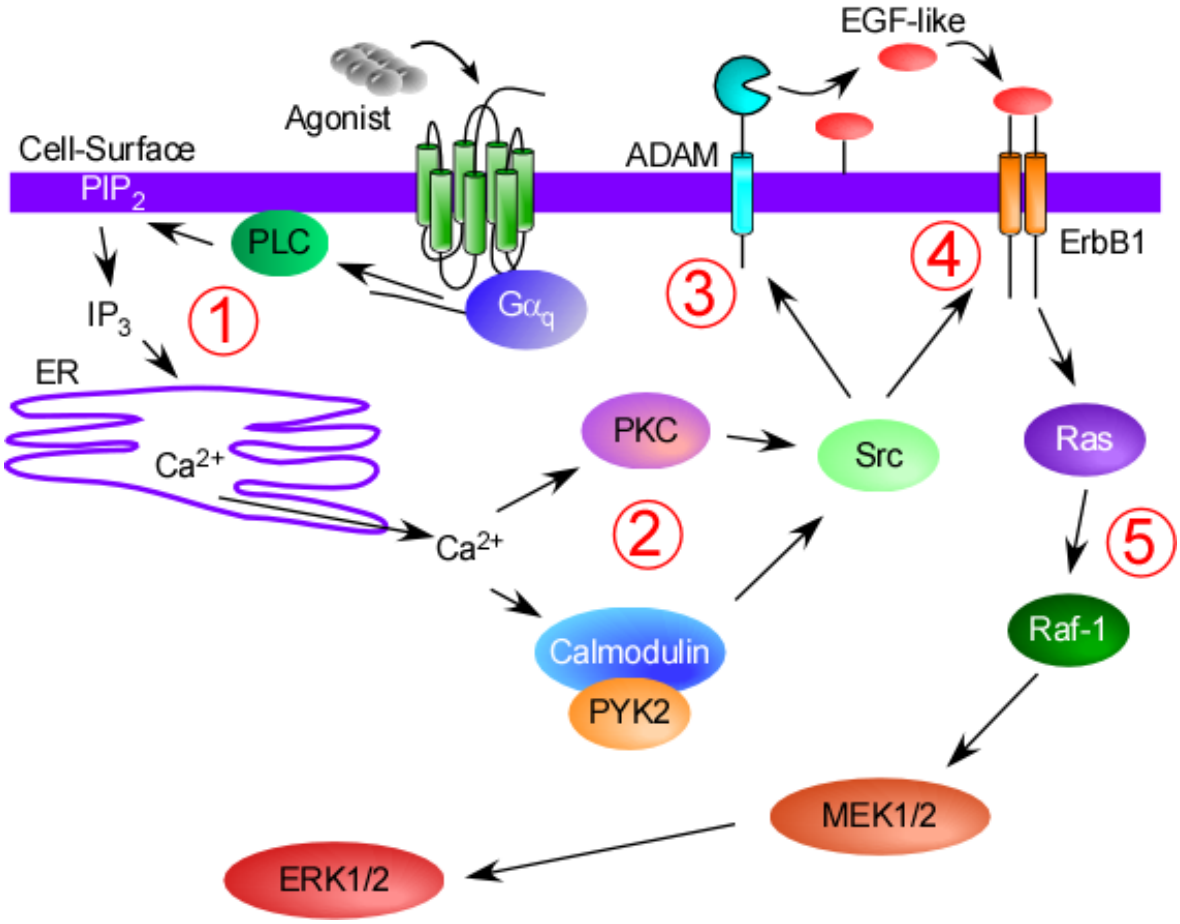

Figure 1.13 **ErbB1 transactivation-mediated ERK1-2 activation.** GPCRs can promote RTK transactivation that leads to ERK1-2 activation. Many mechanisms have been described depending on the cell type and the GPCR type. (1) The most characterised mechanism involve increase of intracellular Ca^{2+} that lead to activation of Src (2) through PKC or calmodulin/PYK2 activation. (3) Src has been shown to either induce activation of metalloproteases called ADAM that promote release of extracellular EGF-like ligands leading to the activation of ErbB1. (4) Alternatively Src can directly activate ErbB1. (5) Stimulated ErbB1 receptors lead to ERK1-2 activation via the activation of Ras/Raf-1 pathway.

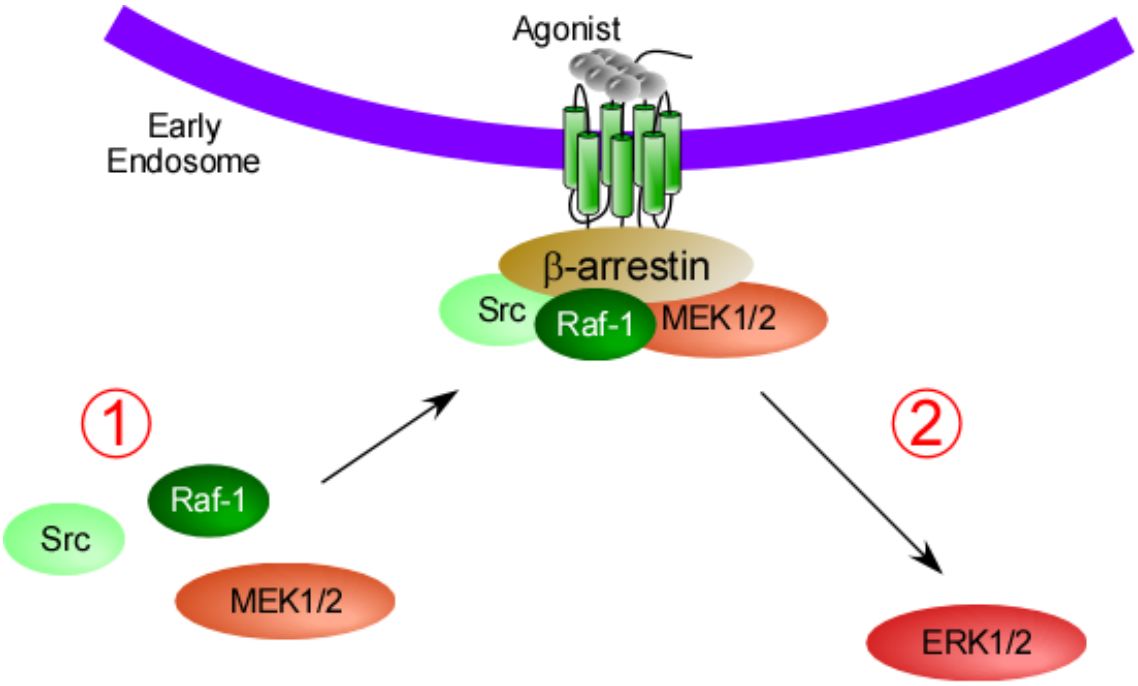

Figure 1.14 **β-arrestin-dependent endosomal signalling.** The sequestered agonist/GPCR/ β-arrestin complex in endosomes can mediate a second wave of ERK signalling distinct from that which is induced at the cell-surface. (1) Specifically, β-arrestins acts as molecular scaffolds to recruit many effector proteins such as the ERK1-2 module: MEK1-2, Raf-1 and Src. (2) This complex leads to the activation of ERK1-2. The signal is terminated by dissociation of the agonist/GPCR/ β-arrestin complex.

1.5 Aims of this Project

This report is divided in two different parts. The first part describes the mechanisms and function of CGRP-induced ERK activation. The second part describes mechanisms of the post-endocytic sorting of the GPCR for ADM, namely, CLR•RAMP2.

It is well documented that CGRP can promote activation of ERK. However, the biological functions of CGRP-induced ERK activation remain poorly defined. CGRP-induced ERK activation has recently been linked with the induction of iNOS in trigeminal ganglion glial cells (Vause and Durham, 2009). The induction of iNOS produces large amounts of NO (Nathan and Xie, 1994) and iNOS is upregulated in different pathologies including migraine (Olesen and Jansen-Olesen, 2000), atherosclerosis (Ginnan et al., 2008) and sepsis (Hauser et al., 2005). CGRP is similarly upregulated in migraine and sepsis (Goadsby et al., 1990; Zhou et al., 2001). In the cardiovascular system, CGRP together with interleukin-1β, has been shown to promote upregulation of iNOS and NO release in SMC (Schini-Kerth et al., 1994). As both CGRP and NO are important signalling molecules in the cardiovascular system, I aimed to determine the exact mechanisms through which CGRP activates ERK1-2 as a first step towards deciphering the mechanisms in SMC and whether CGRP upregulates iNOS via an ERK-dependent pathway. The first part of this project using HEK cells as a model is:

- To determine whether CGRP induces transactivation of ErbB1.
- To elucidate the role of endosomal signalling and β-arrestin in CGRP-induced ERK activation.
- To investigate whether CGRP-induced ERK activation is mediated by cAMP/PKA pathway or PLC/PKC/Ca^{2+} pathway.
- Finally to characterise primary rat thoracic artery SMC as a model to study the involvement of ERK activation in CGRP-induced iNOS expression.

It has been shown that both CLR•RAMP1 and CLR•RAMP3 can recycle after transient stimulation (Bomberger et al., 2005; Cottrell et al., 2007). Moreover, it has been shown that ECE-1 regulates the recycling of CLR•RAMP1 by cleaving CGRP (Padilla et al., 2007). However, nothing is known about the regulation of CLR•RAMP2. As ADM is also cleaved by ECE-1, only at endosomal pH (unpublished data, G. S. Cottrell), then it was hypothesised that ECE-1 would similarly regulate CLR•RAMP2. It is important to study such mechanisms, as a better understanding of how receptors are trafficked may lead to the development

of new therapies to treat disease. I first used a HEK cell model in the aim to undertake the key findings of this study to a more physiological model such as HMEC-1. The second part of this project is:

- To determine whether ADM induces the recycling or the degradation of CLR•RAMP2.

- To investigate the molecular mechanisms involved in the post-endocytic sorting of CLR•RAMP2, such as ubiquitination.

- To establish the role of ubiquitination in the ADM-induced degradation of CLR•RAMP2.

- Finally, to characterise a more suitable model such as HMEC-1 cells, to study CLR•RAMP2 post-endocytic sorting.

Chapter 2. Materials and Methods

2.1 Materials

All reagents, chemicals, peptides and inhibitors used in this study are listed in **Appendix I**. The compositions of buffers and growths media are details in **Appendix II**.

2.1.1 Cell Lines

Cell type	Cell line	Source	Medium
Human Embryonic Kidney (**HEK**) 293 cells	Flp-In™293 (HEK-FLP)	Invitrogen (R750-07)	AdDMEM*, HIFBS* (2% (v:v)), L-glu* (2 mM), zeocin (100 µg/mL)
	HEK-CLR•RAMP1	G.S. Cottrell	AdDMEM, HIFBS (2% (v:v)), L-glu (2 mM), hygromycin B (200 µg/mL)
	HEK-CLR•RAMP2	G.S. Cottrell	
Human dermal micro-vascular endothelial cells-1 (**HMEC-1**)	HMEC-1	Centre for Disease Control and Prevention (USA)	MCBD, HIFBS (10% (v:v)), L-glu. (2 mM), EGF* (10 ng/mL), HCORT* (1 µg/mL)
Primary rat thoracic aorta smooth muscle cells (**TA-SMC**)	TA-SMC	See **2.2.2**	DMEM, HIFBS (10% (v:v)), NEAA* (1% (v:v)), P/S* (1% (v:v)), fungizone (0.1% (v:v))

Table 2.1 **List of Cell Lines.** *AdDMEM = Advanced DMEM, HIFBS = heat inhibited foetal bovine serum, L-glu. = L-glutamine, EGF = epidermal growth factor, HCORT = hydrocortisone, NEAA = non-essential amino acids, P/S = penicillin/streptomycin. The medium DMEM and MCDB are described in **Appendix I**.

2.1.2 Animals

Male Wistar rats (80–100 g) were killed by cervical dislocation following institutional guidelines for animal welfare and schedule 1 of the Animals (scientific procedures) Act 1986.

2.1.3 Antibodies

Antibodies	Host	Dilution		Supplier	Cat. number
		WB*	ICC*		
α-smooth muscle actin	Mouse	-	1/250	Sigma-Aldrich	A5228
β-actin	Mouse	1/100,000	-	Sigma-Aldrich	A1978
CLR (RK11)	Rabbit	1/2,000	1/2,000	(Cottrell et al., 2005)	N/A
EEA1	Mouse	-	1/100	BD Bioscience	610457
Phospho ERK1/2	Mouse	1/1,000	-	Santa Cruz	sc-7383
ERK2	Rabbit	1/10,000	-	Santa Cruz	sc-154
HA	Rabbit	1/5,000	1/500	Sigma-Aldrich	H6908
iNOS	Rabbit	1/2,500	1/100	Cell signalling	2977S
LAMP1	Mouse	-	1/1,000	Santa Cruz	sc-20011
c-Myc	Rabbit	1/10,000	1/500	Sigma-Aldrich	C3956
Transferrin receptor	Mouse	1/5,000	-	Invitrogen	13-6800
Ubiquitin	Mouse	1/5,000	-	Santa Cruz	sc-8017

Table 2.2 **List of Primary Antibodies.** *ICC = immunocytochemistry; *WB = Western blot. All stock of antibodies, if not supplied in glycerol, were diluted in glycerol (50% (v:v)) and stored at -20°C. The factor of dilution is not included in the table and therefore was added during experimentation.

Antibodies	Host	Dilution		Supplier	Cat. number
		WB	ICC		
Mouse (Peroxidase)	Goat	1/10,000	-	Stratech Scientific Limited	115-035-146-JIR
Rabbit (Peroxidase)	Goat	1/10,000	-	Stratech Scientific Limited	111-035-144-JIR
Mouse (FITC)	Donkey	-	1/500	Stratech Scientific Limited	715-095-150-JIR
Mouse (Cy5)	Donkey	-	1/500	Stratech Scientific Limited	715-175-150-JIR
Rabbit (RRX)	Donkey	-	1/500	Stratech Scientific Limited	711-295-152-JIR
Rabbit (DyLight 649)	Donkey	-	1/500	Stratech Scientific Limited	711-495-152-JIR

Table 2.3 **List of Secondary Antibodies.** All stock of antibodies, if not supplied in glycerol, were diluted in glycerol (50% (v:v)) and stored at -20°C. The factor of dilution is not included in the table and therefore was added during experimentation.

2.1.4 Plasmid DNA

Plasmid	Resistance	Source/Reference
pOG44	-	Invitrogen (R750-07)
pcDNA5/FRT	Hygromycin B	Invitrogen (R750-07)
pcDNA5/FRT-CLR-HA	Hygromycin B	G.S. Cottrell, unpublished
pcDNA3.1/Blasticidin-RAMP1-Myc	Blasticidin	(Cottrell et al., 2005)
pcDNA3.1/Blasticidin-RAMP2-Myc	Blasticidin	G.S. Cottrell, unpublished
pcDNA5/FRT-CLR•RAMP1	Hygromycin B	(Cottrell et al., 2007)
pcDNA5/FRT-CLR•RAMP2	Hygromycin B	G.S. Cottrell, unpublished
pcDNA5/FRT-CLRΔ9KR•RAMP2	Hygromycin B	(see **Chap. 5.5**)
pcDNA3-β-arrestin1-FLAG WT	-	(Luttrell et al., 1999)
pcDNA3-β-arrestin1-FLAG$^{P91G\ P121E}$	-	(Luttrell et al., 1999)

Table 2.4 **List of Plasmid DNA**. All plasmid DNA were stored at -20°C. The CLR, RAMP1 and RAMP2 vectors were a gift from G. S. Cottrell. The β-arrestin1 vectors were a gift from R. J. Lefkowitz.

2.1.5 Primers

Gene	Primers		Product size (base pair)
CLR	Forward	5'-TGCTGGATCAGCTCAGACAC-3'	442 bp
	Reverse	5'-CATCGCTGATTGTTGACACC-3'	
RAMP1	Forward	5'-CATCCAGGAGCTGTGTCTCA-3'	277 bp
	Reverse	5'-AATGGGGAGCACAATGAAAG-3'	
RAMP2	Forward	5'-GTTACTGCTGCTGTTGCTGC-3'	446 bp
	Reverse	5'-CATCGCCGTCTTTACTCCTC-3'	
RAMP3	Forward	5'-TTGCAATGAGACAGGAATGC-3'	313 bp
	Reverse	5'-CACGGTCAACAAGACTGGAA-3'	

Table 2.5 **List of Primers.** All primers were purchased from Sigma-Aldrich and stored at -20°C.

2.1.6 Bacteria Strain

MACH1 cells are derivatives of *Escherichia coli* (*E. coli*). Genotype: F-ϕ80(*lac*Z)ΔM15 Δ*lac*X74 *hsd*R($r_{K-}m_{K+}$) Δ*rec*A1398 *end*A1 *ton*A. MACH1 cells were used for routine transformation and cloning (see **2.4** and **2.5**). Cells purchased from Invitrogen (C8620-03) and stored at -80°C.

2.2 Mammalian Cell Culture

2.2.1 Cell Culture

All cells were routinely grown at 37°C in a humidified 95% (v:v) air/5% (v:v) CO_2 atmosphere in 75 cm² plastic tissue culture flask (BD Biosciences). The growth medium of each cell line is described in **Table 2.1**.

2.2.2 Preparation of Primary Smooth Muscle Cells

Thoracic aorta smooth muscle cells were obtained using an explant method. Briefly, the thoracic aorta was excised and immediately placed in ice cold phosphate-buffered saline (PBS) supplemented with 1% (v:v) P/S and 0.1% (v:v) fungizone. The aorta was cleaned of surrounding fat tissue and nerves, transversally cut open and chopped into small pieces (~1 mm). Finally, the pieces were washed 3 times with sterile PBS and cultured as described in **Table 2.1** and **2.2.1**.

2.2.3 Subculturing of Mammalian Cells

Cells were subcultured upon reaching 80-90% confluency. Culture medium was aspirated and cells were then washed with PBS (without Ca^{2+} and Mg^{2+}) (PBS-CM). To detach adherent cells from the culture plate, cells were incubated in trypsin/EDTA (2-3 min, 37°C). An equal volume of fresh culture medium was added to neutralise the trypsin, before cells were transferred to a sterile centrifuge tube and collected by centrifugation (1,000 *g*, 5 min, RT). The cell pellet was resuspended in culture medium (10 mL) and cells were subcultured in a ratio of 1:5 (HEK and HMEC cells) or 1:3 (TA-SMC). Culture medium was replaced every 2-3 days.

2.2.4 Preparation of Cells for Storage in Liquid Nitrogen

Cell pellets were resuspended in HIFBS containing 10% (v:v) DMSO and aliquots (1 mL) were placed into cryovials (Fisherbrand). Aliquots were placed in freezing container (Mr. Frosty, Nalgene®, Sigma-Aldrich) incubated (overnight, -80°C) and then transferred to liquid nitrogen for long-storage.

2.2.5 Recovery of Mammalian Cells from Liquid Nitrogen Storage

Cells were thawed in a water bath (2-3 min, 37°C) and combined with fresh culture medium (9 mL) in a centrifuge tube. Cells were collected by centrifugation (1,000 *g*, 5 min), the pellet resuspended in fresh medium (10 mL) and then transferred to a culture flask. Cells were then cultured as described in **2.2.1**.

2.2.6 Transfection of Mammalian Cells

Transient Transfection:

HEK-FLP cells were plated at $5x10^6$ cells/well in 6-well plates or 35 mm dishes (BD Biosciences) in antibiotic-free medium 24 h prior to transfection. The following day plasmid DNA (3 µg/well) and lipofectamine (8 µL/well) were incubated in separate tubes with Opti-MEM® (250 µL, 5 min, RT). The DNA and lipofectamine mixes were then combined and incubated further (20 min, RT). The medium on the cells was replaced by fresh medium (1.5 mL), before addition of the DNA:Lipofectamine complexes in a drop-wise action. The cells were then incubated for 4-6 h before they were subcultured for subsequent experimentation. Alternatively, HMEC-1 cells were plated at $5x10^4$ cells/well in 12-well plates (BD Biosciences). DNA:lipofectamine complexes were generated using the same protocol, but quantities were varied to optimise transfection efficiency (see **Chapter 5.10**)

Stable Transfection:

For stable transfection, the Flp-in™ system was used (**Fig. 2.1**). This system allows integration and expression of a gene of interest. The Flp-In™ System involves introduction of a Flp recombination target (FRT) site into the genome of HEK cells. An expression vector containing a FRT site and the gene of interest is then integrated into the genome via Flp recombinase-mediated DNA recombination (expressed by the vector pOG44) at the FRT site (O'Gorman et al., 1991).

The same protocol as described above in transient transfection was used, as an exception that DNA pOG44 was added to the DNA of interest with a ratio of 9:1 (2.7 µg pOG44 + 300 ng DNA). At the end of the incubation with the mixture DNA:Lipofectamine, cells were split and put into antibiotic-free medium for 24h. Then the cells were put into selection by adding Hygromycin B (50-200 µg/mL).

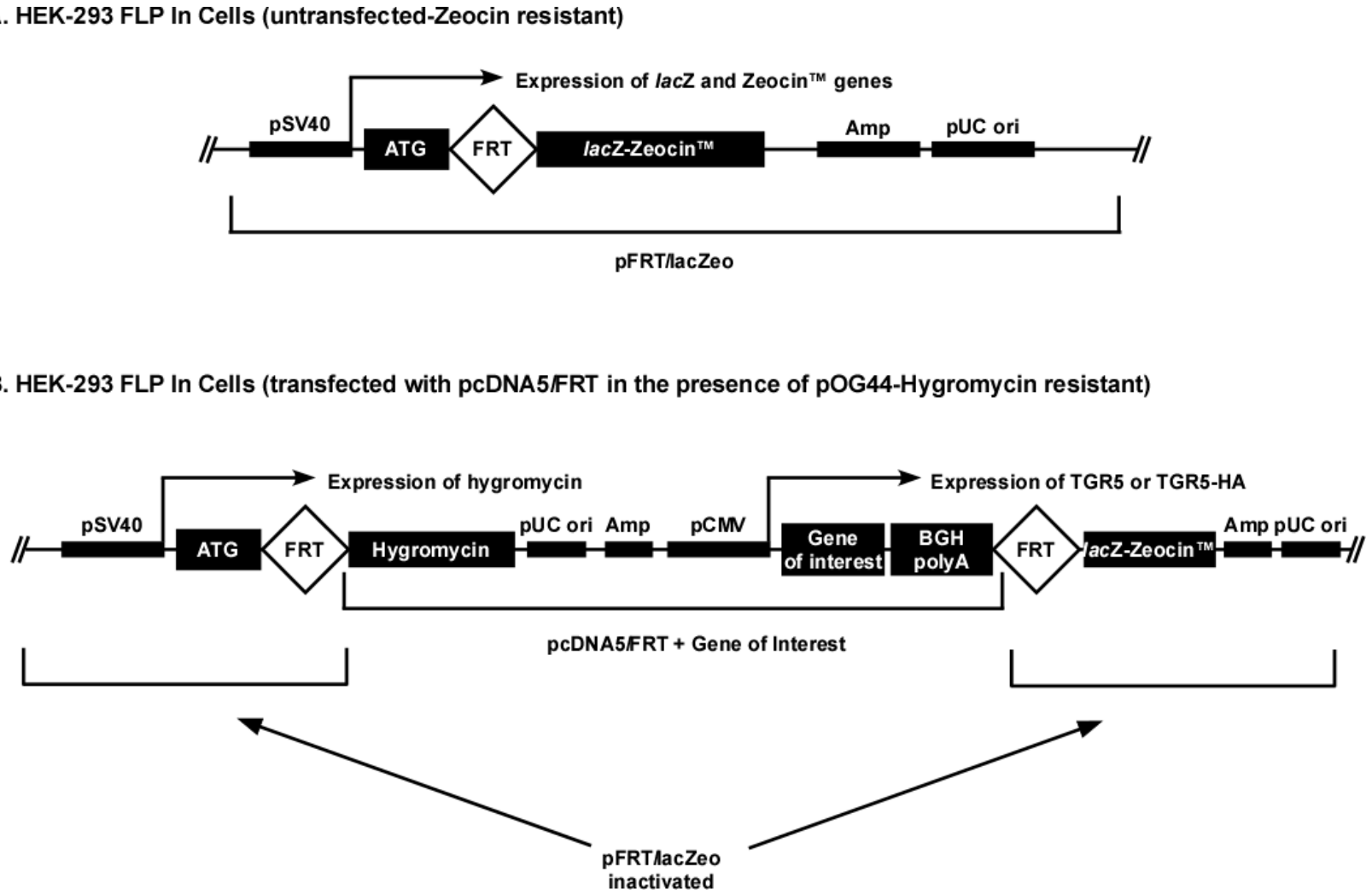

Figure 2.1 **Diagram of the Flp-in® system.** (**A**) pFRT/*Lac*Zeo stably transfected into HEK cells generate a resistance to Zeocin™ (HEK-FLP). (**B**) Transfection of HEK-FLP with gene of interest (pcDNA5/FRT-"gene of interest") and Flp recombinase (pOG44), allows integration of pcDNA5/FRT-"gene of interest" into the FRT site.

2.3 Biochemical Techniques

2.3.1 Drug Treatments

HEK cells were seeded at: $1.2x10^6$ cells/well in 12-well plate; $3x10^6$ cells/well in 6-well plate or 35 mm dishes; and $2\text{-}5x10^6$ cells/dish in 100 mm dishes (BD Biosciences), all coated with poly-D-lysine (50 µg/mL). HMEC-1 and TA-SMC cells were seeded at: $7x10^4$ cells/well in 12-well plate; $1.7x10^5$ cells/well in 6-well plate or 35 mm dishes; and $1x10^6$ cells/dish in 100 mm dishes. All cells were plated 48 h before experiment. Cells were washed 3 times with 1x PBS and incubated in appropriate serum-free medium supplemented with 0.1% bovine serum albumin (BSA) (DMEM-, MCDB-, SMC-BSA), with appropriate vehicle or inhibitors for 30 min. Cells were stimulated with agonist (CGRP or ADM, 0.1-1 µM, 0-16 h, 37°C), washed 3 times with 1x PBS and incubated in agonist-free medium (± inhibitors) for 0-16 h (recovery time). In some experiments, cells were deprived of serum by incubating cells in medium containing 0.1% BSA (16 h).

2.3.2 Lysis of Mammalian Cells

Cells were placed on ice, washed 3 times in ice-cold 1x PBS, and lysed in Lysis buffer (150-350 µL, 10 min, 4°C) with gentle rocking. Cells were then scraped and lysates were collected into microcentrifuge tubes and centrifuged (10,000 *g*, 10 min, 4°C) to pellet insoluble cell debris. Supernatants were then transferred to fresh tubes.

2.3.3 Protein Determination and Sample Preparation

Proteins concentrations were determined by BCA assay (Smith et al., 1985) and modified to a 96-well plate format (Hooper, 1993). Briefly, dilutions of BSA from 0-10 µg/µL were used as a standard. Samples (3-10 µL) were added to deionized distilled water (DDW) to a final volume of 10 µL. BCA solution and 4% (w:v) $CuSO_4$ solution of the BCA kit were mixed (50:1) and 200 µL of the mixture was added to each well. Plates were then incubated for 30 min at 37°C. Plates were read at 562 nm using a VersaMax plate reader (Molecular Devices) and analysed using SoftMax Pro 4.8 software (Molecular Devices). Samples (20-50 µg protein) for analysis by Western blotting were prepared by mixing with 5x SDS-loading buffer. Samples were then heated (3-5 min, 100°C) and centrifuged (10,000 *g*, 1 min, RT) before analysis by SDS-PAGE and Western blotting (see **2.3.4**).

2.3.4 SDS-PAGE Electrophoresis

Proteins were separated using appropriate percentage acrylamide gels (8-15% (w:v)).

Component	Stacking gel	Resolving gel			
	3%	8%	10%	12%	15%
0.5 M Tris/HCl, pH	1.25 mL	-	-	-	-
1.5 M Tris/HCl, pH	-	2.5 mL	2.5 mL	2.5 mL	2.5 mL
10% (w:v) SDS	50 µL	100 µL	100 µL	100 µL	100 µL
10% (w:v) APS*	50 µL	100 µL	100 µL	100 µL	100 µL
40% (w:v)	375 µL	2 mL	2.5 mL	3 mL	3.75 mL
DDW	3.275 mL	5.3 mL	4.8 mL	4.3 mL	3.55 mL
Temed	2.5 µL	5 µL	5 µL	5 µL	5 µL
Total volume	5 mL	10 mL	10 mL	10 mL	10 mL

Table 2.6 **Composition of SDS-Acrylamide Gels.** *APS = ammonium persulphate

The SDS gels were prepared using the Mini-PROTEAN Tetra Electrophoresis System (BioRad). The resolving gel (**Table 2.6**) was poured first and water saturated butan-2-ol layered on top and the gel left to polymerise for about 30 minutes. After the resolving gel had set, the butan-2-ol was washed away using DDW and the stacking gel was then poured on top. A 10-well comb was then placed to form the wells for the loading of the protein and allowed to polymerise for another 15 minutes. Once set, the comb was gently removed and the gel mounted on the apparatus. The tank was filled in with running buffer and non-polymerised acrylamide was removed from by using a syringe to dispel buffer from each well. The samples were then loaded and gel was run at constant current (0.2 mA/gel) until the dye in the loading buffer emerged from the bottom of the gel.

2.3.5 Transfer of Protein on PVDF Membrane

At the end of the separation the proteins were transferred onto a PVDF membrane, by wet-transfer procedure using Mini Trans-Blot® Electrophoretic Transfer Cell (BioRad). The gel was placed onto the membrane, sandwiched between two soaked-extra thick blot papers in child transfer buffer. The tank was filled in with transfer buffer and a constant current was applied (1 A, 1 h). The tank was cooled down by using dry ice changed every 20 minutes.

2.3.6 Western Blotting of Membranes

At the end of the transfer the membranes were rinsed in 1x PBS and blocked (1 h, RT) in blocking. Membranes were incubated in fresh blocking buffer with the appropriate primary antibodies (overnight, 4°C) on a rocker. Membranes were washed (3x10 min) in 1x PBS-T and incubated with fresh blocking buffer containing appropriate secondary antibodies conjugated to horseradish peroxidase (1 h, RT) on a rocker. Membranes were washed (3x10 min) with PBS-T and immunoreactive proteins were detected by using chemiluminescence (incubation 1-5 min, RT). Membranes were exposed to X-ray film (Kodak), developed, digitised (EPSON Perfection 1250) and quantified using ImageJ. Alternatively membranes were read using an ImageQuant RT ECL (GE Healthcare) and quantified with ImageQuantTL software.

In experiments looking at the effect of inhibitors or different conditions compared to control, results were normalised at 10 min time point, in order to be consistent between time course experiments. Results were either expressed in fold-increase over unstimulated cells, when the 10 min time point between control and treated cells was different; or expressed in % of maximal response, when the 10 min time point between control and treated cells was similar.

2.3.7 Removal of Antibodies from PVDF Membrane

PVDF membrane were incubated in stripping buffer (10-60 min, 60°C) and rinsed with 1x PBS. Membranes were then blocked again and blotted as described (see **2.3.6**).

2.3.8 Immunoprecipitation

HEK cells were plated on 100 mm dishes 48 h prior experiment. After treatment, cells were lysed in radio-immunoprecipitation assay (RIPA) buffer (2 mL, 10 min, 4°C). Cells were then scraped, lysates were collected into centrifuge tubes and centrifuged (10,000 *g*, 10 min, 4°C). Samples were divided into two aliquots and immunoprecipitating antibodies added to isolate CLR or CLRΔ9KR (RK11, 1:2000) and RAMP2 (myc, 1:500) and incubated (overnight, 4°C) on rotation. Samples were then incubated (2 h, 4°C) with 20 µL/tube of protein A/G Plus on rotation and immuno-complexes captured by centrifugation (4,000 *g*, 1 min, RT). Immuno-complexes were washed 3 times in of RIPA buffer (1 mL). After the final wash immuno-complexes were resuspended in 20 µL of 2x SDS-loading buffer. Samples were then analysed by SDS-PAGE and Western blotting (see **2.3.4**).

2.3.9 Degradation Assays

Degradation Assay Using Cycloheximide (CHX):

HEK cells were plated in 100 mm dishes 48 h prior experiment. Cells were washed 3 times in 1x PBS and incubated (30 min) in DMEM-BSA and 140 µM of CHX. Cells were stimulated with ADM or CGRP (100 nM, 10 min, 37°C), washed 3 times with 1x PBS and incubated (16 h) in DMEM-BSA supplemented with CHX. Or instead, cells were stimulated continuously with ADM or CGRP (100 nM, 16 h, 37°C) in DMEM-BSA supplemented with CHX. Cells were lysed and samples prepared for SDS-PAGE and Western blotting (see **2.3.4**).

Degradation Assay Using Biotin/Avidin Complex:

HEK cells were plated in 100 mm dishes 48 h prior experiment. Cells were washed 3 times in ice-cold 1x PBS and then cell surface proteins were labelled using Sulfo-NHS-SS-Biotin according to the manufacturer's guidelines. Briefly, cells were incubated (30 min, 4°C) with ice cold 1x PBS containing Sulfo-NHS-SS-Biotin with gentle shaking. Cells were washed 3 times with ice-cold 1x PBS and incubated (30 min, 37°C) in DMEM- or MCDB-BSA supplemented with vehicle, lysosome inhibitor cocktail (pepstatin A and E-64d, both at 10 µM; and Z-PAD at 200 µM) or proteasome inhibitor MG-132 (20 µM). Cells were stimulated with ADM (100 nM, 0-16 h, 37°C), lysed in RIPA buffer (2 mL) and centrifuged (10,000 *g*, 10 min, 4°C). Supernatants were transferred to fresh microcentrifuge tubes and rotated (overnight, 4°C) with 20 µL/tube of NeutrAvidin agarose. Complexes were collected by centrifugation (4,000 *g*, 1 min, 4°C), washed 3 times in RIPA buffer (1 mL), supernatants discarded and the complexes resuspended in 20 µL of 2x SDS-loading buffer. Samples were then analysed by SDS-PAGE and Western blotting (see **2.3.4**).

2.3.10 Immunocytochemistry

HEK, HMEC-1 or TA-SMC cells were plated on coverslips (coated with poly-D-lysine for HEK cells) in 6-well plate or 35 mm dishes 48 h prior experiment. After treatment, cells were washed 3 times in 1x PBS. Coverslips were then incubated (20 min, 4°C) in 4% (w:v) paraformaldehyde (PFA). Coverslips were incubated (30 min, RT) in blocking solution and incubated with the appropriate primary antibodies (~45 µL/coverslip, overnight, 4°C). Coverslips were washed in blocking solution, incubated with appropriate secondary antibodies (~45 µL/coverslip, 1-2 h, RT) and washed (3x10 min) in blocking solution. Coverslips were rinsed with 1x PBS before mounting on microscope slides using Vectashield mounting medium with DAPI (Vector Laboratories).

2.3.11 Confocal Microscopy

For confocal microscopy, cells mounted on slides (see **2.3.10**) were observed with a Zeiss laser-scanning confocal microscope (LSM Meta 510) using EC Plan-Neofluar 20x/0.5, EC Plan-Neofluar 40x/1.3 Oil DIC and Plan-Apochromat 63x/1.4 Oil DIC objectives. Images were collected at a zoom of 1-2 and an iris of <3 µm, and at least five optical sections were taken at intervals of 0.5 µm. Single sections are shown. Images were processed using ImageJ and Adobe Photoshop software.

2.3.12 Internalisation of Receptors

HEK cells were seeded in 12-well plate 48 h prior experiment. Cells were washed 1 time in 1x PBS and incubated (30 min, 37°C) with anti-Myc antibody (1/250) in DMEM-BSA. Cells were washed once with 1x PBS and stimulated with ADM (100 nM, 0-30 min). Cells were washed once with 1x PBS and incubated (0-60 min, 37°C) in DMEM-BSA agonist-free. Cells were washed with 1x PBS-CM and incubated in trypsin/EDTA (250 µL/well, 2-3 min, 37°C). Cells were detached by pipetting up and down and collected into a microcentrifuge tube. Cells were centrifuged (1,000 *g*, 5 min, 4°C). Supernatant was discarded and pellet resuspended in ice cold PBS-CM (500 µL). An anti-rabbit DyLight 649 (1/500) was added to each tube and incubated (1 h, 4°C) on rotation. Cells were washed 3 times, centrifuged (1,000 *g*, 1 min, 4°C) in PBS-CM and resuspended in ice cold PBS-CM. Cells were analysed using Fluorescence-activated cell sorting (FACS) flow cytometry method assessed on a FACSCanto II (BD Biosciences) and analysed with BDFacs DiVa software.

2.4 Molecular Biology Techniques

2.4.1 Extraction of RNA

RNA was extracted using TRIzol® Reagent (Invitrogen, 15596-026) according to the manufacturer's guidelines. In brief, cells were cultured in 35 mm dish, media was removed from the culture dish and TRIzol® (1 mL) was added directly on the cells. Cells were lysed by pipetting up and down on the dish. The homogenised sample was transferred in a fresh microcentrifuge tube and incubated (5 min, RT). Chloroform (0.2 mL) was added to the tube, shacked vigorously for 15 seconds and left incubated (5 min, RT). The mixture was then centrifuged (12,000 *g*, 15 min, 4°C). The mixture is separated in two phases. The top colourless phase (containing the RNA) was transferred in a fresh tube. Propanol-2-ol (500 µL) was added to the tube, incubated (10 min, RT) and centrifuged (12,000 *g*, 10 min, 4°C). The supernatant was discarded and the pellet was washed with 75% (v:v) ethanol/DDW (1 mL), vortexed briefly and centrifuged (7,500 *g*, 5 min, 4°C). The supernatant was discarded and the tube was left air dry (5 min, RT). The RNA was resuspended (50 µL) in DEPC-H_2O by pitting up and down. The solution was then incubated (10-15 min, 55-60°C) and quantified (see **2.4.2**). The RNA was used immediately or stored at -80°C.

2.4.2 Quantification of Nucleic Acids

The quantification of nucleic acids (DNA or RNA) was determined by using the Beer Lambert Law reading the absorbance at 260 nm, where A_{260} = 1 for 40 µg/mL of RNA and A_{260} = 1 for 50 µg/mL of DNA. The purity was measured using the ratio of the absorbance at 260 and 280 nm ($A_{260/280}$). The absorbance was read using BioPhotometer (Eppendorf).

2.4.3 Reverse-Transcriptase Polymerase Chain Reaction (RT-PCR)

TaqMan® Reverse Transcription Reagents (Invitrogen, N8080234) was used to generate complementary DNA (cDNA) from RNA. The reaction mix was made according to the manufacturer's guidelines (**Table 2.7**). Samples were placed into a thermal cycler and subjected to cycling as follows:

25°C, 10 min
48°C, 30 min
99°C, 5 min

The cDNA produced were used as a template for PCR or stored at -20°C.

Component	Volume (µL)	Final concentration
10x Reverse Transcriptase buffer	4	1x
10 mM dNTPs	8	2 µM
25 mM $MgCl_2$	8.8	5.5 mM
Oligo $d(T)_{16}$ or Random Hexamers	2	2.5 µM
RNAse inhibitor	0.8	0.4 U/µL
MultiScribe Reverse Transcriptase	1	1.25 U/µL
RNA (1-4 µg)	varied	-
DEPC-H_2O	Until 40	-

Table 2.7 **Reaction mix for RT-PCR.**

2.4.4 PCR Following cDNA Production

PCR reagents were from Qiagen (201203). The reaction mix was made according to the manufacturer's guidelines (**Table 2.8**) Samples were placed into a thermal cycler and subjected to cycling as follows:

94°C, 10 min
94°C, 30 s
60°C, 30 s
72°C, 1 min
} 35 cycles
72°C, 10 min

The PCR products were ran on agarose gel electrophoresis or stored at -20°C (see **2.4.6**).

Component	Volume (µL)	Final concentration
10x PCR buffer	5	1x
cDNA (template) (≈1 µg)	5	≈0.2 M
Forward primer	2	0.5 µM
Reverse primer	2	0.5 µM
Taq	0.05	$5x10^{-3}$ U/µL
DDW	Until 50 µL	-

Table 2.8 **Reaction Mix for PCR following cDNA production.**

2.4.5 Screening of Bacterial Colonies

Single colonies were picked from LB-agar plates (see **Appendix II**) and resuspended in DDW (10 µL). An aliquot (2 µL) of this mix was then used as template for PCR. PCR reagents were from Qiagen (201203). The reaction mix was made according to the manufacturer's guidelines (**Table 2.9**). Samples were placed into a thermal cycler and subjected to cycling as follows:

96°C, 10 min
96°C, 30 s
55°C, 30 s } 35 cycles
72°C, 1 min
72°C, 10 min

PCR products were then analysed by DNA gel electrophoresis as described (see **2.4.6**).

Component	Volume (µL)	Final concentration
10x PCR buffer	2	1x
10 mM dNTPs	0.4	0.2 µM
Template	2	-
Forward primer	1	0.5 µM
Reverse primer	1	0.5 µM
Taq (5U/µL)	0.05	$1.25x10^{-3}$ U/µL
DDW	Until 20 µL	-

Table 2.9 **Reaction mix for colony PCR.**

2.4.6 Electrophoresis of DNA

Separation of DNA was performed on agarose gel electrophoresis. 1-2% (w:v) of agarose (Fisher Scientific, BP1356) was melted in 1x Tris-acetate EDTA (TAE) buffer. The mixture was allowed to cool down, ethidium bromide was added (0.1 µg/mL) and the gel was poured into a gel casting tray until it sets. The gel was then placed into an electrophoresis tank with 1x TAE and the samples were mixed with 0.5 µL of 10x DNA loading buffer, loaded and ran at constant voltage (5-20 V/cm). Gel was then exposed under UV light to visualise the DNA. Images of the gel were captured in a Syngene UV transluminator using Genesnap software.

2.4.7 Restriction Enzyme Digestion of DNA

Restriction enzymes were used to cut at specific site the DNA. All the enzymes were purchased from New England BioLabs (NEB). The reactions were performed in total volume of 20 µL (**Table 2.10**). The reaction mix was then incubated at 37°C for at least 2 h. The digestion products were ran on agarose gel electrophoresis or stored at -20°C (see **2.4.6**).

Component	Volume (µL)	Final concentration
10x buffer 1-4 (according to the enzyme(s) used)	2	1x
10x BSA (10 mg/mL)	2	1 mg/mL
Enzyme(s)	Total of 1 µL	Varied
Template (DNA) (1-5 µg)	Varied	Varied
DDW	Until 20 µL	-

Table 2.10 **Reaction Mix for Digestion of Restriction Enzyme.** For double digestion, the volume of enzymes added was adjusted to keep an equivalent activity (i.e. 50:50). The maximum volume of enzymes was 1 µL (5% of glycerol) to avoid any star activity.

2.4.8 Extraction of DNA

The bands of interest were excise of a gel using a sterile blade and DNA was purified using Qiagen QIAquick Gel Extraction Kit (28704) according to the manufacturer's guidelines. Briefly, the agarose gel was melted (50°C, water bath) and the DNA fragment was purified by bind-wash-elute procedure.

2.4.9 Ligation of DNA Fragments

The fragments were ligated using the T4 DNA ligase (NEB, M0202T) in 10 µL of reaction (**Table 2.11**). The reaction was incubated in a thermal cycler (14°C, 4-16 h) and an aliquot (1-5 µL) used to transform chemically competent *E. coli* (**2.1.6**).

Component	Volume (µL)	Final concentration
10x Ligase buffer	1	1x
Inserts	Ratio 1:1 to 1:3	Varied
Ligase	0.5	1.5 Weiss U*/µL
DDW	Until 10 µL	-

Table 2.11 **Reaction Mix for Ligation.** *1 Cohesive End unit from NEB=0.015 Weiss unit

2.4.10 Purification of Plasmid DNA

A QIAprep Spin Miniprep Kit (27104) or EndoFree Plasmid Maxi Kit (12362) from Qiagen were used to purify plasmid DNA following the manufacturer's guidelines. Cultures were set up as described in **2.5.4**. The plasmid DNA was dissolved in water, quantified as described in **2.4.2** and stored at -20°C.

2.5 Bacterial Work

2.5.1 Bacterial Broth

Two broths were used: Lysogeny broth (LB) a nutritionally rich medium, used routinely to culture bacteria; and super optimal broth (SOB) was used to culture cells when preparing chemically competent cells. See **Appendix II** for broth preparation.

2.5.2 Preparation of Competent Cells

The protocol described by Inoue *et al.* was used to prepare competent cells (Inoue et al., 1990). In brief, bacteria were spread and grown on an antibiotic-free LB-agar plate (overnight, 37°C). Then 10-12 colonies were picked and incubate in SOB media (250 mL, 24-48 h, 18°C) until the bacteria growth reach a value of optical density at 600 nm (OD_{600}) of 0.5-0.6, read on a BioPhotometer (Eppendorf). Bacteria were then put on ice (10 min), centrifuged (2,500 *g*, 10 min, 4°C) and the pellet was resuspended (80 mL) in transformation buffer (TB). Bacteria were incubated on ice (10 min) and centrifuged again (2,500 *g*, 10 min, 4°C). Finely, the pellet was resuspended (20 mL) in TB buffer + 7% (v:v) of DMSO. Cells were then aliquoted (250 µL) and frozen directly in liquid nitrogen. Cells were stored in -80°C.

2.5.3 Transformation of Bacteria

Chemically competent *E. coli* (50 µL) were thawed on ice. After thawing, *E. coli* were incubated with plasmid DNA (~20 ng) or ligation mix (1-5 µL) on ice (30 min). Bacteria were heat-shocked (30 s, 42°C) using a water bath and then allowed for recover on ice (5 min), before spreading on LB-agar (see **Appendix II**) containing ampicillin (100 mg/mL in 50% (v:v) ethanol/DDW). Plates were then inverted and placed in an incubator overnight to allow growth to proceed. MACH1 cells were grown at 37°C.

2.5.4 Culture of Bacteria

Single colonies were picked from LB-agar plates and LB broth (5 mL) containing ampicillin (100 mg/mL in 50% (v:v) ethanol/DDW), inoculated and placed in a shaking incubator (200 rpm, overnight, 37°C). For larger culture volumes (250 mL) a starter culture (5 mL) was set up as described, grown during the day and then

used to inoculate the larger volume. The larger volume culture was then placed in a shaking incubator (200 rpm, overnight, 37°C).

2.5.5 Preparation of Bacterial Glycerol Stocks

To prepare glycerol stocks of bacterial cultures, an aliquot of an overnight culture (1 mL) was mixed with glycerol (250 µL) and then stored at -80°C.

2.6 Analysis and Statistics

Experiments were repeated n≥3 times. Data are presented as mean ± standard error of the mean (S.E.M.). Results were compared by Student's t test, with $p<0.05$ considered significant.

Chapter 3. Mechanisms of CGRP-Induced ERK Activation

3.1 Background and Objectives

The mitogenic-activated protein kinase (MAPK) pathways play a key role in the development and the cell cycle. One of these pathways, the extracellular signal-regulated kinase (ERK)1-2 module is involved in many biological responses and is notably responsible for cell proliferation and survival (reviewed in (Pearson et al., 2001; Seger and Krebs, 1995)). Typically, ERK1-2 is activated by two types of cell-surface receptor, the receptor tyrosine kinases (RTK) and G protein-coupled receptors (GPCR).

CGRP has been found to induce ERK activation in different cell types. CGRP induces proliferation in ERK-dependent manner in alveolar epithelial cells (Kawanami et al., 2009) and primary rat osteoblast (Han et al., 2010), whereas it has been shown to inhibit proliferation in aortic smooth muscle cells and pulmonary artery smooth muscle cells (Chattergoon et al., 2005). Moreover CGRP-induced ERK1-2 activation has been found to promote iNOS upregulation in trigeminal ganglion glial cells (Vause and Durham, 2009).

Several signalling pathways can lead to GPCR-dependent ERK activation as reviewed in (Rozengurt, 2007) (**Fig. 3.1**). By using different inhibitors, three main pathways were investigated in CGRP-induced ERK activation, that is the cAMP/PKA, PLC/PKC/Ca^{2+} or the transactivation of the epidermal growth factor receptor (ErbB1) pathway in HEK cells. Additionally, the G protein-independent mediated by β-arrestins was also investigated in CGRP-induced ERK activation.

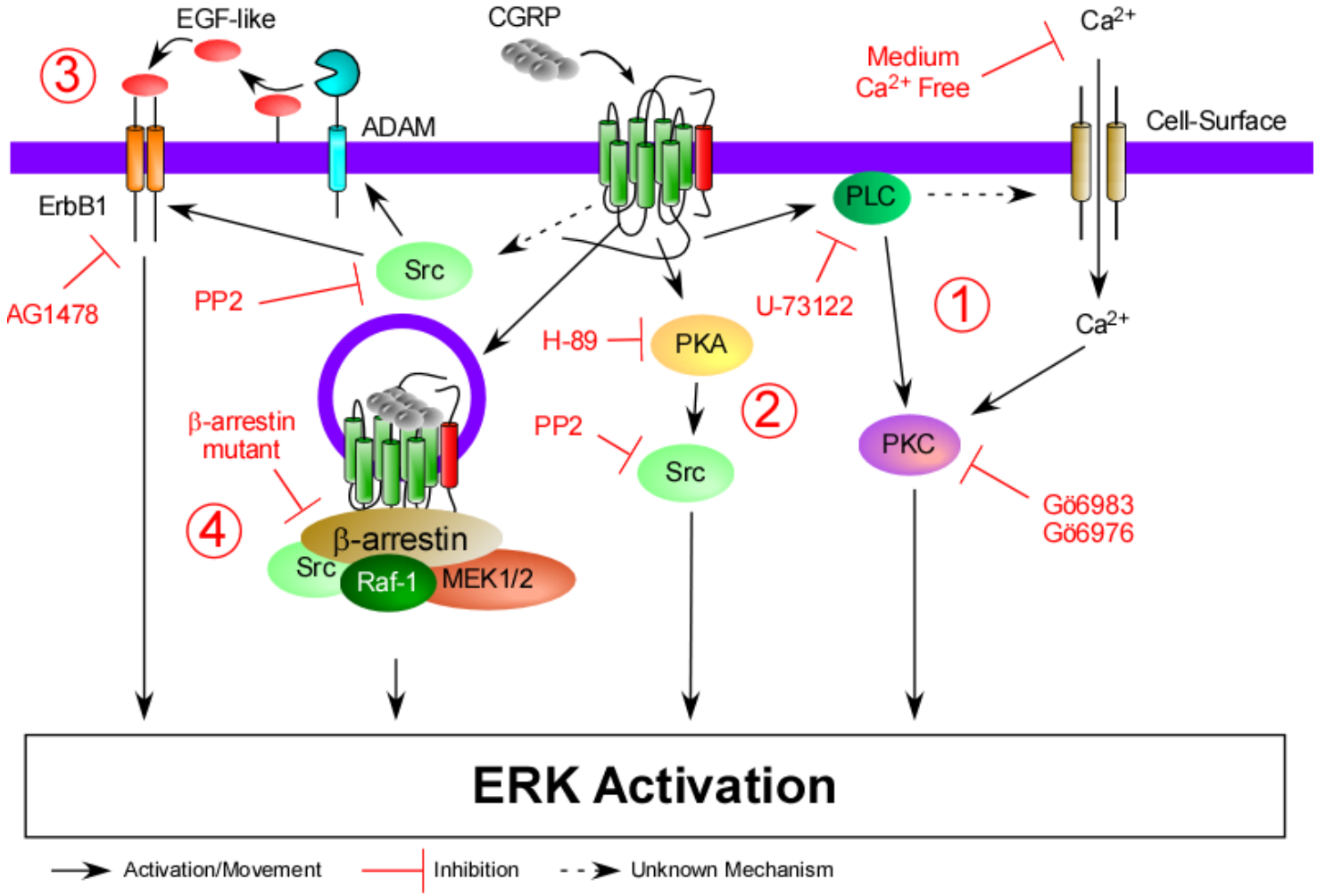

Figure 3.1 **Schematic representation of all ERK pathways potentially involved in CGRP-induced ERK activation.** Four main pathways can be involved in ERK activation, the (1) PLC/PKC/Ca^{2+}, (2) cAMP/PKA, (3) ErbB1 transactivation and (4) the β-arrestin-dependent pathway. To determine which pathways are involved in CGRP-induced ERK activation, different inhibitors (highlighted in red) targeting these pathways were used.

3.2 CGRP-Induced ERK Activation

Like many GPCRs, CLR•RAMP1 induces ERK activation in many different cell types (Cady et al., 2011; Kawanami et al., 2009; Kawase et al., 1999; Vause and Durham, 2009; Yu et al., 2006). To determine whether HEK-CLR•RAMP1 cells are a suitable model for studying CGRP-induced ERK activation, HEK-CLR•RAMP1 cells were incubated in serum-free medium and stimulated with CGRP (0-60 min). Levels of phosphorylated ERK (pERK) 1, pERK2 and ERK2 were determined by Western blotting. In unstimulated cells levels of pERK1 and 2 were low (**Fig. 3.2**). CGRP treatment increased dramatically pERK1 and 2 with a peak at 2 min and then progressively decreased (**Fig. 3.2B**, 24.4±10.5 for pERK1; and 7.9±10.5 for pERK2 fold-increase compared to basal at 2 min). This result shows that CGRP is able to induce ERK activation in HEK-CLR•RAMP1 cells, which suggest that HEK-CLR•RAMP1 cells are a suitable model.

3.3 CGRP Induces Transactivation of the Epidermal Growth Factor Receptor

Many GPCRs can activate mitogenic signalling by transactivating ErbB1 ((Daub et al., 1996) and reviewed in (Goldsmith and Dhanasekaran, 2007; Rozengurt, 2007)). The molecular mechanism of this pathway is not fully understood and varies from cell-type to cell-type and GPCR to GPCR. However, in many cases GPCRs induce activation of cell-surface peptidases to release EGF-like ligands such as HB-EGF or TGF-α that directly activate ErbB1 leading to ERK activation. To determine whether CGRP induces transactivation of the ErbB1 a specific ErbB1 inhibitor, AG1478 (Osherov and Levitzki, 1994), was used. HEK-CLR•RAMP1 cells were incubated with vehicle (DMSO) or AG1478, stimulated with CGRP (0-10 min), washed, incubated in CGRP-free medium ± AG1478 (0-50 min) and levels of pERK1, pERK2 and ERK2 determined by Western blotting. In unstimulated cells, levels of pERK1 and 2 were low (**Fig. 3.3**). CGRP (10 min) caused a prompt increase in levels of pERK1 and 2 in both vehicle- and AG1478-treated cells. However, the increase in AG1478-treated cells was reduced compared to vehicle-treated cells (**Fig. 3.3B**, 65.2±29.7 (vehicle) versus 19.1±9.1 (AG1478) for pERK1 and 18.6±6.5 (vehicle) versus 8.6±3.0 (AG1478) for pERK2; fold-increase at 10 min compared to basal). Indeed, when expressed in fold-decrease over vehicle-treated cells, AG1478 significantly reduced levels of pERK1 and 2 at all time points examined (**Fig. 3.3D** and **E**). Furthermore, basal levels of pERK1 and 2 were not affected by AG1478 (**Fig. 3.3C**). Thus, CGRP can activate ERK by causing transactivation of ErbB1 in HEK cells.

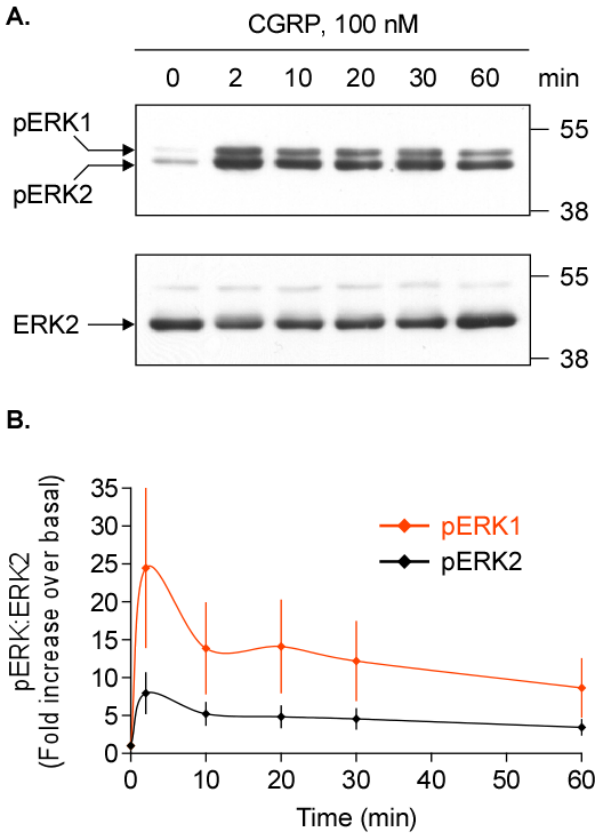

Figure 3.2 **CGRP induces ERK activation.** (**A**) Serum-starved HEK-CLR•RAMP1 cells were stimulated with CGRP (100 nM, 0-60 min) and levels of pERK1, pERK2 and ERK2 determined by Western blotting. Blots were quantified using ImageJ and ratio of pERK1:ERK2 and pERK2:ERK2 calculated. Representative blots are shown. (**B**) Results, expressed in fold-increase over basal, show that CGRP induces a prompt increase of pERK1 and 2 levels, which is sustained by decreases over time. Thus CGRP promotes ERK activation in HEK-CLR•RAMP1 cells. n=4.

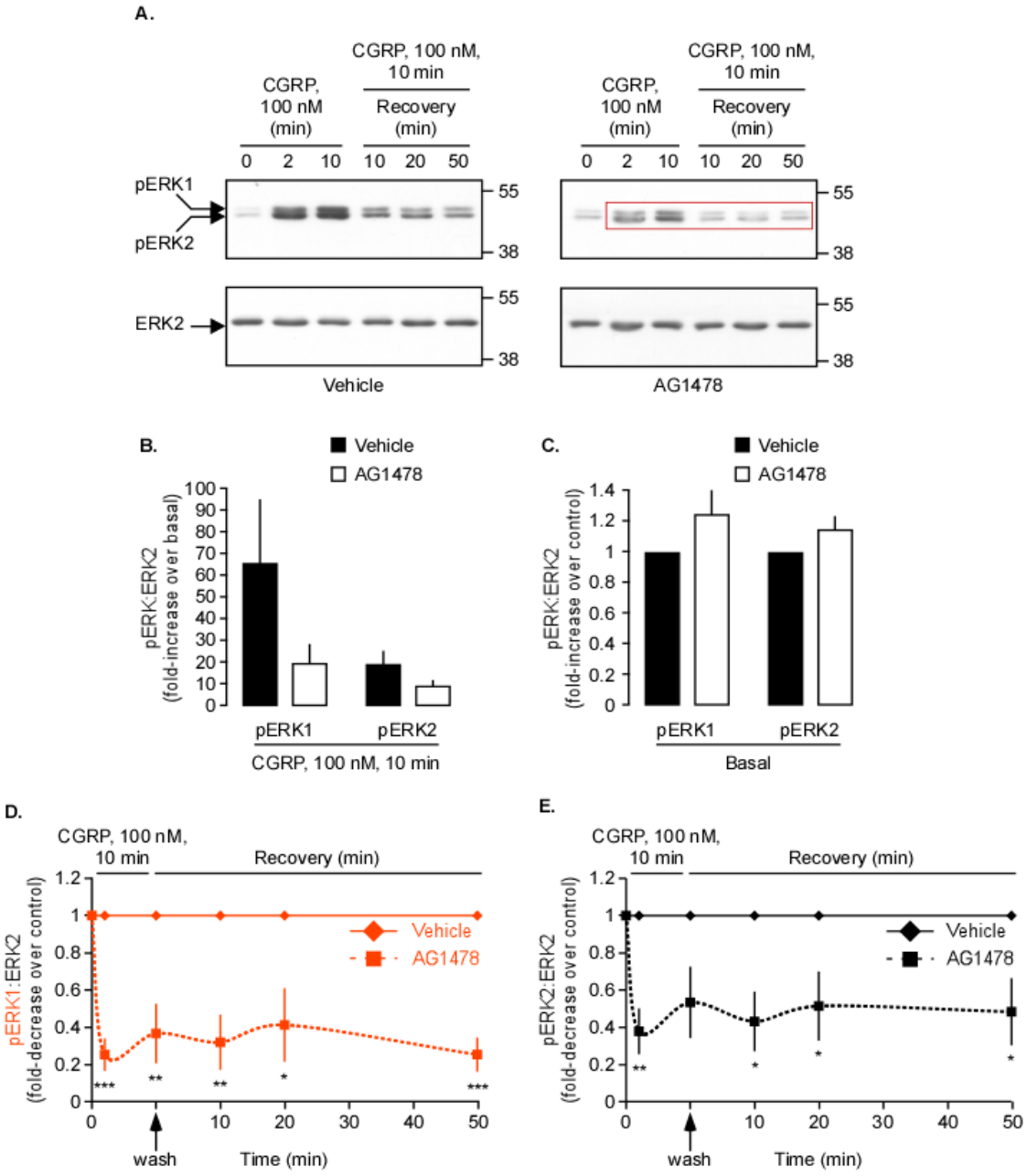

Figure 3.3 **CGRP induces ErbB1-dependent ERK activation.** (**A**) Serum-starved HEK-CLR•RAMP1 cells were incubated with vehicle or AG1478 (1 µM), stimulated with CGRP (100 nM, 0-10 min), washed, incubated in CGRP-free medium ± AG1478 (0-50 min) and levels of pERK1, pERK2 and ERK2 determined by Western blotting. Blots were quantified using ImageJ and ratio of pERK1:ERK2 and pERK2:ERK2 calculated. Representative blots are shown. The red box highlights the difference between vehicle- and AG1478-treated cells. (**B**) The maximal CGRP-induced ERK phosphorylation, expressed in fold-increase over basal, is higher in vehicle- compared to AG1478-treated cells. (**C**) Basal levels of pERK1 and 2 are expressed in fold-increase over vehicle-treated cells. The effect of AG1478 on the basal of pERK1 and 2 shows no significant difference compared to vehicle-treated cells. (**D**, **E**) The CGRP-induced ERK activation of the full time course, expressed in fold-decrease over vehicle of pERK1 (**D**) and pERK2 (**E**) is significantly reduced in AG1478-treated cells. Thus, the CGRP-mediated ERK activation is ErbB1-dependent, suggesting that CGRP induces transactivation of ErbB1 in HEK cells. n=4, *=p<0.05 and **=p<0.01 compared to vehicle-treated cells at the same time point.

3.4 CGRP-Induced ERK Activation is Src-Dependent

The tyrosine kinase Src plays a central role in the GPCR-mediated ERK activation (reviewed in (McGarrigle and Huang, 2007)). Src has been involved in all the ERK pathways described in this study (Daub et al., 1997; Dikic et al., 1996; Eguchi et al., 1998; Luttrell et al., 1999; Schmitt and Stork, 2002). However, Src has been mostly described and characterised within the transactivation of ErbB1. Indeed, Src has been found to be required to promote ERK activation following ErbB1 transactivation, either downstream of ErbB1 (Daub et al., 1997) or involved in the activation of ErbB1 itself (Buteau et al., 2003; Eguchi et al., 1998). To determine whether CGRP induces ERK in a Src-dependent manner a specific Src inhibitor, PP2 (Bain et al., 2007; Hanke et al., 1996), was used. HEK-CLR•RAMP1 cells were serum-starved, incubated with vehicle (DMSO) or PP2, stimulated with CGRP (0-10 min), washed, incubated in CGRP-free medium ± PP2 (0-50 min) and levels of pERK1, pERK2 and ERK2 determined by Western blotting. In unstimulated cells, levels of pERK1 and 2 were low (**Fig. 3.4**). CGRP (10 min) caused a prompt increase in levels of pERK1 and 2 in both vehicle- and PP2-treated cells. However, the increase in PP2-treated cells was significantly reduced compared to vehicle-treated cells (**Fig. 3.4B**, 5.3±1.0 (vehicle) versus 2.7±0.4 (PP2) for pERK1 and 3.9±0.5 (vehicle) versus 2.4±0.3 (PP2) for pERK2; fold-increase at 10 min compared to basal). Indeed, when expressed in fold-decrease over the vehicle-treated cells, PP2 significantly reduced levels of pERK1 and 2 at all time points examined (**Fig. 3.4D** and **E**). Furthermore, basal levels of pERK1 and 2 were not affected by PP2 (**Fig. 3.4C**). Thus, CGRP-induced ERK1-2 activation is Src-dependent in HEK cells.

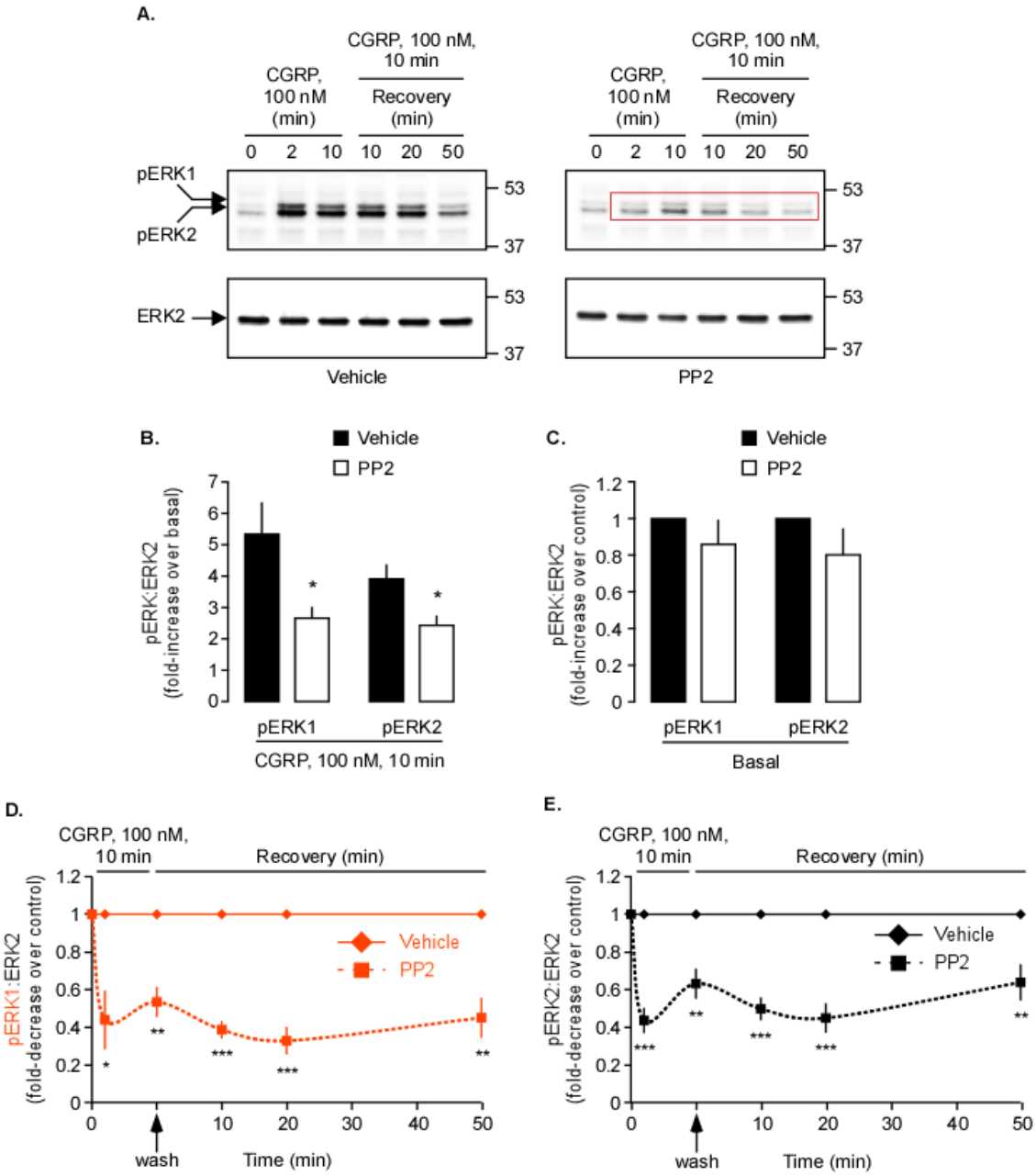

Figure 3.4 **CGRP-induced ERK activation is Src-dependent.** (**A**) Serum-starved HEK-CLR•RAMP1 cells were incubated with vehicle or PP2 (10 µM), stimulated with CGRP (100 nM, 0-10 min), washed, incubated in CGRP-free medium ± PP2 (0-50 min) and levels of pERK1, pERK2 and ERK2 determined by Western blotting. Blots were quantified using ImageQuantTL and ratio of pERK1:ERK2 and pERK2:ERK2 calculated. Representative blots are shown. The red box highlights the difference between vehicle- and PP2-treated cells. (**B**) The maximal CGRP-induced ERK phosphorylation, expressed in fold-increase over basal, is higher in vehicle- compared to PP2-treated cells. (**C**) Basal levels of pERK1 and 2 are expressed in fold-increase over vehicle-treated cells. The effect of PP2 on the basal of pERK1 and 2 shows no significant difference compared to vehicle-treated cells. (**D**, **E**) The CGRP-induced ERK activation of the full time course, expressed in fold-decrease over vehicle of pERK1 (**D**) and pERK2 (**E**) is significantly reduced in PP2-treated cells. Thus, the CGRP-mediated ERK activation is Src-dependent in HEK cells. n=5, *=p<0.05 and **=p<0.01 ***=p<0.001 compared to vehicle-treated cells at the same time point.

3.5 CGRP-Induced ERK Activation is not Promoted by Endosomal Signalosome

ECE-1-dependent degradation of SP (Roosterman et al., 2007) and CGRP (Padilla et al., 2007) only occurs at acidic pH and can be prevented by inhibiting the proteolytic activity of ECE-1 or by preventing endosomal acidification. This degradation induces disruption of the endosomal complexes comprising SP/NK_1R/β-arrestin and CGRP/CLR•RAMP1/β-arrestin to promote recycling of NK_1R and CLR•RAMP1 to the cell-surface (Padilla et al., 2007; Roosterman et al., 2007), and also terminates SP-induced, β-arrestin-dependent ERK signalling (Cottrell et al., 2009). It was hypothesised that by inhibiting ECE-1 or preventing endosomal acidification, the endosomal complex of CGRP/CLR•RAMP1/β-arrestin would be stabilised and thus, promote sustained CGRP-induced ERK activation.

3.5.1 CGRP-Induced ERK Activation is not Regulated by Proteolytic Activity of ECE-1

To determine if ECE-1 regulates CGRP-induced ERK signalling a specific ECE-1 inhibitor, SM-19712 (Umekawa et al., 2000), was used. HEK-CLR•RAMP1 cells were serum-starved, all incubated with AG1478, as a large proportion of the CGRP-induced ERK signalling is ErbB1-dependent. Then by blocking this pathway only G protein-dependent ERK activation would be observed. Cells were also incubated with vehicle (DDW) or SM-19712, stimulated with CGRP (10 min), washed and incubated in CGRP-free medium ± SM-19712 (0-110 min). Levels of pERK1, pERK2 and ERK2 were quantified by Western blotting. In unstimulated cells, levels of pERK1 and 2 were similarly low (**Fig. 3.5**). CGRP (10 min) similarly increased levels of pERK1 and 2 in both vehicle- and SM-19712-treated cells (**Fig. 3.5B**, 15.8±3.4 (vehicle) versus 14.7±4.3 (SM-19712) for pERK1 and 9.9±1.9 (vehicle) versus 9.8±4.2 (SM-19712) for pERK2; fold-increase at 10 min compared to basal). In vehicle-treated cells, levels of pERK1 and 2 slowly returned to basal levels following removal of CGRP. Incubation with the ECE-1 inhibitor, SM-19712 had no effect on the magnitude or the duration of CGRP-induced ERK activation (**Fig. 3.5D** and **E**, 35.1±9.0% (vehicle) versus 42.8±11.8% (SM-19712) for pERK1 and 39.9±12.2% (vehicle) versus 46.2±12.7% (SM-19712) for pERK2; at 110 min of % of maximal response). Furthermore, SM-19712 was not affecting the basal levels of pERK1 and 2 compared to vehicle-treated cells (**Fig. 3.5C**). Thus, the proteolytic activity of ECE-1 does not regulate CGRP-induced ERK activation.

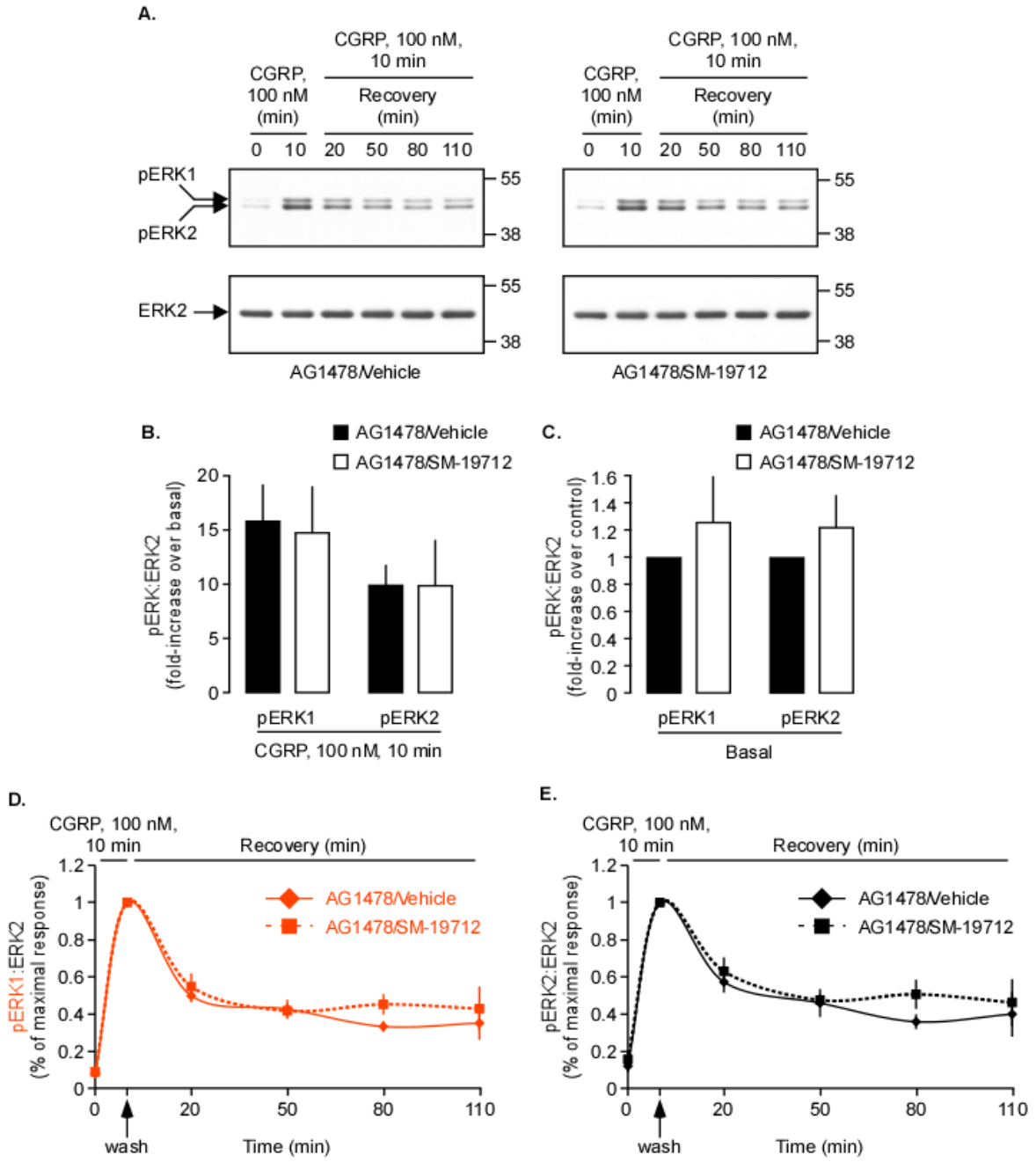

Figure 3.5 **ECE-1 does not affect CGRP-induced ERK activation.** (**A**) Serum-starved HEK-CLR•RAMP1 cells were incubated with AG1478 (1 µM) and with vehicle or SM-19712 (10 µM), stimulated with CGRP (100 nM, 10 min), washed, incubated in CGRP-free medium ± SM-19712 (0-110 min) and levels of pERK1, pERK2 and ERK2 determined by Western blotting. Blots were quantified using ImageJ and ratio of pERK1:ERK2 and pERK2:ERK2 calculated. Representative blots are shown. (**B**) The maximal CGRP-induced ERK phosphorylation, expressed in fold-increase over basal, show no difference in vehicle- compared to SM-19712-treated cells. (**C**) Basal levels of pERK1 and 2 are expressed in fold-increase over vehicle-treated cells. The effect of SM-19712 on the basal of pERK1 and 2 shows no significant difference compared to vehicle-treated cells. (**D**, **E**) The CGRP-induced ERK activation of the full time course, expressed in % maximal of response (10 min) of ERK1 (**D**) and ERK2 (**E**), is similar in both vehicle- and SM-19712-treated cells. Thus, CGRP does not induce ERK activation dependent on the proteolytic activity of ECE-1 in HEK cells. n=4.

3.5.2 Inhibition of Endosomal Acidification does not Affect CGRP-Induced ERK Activation

It has previously been shown that ECE-1-depedent degradation of SP and CGRP only occurs at endosomal pH (Johnson et al., 1999; Padilla et al., 2007). Preventing endosomal acidification with bafilomycin A1, inhibits ECE-1-dependent cleavage of SP, the recycling of NK_1R to the cell-surface (Roosterman et al., 2007) and sustains SP-induced, β-arrestin-dependent ERK activation (Cottrell et al., 2009). To determine the effect of endosomal acidification on CGRP-induced ERK activation, bafilomycin A_1 a vacuolar H^+-ATPase inhibitor was used (Gagliardi et al., 1999). HEK-CLR•RAMP1 cells were all treated with AG1478, to only look at the G protein-dependent ERK activation. Cells were then incubated with vehicle (DMSO) or bafilomycin A_1, stimulated with CGRP (10 min), washed and incubated in CGRP-free medium ± inhibitors (0-110 min). Levels of pERK1, pERK2 and ERK2 were quantified by Western blotting. In unstimulated cells, levels of pERK1 and 2 were similarly low (**Fig. 3.6**). CGRP (10 min) similarly increased levels of pERKs in both vehicle- and bafilomycin A_1-treated cells (**Fig. 3.6B**, 6.1±3.5 (vehicle) versus 5.4±2.1 (bafilomycin A_1) for pERK1 and 3.4±1.4 (vehicle) versus 3.5±0.8 (bafilomycin A_1) for pERK2; fold-increase at 10 min compared to basal). In vehicle-treated cells, levels of pERK1 and 2 slowly returned to basal levels following removal of CGRP. Incubation with bafilomycin A_1 had no effect on the magnitude or the duration of CGRP-induced ERK activation (**Fig. 3.6D** and **E**, 24.8±4.2% (vehicle) versus 37.8±6.3% (bafilomycin A_1) for pERK1 and 28.8±2.9% (vehicle) versus 37.9±5.6% (bafilomycin A_1) for pERK2; at 110 min of % of maximal response). Although, the inhibition of endosomal acidification does not have an effect on CGRP-induced ERK activation, bafilomycin A_1 significantly increases the basal level of pERK1 and 2 (**Fig. 3.6C**, 1.8±0.3 (pERK1) and 1.7±0.2 (pERK2) fold-increase over control). Thus, the effect of bafilomycin A_1 on CGRP-induced ERK activation required further investigation.

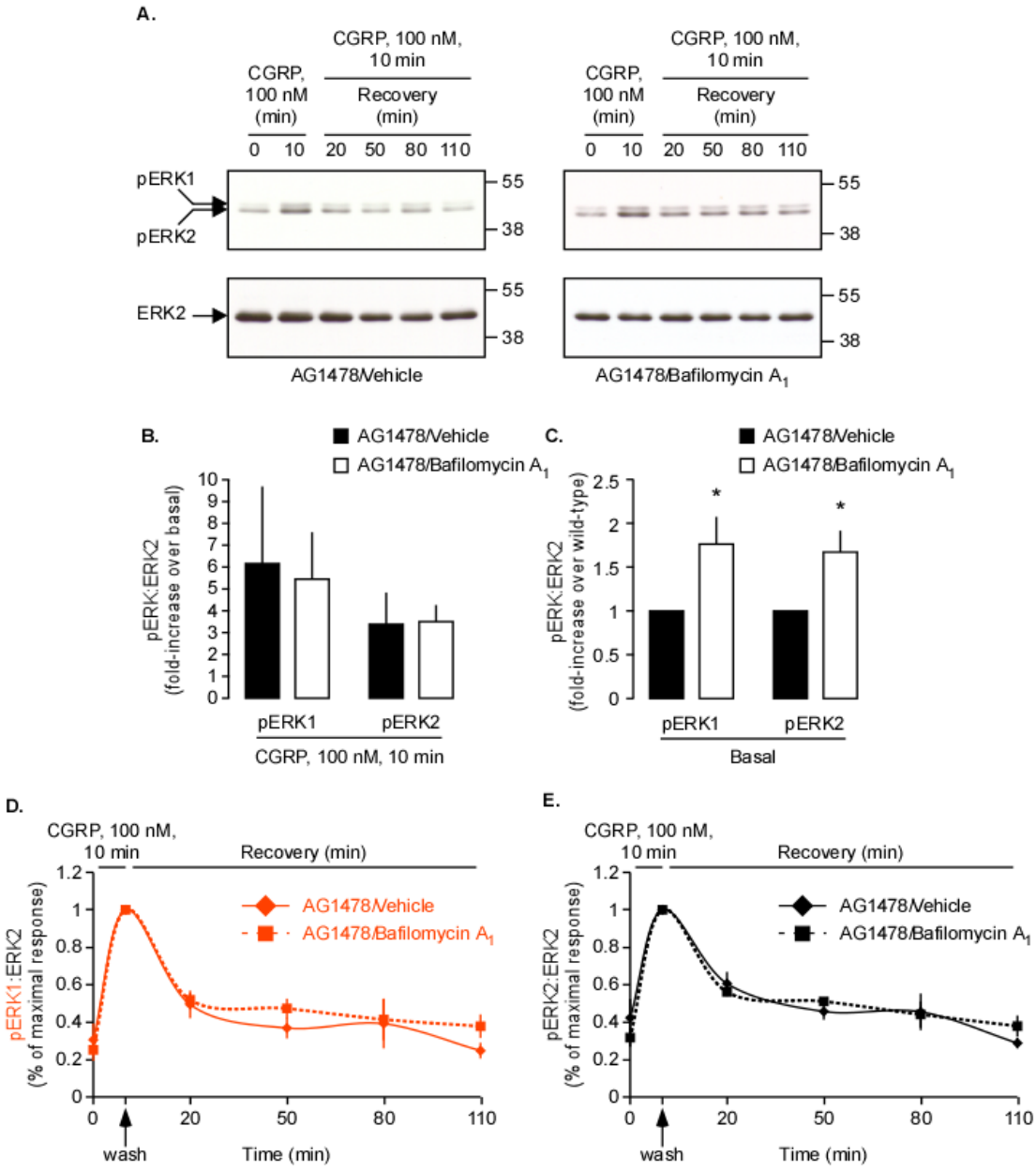

Figure 3.6 **Inhibition of endosomal acidification does not affect CGRP-induced ERK activation.** (**A**) Serum-starved HEK-CLR•RAMP1 cells were incubated with AG1478 (1 µM) and with vehicle or bafilomycin A_1 (1 µM), stimulated with CGRP (100 nM, 10 min), washed, incubated in CGRP-free medium ± bafilomycin A_1 (0-110 min) and levels of pERK1, pERK2 and ERK2 determined by Western blotting. Blots were quantified using ImageJ and ratio of pERK1:ERK2 and pERK2:ERK2 calculated. Representative blots are shown. (**B**) The maximal CGRP-induced ERK phosphorylation, expressed in fold-increase over basal, shows no difference in vehicle- compared to bafilomycin A_1-treated cells. (**C**) Basal levels of pERK1 and 2 are expressed as fold-increase over vehicle-treated cells. The effect of bafilomycin A_1 on the basal of pERK1 and 2 shows a significant increase compared to vehicle-treated cells. (**D**, **E**) The CGRP-induced ERK activation of the full time course, expressed in % maximal of response (10 min) of ERK1 (**D**) and ERK2 (**E**), is similar in both vehicle- and bafilomycin A_1-treated cells. Thus, CGRP does not induce ERK activation dependent on the endosomal acidification in HEK cells, which suggests that CGRP does not induce endosomal signalling of ERK. n=4, *=p<0.05 compared to vehicle-treated cells at the same time point.

3.5.3 β-arrestin1 is not Involved in CGRP-Induced ERK Activation

It is now clear that β-arrestin recruits many catalytically active proteins, which then induce ERK activation ((DeFea et al., 2000a; DeFea et al., 2000b) and reviewed in (Luttrell and Gesty-Palmer, 2010; Murphy et al., 2009)). Moreover, ECE-1 has been shown to regulate the SP-induced β-arrestin-dependent ERK activation (Cottrell et al., 2009). To further investigate the mechanism by which CGRP can induce ERK activation, a β-arrestin1 mutant was used. HEK cells were transiently transfected with CLR•RAMP1 and β-arrestin1 WT or β-arrestin1 P91G P121E (a mutant that is unable to bind Src (Luttrell et al., 1999)). This mutant has two main actions, first it prevents the internalisation of the receptor, because Src phosphorylates dynamin to facilitate internalisation (Ahn et al., 1999); and secondly, it prevents β-arrestin-dependent signalling, as Src activates MAPK while bind to β-arrestin (Luttrell et al., 1999). HEK-CLR•RAMP1 cells were stimulated with CGRP (0-10 min), washed and incubated in CGRP-free medium (0-50 min). Levels of pERK1, pERK2 and ERK2 were quantified by Western blotting. In unstimulated cells basal levels of pERK1 and 2 were similarly low (**Fig. 3.7**). CGRP (10 min) similarly increased levels of pERK1 and 2 in both cell types (**Fig. 3.7B**, 9.4±2.9 (WT) versus 11.1±2.0 (mutant) for pERK1 and 3.6±1.1 (WT) versus 3.9±0.6 (mutant) for pERK2; fold-increase at 10 min compared to basal). In vehicle-treated cells, levels of pERK1 and 2 slowly returned to basal levels following removal of CGRP. There was no significant difference in the magnitude or duration of ERK activation in β-arrestin1 WT- or β-arrestin1 P91G P121E-expressing cells (**Fig. 3.7D** and **E**, 39.5±12.1% (WT) versus 31.2±4.7% (mutant) for pERK1 and 52.8±9.7% (WT) versus 51.4±5.6% (mutant) for pERK2; at 110 min of % of maximal response). Moreover, β-arrestin1 P91G P121E expression did not have an effect on the basal level of pERK1 and 2 compared to β-arrestin1 WT-expressing cells (**Fig. 3.7C**). Thus, CGRP does not induce ERK activation dependent on β-arrestins.

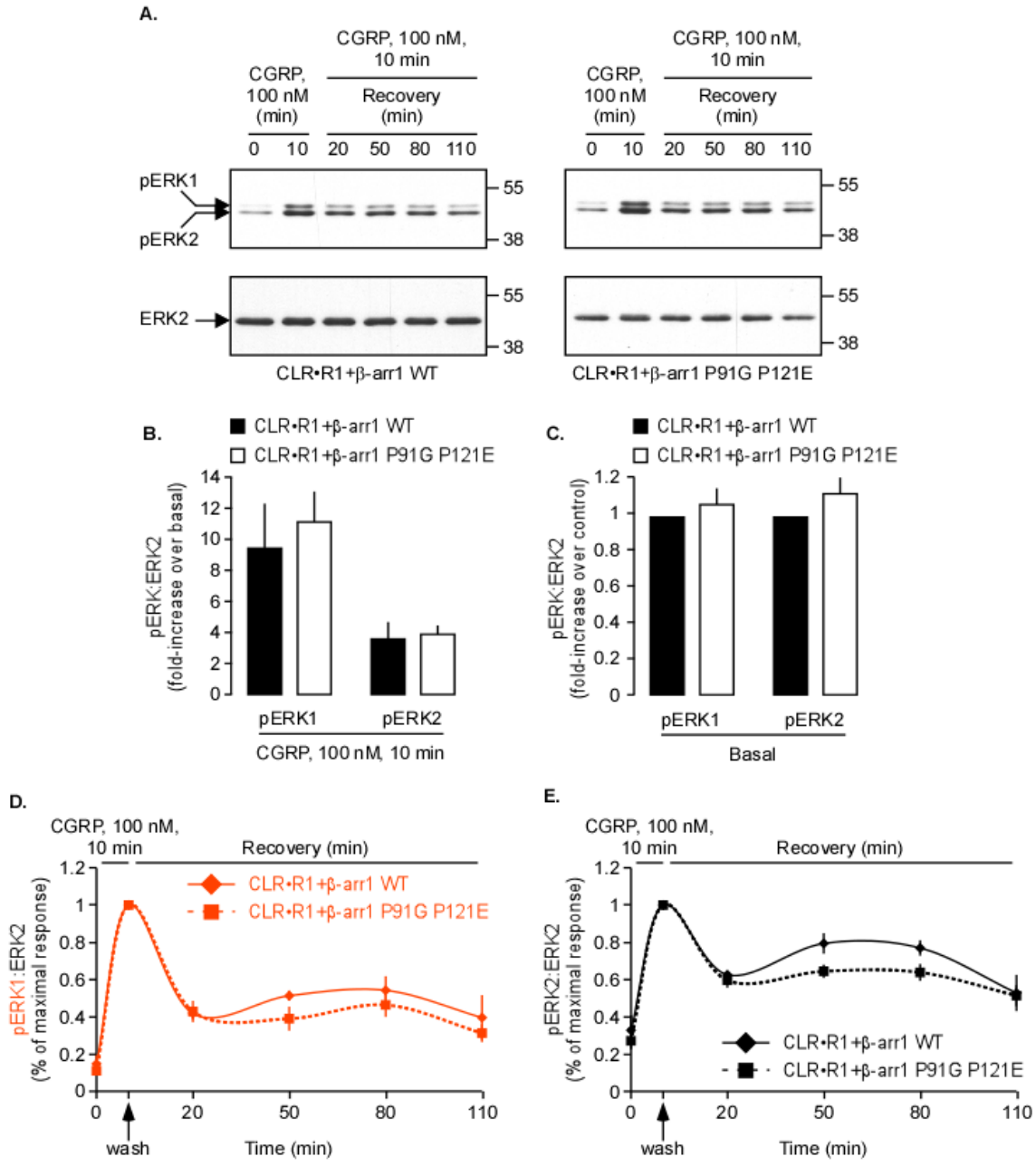

Figure 3.7 **β-arrestin1 does not affect CGRP-induced ERK activation.** (**A**) Serum-starved HEK-FLP cells were transfected with CLR•RAMP1 (CLR•R1) and β-arrestin1 WT (β-arr1 WT) or β-arrestin1 P91G P121E (β-arr1 P91G P121E). Cells were then stimulated with CGRP (100 nM, 0-10 min), washed, incubated in CGRP-free medium (0-110 min) and levels of pERK1, pERK2 and ERK2 determined by Western blotting. Blots were quantified using ImageJ and ratio of pERK1:ERK2 and pERK2:ERK2 calculated. A representative blot is shown. (**B**) The maximal CGRP-induced ERK phosphorylation, expressed in fold-increase over basal, show no difference in β-arrestin1 WT- compared to β-arrestin1 mutant-expressing cells. (**C**) Basal levels of pERK1 and 2 are expressed in fold-increase over β-arrestin1 WT-expressing cells. Expression of β-arrestin1 P91G P121E on the basal of pERK1 and 2 shows no significant difference compared to β-arrestin1 WT-expressing cells. (**D**, **E**) The CGRP-induced ERK activation of the full time course, expressed in % maximal of response of ERK1 (**D**) and ERK2 (**E**), is similar in both β-arrestin1 WT- and β-arrestin1 mutant-expressing cells. Thus, CGRP does not induce ERK activation depending on β-arrestin1 in HEK cells. n=3.

3.6 CGRP-Induced ERK Activation is Protein Kinase A-Dependent

GPCRs coupled to $G\alpha_s$ stimulate the activation of AC to promote the increase of intracellular cAMP levels (reviewed in (Gilman, 1984a; Gilman, 1984b)) that subsequently activates PKA (Brostrom et al., 1970; Gill and Garren, 1971; Tao et al., 1970). GPCRs that activate $G\alpha_s$ proteins have also been shown to regulate the ERK1-2 module, either by promoting activation of ERK via activation of B-Raf pathway, or by promoting inhibition of ERK activation via inhibition of Raf-1. As CLR•RAMP1 has been shown to be coupled to $G\alpha_s$ (activation of adenylate cyclase and accumulation of cAMP) (Aiyar et al., 1999; Van Valen et al., 1990), it was hypothesized that CGRP would induce ERK phosphorylation via the cAMP/PKA pathway. To determine whether CGRP induces cAMP/PKA-dependent ERK activation, HEK-CLR•RAMP1 cells were incubated with vehicle (DMSO) or H-89, a PKA inhibitor (Chijiwa et al., 1990). Cells were stimulated with CGRP (0-10 min), washed and incubated in CGRP-free medium ± H-89 (0-50 min). Levels of pERK1, pERK2 and ERK2 were quantified by Western blotting. In unstimulated cells, levels of pERK1 and 2 were similarly low (**Fig. 3.8**). CGRP (10 min) caused a prompt increase in levels of pERK1 and 2 in both vehicle- and H-89-treated cells. However, the increase in H-89-treated cells was significantly reduced compared to vehicle-treated cells (**Fig. 3.8B**, 10.2±0.7 (vehicle) versus 3.5±0.7 (H-89) for pERK1 and 5.4±0.5 (vehicle) versus 2.6±0.4 (H-89) for pERK2; fold-increase at 10 min compared to basal). Indeed, when expressed in fold-decrease over vehicle-treated cells, H-89 significantly reduced levels of pERK1 and 2 at all time points examined (**Fig. 3.8D** and **E**). Basal levels of pERK1 and 2 show not significant difference between vehicle- and H-89-treated cells (**Fig. 3.8C**). Thus, CGRP induces ERK activation in a PKA-dependent manner in HEK cells.

H-89 has been reported to have non-specific activities by inhibiting other kinases (reviewed in (Lochner and Moolman, 2006)). Therefore the effects of a lower concentration of H-89 (10 µM) was also examined (**Fig. 3.9**). In unstimulated vehicle- and H-89-treated cells, levels of pERK1 and 2 were similarly low. CGRP (10 min) caused a prompt increase in levels of pERK1 and 2 in both vehicle- and H-89-treated cells. However, the increase in H-89-treated cells was reduced compared to vehicle-treated cells (**Fig. 3.9B**, 10.6±2.9 (vehicle) versus 6.0±1.3 (H-89) for pERK1 and 8.1±2.3 (vehicle) versus 4.5±0.9 (H-89) for pERK2; fold-increase at 10 min compared to basal). Indeed, when expressed in fold-decrease over vehicle-treated cells, H-89 significantly reduced levels of pERK1 and 2 at almost all time points examined (**Fig. 3.9D** and **E**). Even though, basal levels of pERK1 and 2 show a slight increase in H-89- compared to vehicle-treated cells (**Fig. 3.9C**, 1.5±0.3 (pERK1) and 1.5±0.2 (pERK2) fold-increase over control), CGRP-induced ERK2 activation is PKA-dependent in HEK cells.

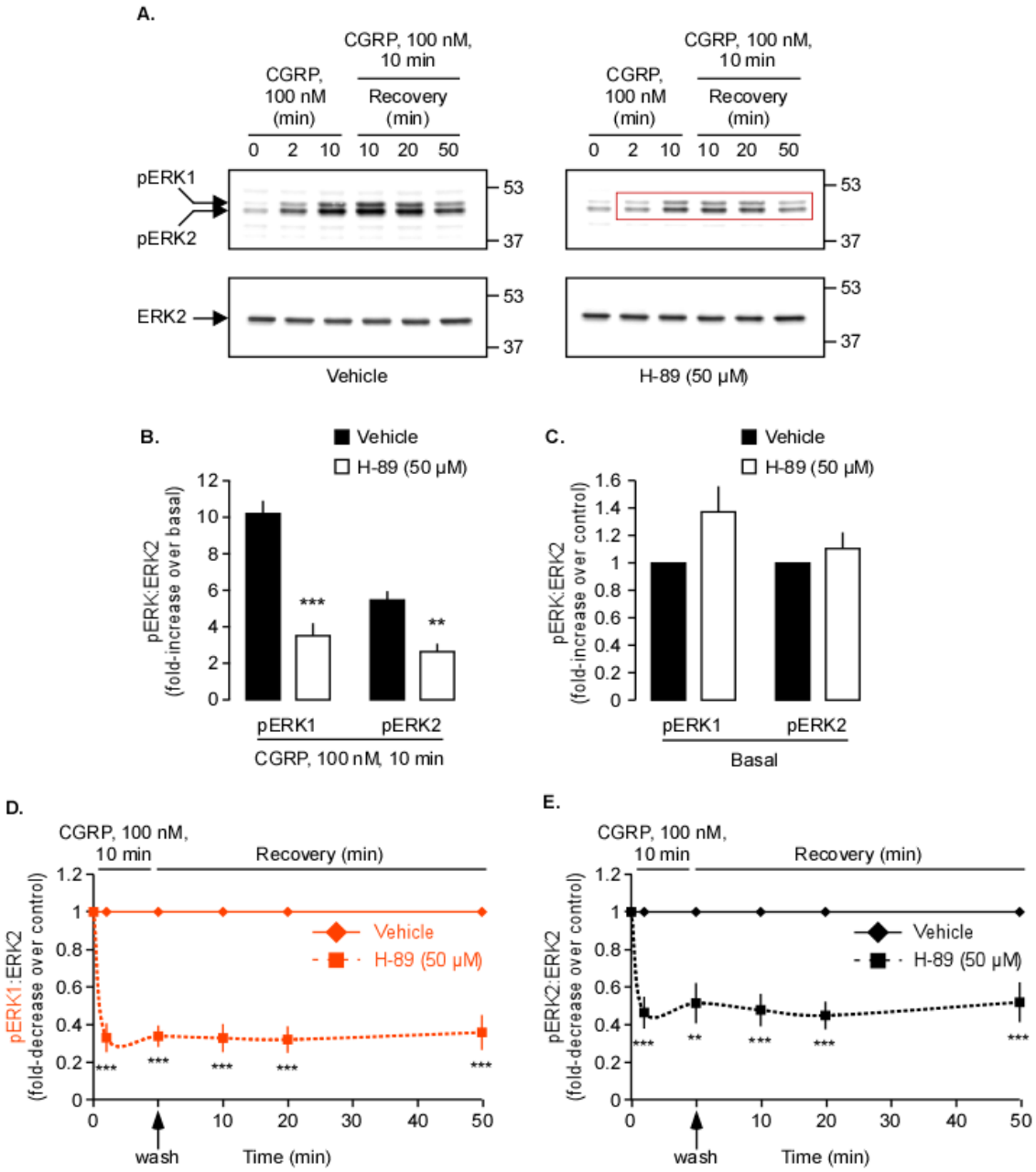

Figure 3.8 **CGRP-induced ERK activation is PKA-dependent.** (**A**) Serum-starved HEK-CLR•RAMP1 cells were incubated with vehicle (DMSO) or H-89 (50 µM), stimulated with CGRP (100 nM, 0-10 min), washed, incubated in CGRP-free medium ± H-89 (0-50 min) and levels of pERK1, pERK2 and ERK2 determined by Western blotting. Blots were quantified using ImageQuantTL and ratio of pERK1:ERK2 and pERK2:ERK2 calculated. Representative blots are shown. The red box highlights the difference between vehicle- and H-89-treated cells. (**B**) The maximal CGRP-induced ERK phosphorylation, expressed in fold-increase over basal, is higher in vehicle- compared to H-89-treated cells. (**C**) Basal levels of pERK1 and 2 are expressed in fold-increase over vehicle-treated cells. The effect of H-89 on the basal of pERK1 and 2, show no significant difference compared to vehicle-treated cells. (**D**, **E**) The CGRP-induced ERK activation of the full time course, expressed in fold-decrease over vehicle of pERK1 (**D**) and pERK2 (**E**) is significantly reduced in H-89-treated cells. Thus, the CGRP-mediated ERK activation is PKA-dependent in HEK cells. n=6, **=p<0.01 and ***=p<0.001 compared to vehicle-treated cells at the same time point.

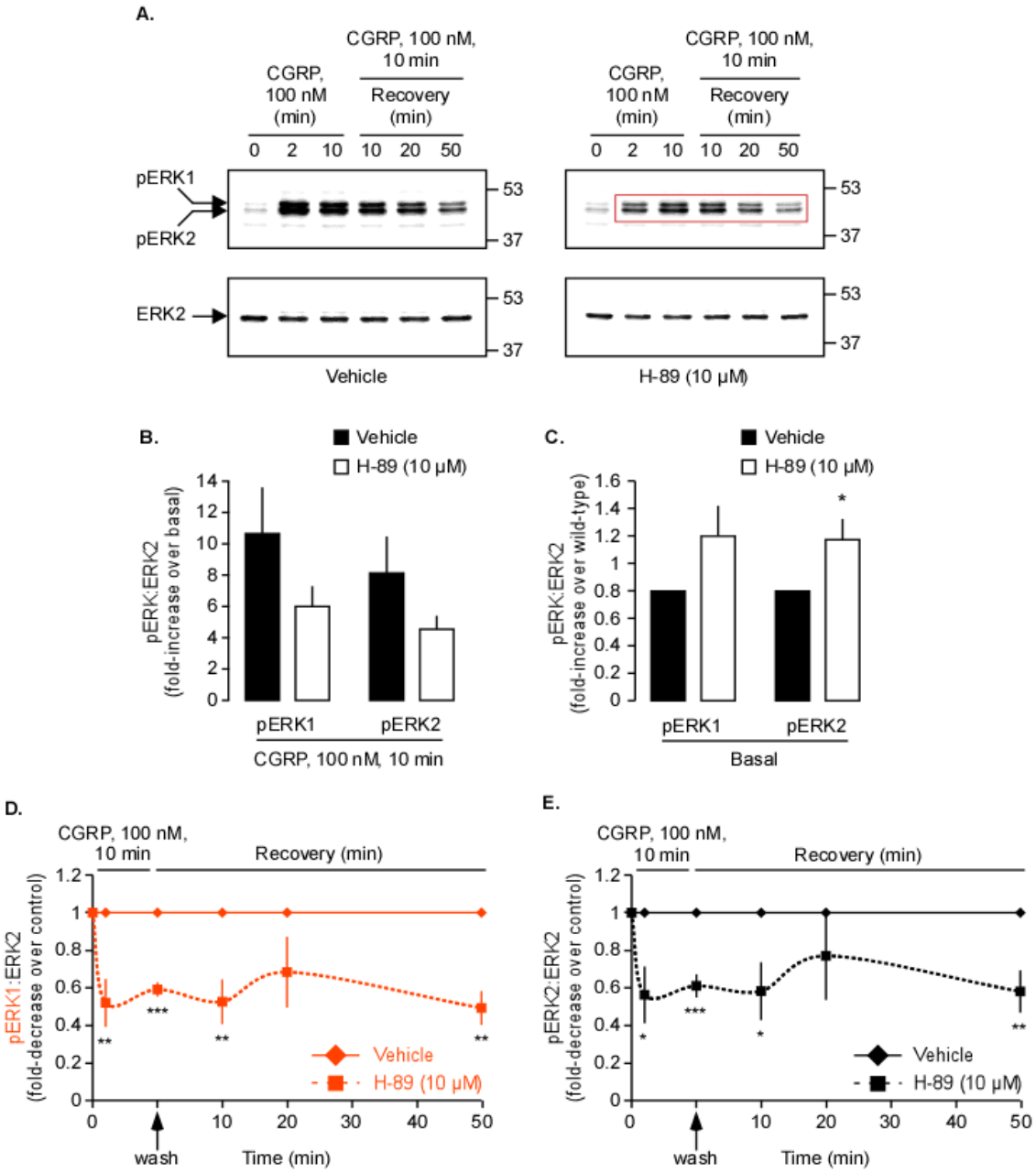

Figure 3.9 **Effect of lower concentration of H-89 on CGRP-induced ERK activation.** (**A**) Serum-starved HEK-CLR•RAMP1 cells were incubated with vehicle (DMSO) or H-89 (10 µM), stimulated with CGRP (100 nM, 0-10 min), washed, incubated in CGRP-free medium ± H-89 (0-50 min) and levels of pERK1, pERK2 and ERK2 determined by Western blotting. Blots were quantified using ImageQuantTL and ratio of pERK1:ERK2 and pERK2:ERK2 calculated. Representative blots are shown. The red box highlights the difference between vehicle- and H-89-treated cells. (**B**) The maximal CGRP-induced ERK phosphorylation, expressed in fold-increase over basal, is higher in vehicle- compared to H-89-treated cells. (**C**) Basal levels of pERK1 and 2 are expressed in fold-increase over vehicle-treated cells. The effect of H-89 on the basal of pERK1 and 2 shows an increase compared to vehicle-treated cells. (**D**, **E**) The CGRP-induced ERK activation of the full time course, expressed in fold-decrease over vehicle of pERK1 (**D**) and pERK2 (**E**) is significantly reduced in H-89-treated cells. Thus, the CGRP-mediated ERK activation is PKA-dependent in HEK cells. n=4, *=p<0.05, **=p<0.01 and ***=p<0.001 compared to vehicle-treated cells at the same time point.

3.7 Effect of the PKC/PLC Pathway in the CGRP-Induced ERK Activation

Stimulation of $G\alpha_{q/11}$ leads to the activation of PLC (reviewed in (Rhee, 2001)), which in turn catalyses the hydrolysis of phosphatidylinositol 4,5-biphosphate into two second messengers: IP_3 and DAG. IP_3 induces mobilisation of Ca^{2+} from endoplasmic reticulum (ER) (Putney, 1986). Together Ca^{2+} and DAG act in synergy to activate PKC. Once activated, PKC phosphorylates Raf kinase inhibitor protein (RKIP), which inhibits Raf-1-mediated phosphorylation of mitogen-activated protein kinase kinase (MEK) by binding to Raf-1. The PKC-mediated phosphorylation of RIKP leads to the dissociation of the complex RKIP/Raf-1 and thereby to the activation of MEK and ERK (Corbit et al., 2003). As CGRP has been shown to induce Ca^{2+} mobilisation through $G\alpha_{q/11}$-mediated activation of PLC-β1 in OHS-4 cells (human bone cell line) (Drissi et al., 1998), it was expected that CGRP promotes ERK activation through the PKC/PLC/Ca^{2+} pathway. To determine if the PKC/PLC/Ca^{2+} pathway is involved in CGRP-induced ERK activation specific inhibitors of this pathway were used.

3.7.1 CGRP-Induced ERK Activation is PLC-Independent

Activation of most PKC isoforms requires upstream activation of PLC (reviewed in (Zeng et al., 2012)). To determine if PLC is involved in the CGRP-induced ERK activation, HEK-CLR•RAMP1 cells were incubated with vehicle (DMSO) or U-73122, a pan inhibitor of PLC (Bleasdale et al., 1990). Cells were stimulated with CGRP (0-10 min), washed and incubated in CGRP-free medium ± U-73122 (0-50 min). Levels of pERK1, pERK2 and ERK2 were quantified by Western blotting. In unstimulated vehicle- and U-73122-treated cells, levels of pERK1 and 2 were similarly low (**Fig. 3.10**). CGRP (10 min) caused a prompt increase in levels of pERK1 and 2 similarly in both vehicle- and U-73122-treated cells (**Fig. 3.10B**, 4.3±1.0 (vehicle) versus 5.1±2.6 (U-73122) for pERK1 and 4.2±0.8 (vehicle) versus 4.0±1.6 (U-73122) for pERK2; fold-increase at 10 min compared to basal). Indeed, when expressed in % of maximal response, U-73122 had no effect on ERK activation compared to vehicle-treated cells (**Fig. 3.10D** and **E**). U-73122 does not affect the basal levels of pERK1 and 2, compared to vehicle-treated cells (**Fig. 3.10C**). Thus, CGRP-induced ERK activation does not require PLC.

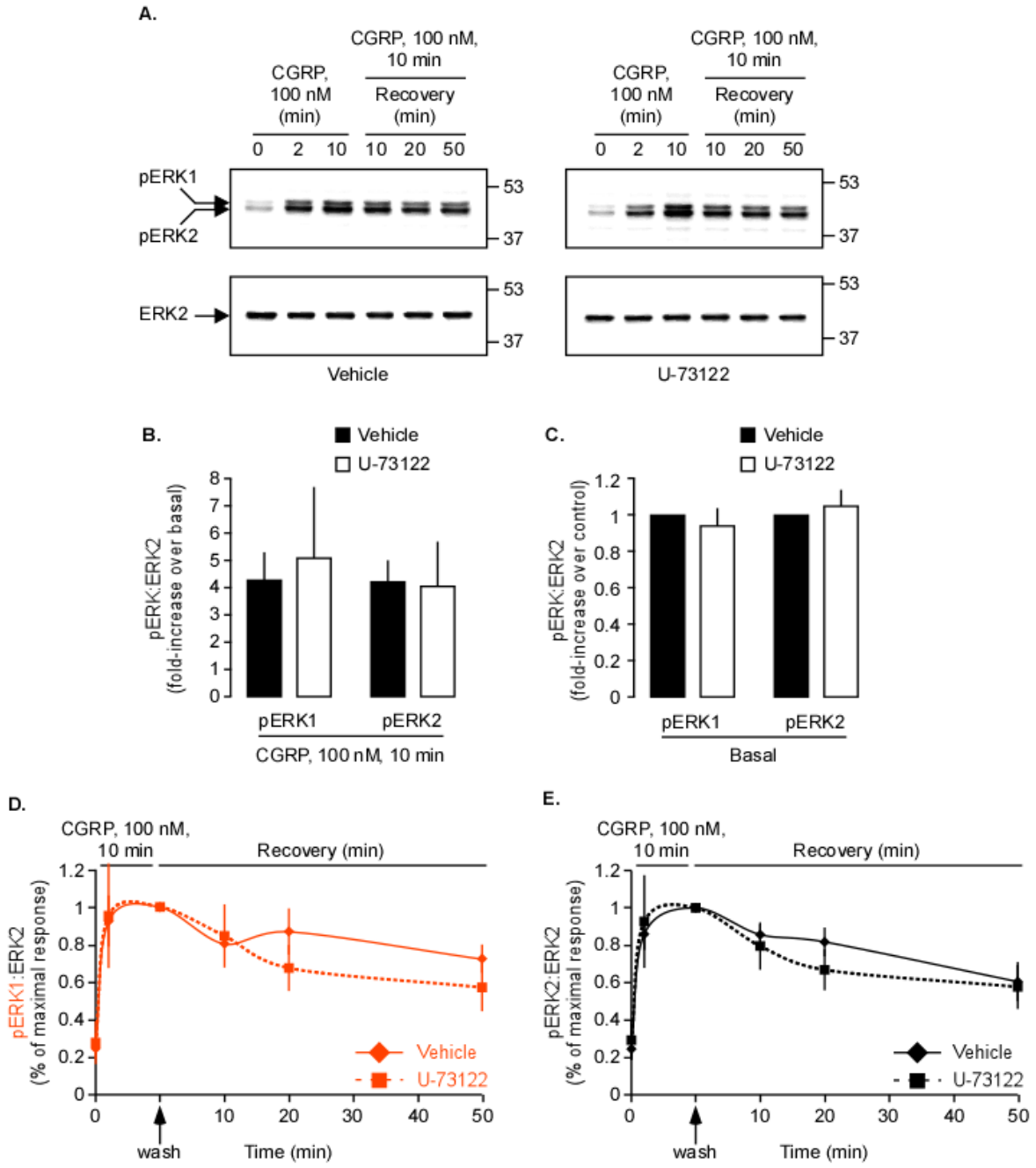

Figure 3.10 **CGRP-induced ERK activation is not PLC-dependent.** (**A**) Serum-starved HEK-CLR•RAMP1 cells were incubated with vehicle or U-73122 (100 µM), stimulated with CGRP (100 nM, 0-10 min), washed, incubated in CGRP-free medium ± U-73122 (0-50 min) and levels of pERK1, pERK2 and ERK2 determined by Western blotting. Blots were quantified using ImageQuantTL and ratio of pERK1:ERK2 and pERK2:ERK2 calculated. Representative blot are shown. (**B**) The maximal CGRP-induced ERK phosphorylation, expressed in fold-increase over basal show no difference in vehicle- compared to U-73122-treated cells. (**C**) Basal levels of pERK1 and 2 are expressed in fold-increase over vehicle-treated cells. The effect of U-73122 on the basal of pERK1 and 2 shows no difference compared to vehicle-treated cells. (**D**, **E**) The CGRP-induced ERK activation of the full time course, expressed in % of maximal response of pERK1 (**D**) and pERK2 (**E**), shows no difference between vehicle- and U-73122-treated cells, suggesting that CGRP activates ERK in PLC-independent manner in HEK cells. n=3.

3.7.2 Effect of PKC Inhibitors on the CGRP-Induced ERK Activation

To determine if CGRP induces PKC-dependent ERK activation, HEK-CLR•RAMP1 cells were incubated with vehicle (DMSO) or Gö6976, a conventional PKC (cPKC) isoform inhibitor (Martiny-Baron et al., 1993). Cells were stimulated with CGRP (0-10 min), washed and incubated in CGRP-free medium ± Gö6976 (0-50 min). Levels of pERK1, pERK2 and ERK2 were quantified by Western blotting. In unstimulated cells, levels of pERK1 and 2 were similarly low (**Fig. 3.11**). CGRP (10 min) caused a prompt increase in levels of pERK1 and 2 in both vehicle- and Gö6976-treated cells. However, the increase in Gö6976-treated cells was significantly reduced compared to vehicle-treated cells (**Fig. 3.11B**, 9.0±1.9 (vehicle) versus 4.0±0.9 (Gö6976) for pERK1 and 3.2±0.3 (vehicle) versus 2.2±0.2 (Gö6976) for pERK2; fold-increase at 10 min compared to basal). Indeed, when expressed in fold-decrease over vehicle-treated cells, Gö6976 reduced levels of pERK1 and 2 significantly only after the initial stimulation (2 and 10 min) (**Fig. 3.11D** and **E**). This result implicates cPKC isoforms in the early stages of CGRP-induced ERK activation. However, Gö6976 significantly increases the basal levels of pERK1 and 2 compared to vehicle-treated cells (**Fig. 3.11C**, 2.0±0.1 (pERK1) and 1.7±0.0 (pERK2) fold-increase over control). Thus, involvement of cPKC in CGRP-induced ERK activation required further investigation.

Additionally, a pan inhibitor of PKC isoforms, Gö6983 (Gschwendt et al., 1996), was also used. HEK-CLR•RAMP1 cells were incubated with vehicle (DMSO) or Gö6983. Cells were stimulated with CGRP (0-10 min), washed and incubated in CGRP-free medium ± Gö6983 (0-50 min). Levels of pERK1, pERK2 and ERK2 were quantified by Western blotting. In unstimulated vehicle- and Gö6983-treated cells, levels of pERK1 and 2 were similarly low (**Fig. 3.12**). CGRP (10 min) caused similarly a prompt increase in levels of pERK1 and 2 in both vehicle- and Gö6983-treated cells (**Fig. 3.12B**, 23.4±10.2 (vehicle) versus 18.5±7.6 (Gö6983) for pERK1 and 16.9±6.4 (vehicle) versus 14.8±6.2 (Gö6983) for pERK2; fold-increase at 10 min compared to basal). In vehicle-treated cells, levels of pERK1 and 2 slowly returned to basal levels following removal of CGRP. Incubation with the PKC inhibitor, Gö6983 had no significant effect on CGRP-induced ERK activation (**Fig. 3.12D** and **E**). These data show that PKC is not involved in CGRP-induced ERK activation. However, as Gö6983 significantly reduces the basal levels of pERK, compared to the vehicle (**Fig. 3.12C**, 0.7±0.0 (pERK1) and 0.7±0.0 (pERK2) fold-decrease over control), then, this result is again difficult to interpret. However, together the data obtained with Go6976 and Go6983 imply that PKC has little, if any effect on CGRP-induced ERK activation.

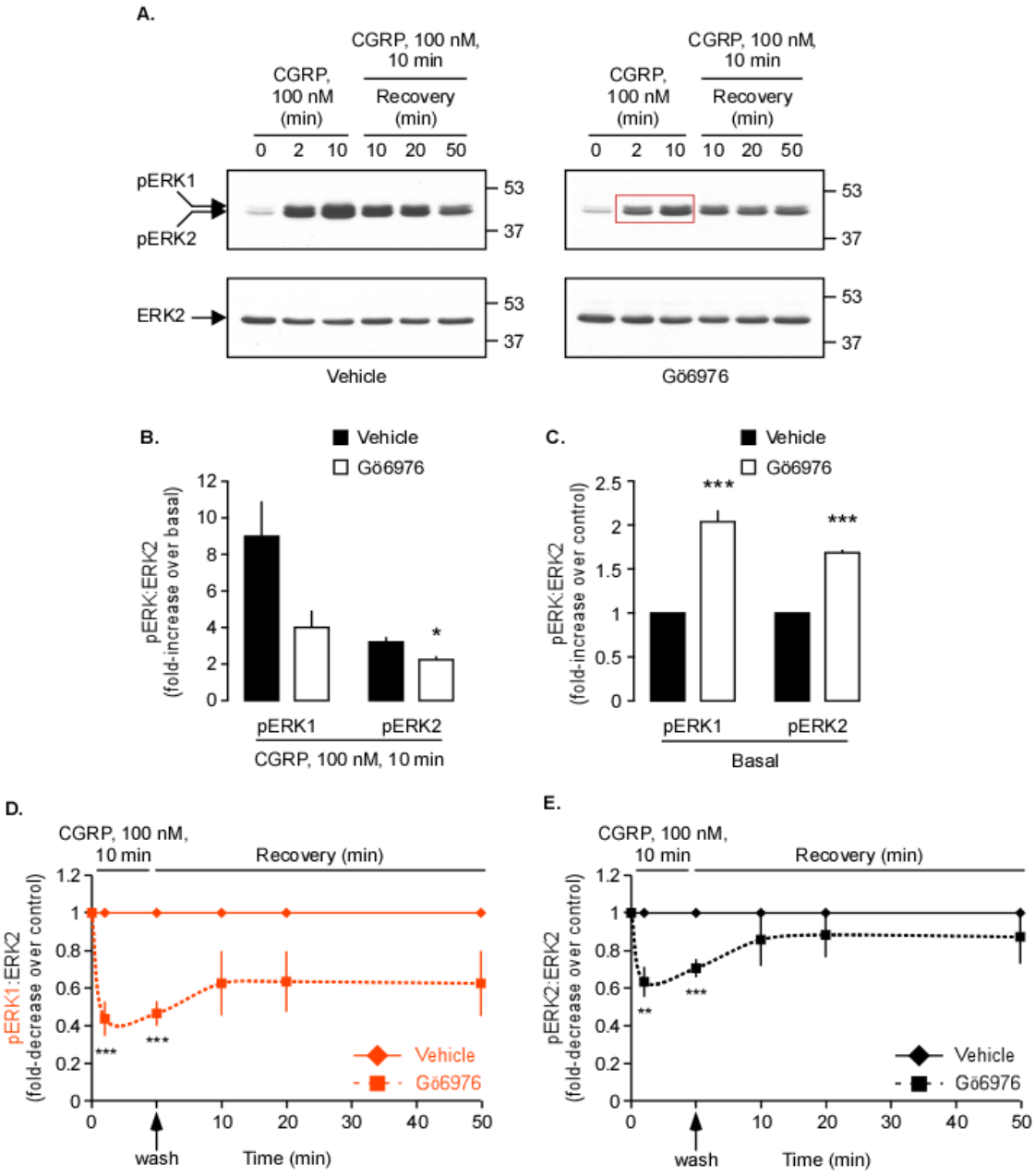

Figure 3.11 **CGRP-induced ERK activation is PKC-dependent.** (**A**) Serum-starved HEK-CLR•RAMP1 cells were incubated with vehicle (DMSO) or Gö6976 (10 µM), stimulated with CGRP (100 nM, 0-10 min), washed, incubated in CGRP-free medium ± Gö6976 (0-50 min) and levels of pERK1, pERK2 and ERK2 determined by Western blotting. Blots were quantified using ImageJ and ratio of pERK1:ERK2 and pERK2:ERK2 calculated. Representative blots are shown. The red box highlights the difference between vehicle- and Gö6976-treated cells. (**B**) The maximal CGRP-induced ERK phosphorylation, expressed in fold-increase over basal, is higher in vehicle- compared to Gö6976-treated cells. (**C**) Basal levels of pERK1 and 2 are expressed in fold-increase over vehicle-treated cells. The effect of Gö6976 on the basal of pERK1 and 2 shows a significant increase compared to vehicle-treated cells. (**D**, **E**) The CGRP-induced ERK activation of the full time course, expressed in fold-decrease over vehicle of pERK1 (**D**) and pERK2 (**E**) is significantly reduced in Gö6976-treated cells only at 2 and 10 min. Thus, CGRP partially activates ERK in PKC-dependent manner in HEK cells. n=4, *=p<0.05, **=p<0.01 and ***=p<0.001 compared to vehicle-treated cells at the same time point.

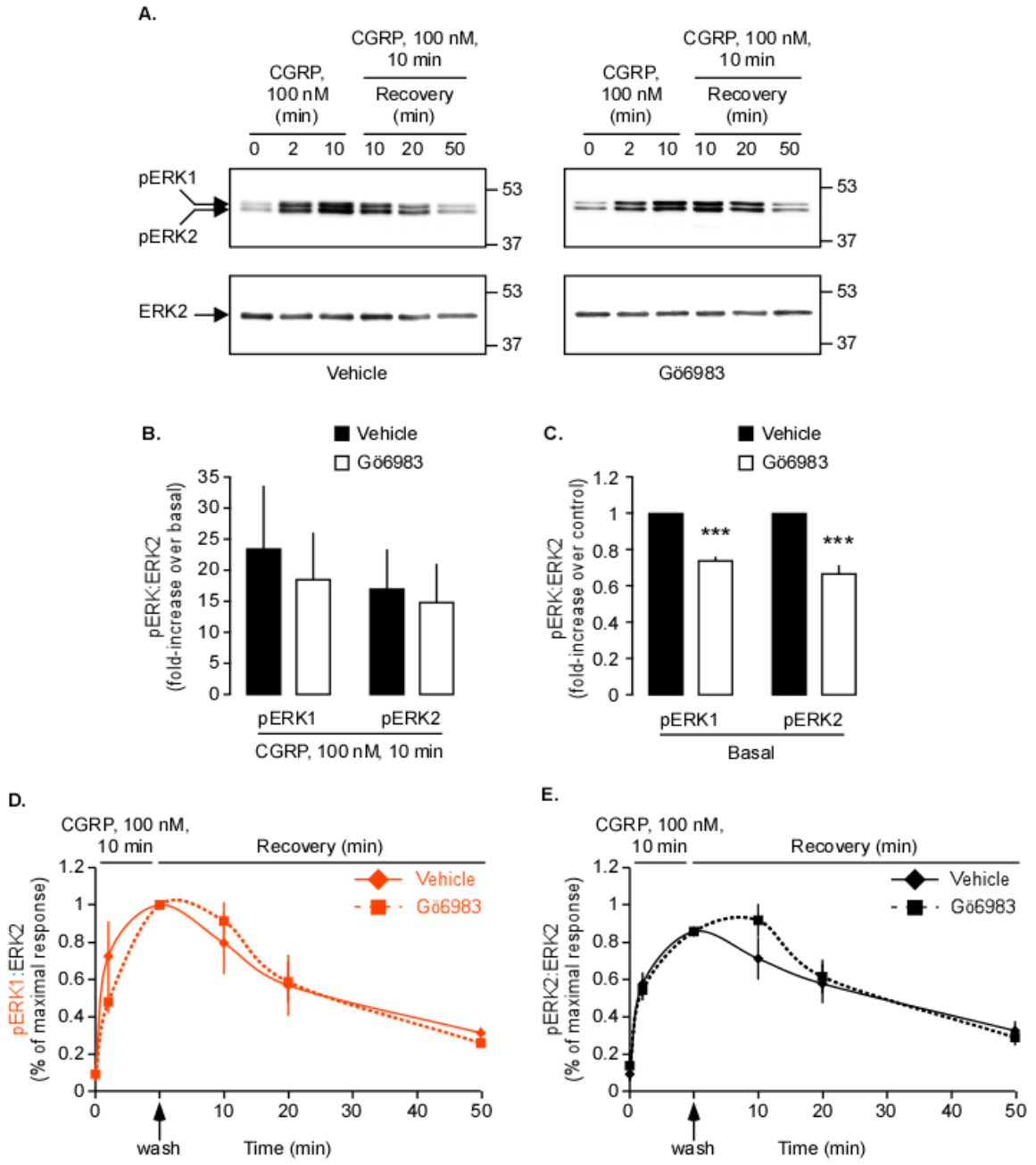

Figure 3.12 **CGRP-induced ERK activation is PKC-independent.** (**A**) Serum-starved HEK-CLR•RAMP1 cells were incubated with vehicle (DMSO) or Gö6983 (10 µM), stimulated with CGRP (100 nM, 0-10 min), washed, incubated in CGRP-free medium ± Gö6983 (0-50 min) and levels of pERK1, pERK2 and ERK2 determined by Western blotting. Blots were quantified using ImageQuantTL and ratio of pERK1:ERK2 and pERK2:ERK2 calculated. Representative blots are shown. (**B**) The maximal CGRP-induced ERK phosphorylation, expressed in fold-increase over basal, shows no difference in vehicle- compared to Gö6983-treated cells. (**C**) Basal levels of pERK1 and 2 are expressed in fold-increase over vehicle-treated cells. The effect of Gö6983 on the basal of pERK1 and 2 shows a significant decrease compared to vehicle-treated cells. (**D**, **E**) The CGRP-induced ERK activation of the full time course, expressed in fold-decrease over vehicle of pERK1 (**D**) and pERK2 (**E**), is similar in vehicle- and Gö6983-treated cells. Thus, CGRP activates ERK in PKC-independent manner in HEK cells. n=4, ***=p<0.001 compared to vehicle-treated cells at the same time point.

3.7.3 CGRP-Induced ERK Activation is Extracellular Ca^{2+}-Independent

Ca^{2+} is required for the activation of conventional PKC isoforms ((Ogawa et al., 1981) and reviewed in (Zeng et al., 2012)). To determine the effect of extracellular Ca^{2+}, HEK-CLR•RAMP1 cells were incubated in medium with Ca^{2+} (Ca^{2+}-plus) or without Ca^{2+} (Ca^{2+}-free). Cells were stimulated with CGRP (0-10 min), washed and incubated in CGRP-free Ca^{2+}-plus or -free buffer (0-50 min). Levels of pERK1, pERK2 and ERK2 were quantified by Western blotting. In unstimulated Ca^{2+}-plus- and -free-treated cells, levels of pERK1 and 2 were similarly low (**Fig. 3.13**). CGRP (10 min) caused similarly a prompt increase in levels of pERK1 and 2 in both Ca^{2+}-plus- and –free-treated cells (**Fig. 3.13B**, 11.9±2.5 (plus) versus 11.9±3.1 (free) for pERK1 and 5.6±1.5 (plus) versus 5.8±1.4 (free) for pERK2; fold-increase at 10 min compared to basal). Indeed, when expressed in % of maximal response, Ca^{2+}-free had no difference on ERK activation compared to Ca^{2+}-plus-treated cells (**Fig. 3.13D** and **E**). Thus, extracellular Ca^{2+} is not required in CGRP-induced ERK activation. However, Ca^{2+}-free increases the basal of pERK1 and 2, compared to the Ca^{2+}-plus-treated cells (**Fig. 3.13C**, 1.3±0.2 (pERK1) 1.2±0.1 (pERK2) fold-increase over control).

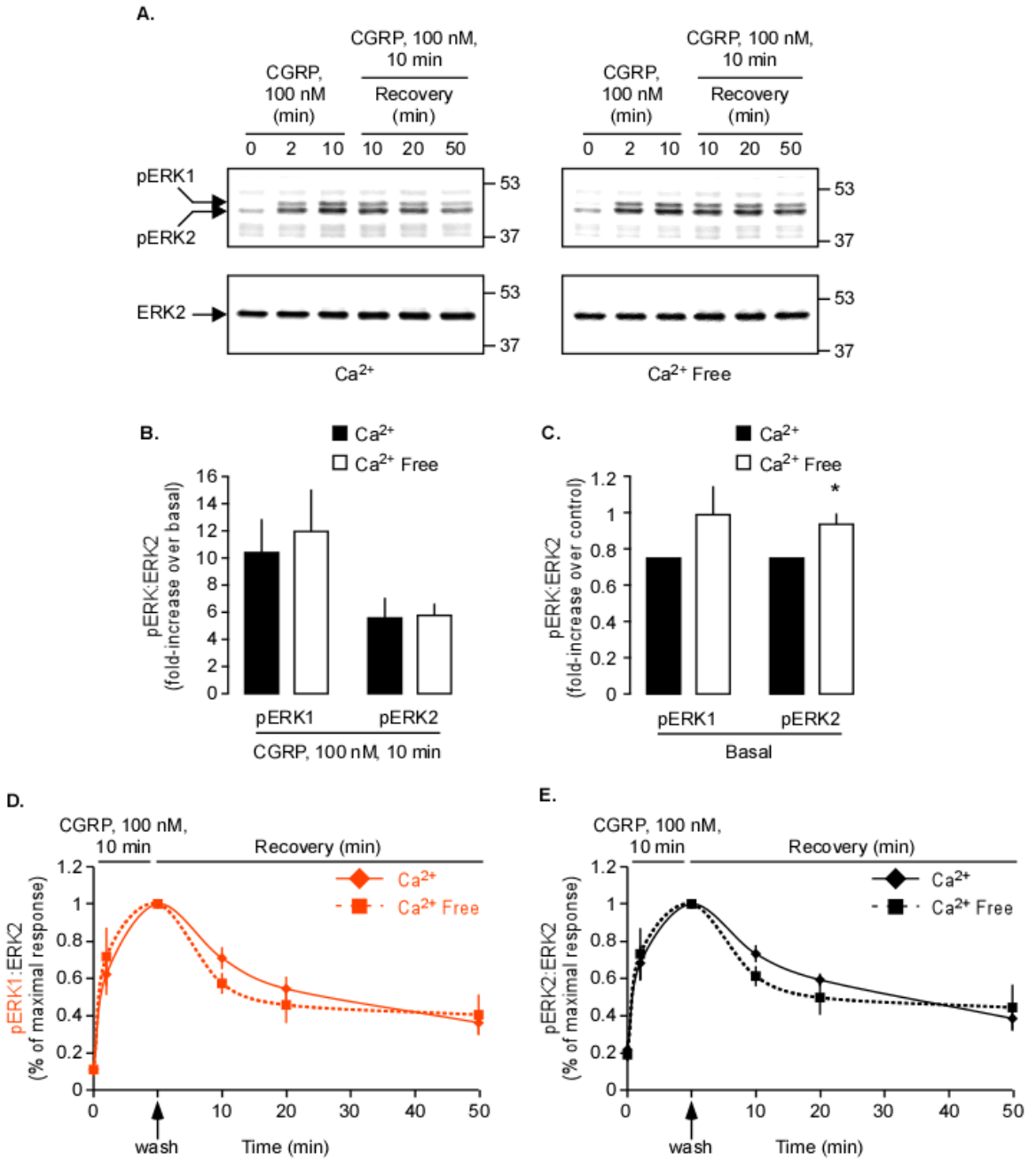

Figure 3.13 **CGRP-induced ERK activation is not dependent on extracellular Ca^{2+}.** (**A**) Serum-starved HEK-CLR•RAMP1 cells were incubated with Ca^{2+} or Ca^{2+} Free, stimulated with CGRP (100 nM, 0-10 min), washed, incubated in CGRP-free Ca^{2+} or Ca^{2+}-free buffer (0-50 min) and levels of pERK1, pERK2 and ERK2 determined by Western blotting. Blots were quantified using ImageQuantTL and ratio of pERK1:ERK2 and pERK2:ERK2 calculated. Representative blot are shown. (**B**) The maximal CGRP-induced ERK phosphorylation, expressed in fold-increase over basal, shows no difference in Ca^{2+} compared to Ca^{2+} Free-treated cells. (**C**) Basal levels of pERK1 and 2 are expressed in fold-increase over Ca^{2+}-treated cells. The effect of Ca^{2+} Free on the basal of pERK1 and 2 shows a significant increase compared to Ca^{2+}-treated cells. (**D**, **E**) The CGRP-induced ERK activation of the full time course, expressed as % of maximal response of pERK1 (**D**) and pERK2 (**E**), shows no difference between Ca^{2+}- and Ca^{2+} Free-treated cells, suggesting that CGRP activates ERK in extracellular Ca^{2+}-independent manner in HEK cells. n=4, *=p<0.05 compared to Ca^{2+}-treated cells at the same time point.

3.8 Discussion

HEK cells stably transfected with CLR•RAMP1, have already been used to study CGRP-induced ERK activation (Parameswaran et al., 2000a) where it has been shown that CGRP induces a concentration-dependent increase of ERK phosphorylation. I also showed that CGRP induces ERK activation in HEK cells, suggesting that HEK cells are a good model to study CGRP-induced ERK activation.

Many GPCRs have been shown to induce transactivation of ErbB1 (Daub et al., 1996; Eisinger and Ammer, 2008; Maudsley et al., 2000; Zajac et al., 2011). This signalling pathway is G protein-independent and could mask any subtle changes in CLR•RAMP1-mediated ERK activation. I was then interested to see whether CGRP can induce transactivation of ErbB1 by using a specific ErbB1 inhibitor, AG1478 (Osherov and Levitzki, 1994). I showed for the first time, that CGRP can cause transactivation of ErbB1 to activate ERK1-2 in HEK cells. ErbB1 transactivation has been reported to play an important role in cancer-related disorders (reviewed in (Fischer et al., 2003)), including by promoting angiogenesis (de Jong et al., 1998; Schreiber et al., 1986). Moreover, CGRP has also been shown to enhance tumour-associated angiogenesis (reviewed in (Majima et al., 2011)). However, the CGRP-mediated molecular mechanism of angiogenesis remains unknown. It is then possible to think that CGRP induce angiogenesis via transactivation of ErbB1. Interestingly, β_1-AR has been shown to also induce transactivation of ErbB1 in HEK cells, however only stimulation with EGF and not catecholamine causes pERK1-2 translocation into the nucleus (Tilley et al., 2009). These results suggest that GPCR-mediated transactivation of ErbB1 induce activation of ERK that promotes activation of cytoplasmic mediators only. It is currently unknown if CGRP-induced ErbB1 transactivation causes translocation of pERK1-2 into the nucleus. However, as HEK cells do not express endogenously CLR•RAMP1, it would be first necessary to verify that CGRP induces ErbB1 transactivation in cells naturally expressing CGRP receptors. Further experiments remain to determine the role and the mechanisms of CGRP-induced ErbB1 transactivation. I showed that CGRP-induced ErbB1 transactivation provides about 60% of total CGRP-induced ERK signal. Therefore, when performing experiments to determine the effects of ECE-1 inhibition and endosomal acidification, I inhibited this pathway so that only the G protein-dependent ERK activation would be observed.

The tyrosine kinase Src is known to play an important role in GGRP-mediated ERK activation (reviewed in (McGarrigle and Huang, 2007)). Moreover, Src has been described to be involved in ERK activation through cAMP/PKA, PKC/PLC/Ca^{2+} and β-arrestins-dependent pathways (Dikic et al., 1996; Luttrell et al., 1999; Schmitt and Stork, 2002). However, many studies reported that the

protein kinase Src was mediating ErbB1 transactivation (Buteau et al., 2003; Daub et al., 1997; Eguchi et al., 1998). By using PP2, a Src inhibitor, I showed that CGRP-induced ERK activation was reduced. Thus, Src is required for CGRP-induced ERK activation. I showed that CGRP-induced ERK activation was mainly mediated through the cAMP/PKA pathway and the transactivation of ErbB1. As, Src has been described to be involved in both pathways, further experiments remain to determine in which pathway Src induces ERK activation.

ECE-1 regulates the recycling and the SP-induced β-arrestin-dependent ERK signalling of NK_1R (Cottrell et al., 2009; Roosterman et al., 2007). Furthermore, CLR•RAMP1 trafficking is also regulated by ECE-1 (Padilla et al., 2007). I was then expected that ECE-1 would similarly regulate CGRP-induced β-arrestin-dependent ERK activation. Surprisingly, preventing endosomal acidification with bafilomycin A_1 and inhibiting ECE-1 had no effect on the magnitude or duration of CGRP-induced ERK activation. Thus, it seems that ECE-1 does not regulate CGRP-induced β-arrestin-dependent ERK activation. Besides, it has been shown that CGRP can be cleaved by other metalloprotease such as insulin-degrading enzyme (Kim et al., 2012). Theoretically, it is then possible that CGRP can be cleaved by other endosomal metalloproteases, which would regulate CGRP-induced β-arrestin-dependent ERK activation. However, it is unlikely as when inhibiting ECE-1 alone, CLR•RAMP1 has been showed to be sequestered in endosomes (Padilla et al., 2007). These results suggest that only ECE-1 degrades CGRP in endosome, because if another metalloprotease was able to degrade CGRP, by inhibiting ECE-1 only, CLR•RAMP1 would not be blocked in endosome. Moreover, it is known that enzymes in general, are pH sensitive and required optimal pH to be fully active, meaning that the pH of every cellular organelles must be strictly regulated (reviewed in (Demaurex, 2002)). I showed that inhibiting the endosomal acidification does not affect CGRP-induced ERK activation, which again shows that it is unlikely that other metalloproteases are able to degrade CGRP. Another explanation would be that CGRP-induced ERK activation is not depending on β-arrestin, and therefore would not be regulated by the endosomal proteases activity as it has been shown for NK_1R (Cottrell et al., 2009). It is known that many GPCRs can activate ERK via β-arrestin-dependent pathways (Cottrell et al., 2009; Luttrell et al., 2001; Shenoy et al., 2006). Even though, CGRP induces the translocation of β-arrestin to the cell-surface and traffic together with CLR•RAMP1 to early endosome (Padilla et al., 2007), I hypothesised that CGRP would not induce a β-arrestin-dependent ERK activation. To assess this hypothesis, I use a β-arrestin1 mutant. I did not use the ErbB1 inhibitor, AG1478 in these experiments as β-arrestins have also been shown to play a role in ErbB1 transactivation. β_1-AR-induced ErbB1 transactivation depends on a mechanism in which GRK phosphorylation recruits β-arrestins and Src to the cell-surface to promote ErbB1 transactivation (Noma et al., 2007; Tilley et al., 2009). By using the dominant-negative β-arrestin1 mutant (β-arrestin1 P91G P121E) that cannot bind

to Src, I showed that CGRP-induced ERK activation was not altered, suggesting as expected that CGRP does not promote a β-arrestin-dependent ERK activation. In contrast, expression of this mutant does affect the isoproterenol-induced ERK activation of the β_2-AR (Luttrell et al., 1999). Together, these data suggest that CGRP does not activate ERK via a β-arrestin-dependent mechanism, nor does it use the endosome as a signalling platform to activate ERK. However, it does not mean that CGRP does not induce β-arrestin-dependent endosomal signalling. β-arrestins are binding partners for many other signalling proteins, including p38 (Gong et al., 2008), Akt (Cianfrocca et al., 2010) and JNK (McDonald et al., 2000). It remains to be determined whether CGRP promotes a β-arrestins-dependent activation of other MAPK.

The cAMP/PKA pathway is commonly involved in GPCR-induced ERK activation (reviewed in (Goldsmith and Dhanasekaran, 2007; Rozengurt, 2007)). CLR•RAMP1 is known to couple $G\alpha_s$ subunit (Aiyar et al., 1999; Van Valen et al., 1990), which leads to accumulation of cAMP. I then expected that CGRP would induce ERK phosphorylation via the cAMP/PKA pathway. Indeed, by using H-89, a PKA inhibitor (Chijiwa et al., 1990), I showed that CGRP-induced ERK activation was PKA-dependent. This result is consistent with another study (Parameswaran et al., 2000a), which showed that 20 μM of H-89 was sufficient to reduced CGRP-induced ERK activation. H-89 has been commonly used at 50 μM (Chao and Hamilton, 2009; Lee and Linstedt, 2000; Murphy et al., 2010). However, it has been shown that H-89 can inhibit other kinases (reviewed in (Lochner and Moolman, 2006)), which suggests that the effect seen could be due to off-target effects. Therefore, I used two different concentrations of H-89 and obtained similar results. The lower concentration (10 μM) of H-89 gives a more specific inhibition of PKA. Thus, I can say with more certainty that CGRP activates ERK through PKA. However, it would be interesting to use other PKA inhibitors and confirm that the same effect is observed. It should be noted that I did not use AG1478 in these experiments as it has been shown that ErbB1 transactivation can be mediated by PKA (Donnini et al., 2007) and therefore promote CGRP-induced ERK activation. However, further experiments remains to determine whether PKA is involved in CGRP-mediated ErbB1 transactivation.

GPCRs can also induce ERK activation through the PLC/PKC/Ca^{2+} pathway (reviewed in (Belcheva and Coscia, 2002; Goldsmith and Dhanasekaran, 2007; Rozengurt, 2007)) either through the coupling with a $G\alpha_q$ subunit or through $\beta\gamma$ subunits-dependent mechanism of the G protein. Moreover, CGRP has been described to promote Ca^{2+} mobilisation through $G\alpha_q$ subunit-mediated PLC activation in human bone cells OHS-4 (Drissi et al., 1998). Interestingly, it has been shown in HEK cells that expression and stimulation of the CGRP receptor, promotes ERK activation in a PKA- and PI3K-dependent manner (Parameswaran et al., 2000b). Conversely, in COS-7 cells, expression and stimulation of CGRP

receptor leads to ERK activation predominantly through PI3K activation (Conner et al., 2008). I was then interested to see if this pathway was involved in CGRP-induced ERK activation. I then used different inhibitors targeting three components of this pathway: PLC, PKC and Ca^{2+}.

When I used a PLC inhibitor, I showed no effect on CGRP-induced ERK activation, neither on the basal level nor on the initial activation of pERK. Therefore, PLC is not involved in the CGRP-induced ERK activation. This result suggests that CGRP-induced ERK activation is not mediated through the PLC/PKC/Ca^{2+} pathway. Interestingly, when I used Gö6976, a cPKC inhibitor (Martiny-Baron et al., 1993), I showed that CGRP-induced ERK phosphorylation was reduced. This result suggests that cPKC are involved in CGRP-induced ERK activation, which contradicts the effects seen with the PLC inhibitors, as cPKC required activation of PLC to be activated (reviewed in (Webb et al., 2000)). One explanation is that Gö6976 inhibits CGRP-induced ERK activation through off-target effects. Indeed, it has been shown that Gö6976 was able to inhibit other kinases including Janus kinase 2 (Grandage et al., 2006). Another explanation is that I showed that Gö6976 significantly increased the basal level of pERK. This basal activity has already been observed in another study (Sellers et al., 2001). It becomes then difficult to interpret the effect of the inhibitor, as the reduction of pERK seen in the initial activation of ERK could be due to the fact that starting from higher level of phosphorylation, ERK would reach its maximum phosphorylation level more rapidly. Then by comparing the level of pERK over the basal, it would appear to be reduced in the Gö6976-treated cells compared to vehicle-treated cells. Interestingly, it has been shown that cPKC isoforms were responsible of a negative feedback on ErbB1 phosphorylation (Santiskulvong and Rozengurt, 2007). Therefore, by inhibiting PKC, basal phosphorylation level of ErbB1 can increase, leading to an augmentation of ERK activation. This could explain why Gö6976 increases basal level of pERK.

I then decided to use Gö6983, a broad-spectrum of PKC isoforms inhibitor (Gschwendt et al., 1996). Gö6983 has already been shown to inhibit GPCR-induced ERK activation (Shah et al., 2005). Even though, Gö6983 reduces significantly the basal level of pERK, I showed that CGRP-induced ERK activation was not reduced in Gö6976-treated cells compared to vehicle-treated cells. This result suggests that CGRP does not induce ERK activation through PKC, which confirms the results observed with the PLC inhibitor and that the effect seen with Gö6976 seems to be due to off-target effects. Thus, it is likely that CGRP-induced ERK activation is PLC/PKC-independent.

Finally, I wanted to see the effect of Ca^{2+} on the CGRP-induced ERK activation. It is known that some isoforms of PKC required Ca^{2+} to be activated (Ogawa et al., 1981) and reviewed in (Rozengurt, 2007; Zeng et al., 2012)). To assess the role of Ca^{2+}, I stimulated the cells in presence or not of extracellular Ca^{2+}. I am aware that

it is mainly a mobilisation of Ca^{2+} from intracellular store that trigger PKC activation. However, it is known that this rapid Ca^{2+} mobilisation is followed by a slower entry of Ca^{2+} from the outside (reviewed in (Parekh and Putney, 2005)). It also has been shown that this entry of Ca^{2+} could sustain PKC and ERK activation (Numaga et al., 2010). In our experiment, I showed that extracellular Ca^{2+} did not seem to have any effect on the CGRP-induced ERK activation. Which again, suggests that Ca^{2+}-dependent PKC isoforms are not involved in the CGRP-induced ERK activation, because I should have seen a faster decrease in pERK level in the Ca^{2+}-free treated cells. However, the fact that the basal level of pERK was significantly higher in Ca^{2+}-free treated cells complicates the interpretation of the involvement of Ca^{2+} in the CGRP-induced ERK activation, but could also be explain by the negative feedback of Ca^{2+}-dependent PKC isoforms. It should be noted that I did not use AG1478 in these experiments as it has been shown that ErbB1 transactivation can be mediated by PKC (Stewart and O'Brian, 2005). Altogether, these results suggest that the PLC/PKC/Ca^{2+} pathway is not involved in the CGRP-induced ERK activation.

3.9 Summary and Conclusion

To investigate the mechanism of CGRP-induced ERK-dependent upregulation of iNOS, I first determined whether CGRP activates ERK in HEK-CLR•RAMP1 cells. I used transfected HEK cells as they are an easy model to manipulate and provide strong signals to analyse. Using these findings, key experiments could then be repeated in a more appropriate model such as primary thoracic artery smooth muscle cells.

As expected, CGRP induces ERK activation in HEK-CLR•RAMP1 cells. By using different inhibitors I show that CGRP-induced ERK activation is mainly activated through two major pathways. I show for the first time that CGRP induces transactivation of ErbB1, which then lead to the activation of ERK (**Fig. 3.14**). This pathway seems to be quite important as the use of an ErbB1 inhibitor reduces CGRP-induced ERK activation by about 60%. Surprisingly, even if ECE-1 is regulating the traffic of CLR•RAMP1 (Padilla et al., 2007), the inhibition of ECE-1 or the endosomal acidification did not affect the magnitude or duration of CGRP-induced ERK signalling, as it has been shown for NK_1R (Roosterman et al., 2007). Moreover, I showed that CGRP-induced ERK activation is β-arrestin1-independent. The other pathway involved in the CGRP-induced ERK activation is the cAMP/PKA pathway, which was expected as is has been shown that CLR•RAMP1 couples with a $G\alpha_s$ subunit (Aiyar et al., 1999; Van Valen et al., 1990). By using a PKA inhibitor, I showed that CGRP-induced ERK activation was reduced by about 50% (**Fig. 3.14**). I also showed that Src is involved in CGRP-induced ERK activation, potentially involved either in the transactivation of ErbB1

pathway or the cAMP/PKA pathway. Also, I showed that the PLC/PKC/Ca^{2+} pathway is not involved in CGRP-induced ERK activation. Altogether those results give us a better understanding of the CGRP-induced ERK signalling in HEK-CLR•RAMP1 cells.

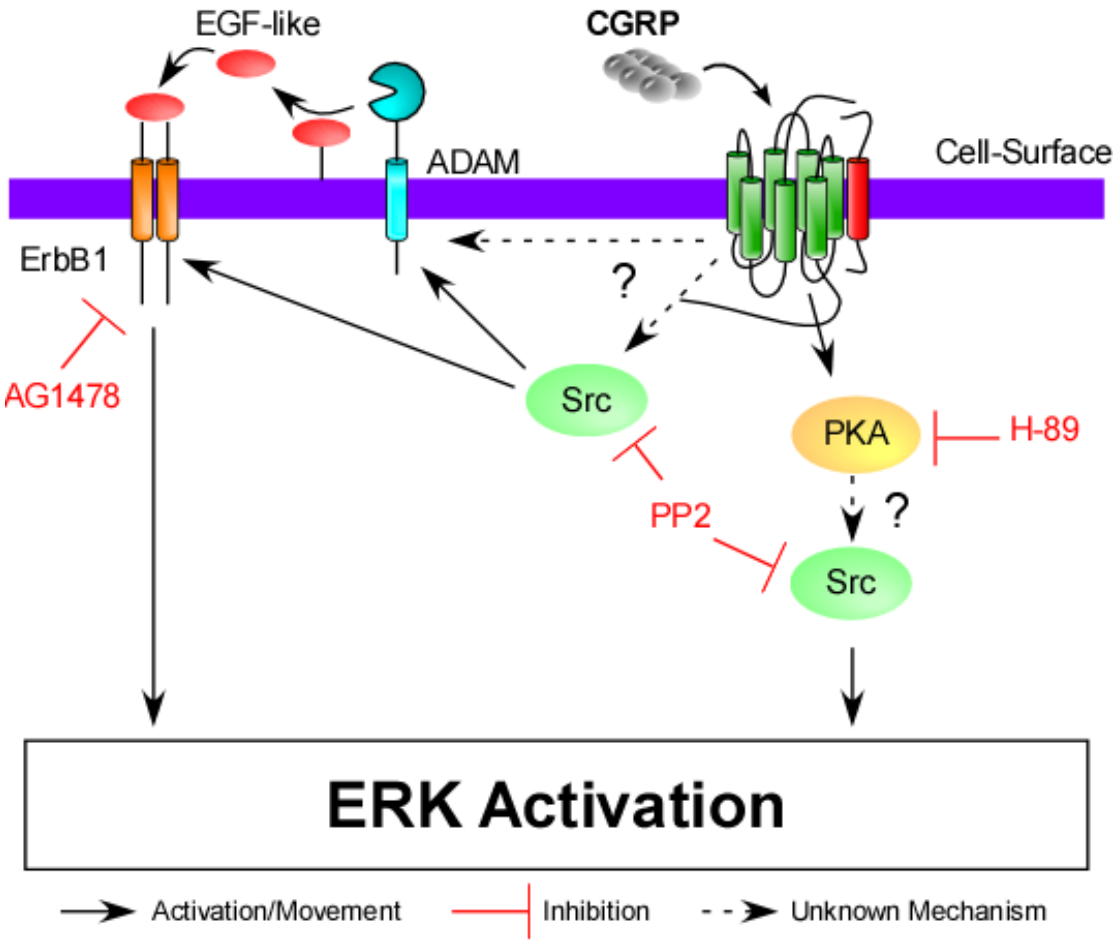

Figure 3.14 **Schematic representation of ERK pathways involved in CGRP-induced ERK activation.** CGRP induce transactivation of ErbB1 which leads to the activation of ERK. This pathway can be blocked by using ErbB1 inhibitor: AG1478. However, the exact mechanism of CGRP-induced ErbB1 transactivation remains to be determined. The other pathway involved in CGRP-induced ERK activation is cAMP/PKA, where H-89, a PKA inhibitor, was shown to reduce CGRP-induced ERK activation. By using PP2 a Src inhibitor, Src has been shown to be also involved in CGRP-induced ERK activation. The role of Src remains to be determined: Src can either be involved in the transactivation of ErbB1 or in the cAMP/PKA pathway.

Chapter 4. Upregulation of iNOS by CGRP in Primary Smooth Muscle Cells

4.1 Background and Objectives

It is known that CGRP can induce ERK activation in different cell types (Kawanami et al., 2009; Kawase et al., 1999; Yu et al., 2006), which is mainly involved in the proliferation of those cell types. However, CGRP has also been shown to regulate other biological responses in ERK dependent manner, such as inducing expression of VEGF in HaCat keratinocyte cells (Yu et al., 2006), promoting inflammation in astrocytes and microglia cells (Wang et al., 2009) and inducing iNOS in trigeminal ganglion glial cells (Vause and Durham, 2009).

iNOS produces large amounts of NO (Nathan and Xie, 1994) and is upregulated in different pathologies such as migraine (Olesen and Jansen-Olesen, 2000), atherosclerosis (Ginnan et al., 2008) and sepsis (Hauser et al., 2005). CGRP is similarly upregulated in migraine and sepsis (Goadsby et al., 1990; Zhou et al., 2001). CGRP has been shown to upregulate iNOS and NO release in trigeminal ganglion glial cells in a p38- and ERK-dependent mechanism (Vause and Durham, 2009). Moreover, when SMCs are pretreated with interleukin-1β, CGRP also promotes upregulation of iNOS and NO release by inducing elevation of cAMP, whereas CGRP alone had no effect on iNOS expression (Schini-Kerth et al., 1994). However, the specific molecular mechanisms of CGRP-induced iNOS upregulation remain unknown. First, to determine if primary rat thoracic artery SMCs (TA-SMCs) are a suitable model to study CGRP-induced iNOS upregulation, cells were isolated, cultured and then characterised. The aim of this study is to investigate if CGRP promotes ERK-dependent iNOS expression in TA-SMC.

4.2 Characterisation of Primary Smooth Muscle Cells from Rat Thoracic Aorta

4.2.1 TA-SMC Express α-Smooth Muscle Actin

CGRP induces ERK activation in HEK-CLR•RAMP1 cells. However, these cells do not express endogenously CLR•RAMP1, and do not represent the best physiological model to study whether CGRP-induced iNOS upregulation in an ERK activation dependent manner. Indeed, CGRP was unable to induce iNOS expression in HEK-CLR-RAMP1 cells (unpublished observation, G.S. Cottrell). Therefore, primary rat TA-SMCs were used. Cells were extracted by an explant method. Explants were then cultured until the cells formed a monolayer. To determine if the cells were actual SMC, the cells in cultures were characterised using a specific SMC markers: α-smooth muscle actin (α-SMA) (Skalli et al., 1989). Primary TA-SMCs were fixed and α-SMA and DAPI (DNA marker) detected by immunofluorescence and confocal microscopy (**Fig. 4.1A**). α-SMA staining

shows characteristic actin fibres. Thus, the cultures from rat thoracic aorta contain SMCs.

4.2.2 TA-SMC Express mRNA for CLR and RAMP1

The cells issued from an explant method are SMC. In order to be a suitable model these cells must express all the components of the CGRP receptor. To determine if TA-SMCs express CLR, RAMP1, 2 and 3, mRNA was extracted from TA-SMC culture. Reverse transcriptase (RT)-PCR was then performed with or without reverse transcriptase polymerase (MultiScribe) in order to generate cDNA. By using specific primers for CLR, RAMP1, 2 and 3, cDNA were then amplified by PCR and products were run on 1.5% agarose gel (**Fig. 4.1B**). In the absence of MultiScribe, no product was amplified for any reaction. However, in reaction with Multiscribe products of expected size for CLR (442 bp), RAMP1 (277 bp), RAMP2 (446 bp) and RAMP3 (313 bp) were detected. Thus, TA-SMC endogenously express mRNA for CGRP and ADM receptors. Altogether, these results suggest that TA-SMC have the potential to respond to CGRP.

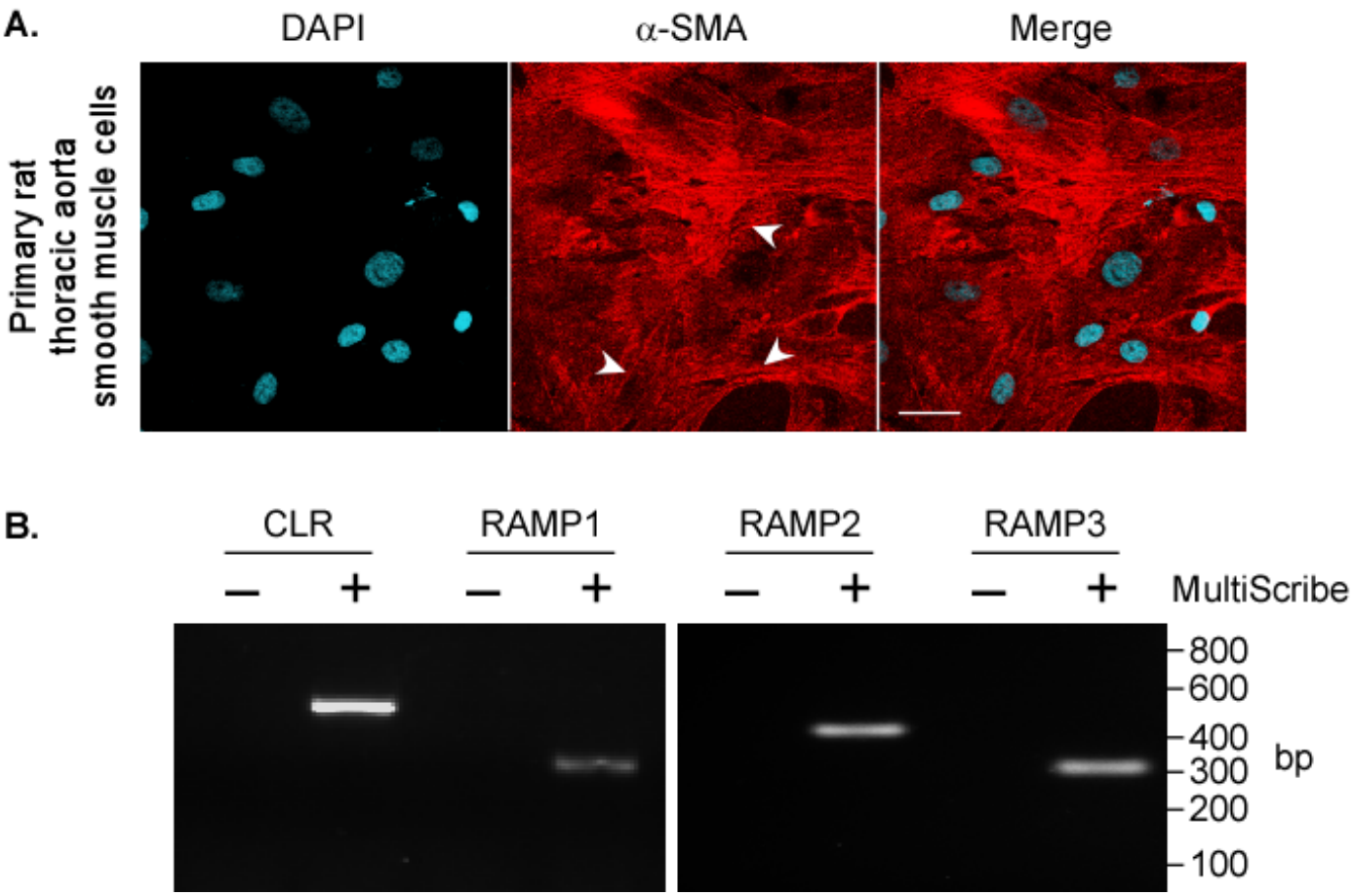

Figure 4.1 **Characterisation of TA-SMC.** (**A**) Primary cells obtained from explant methods from rat thoracic aorta were fixed and stained simultaneously with DAPI and α-SMA. Immunoreactive proteins were detected by immunofluorescence and analysed by confocal microscopy. Cells show a bright staining for α-SMA with characteristic actin fibres (arrowheads), which suggest that the primary cells are SMC. Scale bar = 10 μm. (**B**) RNA was extracted from TA-SMC culture and cDNA were generated with or without reverse transcriptase (MultiScribe). cDNA were then amplified by PCR with specific primers for CLR (442 bp), RAMP1 (277 bp), RAMP2 (446 bp) and RAMP3 (313 bp).

4.3 CGRP Induces iNOS Expression in TA-SMC

TA-SMCs express mRNA for CLR•RAMP1, suggesting that these cells are able to respond to CGRP. Therefore, to confirm this hypothesis, TA-SMCs were stimulated with CGRP and iNOS expression analysed by Western blotting and by immunofluorescence and confocal microscopy. In our primary cells culture, a higher concentration of CGRP (1 μM) was used, similarly to previous study (Schini-Kerth et al., 1994).

4.3.1 Western Blot Analysis of CGRP-Induced iNOS Production

To determine if primary smooth muscle cells can promote iNOS upregulation, cells were stimulated with CGRP (0-6 h) and analysed by Western blotting for the presence of iNOS and β-actin (loading control). In unstimulated cells there was a low basal level of iNOS (**Fig. 4.2**). After 6 h, a significant increase of iNOS signal was observed (**Fig. 4.2B**, 4.3±1.3 fold-increase over basal). Thus, CGRP induces iNOS production in TA-SMC.

4.3.2 Confocal Analysis of CGRP-Induced iNOS Production

To determine if CGRP can promote iNOS expression TA-SMCs, cells were stimulated with CGRP (6 h) and iNOS and α-SMA (used to identify SMCs) were simultaneously analysed by immunofluorescence and confocal microscopy (**Fig. 4.3**). Each image was analysed by ImageJ, where extracellular background signals have been manually removed and level of cellular signals were quantified. Ratio of iNOS:SMA was calculated and expressed as fold-increase over control. In unstimulated cells, analysis showed low levels of iNOS (**Fig. 4.3A**). Stimulation with CGRP induced a significant increase of iNOS signal (**Fig. 4.3B**, 1.7±0.1 fold-increase over unstimulated). Thus, CGRP causes upregulation of iNOS in TA-SMCs.

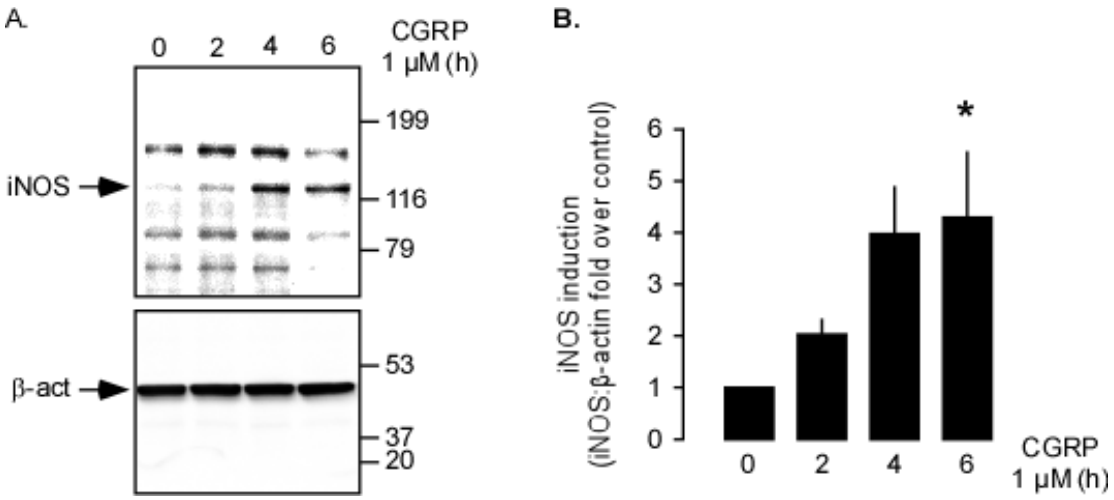

Figure 4.2 **CGRP induces iNOS production in TA-SMCs.** (**A**) TA-SMCs were stimulated with CGRP (1 µM, 0-6 h). Blots were probed for levels of iNOS and β-actin. Immunoreactive bands were quantified by ImageQuantTL. Representative blots are shown. (**B**) Ratios of iNOS:β-actin calculated and results expressed in fold-increase over unstimulated cells. Basal levels of iNOS are low. CGRP induces a significant iNOS upregulation at 6 h. n=4, *p<0.05 compared to unstimulated cells.

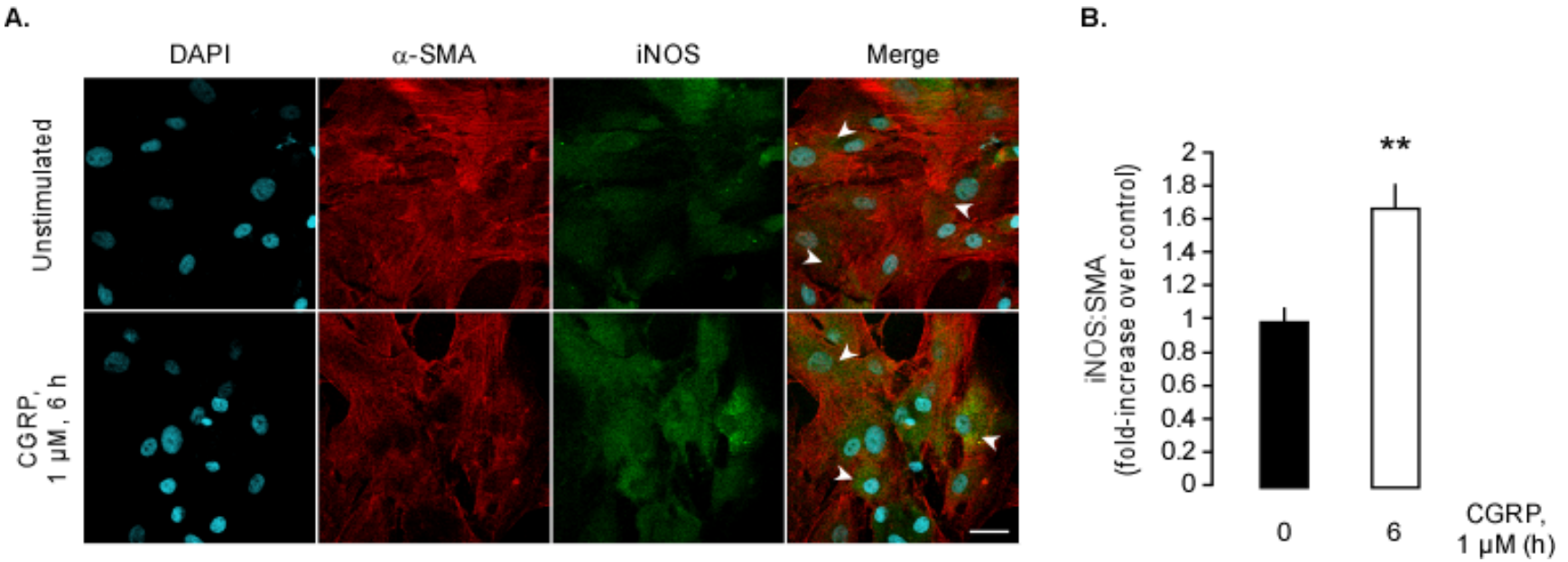

Figure 4.3 **Visualisation of CGRP-induced iNOS production in primary smooth muscle cells by confocal microscopy.** (**A**) Primary smooth muscle cells were stimulated with CGRP (1 µM, 0-6 h), and immunoreactive proteins were detected by immunofluorescence and analysed by confocal microscopy. (**B**) Signal for iNOS and SMA were analysed and quantified by ImageJ. Ratio of iNOS:SMA are expressed as fold-increase over control. (**A**, **B**) In unstimulated cells, levels of iNOS are low. After stimulation with CGRP, level of iNOS are significantly increased (arrowheads). Thus, CGRP induces iNOS upregulation in primary smooth muscle cells. **=p<0.01 compared to unstimulated cells, scale bar = 10 µm.

4.4 CGRP-Induced iNOS Upregulation is ERK-Dependent in TA-SMC

CGRP induces iNOS expression in TA-SMC. However, the exact molecular mechanism of CGRP-induced iNOS upregulation remains unknown. As a first step to determine if CGRP-induced iNOS upregulation in TA-SMC is ERK dependent, a MEK inhibitor, U-0126 (Favata et al., 1998), was used. TA-SMCs were incubated with vehicle (DMSO) or U-0126 (30 min), stimulated with CGRP (0-6 h) and levels of iNOS and β-actin determined by Western blotting. In unstimulated vehicle- and U-0126-treated cells, levels of iNOS were low (**Fig. 4.4**). CGRP caused increase in levels of iNOS in both vehicle- and U-0126-treated cells. However, the increase in U-0126-treated cells was reduced compared to vehicle-treated cells (**Fig. 4.4B**, 10.4±1.4 (vehicle) versus 2.8±0.5 (U-0126) fold-increase over basal at 6 h). Thus, CGRP-induced iNOS upregulation is ERK-dependent in TA-SMC. Furthermore, these results suggest that TA-SMC is a suitable model to study the involvement of ERK activation in CGRP-induced iNOS upregulation.

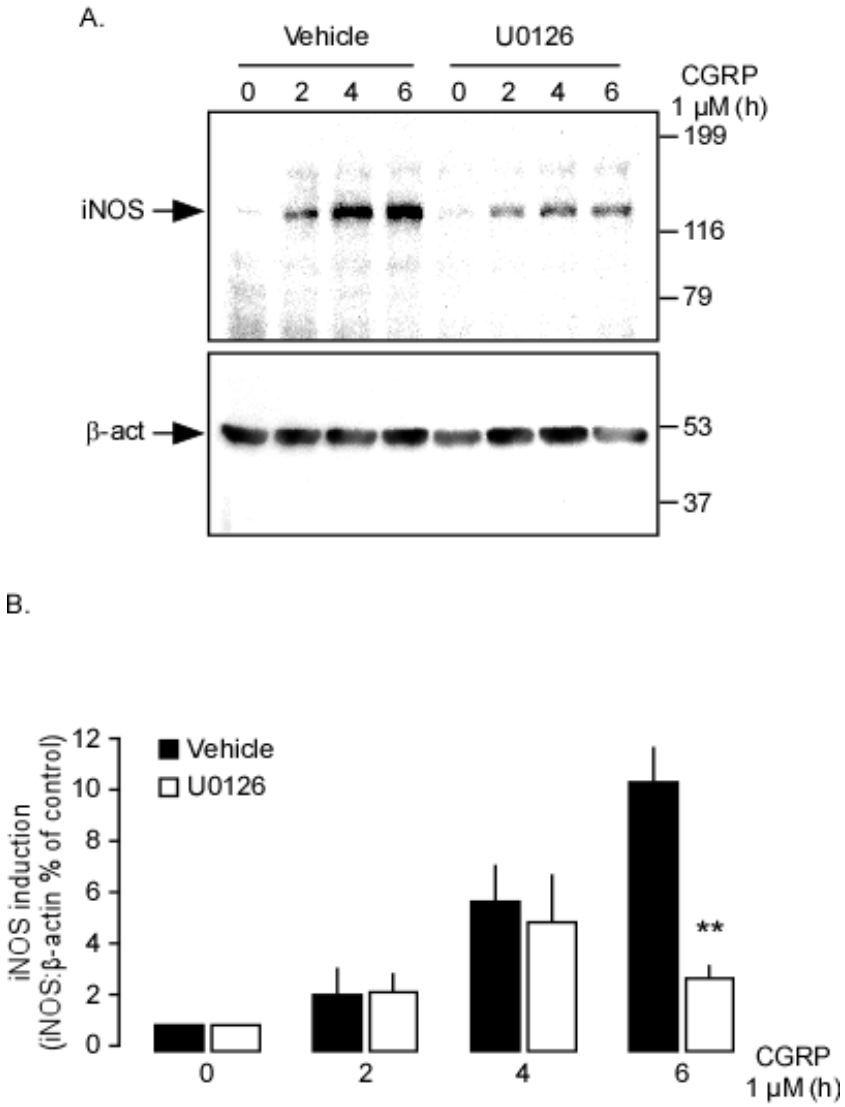

Figure 4.4 **CGRP-induced iNOS upregulation is ERK-dependent.** (**A**) TA-SMCs were incubated with vehicle (DMSO) or U-0126 (10 µM), stimulated with CGRP (1 µM, 0-6 h) and levels of iNOS and β-actin determined by Western blotting. Blots were quantified by ImageQuantTL. Representative blots are shown. (**B**) The CGRP-induced iNOS production expressed in fold-increase over basal of iNOS:β-actin, is significantly reduced at 6 h in U-0126-treated cells compared to vehicle-treated cells, indicating that CGRP induces iNOS upregulation in a ERK-dependent manner. n=3, **=p<0.01 compared to vehicle-treated cells at each time point.

4.5 Discussion

As HEK-CLR•RAMP1 cells do not endogenously express CLR•RAMP1 and CGRP does not induce iNOS expression in these cells, I required a more physiological model to evaluate the role of CGRP-induced ERK activation in the upregulation of iNOS. Many studies have shown that primary SMCs respond to CGRP leading to an increase of cAMP (Schini-Kerth et al., 1994; Vallotton et al., 1989; Wisskirchen et al., 1999). I then decided to use SMC issued from rat thoracic artery. I isolated cells using an explant method. Other groups have already used this method to isolate this type of cells (Campbell and Campbell, 1993; Xu et al., 2009). The cells were then characterised by using a specific marker of SMC that is α-SMA (Skalli et al., 1989) in order to confirm that the cells issued from the explant were SMC. I also determined if these cells were expressing components of the CGRP receptor. PCR products amplified from cDNA generated from mRNA extracted from TA-SMC, indicated the presence of mRNA for CLR, RAMP1, RAMP2 and RAMP3. As this type of cell has already been shown to respond to CGRP, it was not surprising to find that they express CLR and RAMP1. Moreover, the fact that TA-SMCs also express RAMP2 and 3, suggests that they may also express a functional ADM receptor. Indeed, studies have shown that ADM inhibits the proliferation of SMCs, indicating that SMCs can express a functional ADM receptor (Kano et al., 1996). Altogether, I showed that TA-SMCs are expressing mRNA for CLR•RAMP1. Furthermore, I also show that TA-SMCs responded to CGRP and promoted upregulation of iNOS. However, it is not an unfamiliar result, as a previous study showed that CGRP also induces iNOS upregulation in TA-SMC (Schini-Kerth et al., 1994). Interestingly, in this study the authors showed that CGRP (1 µM) on its own was not sufficient to induce iNOS upregulation. Indeed, only when the cells were pretreated with IL-1β, CGRP was able to promote iNOS upregulation. In contrast, my results showed that when applied alone the same concentration of CGRP (1 µM) is sufficient to induce iNOS expression. Moreover, by using the MEK inhibitor, U-0126 I show that CGRP-induced iNOS upregulation was reduced. The fact that CGRP is used at high concentration, could induce stimulation of CLR•RAMP2 or 3. Therefore to confirm these effects a CGRP inhibitor could be used and see whether iNOS upregulation is affected or not. If not it means that the effect of CGRP are not mediated by CLR•RAMP1. Nevertheless, this result suggests that CGRP-induced iNOS production is ERK-dependent. However, I noticed that the TA-SMC tends to lose the expression of CLR•RAMP1. Indeed, some explants after few weeks were not responding at all to CGRP, which make it difficult to carry out any experiments due to the inconsistency of the results. Other studies also reported that primary SMC put on culture tend to lose expression of some cell-surface protein such as the α7 integrin (Yao et al., 1997) and the muscarinic acetylcholine receptor M2 (Hsieh and Farley, 2002) due to differentiation of these cells. I also observed a similar process where cells after 5 passages start to change morphology

becoming smaller and epithelial-like shape (**Fig. 4.5**). Further experiment and characterisation would be necessary to confirm these observations. As a consequence, one way to overcome the loss of CGRP receptor would be to use exogenously expressed CLR and RAMP1 in TA-SMC, for example by using the lentivirus or adenovirus system.

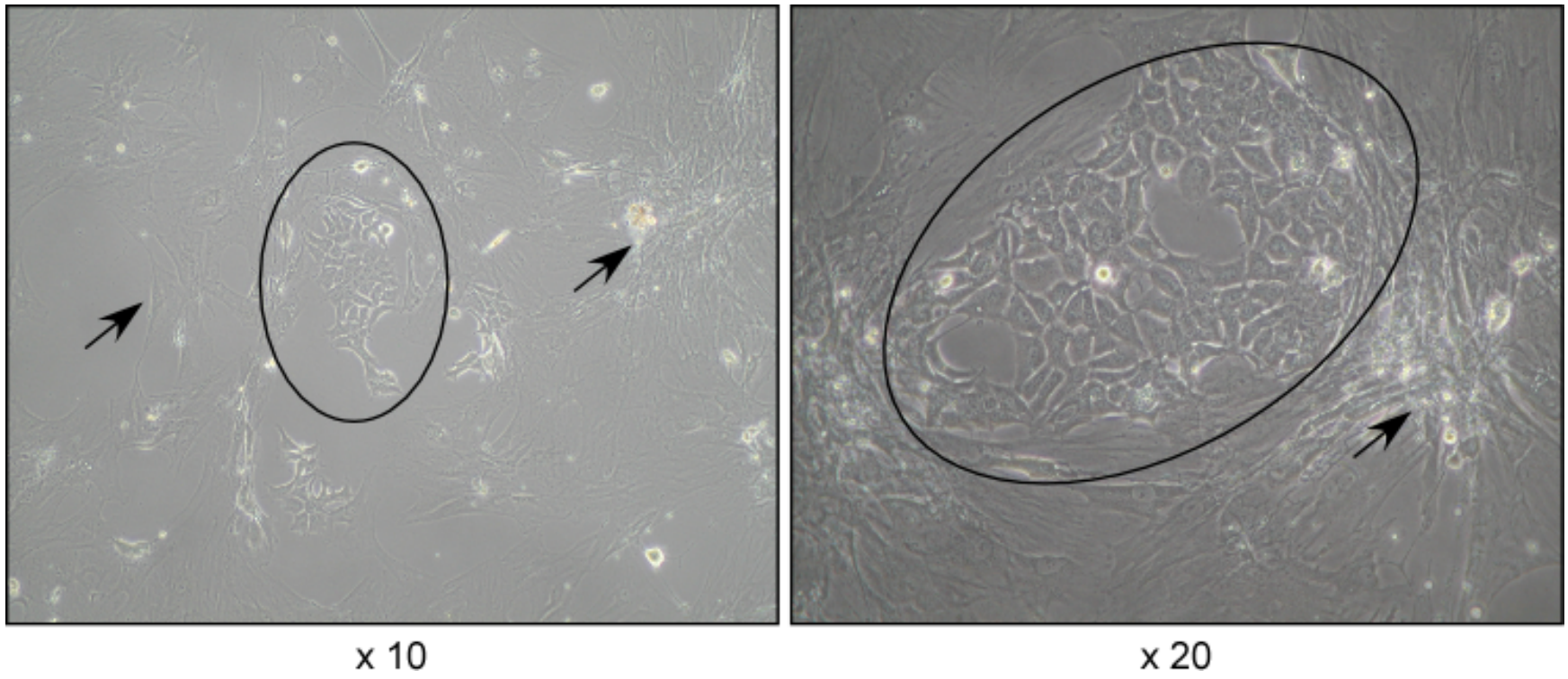

Figure 4.5 **Morphological change of TA-SMC.** Culture of primary TA-SMC at passage 5 grown in DMEM supplemented with HIFBS (10% (v:v), NEAA (1% (v:v)), P/S (1% (v:v)) and fungizone (0.1% (v:v)). Until passage 5, cells display characteristic morphology of SMC, such as flat cell presenting long and thin ramifications and growing on top of each other forming “hills and valleys” (arrows). However, from passage 5, another population is emerging presenting distinctive morphological features such as smaller cell, growing on monolayer and presenting characteristic epithelial cell-like feature (circle).

4.6 Summary and Conclusion

I aimed to determine a suitable model to study the molecular mechanisms regulating CGRP-induced iNOS upregulation. I used primary smooth muscle cells isolated from rat thoracic aorta. I first confirmed that the cells isolated from the explants were SMC, by confirming the expression of a specific marker of SMC, α-SMA, which is a characteristic constituent of the cytoskeleton of SMC (Skalli et al., 1989). I then investigated whether these cells expressed mRNA for CLR and RAMP1. Using RT-PCR, I amplified products for CLR, RAMP1, RAMP2 and RAMP3. Thus, primary smooth muscle cells issued from rat thoracic artery express α-SMA, which confirms that they are smooth muscle cells; and express all the components for CGRP and ADM receptors. I then investigated whether CGRP promotes iNOS upregulation in TA-SMC. Indeed, I showed by Western blotting and by confocal microscopy that stimulation with CGRP induces a significant increase of iNOS expression. Moreover, when I incubated TA-SMC cells with U-0126, a MEK inhibitor, CGRP-mediated iNOS upregulation was reduced, which suggests that iNOS production is ERK-dependent. Therefore, these results suggest that TA-SMCs are a suitable model to study the molecular mechanisms that regulate CGRP-induced iNOS production. Further experiments would be necessary to determine which particular ERK pathway is involved in CGRP-mediated iNOS upregulation.

Chapter 5. Post-Endocytic Sorting of CLR•RAMP2 in Human Embryonic Kidney Cells

5.1 Background and Objectives

GPCRs represent the largest family of membrane receptors and are involved in many diseases and dysfunctions. Understanding the molecular mechanisms that regulate GPCRs is critical for the development of new therapies.

CGRP and ADM are widely distributed throughout the body and play important roles in cardiovascular homeostasis, nociception and development. They are implicated in many diseases including migraine, heart failure and sepsis and as such mechanisms regulating their functions could be sites potential therapeutic intervention. However, as many aspects of the mechanisms regulating the receptors for ADM and CGRP are still poorly understood, it is then important to define these regulatory mechanisms.

CGRP and ADM receptors are heterodimeric complexes composed of a common class B GPCR, the calcitonin receptor-like receptor (CLR), and a receptor activity-modifying protein (RAMP). There are three types of RAMP: RAMP1, RAMP2 and RAMP3. Association with RAMP1 gives a high affinity CGRP receptor, whereas association with RAMP2 or RAMP3 gives high affinity ADM receptors. The same group, who identified ADM, showed that CGRP or ADM-mediated stimulation induces CLR and RAMPs internalisation via clathrin-coated vesicles (Kuwasako et al., 2000). They also reported that after internalisation, CLR and RAMPs did not recycle back to the cell-surface and were targeted to acidic vesicles believed to be lysosomes. However, other studies showed that both CLR•RAMP3 (Bomberger et al., 2005) and CLR•RAMP1 (Cottrell et al., 2007) were recycled back to the cell-surface after transient stimulation. Still, little is known about the mechanisms regulating CLR•RAMP2. Therefore, the mechanisms of the post-endocytic sorting of CLR•RAMP2 were first determined in HEK cells.

5.2 Characterisation of a HEK-CLR•RAMP2 Cell Line

Tagged HA-CLR and myc-RAMP2 were stably transfected into HEK-FLP cells to facilitate the study of the post-endocytic sorting of CLR•RAMP2. HEK cells are a good model as they are easy to manipulate e.g. transfection, overexpression of receptors, which gives strong signals to analyse.

5.2.1 Expression of CLR•RAMP2 and Trafficking

ADM induces internalisation of CLR•RAMP2 in HEK cells (Kuwasako et al., 2000). To determine if CLR•RAMP2 is expressed at the cell-surface, and internalises normally upon ADM stimulation, cell-surface receptors were labelled by incubating (30 min) HEK-CLR•RAMP2 cells with antibodies to extracellular CLR (HA) and RAMP1 (myc) epitopes. Cells were then stimulated with ADM (30 min). Receptors were then localised by immunofluorescence and confocal microscopy (**Fig. 5.1**). In unstimulated cells, CLR is localised at the cell-surface as well as RAMP2. Stimulation with ADM induces internalisation of CLR and RAMP2 together in the same intracellular vesicles. Thus, CLR•RAMP2 is expressed at the cell-surface and ADM causes its internalisation, which suggest that CLR•RAMP2 is functional.

5.2.2 ADM-Induced ERK Activation

It has been shown that ADM induces ERK activation in many different cell types (Kim et al., 2003; Niu et al., 2004; Uzan et al., 2008). To determine if ADM was able to induce ERK activation in HEK-CLR•RAMP2, cells were incubated in serum-free medium and stimulated with ADM (0-60 min). Levels of phosphorylated ERK1 and 2 (pERK1 and pERK2) and ERK2 were determined by Western blotting. In unstimulated cells levels of pERK1-2 were low (**Fig. 5.2**). ADM treatment increased dramatically pERK1-2 with a peak at 2 min and then progressively decreased (**Fig. 5.2B**, 11.0±3.0 for pERK1; and 4.6±0.8 for pERK2 fold increase compare to basal at 2 min). This result shows that ADM is able to induce ERK activation in HEK-CLR•RAMP2 cells. Thus, CLR•RAMP2 forms a functional receptor in HEK cells and this model system represents a suitable model to study the regulation of CLR•RAMP2.

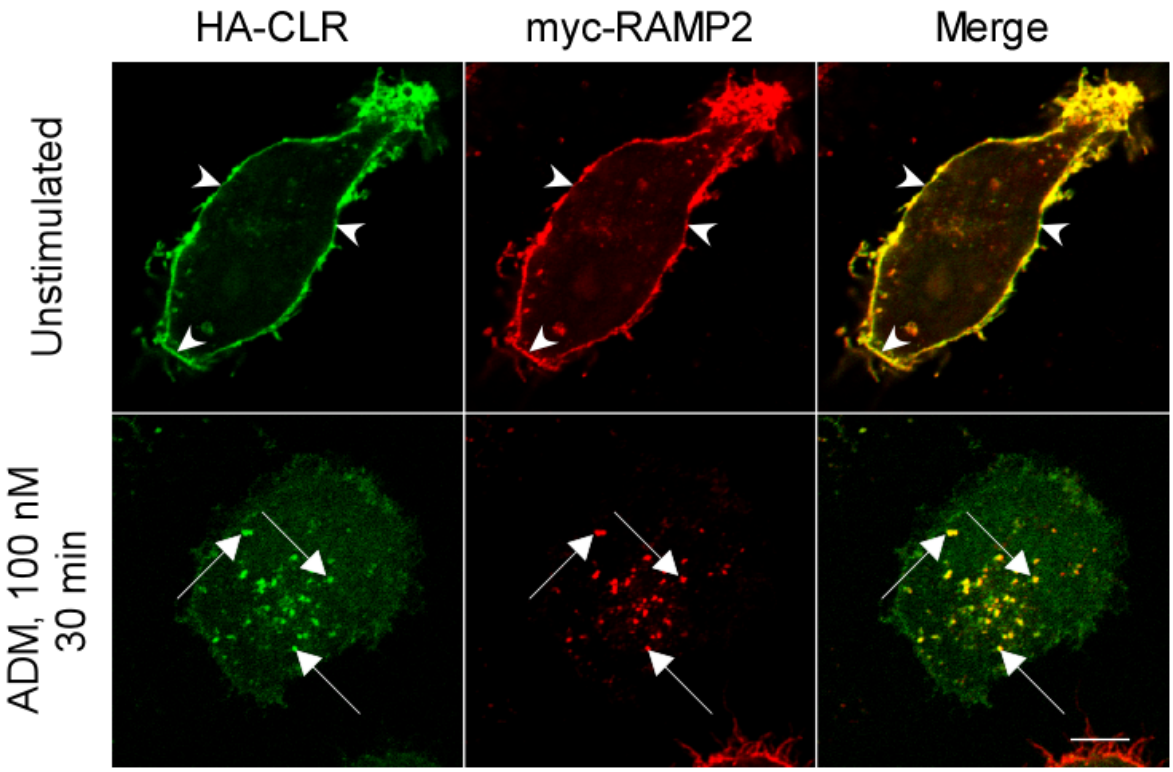

Figure 5.1 **ADM induces internalisation of CLR•RAMP2.** HEK-CLR•RAMP2 cells were incubated (30 min, 37°C) with antibody against the extracellular epitope tag of CLR (HA) and RAMP2 (myc), stimulated with ADM (100 nM, 30 min). Immunoreactive proteins were then detected by immunofluorescence and analysed by confocal microscopy. In unstimulated cells, CLR and RAMP2 are present at the cell-surface (arrowheads). ADM induces trafficking of CLR and RAMP2 together in intracellular vesicles (arrows). Thus CLR•RAMP2 is expressed at the cell-surface of HEK-CLR•RAMP2 and internalised upon ADM stimulation. Scale bar = 10 μm.

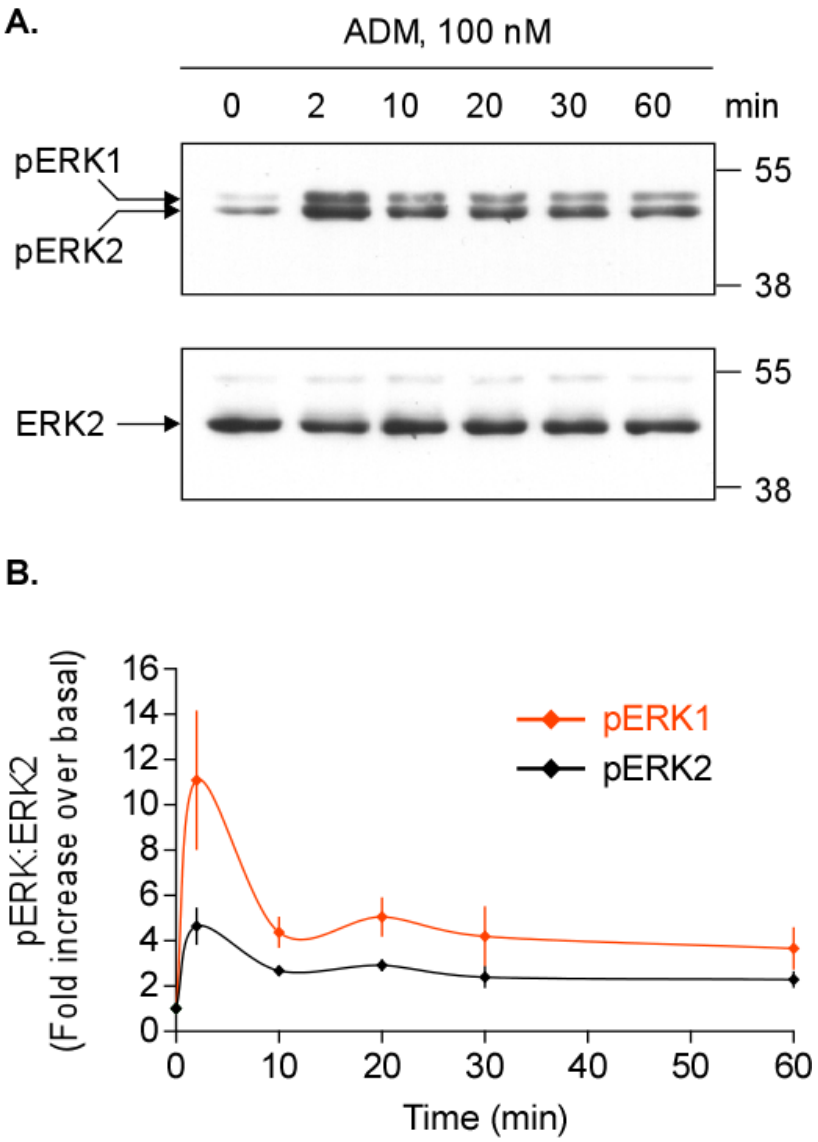

Figure 5.2 **ADM induces ERK activation.** (**A**) Serum-starved HEK-CLR•RAMP2 cells were stimulated with ADM (100 nM, 0-60 min) and levels of pERK1-2 and ERK2 determined by Western blotting, where a representative blot is shown. Blots were quantified using ImageJ. (**B**) Ratios of pERK1:ERK2 and pERK2:ERK2 calculated and expressed as fold increase over basal, show that ADM induces a prompt increase level of pERK1-2 activation, which is sustained by decreases over time. n=4.

5.3 ADM Induces Degradation of CLR•RAMP2

Compared to our understanding of the trafficking of CLR•RAMP1, nothing is known about the post-endocytic sorting of CLR•RAMP2. It has been shown that following a transient stimulation (1 h) with CGRP, CLR•RAMP1 recycles back to the cell-surface in about 6 h. However, following a continuous stimulation (16 h), CLR•RAMP1 is degraded and therefore does not recycle (Cottrell et al., 2007).

Moreover, it has been shown that CGRP is degraded in endosome by ECE-1, which then promotes the recycling of CLR•RAMP1 to the cell-surface (Padilla et al., 2007). As ADM is degraded by ECE-1 at endosomal pH (5.5) and not extracellular pH (7.4) (unpublished data, G. S. Cottrell) and that both CGRP and ADM receptor share a common GPCR, it was anticipated that following a transient stimulation with ADM, ECE-1 would regulate the recycling of CLR•RAMP2 to the cell-surface, similarly to CLR•RAMP1.

5.3.1 Quantification of CLR•RAMP2 Degradation by Western Blot

To determine if CLR•RAMP2 traffics in a similar way to CLR•RAMP1, the degradation of CLR following both transient and continuous stimulation with ADM was examined. HEK-CLR•RAMP1 and HEK-CLR•RAMP2 cells were incubated with cycloheximide (CHX), an inhibitor of protein synthesis (Obrig et al., 1971), to block the production of newly synthesised receptors. Cells were transiently stimulated with CGRP or ADM (10 min), washed and incubated in agonist-free medium (16 h). Alternatively, cells were continuously stimulated with CGRP or ADM (16 h). Levels of CLR and β-actin (loading control) were quantified by Western blotting (**Fig. 5.3**). As expected for CLR•RAMP1, transient stimulation with CGRP did not induce degradation of CLR (**Fig. 5.3B**, 84.6±9.7% compared to control). However, when CLR•RAMP1 are continuously stimulated with CGRP, CLR are almost completely degraded (**Fig. 5.3B**, 13.0±2.7% compared to control). In contrast, stimulation of CLR•RAMP2 with ADM induced degradation of CLR irrespective of whether the stimulation was transient or continuous (**Fig. 5.3D**, 25.1±6.9% (10 min) and 0.7±0.4% (16 h) compared to control). Thus, CLR•RAMP2 is degraded following stimulation with ADM and does not recycle.

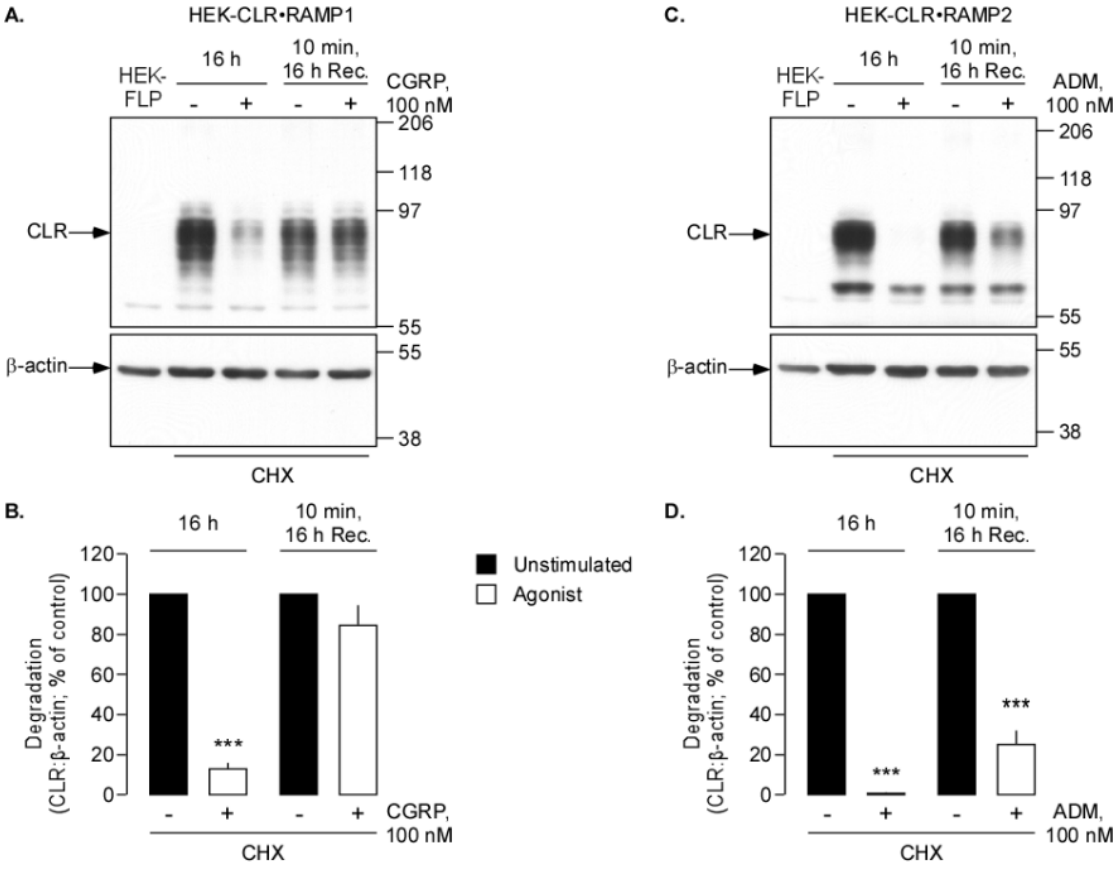

Figure 5.3 **Effect of transient and continuous stimulation on levels of CLR•RAMP1 and CLR•RAMP2.** (**A**) HEK-CLR•RAMP1 and (**C**) HEK-CLR•RAMP2 cells incubated with CHX (140 µM), stimulated transiently with agonist (100 nM, 10 min), washed and incubated in agonist-free medium (16 h); or stimulated continuously with agonist (100 nM, 16 h) and levels of CLR and β-actin determined by Western blotting. There were no signals for CLR in untransfected HEK-FLP cells, indicating specificity of the anti-CLR (HA) antibody. (**A**, **C**) Representative blots are shown. (**B**, **D**) Blots were quantified using ImageJ, ratios of CLR:β-actin calculated and results expressed as the % of appropriate unstimulated controls. (**B**) Continuous stimulation (16 h) with CGRP induces significant degradation of CLR. In contrast, transient stimulation (10 min) does not cause degradation of CLR. (**D**) Continuous and transient stimulation of ADM causes significant degradation of CLR. n=4, ***=p<0.001 compared to vehicle-treated cells at the same time point.

5.3.2 Localisation of CLR•RAMP2 by Immunostaining

To confirm that CLR•RAMP2 does not recycle after transient stimulation, the localisation of CLR•RAMP2 was analysed by confocal microscopy. The same method has already been used to show that CGRP-induced CLR•RAMP1 recycles back to the cell-surface after 6 h recovery (Padilla et al., 2007). Cell-surface receptors were labelled by incubating (30 min) HEK-CLR•RAMP2 cells with antibodies to extracellular RAMP1 (myc) epitopes. Cells were then stimulated with ADM (10 min), washed and incubated in ADM-free medium (0-6 h). Receptors were then localised by immunofluorescence and confocal microscopy (**Fig. 5.4**). In unstimulated cells, RAMP2 is at the cell-surface. Stimulation with ADM induces internalisation of RAMP2 to intracellular vesicles. After 6 h of recovery, the receptor has not recycled to the membrane. Moreover, the signal has almost completely disappeared, showing that the antibodies have been degraded, which suggests that the receptor is also degraded. Thus, CLR•RAMP2 does not recycle after transient stimulation.

5.4 ADM Induces Ubiquitination of CLR, but not RAMP2

Ubiquitin is a small regulatory protein which can be covalently attached to lysine residues of targets proteins. Modification by ubiquitination plays important roles in the life of a GPCR (reviewed by (Hanyaloglu and von Zastrow, 2008; Marchese et al., 2008)), such as to target GPCR for degradation. Therefore, as ADM induces degradation of CLR, it was investigated whether ADM also causes ubiquitination of CLR•RAMP2. To determine if CLR•RAMP2 was ubiquitinated, HEK-CLR•RAMP2 cells were stimulated with ADM (0-60 min) and CLR and RAMP2 immunoprecipitated and analysed by Western blotting for the presence of ubiquitin. In unstimulated HEK-CLR•RAMP2 cells there was a low basal level of ubiquitination of CLR compared to untransfected cells (**Fig. 5.5**). ADM stimulation, after 60 minutes, ADM induces further ubiquitination of CLR (**Fig. 5.5C**, 4.7±1.2 fold increase over basal). Under the same conditions ubiquitination of RAMP2 was not observed (**Fig. 5.5B**). There were no signals in untransfected HEK-FLP cells indicating specificity of the immunoprecipitating antibodies. Thus, ADM induces ubiquitination of CLR, but not RAMP2.

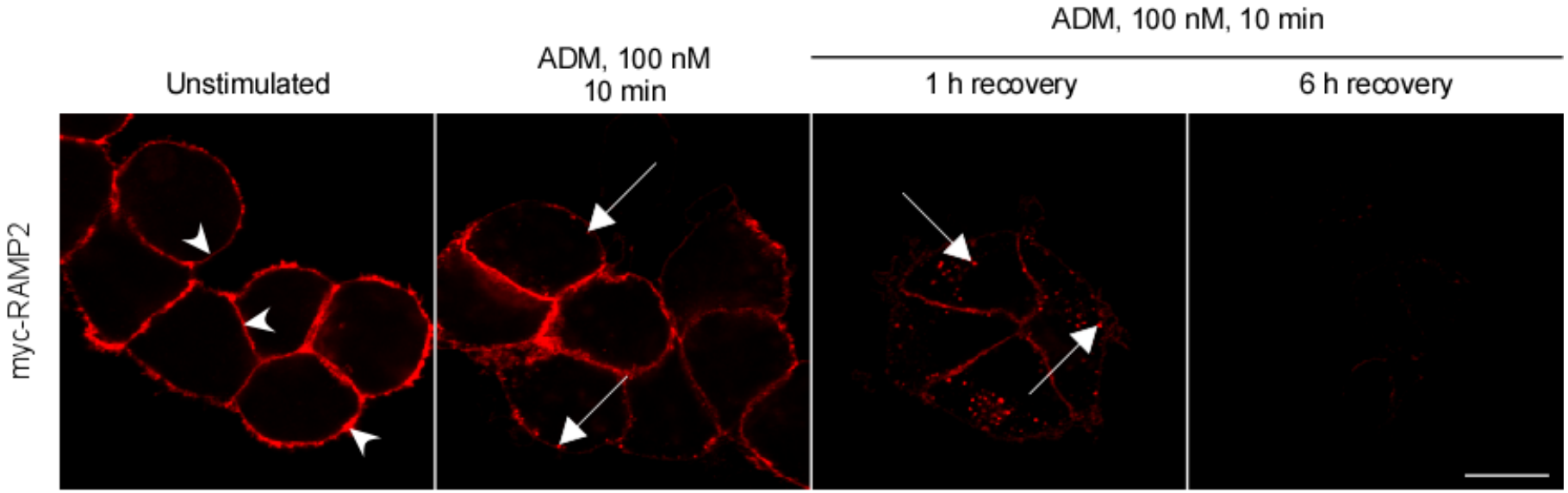

Figure 5.4 **CLR•RAMP2 does not recycle after transient stimulation.** HEK-CLR•RAMP2 cells were incubated (30 min, 37°C) with antibody against the extracellular epitope tag of RAMP2 (myc), stimulated with ADM (100 nM, 10 min), washed and incubated in ADM-free medium (0-6 h). Immunoreactive proteins were detected by immunofluorescence and analysed by confocal microscopy. In unstimulated cells, CLR are present at the cell-surface (arrowheads). ADM induces trafficking of CLR in intracellular vesicles (arrows). After 6 h of recovery, the receptor has not recycled to the cell-surface and the signal has almost completely disappeared, which implies the degradation of the antibodies. This result suggests that CLR•RAMP2 does not recycle to the cell-surface and is degraded. Scale bar = 10 µm.

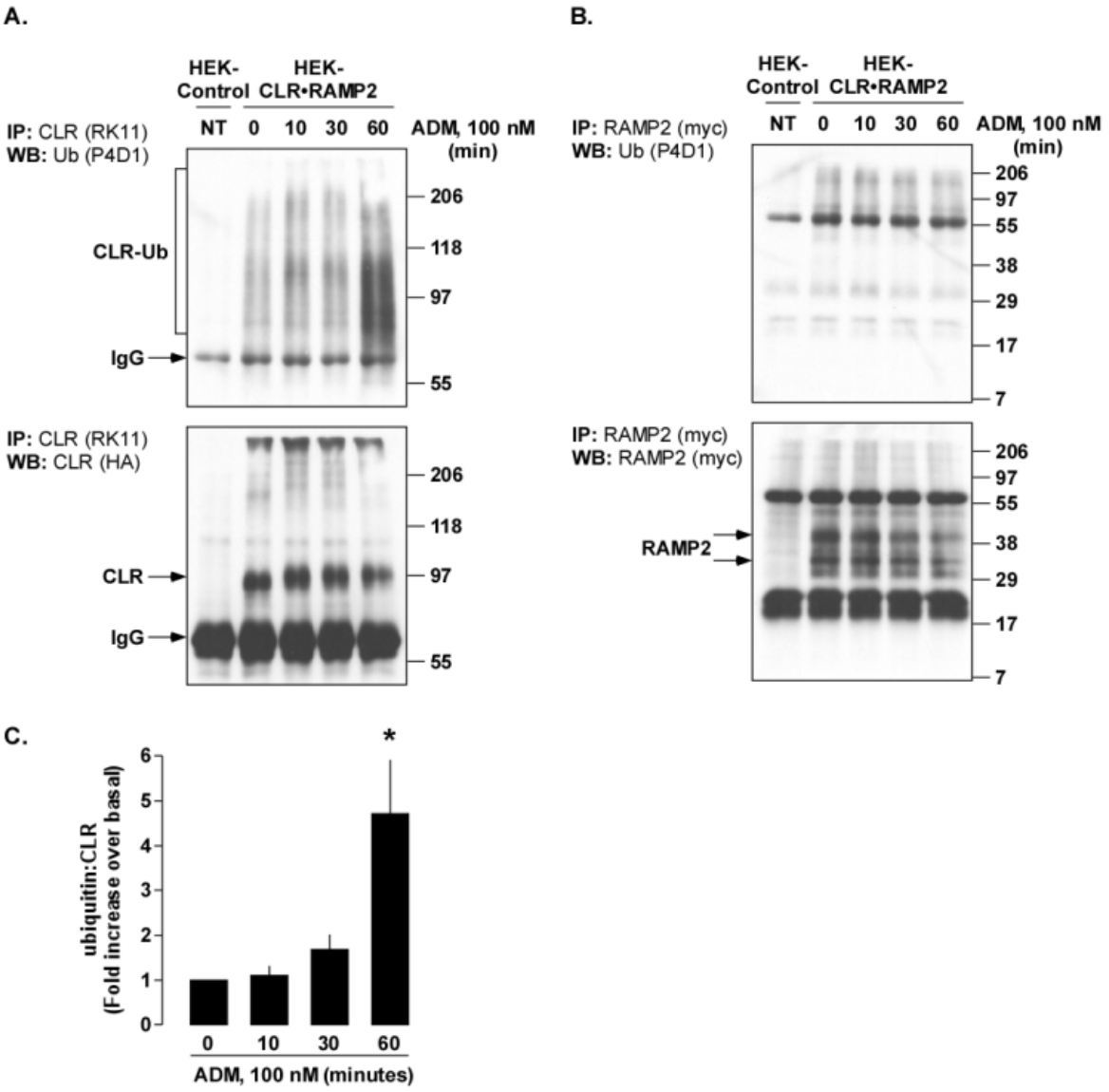

Figure 5.5 **ADM induces ubiquitination of CLR.** (**A, B**) HEK-CLR•RAMP2 cells were stimulated with ADM (100 nM, 0-60 min) and CLR and RAMP2 immunoprecipitated with anti-CLR (RK11) and anti-myc antibodies. Blots were probed for levels of ubiquitin, CLR (anti-HA) and RAMP2 (anti-myc). Immunoreactive bands were quantified using ImageJ. Representative blots are shown. (**C**) Ratios of Ub:CLR calculated and results expressed as fold over the unstimulated control. There were no signals in untransfected HEK cells, indicating specificity of the immunprecipitating antibodies. Basal levels of ubiquitinated CLR are low compared to untransfected cells. ADM significantly further enhances ubiquitination of CLR at 60 min. (**B**) ADM does not induce ubiquitination of RAMP2. n=4, NT=non transfected *=p<0.05 compared to vehicle-treated cells at the same time point.

5.5 Construction of CLR Mutant: CLRΔ9KR

ADM induces ubiquitination of CLR. Ubiquitin is commonly known for its role to target GPCRs to lysosome to be degraded, such as the β2-AR, CXCR4 and PAR2 (Jacob et al., 2005; Marchese et al., 2003; Shenoy et al., 2001). However, ubiquitin has been show to have other roles. In yeast, ubiquitination is required to drive internalisation of the GPCR Ste2 (Hicke and Riezman, 1996), whereas for the ubiquitination of δOR, it affects the rate of degradation of the receptor (Hislop et al., 2009). In order to determine the role of ADM-induced CLR ubiquitination, a CLR mutant was made. By using a site-directed mutagenesis method, all intracellular facing lysine residues (site of binding of ubiquitin to its target protein) of CLR were replaced by arginine residues.

5.5.1 Identification of the Lysine Residues and Design of the Method

The sequence of CLR was retrieved from UniProtKB database (Q16602). All lysine residues were then identified on the predicted intracellular loops and the C-terminal tail of CLR (**Fig. 5.6**). In total, 9 lysine residues were identified.

Lysine residues are defined by the genetic code by two sets of codon: AAA or AAG, while arginine residues are defined by six sets of codon: AGA, AGG, CGU, CGC, CGA or CGG. However, only the two sets of codon AGA and AGG are relevant to substitute the middle nucleic acid to change a lysine into arginine:

AAA or AAG = Lysine

↓

AGA or AGG = Arginine

The PCR site-directed mutagenesis method was employed to create the CLR mutant (Ho et al., 1989). This method consists of designing sets of oligonucleotide primers, overlapping the lysine residues, which contain the nucleic acid substitution coding for arginine. This method requires multistep PCR and restriction site nearby the mutagenesis site in order to divide the sequence into several fragments. As the 9 lysine residues are spread along the sequence, three unique restriction sites were identified within the sequence to facilitate the design of the primers. Thus, the restriction sites lead to the formation of three main fragments.

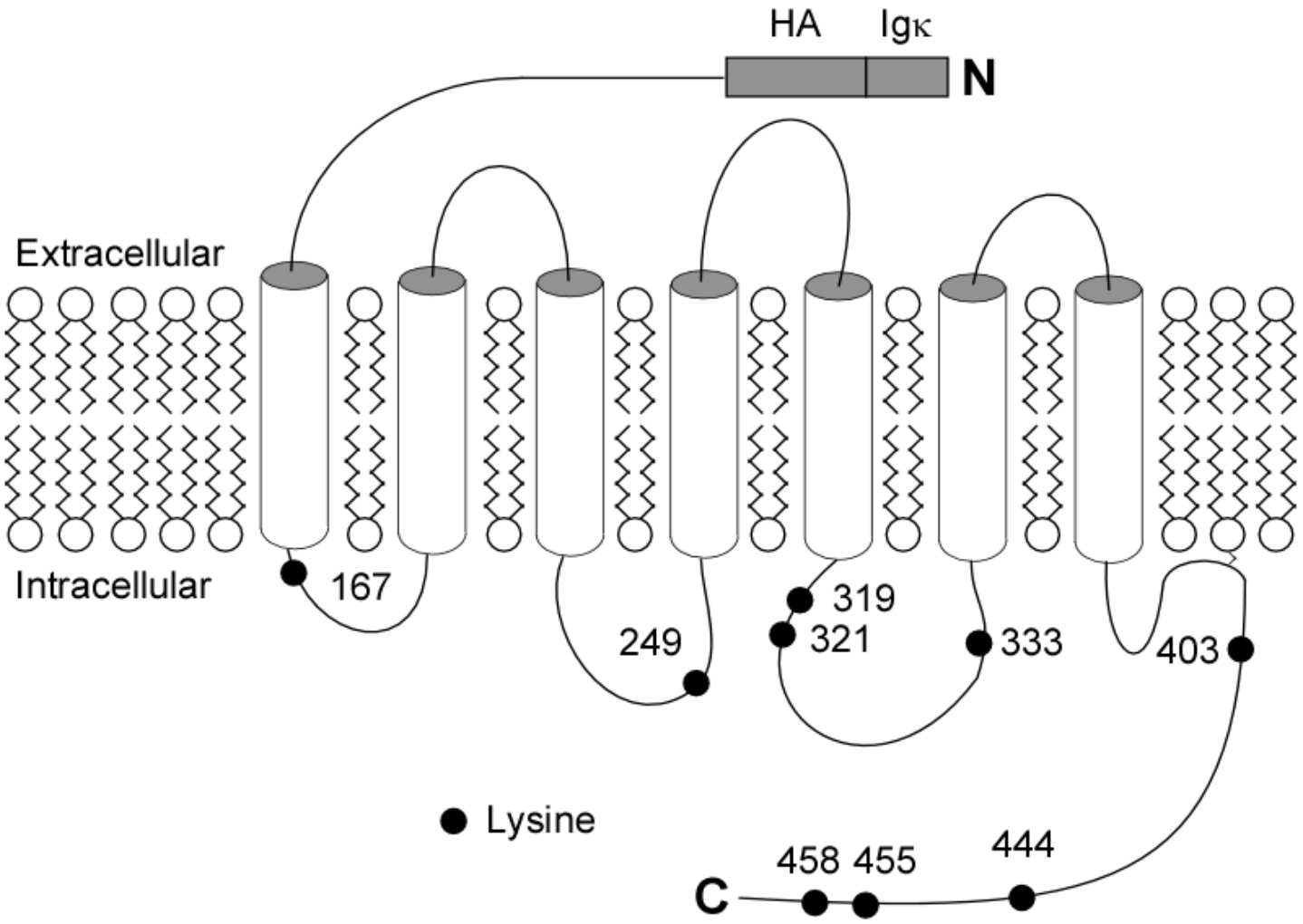

Figure 5.6 **Representation of the topology of CLR.** CLR is represented embed in the plasma membrane. The grey boxes represent the tags HA and Igκ at the N terminal. The black-filled circles are all the lysine residues identified as potential target for ubiquitination.

5.5.2 Production of the Different Fragment by PCR Site-Directed Mutagenesis Method

In order to construct this mutant, the plasmid pcDNA5/FRT-IgκHACLR was used as a template.

5.5.2.1 Production of the First Fragment

For the production of the first fragment, a two-step PCR was required (**Fig. 5.7**). Two pairs of oligonucleotide primers were designed, where in red is represented the codon containing the substitution that codes for arginine residue. The blue sequence represents the restriction site:

- Primer 1: rCLR*BamH*Ifor 5'-TCATGCAGGATCCCATTC-3'
- Primer 2: rCLRK167Rrev 5'-TTTATTTCAGGAGCCTAAGT-3'
- Primer 3: rCLRK249Kfor 5'-TTGCAGAGAGGCAGCACTTG-3'
- Primer 4: rCLR*Afl*IIIrev 5'-ATTGTACGTGTTCTCATCACC-3'

First, two PCR were performed simultaneously using primers 1 and 2 that resulted on the formation of a product called 1-2; and primers 3 and 4 that formed the product 3-4. Then the products 1-2 and 3-4 were used as mega-primer in the second PCR to form the fragment 1-4. The final product was then digested using *BamH* I and *Afl* III enzymes and ready to be ligated.

5.5.2.2 Production of the Second Fragment

For the production of the second fragment, a two-step PCR was required (**Fig. 5.8**). Three oligonucleotide primers were designed, where in red is represented the codon containing the substitution that codes for arginine residue. The blue sequence represents the restriction site:

- Primer 5: rCLR*Afl*IIIK319,321Rfor
  5'-ATATTGTACGTGTTCTCATCACCAGGTTGAGAGTTACAC-3'
- Primer 6: rCLRK333Rfor 5'-TCTACATGAGAGCTGTAAGAG-3'
- Primer 7: rCLR*Kpn*Irev 5'-CATCTTGGTACCACTACTTG-3'

First, PCR using primers 6 and 7 was performed that resulted on the formation of a product called 6-7. Then in the second PCR, the primer 5 and the product 6-7 were used to form the fragment 5-7. The final product was then digested using *Afl* III and *Kpn* I enzymes and ready to be ligated.

5.5.2.3 Production of the Third Fragment

Finally, for the production of the third and last fragment, a two-step PCR was required (**Fig. 5.9**). Three oligonucleotide primers were design, where in red is represented the codon containing the substitution that codes for arginine residue. The blue sequence represents the restriction site:

- Primer 8: rCLR*Kpn*Ifor 5'-CATCTTGGTACCACTACTTG-3'
- Primer 9: rCLRK403Rrev 5'-CCAGTATAGAATCCAATTTG-3'
- Primer 10: rCLRK444,455,458R*Not*Irev
  5'-TAAATGGAAGAAGCATCCAGGATATTGAAAATGTTGCCTTAAGACCA
  GAAAGAATGTATGAGCGGCCGCAT-3'

First, PCR was performed using the primers 8 and 9 that resulted on the formation of a product called 8-9. Then the product 8-9 and the primer 10 were used in the second PCR to form the fragment 8-10. The final product was then digested using *Kpn* I and *Not* I enzymes and ready to be ligated.

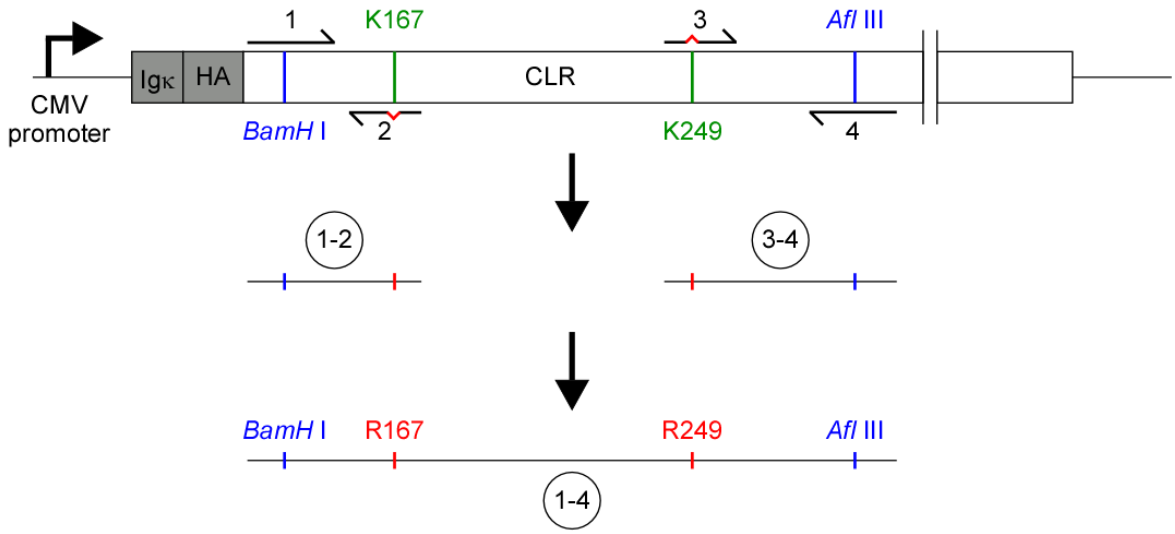

Figure 5.7 **Schematic representation of the production of the fragment 1-4.** The pcDNA5/FRT-IgκHACLR was used as template, where the rectangular box represents the sequence of CLR with Igκ and HA tags highlighted in grey. The lysine residues have been highlighted in green and the arginine residues in red. A two-step PCR led to the formation of the first fragment 1-4 (circle). Two simultaneously PCR were performed, using the primers (semi-arrows, with the red segment representing the substitution of arginine) 1 and 2 to produce the fragment 1-2 and primers 3 and 4 to produce the fragment 3-4. The fragments 1-2 and 3-4 were used as mega-primers to perform the second PCR, which formed the fragment 1-4 containing the arginine-coding sequence. The restriction sites are highlighted in blue.

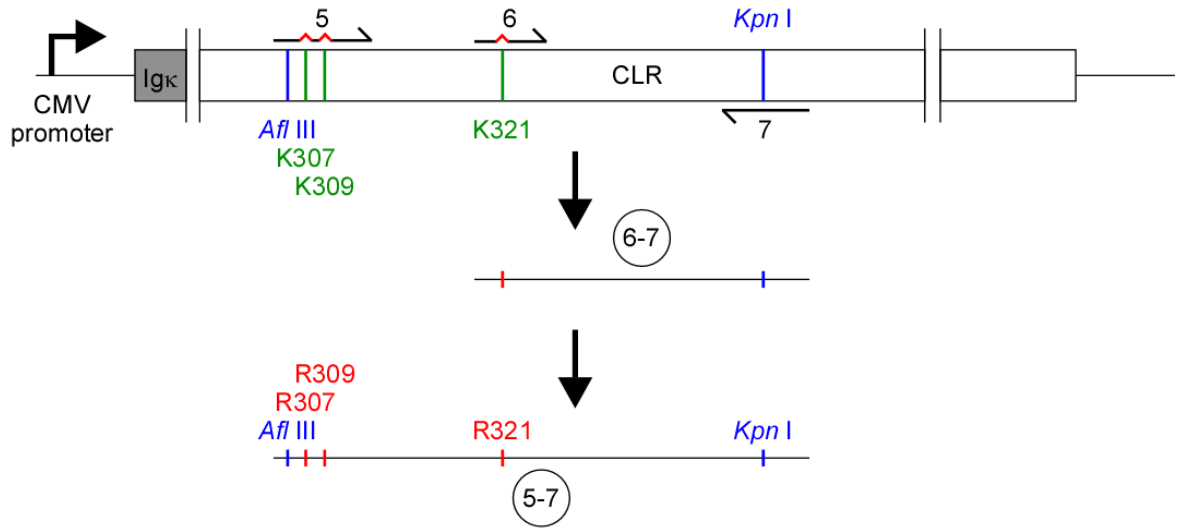

Figure 5.8 **Schematic representation of the production of the fragment 5-7.** The pcDNA5/FRT-IgκHACLR was used as template, where the rectangular box represents the sequence of CLR with Igκ tag highlighted in grey. The lysine residues have been highlighted in green and the arginine residues in red. A two-step PCR led to the formation of the second fragment 5-7 (circle). A PCR was performed, using the primers (semi-arrows, with the red segment representing the substitution of arginine) 6 and 7, to produce the fragments 6-7. The primer 5 and the fragments 6-7 were used as mega-primers to perform the second PCR, which formed the fragment 5-7 containing the arginine-coding sequence. The restriction sites are highlighted in blue.

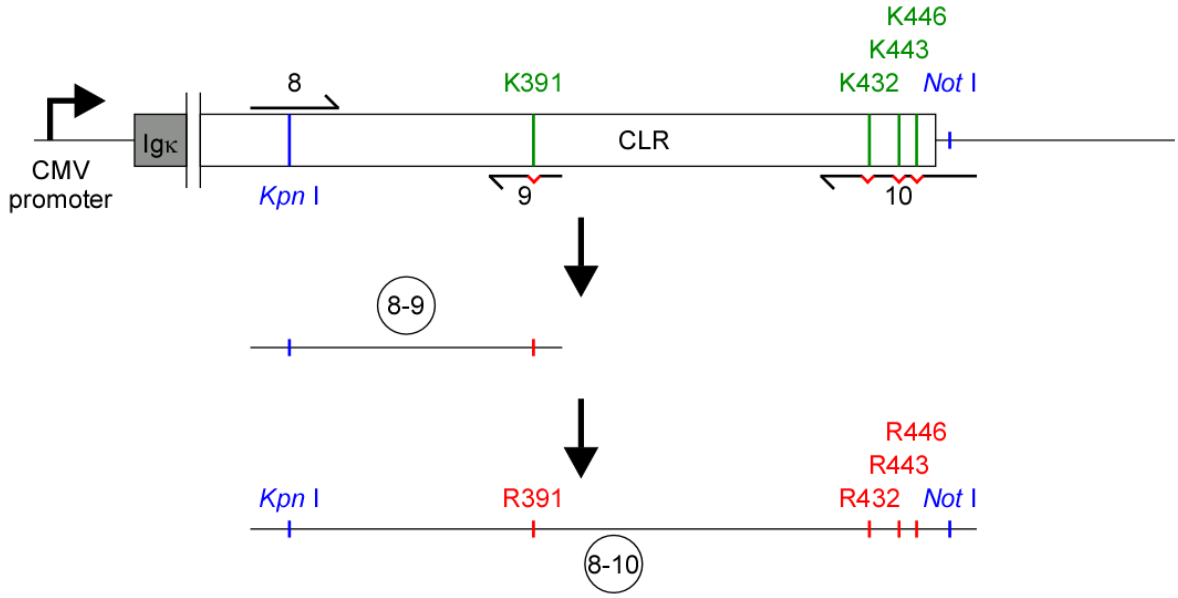

Figure 5.9 **Schematic representation of the production of the fragment 8-10.** The pcDNA5/FRT-IgκHACLR was used as template, where the rectangular box represents the sequence of CLR with Igκ tag highlighted in grey. The lysine residues have been highlighted in green and the arginine residues in red. A two-step PCR led to the formation of the third fragment 8-10 (circle). A PCR was performed, using the primers (semi-arrows, with the red segment representing the substitution of arginine) 8 and 9, to produce the fragments 8-9. The fragments 8-9 and the primer 10 were used as mega-primers to perform the second PCR, which formed the fragment 8-10 containing the arginine-coding sequence. The restriction sites are highlighted in blue.

5.5.2.4 Ligation of the Plasmid pcDNA5/FRT-IgκHACLRΔ9KR

The vector pcDNA5/FRT-IgκHACLR was digested by using the restriction enzymes *BamH* I and *Not* I. The digest was then run on a 1% agarose gel. *BamH* I and *Not* I cut only once in the vector, so two fragments was obtained on the gel: one of ~5000 base pair (bp) that contains the vector sequence and one of ~1200 bp that contain the CLR sequence. The higher fragment was then excised, which contains the vector sequence. Then the three mutated-fragments and the vector where ligated together (**Fig. 5.10**).

5.5.3 Production and Transfection of the Plasmid pcDNA5/FRT-IgκHACLRΔ9KR•RAMP2 into HEK Cells

The plasmid was then transformed into MACH1 bacterium. The DNA of a positive clone was then purified to yield a pcDNA5/FRT-IgκHACLRΔ9KR vector. Finally, the plasmid was transfected into HEK-FLP and cells were selected to express the receptor in a stable manner.

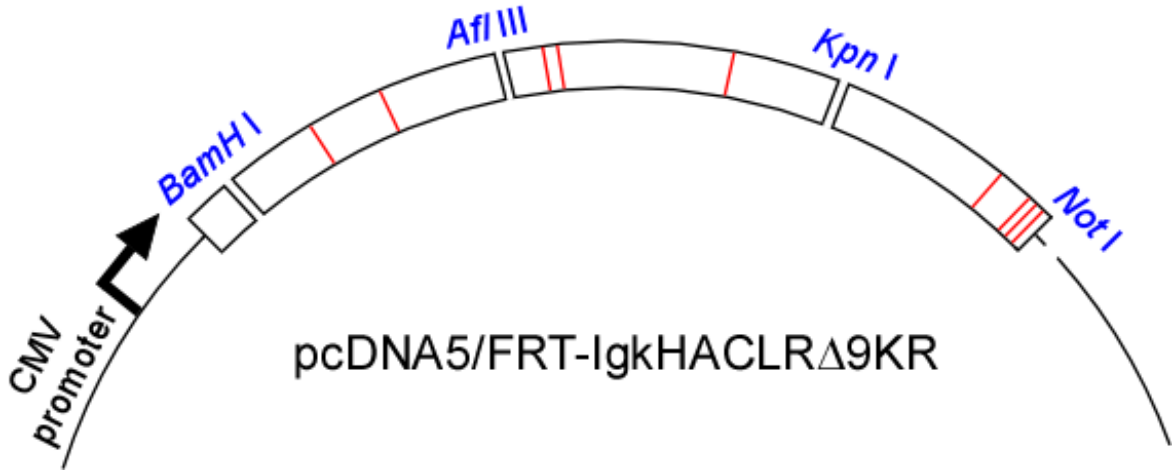

Figure 5.10 **Schematic representation of the ligation procedure.** The vector pcDNA5/FRT-IgκHACLR was cut open using *BamH* I and *Not* I enzyme. The CLR sequence was discarded and the vector sequence purified and ready to be mixed with the three mutated-fragments previously produced. All the fragments were ligated together, and the product was transform into MACH1 bacterium. After ligation the product forms a pcDNA5/FRT-IgκHACLRΔ9KR vector. The restriction enzyme sites are in blue and the substituted-arginine in red.

5.6 Characterisation of HEK-CLRΔ9KR•RAMP2 Cell Line

ADM induces ubiquitination of CLR. Ubiquitin is commonly known for its role to target GPCRs to lysosome to be degraded, such as the CXCR4 (Marchese et al., 2003) and PAR2 (Jacob et al., 2005). However, ubiquitin has been show to promote other responses. In yeast, ubiquitination is required to drive internalisation of the GPCR Ste2 (Hicke and Riezman, 1996), whereas for the δOR ubiquitination affects the rate of degradation (Hislop et al., 2009). In order to determine the role of ADM-induced ubiquitination, a CLR mutant was made (see **5.6**) and stably transfected into HEK-FLP cells. The receptor was then characterised and tested to confirm that it was functional.

5.6.1 CLRΔ9KR•RAMP2 Expression and Trafficking

ADM induces internalisation of CLR•RAMP2 in HEK cells. To determine if CLRΔ9KR•RAMP2 internalises normally, HEK-CLRΔ9KR•RAMP2 cells were stimulated with ADM (30 min) and CLRΔ9KR (HA) simultaneously localised with RAMP2 (myc) by immunofluorescence and confocal microscopy (**Fig. 5.11**). In unstimulated cells, CLRΔ9KR is localised at the cell-surface as well as RAMP2. Stimulation with ADM induces internalisation of CLRΔ9KR together with RAMP2 in the same intracellular vesicles. Thus, CLRΔ9KR•RAMP2 is expressed at the cell-surface and ADM causes its internalisation, which suggest that CLRΔ9KR•RAMP2 is functional.

5.6.2 ADM-Induced ERK Activation in HEK-CLRΔ9KR•RAMP2 Cells

ADM induces ERK activation in HEK-CLR•RAMP2. To determine if ADM induces ERK activation in HEK-CLRΔ9KR•RAMP2, cells were incubated in serum-free medium and stimulated with ADM (0-60 min). Levels of pERK1-2 and ERK2 were determined by Western blotting. In unstimulated cells levels of pERK1-2 were low (**Fig. 5.12**). ADM treatment increased dramatically pERK1-2 with a peak at 2 min and then progressively decreased (**Fig. 5.12B**, 17.5±1.7 for pERK1; and 8.1±3.8 for pERK2 fold increase compare to basal at 2 min). This result shows that ADM is able to induce ERK activation in HEK-CLRΔ9KR•RAMP2 cells.

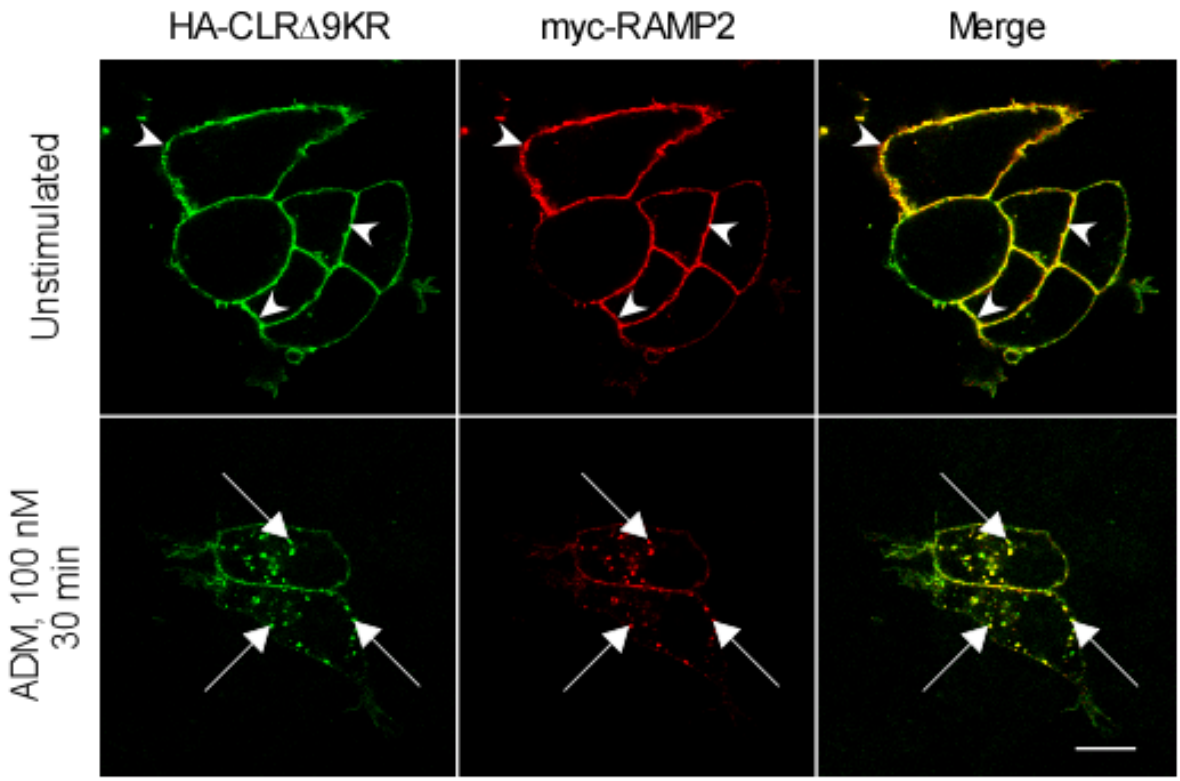

Figure 5.11 **ADM induces internalisation of CLRΔ9KR•RAMP2.** HEK-CLRΔ9KR•RAMP2 cells were stimulated with ADM (100 nM, 30 min), immunoreactive proteins were detected by immunofluorescence and analysed by confocal microscopy. In unstimulated cells, CLRΔ9KR and RAMP2 are co-localised at the cell-surface (arrowheads). ADM induces internalisation of CLRΔ9KR and RAMP2 together in the same intracellular vesicles (arrows). Thus CLRΔ9KR•RAMP2 is expressed at the cell-surface and ADM induces its internalisation. Scale bar = 10 μm.

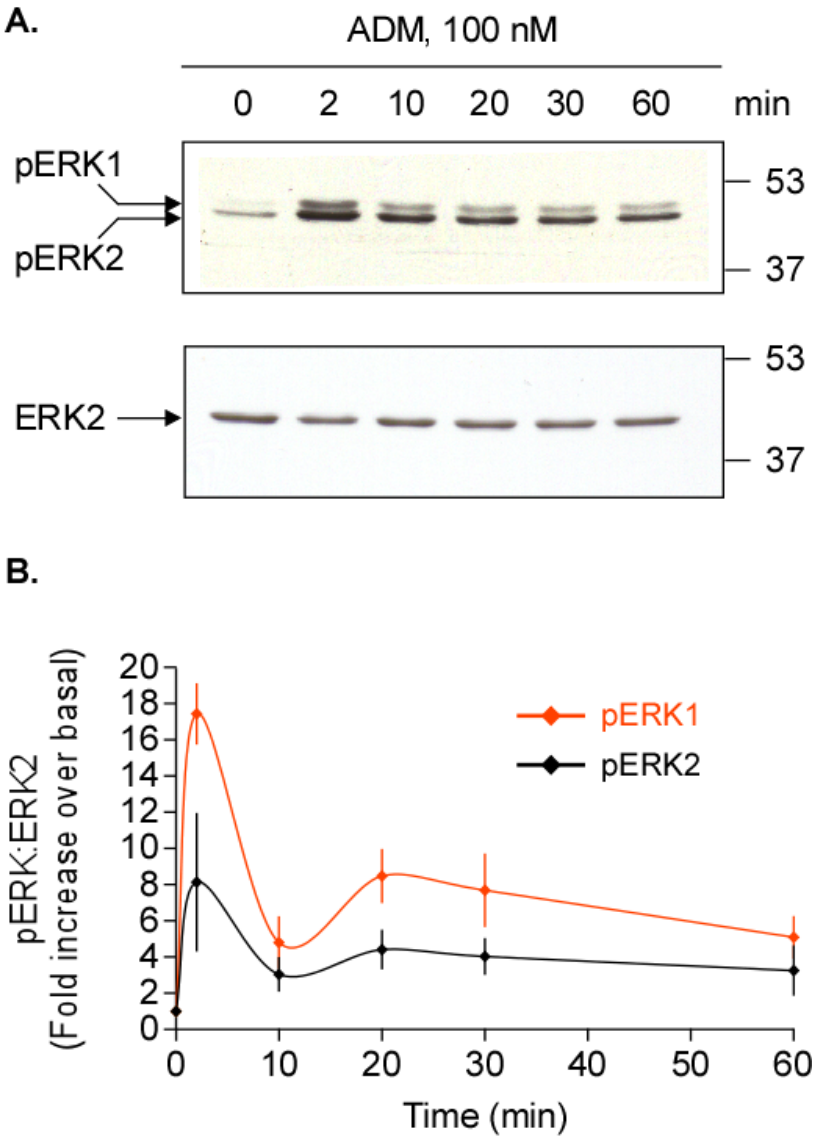

Figure 5.12 **ADM induces ERK activation in HEK-CLRΔ9KR•RAMP2.** (**A**) Serum-starved HEK-CLRΔ9KR•RAMP2 cells were stimulated with ADM (100 nM, 0-60 min) and levels of pERK1-2 and ERK2 determined by Western blotting, where a representative blot is shown. Blots were quantified using ImageJ. (**B**) Ratios of pERK1:ERK2 and pERK2:ERK2 calculated and expressed as fold increase over basal, show that ADM induces a prompt increase level of pERK1-2 activation, which is sustained by decreases over time. n=3.

5.6.3 ADM does not Induce CLR∆9KR Ubiquitination

A lysine-less mutant of CLR was made to study the role of ubiquitination in the regulation of CLR•RAMP2. To verify that CLR∆9KR•RAMP2 was not ubiquitinated, HEK-CLR∆9KR•RAMP2 cells were stimulated with ADM (0-60 min) and CLR∆9KR immunoprecipitated and analysed by Western blotting for the presence of ubiquitin. Either in unstimulated or stimulated HEK-CLR∆9KR•RAMP2 cells, the presence of ubiquitination of CLR∆9KR was not detected (**Fig. 5.13**). There were no signals in HEK-FLP cells for CLR∆9KR indicating specificity of the immunoprecipitating antibodies. Thus, ADM does not induce ubiquitination of CLR∆9KR.

5.7 Determination of the Role of Ubiquitin in CLR•RAMP2 Post-Endocytic Sorting

ADM stimulation of HEK-CLR∆9KR•RAMP2 induces ERK activation and CLR∆9KR•RAMP2 internalisation, suggesting that this receptor is fully functional. Moreover, ADM does not induce ubiquitination of CLR∆9KR. Therefore, HEK-CLR∆9KR•RAMP2 is suitable model to study the role of ubiquitination in the post-endocytic sorting of CLR•RAMP2.

5.7.1 ADM-Induced Trafficking of CLR•RAMP2 and CLR∆9KR•RAMP2

5.7.1.1 Trafficking to Early Endosomes

Many GPCRs undergo agonist-induced endocytosis in order to terminate GPCR-dependent cell membrane signalling (reviewed in (Doherty and McMahon, 2009; Ferguson, 2001)). Generally, following internalisation, GPCRs traffic to a sorting vesicle named early endosome, where they can either be targeted to lysosome for degradation, or redirected to the cell-surface to recycle (reviewed in (Mellman, 1996)). To determine if CLR•RAMP2 and CLR∆9KR•RAMP2 traffics to early endosomes, HEK-CLR•RAMP2 and HEK-CLR∆9KR•RAMP2 cells were stimulated with ADM (30 min) and CLR and CLR∆9KR (RK11) simultaneously localised with EEA1 (an early endosome marker) by immunofluorescence and confocal microscopy (**Fig. 5.14**). In unstimulated cells, both CLR (**Fig. 5.14A**) and CLR∆9KR (**Fig. 5.14B**) are localised at the cell-surface and EEA1 is detected in intracellular vesicles. Stimulation with ADM induces internalisation of CLR and CLR∆9KR to co-localise with EEA1-positive vesicles. Thus, ADM causes trafficking of CLR•RAMP2 and CLR∆9KR•RAMP2 to early endosomes, which

suggest that ubiquitin is not involved in the trafficking of CLR•RAMP2 to endosome.

5.7.1.2 Trafficking to Lysosomes

To be degraded, GPCRs are generally targeted to lysosomes via ubiquitin-dependent mechanisms such as the CXCR4 receptor (Marchese and Benovic, 2001) or -independent mechanisms such as CLR•RAMP1 (Cottrell et al., 2007). To determine if CLR•RAMP2 traffics to the lysosome in an ubiquitin-dependent manner, HEK-CLR•RAMP2 and HEK-CLRΔ9KR•RAMP2 cells were incubated (30 min) with lysosomal protease inhibitors (pepsatin A, E-64d and Z-PAD) to prevent possible degradation of the receptor and facilitate visualisation in lysosome. Cells were then stimulated with ADM (4 h) and CLR and CLRΔ9KR (RK11) simultaneously localised with LAMP1 (a lysosomal marker) by immunofluorescence and confocal microscopy (**Fig. 5.15**). In unstimulated cells, both CLR (**Fig. 5.15A**) and CLRΔ9KR (**Fig. 5.15B**) are localised at the cell-surface and LAMP1 is detected in intracellular vesicles. Stimulation with ADM induces internalisation of CLR and CLRΔ9KR to co-localise with LAMP1-positive vesicles. Thus, ADM causes trafficking of CLR•RAMP2 and CLRΔ9KR•RAMP2 to lysosomes, which suggests that ubiquitin is not involved in the ADM-induced traffic of CLR•RAMP2 to lysosomes.

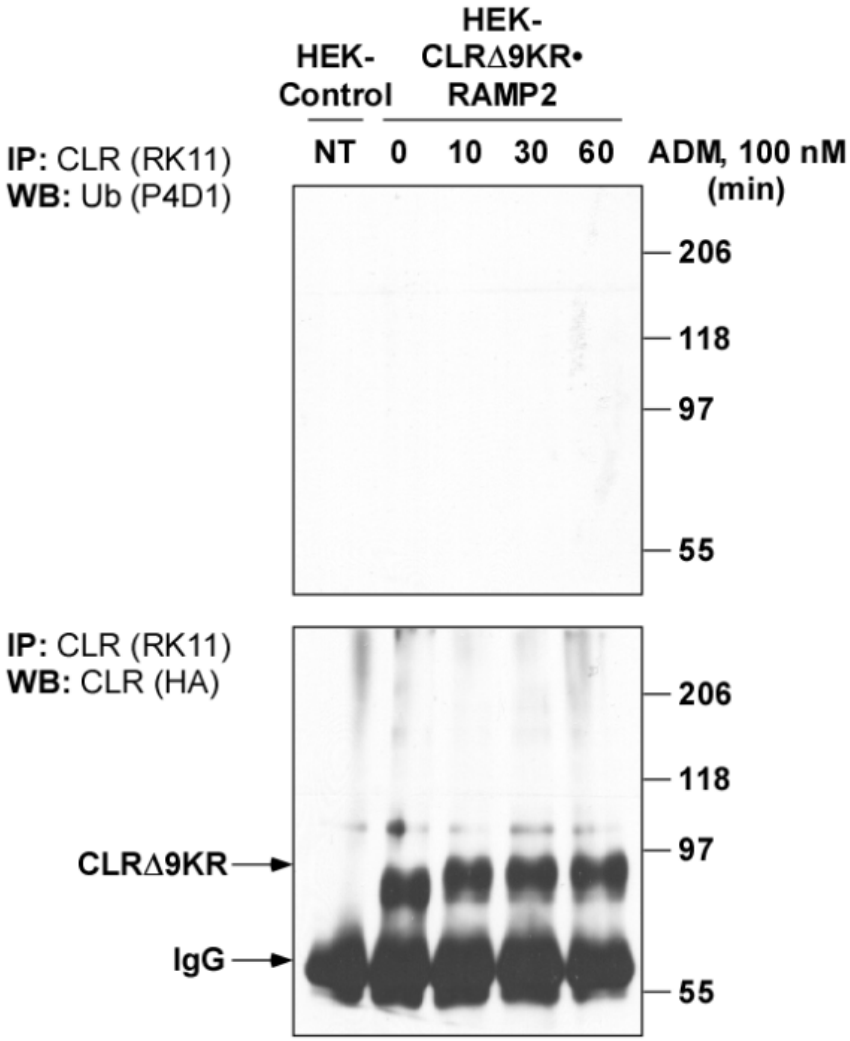

Figure 5.13 **ADM does not induce ubiquitination of CLRΔ9KR.** HEK-CLRΔ9KR•RAMP2 cells were stimulated with ADM (100 nM, 0-60 min) and CLRΔ9KR immunoprecipitated with anti-CLR (RK11). Blots were probed for levels of ubiquitin and CLR (anti-HA). Representative blots are shown. Probing for Ubiquitin shows no signal in treated cells, indicating that ADM does not induce ubiquitination of CLRΔ9KR. Gel was reprobed for CLR (anti-HA) and shows strong signal for CLR. There were no signals in untransfected HEK cells, indicating specificity of the immunprecipitating antibodies. n=4.

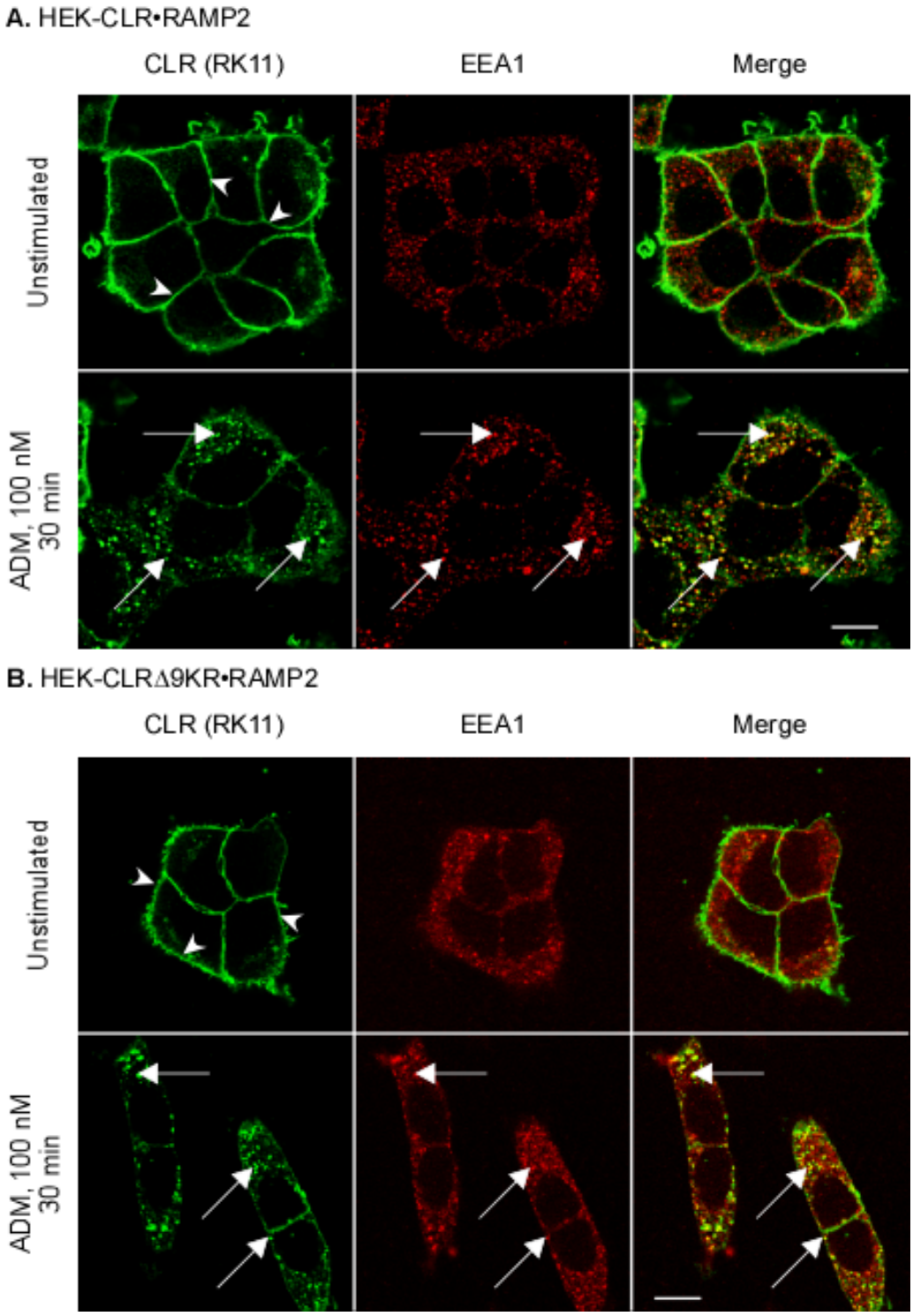

Figure 5.14 **CLR•RAMP2 and CLRΔ9KR•RAMP2 traffic to early endosomes upon ADM stimulation.** HEK-CLR•RAMP2 (**A**) and HEK-CLRΔ9KR•RAMP2 (**B**) cells were stimulated with ADM (100 nM, 0-30 min), immunoreactive proteins were detected by immunofluorescence and analysed by confocal microscopy. In unstimulated cells, CLR and CLRΔ9KR are present at the cell-surface (arrowheads) and EEA1 (early endosomal marker) is detected in intracellular vesicles. ADM induces internalisation of both CLR and CLRΔ9KR to co-localise with EEA1-positive vesicles (arrows). Thus, ADM induces traffic of CLR•RAMP2 and CLRΔ9KR•RAMP2 to early endosomes, which suggests that ubiquitin is not involved in the traffic of CLR•RAMP2 to endosomes. Scale bar = 10 μm.

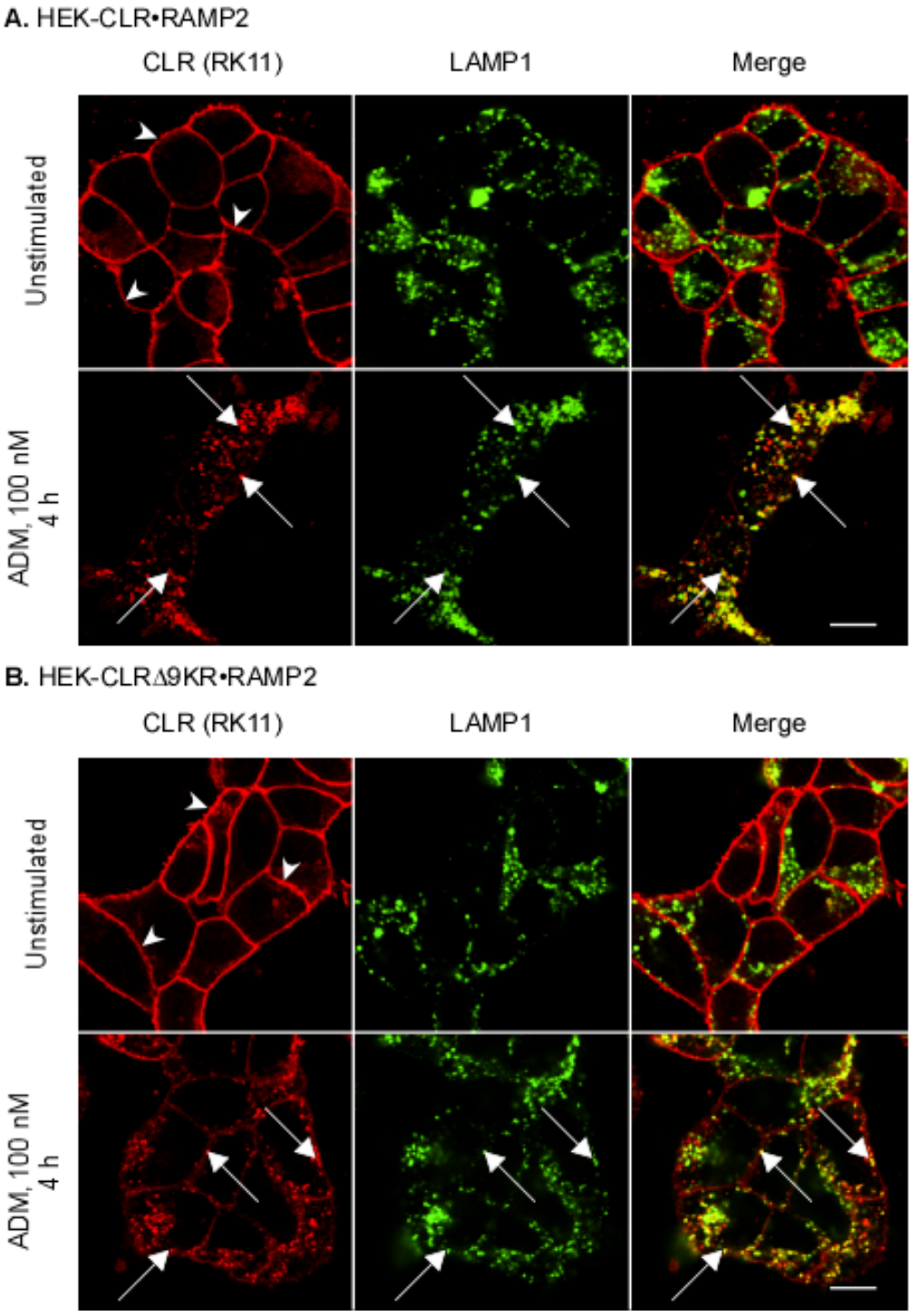

Figure 5.15 **CLR•RAMP2 and CLRΔ9KR•RAMP2 traffic to lysosomes upon ADM stimulation.** HEK-CLR•RAMP2 (**A**) and HEK-CLRΔ9KR•RAMP2 (**B**) cells were incubated with lysosomal protease inhibitors: pepsatin A (10 μM), E-64d (10 μM) and Z-PAD (200 μM), stimulated with ADM (100 nM, 4 h) and immunoreactive proteins detected by immunofluorescence and analysed by confocal microscopy. In unstimulated cells, CLR and CLRΔ9KR are present at the cell-surface (arrowheads) and LAMP1 (lysosomal marker) is detected in intracellular vesicles. ADM induces internalisation of both CLR and CLRΔ9KR to co-localise with LAMP1-positive vesicles (arrows). Thus, ADM induces traffic of CLR•RAMP2 and CLRΔ9KR•RAMP2 to lysosomes, which suggest that ubiquitin is not involved in the traffic of CLR•RAMP2 to lysosomes. Scale bar = 10 μm.

5.7.2 ADM-Induced Degradation of CLR•RAMP2 is Ubiquitin-Independent

5.7.2.1 ADM Induces Degradation of CLR•RAMP2 and CLRΔ9KR•RAMP2

ADM promotes trafficking of both CLR•RAMP2 and CLRΔ9KR•RAMP2 to lysosomes. Given that CLRΔ9KR•RAMP2 is not ubiquitinated, it was concluded that ubiquitination is not involved in the trafficking of CLR•RAMP2 to lysosomes. Next, the role of CLR ubiquitination was investigated, whether it is involved in the degradation of CLR. As CLR is ubiquitinated, a cell-surface biotinylation assay was used to monitor the degradation of CLR and CLRΔ9KR, as CHX can affect the pool of free ubiquitin within the cell (Hanna et al., 2003). HEK-CLR•RAMP2 and HEK-CLRΔ9KR•RAMP2 cells were stimulated with ADM continuously (16 h) or transiently (30 min) and incubated in agonist-free medium (0-16 h). Levels of CLR, CLRΔ9KR, RAMP2 and transferrin receptor (TfR) (loading control: this receptor internalises and recycles back to the cell-surface (reviewed in (Mayle et al., 2012))) were determined by Western blotting (**Fig. 5.16** and **Fig. 5.17**). Following continuous stimulation with ADM both CLR and CLRΔ9KR are similarly degraded (**Fig. 5.16B**, 7.5±3.5% (CLR) and 5.4±1.9% (CLRΔ9KR) of control). RAMP2 was also degraded to similar extents in both cell lines (**Fig. 5.17B**, 20.7±4.9% (CLR) and 14.2±7.5% (CLRΔ9KR) of control). In transient stimulation with ADM in both CLR and CLRΔ9KR are similarly degraded (**Fig. 5.16D**, 74.2±2.6% (CLR) and 60.6±8.0% (CLRΔ9KR) of control); RAMP2 was also degraded to similar extents in both cell lines (**Fig. 5.17D**, 72.1±0.8% (CLR) and 60.0±2.9% (CLRΔ9KR) of control). Thus, ADM induces in both continuous and transient stimulation, degradation of CLR•RAMP2 and CLRΔ9KR•RAMP2, which suggests that ubiquitination is not involved in CLR•RAMP2 degradation.

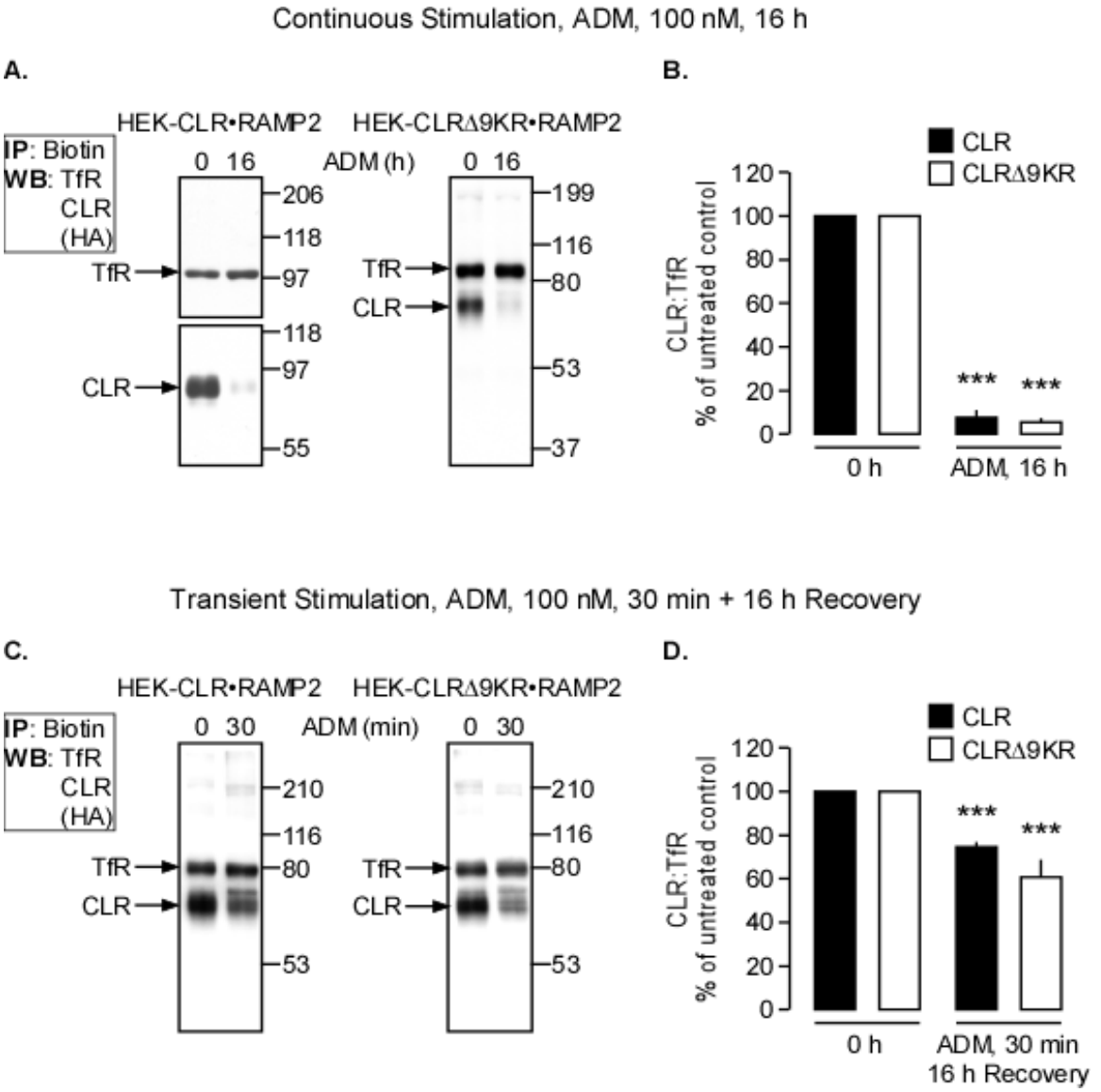

Figure 5.16 **ADM-induced degradation of CLR is ubiquitin-independent.** Cell-surface proteins of HEK-CLR•RAMP2 and HEK-CLRΔ9KR•RAMP2 cells were labelled with biotin. The cells were then stimulated with ADM (100 nM) continuously (16 h) (**A**, **B**) or transiently (30 min) (**C**, **D**). Cells were lysed and biotinylated proteins isolated by immunoprecipitation with Neutravidin. Levels of CLR, CLRΔ9KR and TfR were then analysed by Western blotting. (**A**, **C**) Representative blots are shown. Blots were quantified using ImageJ and ImageQuantTL, ratios of CLR:TfR calculated and results expressed as % of expression compared to the appropriate unstimulated control. In continuous stimulation (**B**), both CLR and CLRΔ9KR are almost completely degraded. In transient stimulation (**D**), CLR and CLRΔ9KR are significantly degraded compared to control. Thus, ADM induces degradation of CLR and CLRΔ9KR, which suggests that ubiquitin is not involved in the degradation of CLR. n≥3, **=p<0.01 and ***=p<0.001 compared to basal of the same cell line.

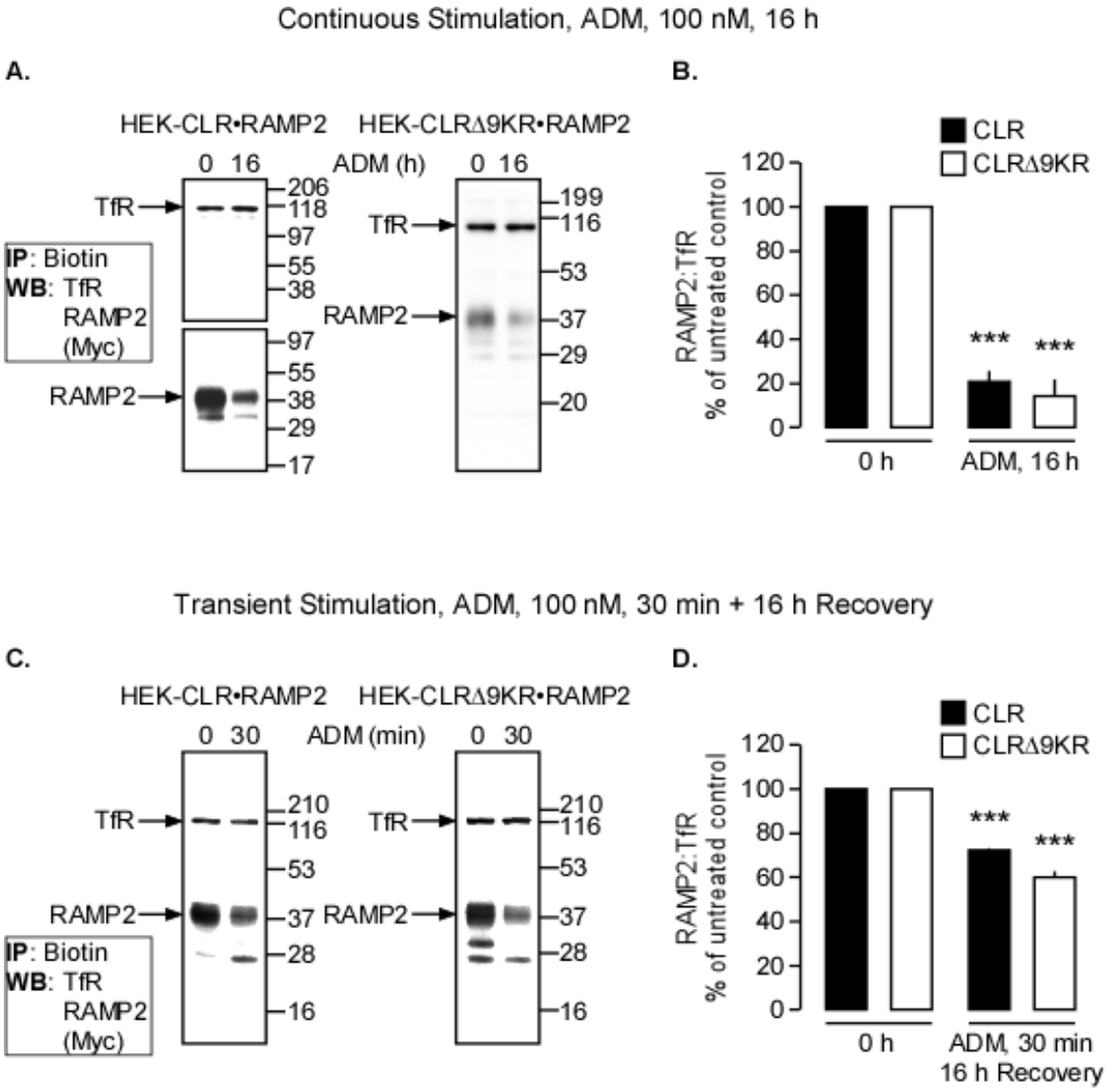

Figure 5.17 **ADM-induced degradation of RAMP2 is ubiquitin-independent.** Cell-surface proteins of HEK-CLR•RAMP2 and HEK-CLRΔ9KR•RAMP2 cells were labelled with biotin. The cells were then stimulated with ADM (100 nM) continuously (16 h) (**A**, **B**) or transiently (30 min) (**C**, **D**). Cells were lysed and biotinylated proteins isolated by immunoprecipitation with Neutravidin. Levels of RAMP2 and TfR in the isolated protein samples were then analysed by Western blotting. (**A**, **C**) Representative blots are shown. Blots were quantified using ImageJ and ImageQuantTL, ratios of RAMP2:TfR calculated and results expressed as % of expression compared to the appropriate unstimulated control. In continuous stimulation (**B**), in both cell lines, RAMP2 is largely degraded. In transient stimulation (**D**), in both cell lines, RAMP2 is significantly degraded compared to control. Thus, ADM induces degradation of RAMP2 in both cell lines, which suggests that ubiquitin of CLR is not involved in the degradation of RAMP2. $n \geq 3$, **=$p<0.01$ and ***=$p<0.001$ compared to basal of the same cell line.

5.7.2.2 Cell-Surface Expression and Internalisation of CLR•RAMP2 and CLRΔ9KR•RAMP2

In previous experiment looking at the degradation of CLR•RAMP2 using CHX (see **5.3.1**), transient ADM stimulation was shown to induce larger amount of degradation (see **Fig. 5.3A**, 28.2±5.4% expression over control), than observed in the biotinylation assay experiments (see **Fig. 5.16D**, 74.2±2.6% expression over control). To investigate this difference, the level of cell-surface expression and internalisation upon ADM stimulation of CLR•RAMP2 and CLRΔ9KR•RAMP2, were investigated. HEK-CLR•RAMP2 and HEK-CLRΔ9KR•RAMP2 cells were incubated (30 min) with an antibody (myc) against the receptor, stimulated with ADM (30 min) and incubated in agonist-free medium (0-1 h). Cells were then detached, suspended in ice-cold PBS and incubated (1 h, 4°C) with immunoreactive protein. Cells were then analysed using FACS flow cytometry method (**Fig. 5.18**). The measure of the fluoresence intensity of each cell population shows that in unstimulated cells, the level of fluorescence intensity is higher compared to stimulated cells (**Fig. 5.18A**). The quantification of the mean fluorescence intensity of all the different cell population reveals a significant reduction of intensity in both cell lines upon stimulation (**Fig. 5.18**B, 61.3±1.1% at 30 min vs 50.1±2.0% at 30 min+1 h Recovery (CLR) and 60.8±1.7% at 30 min vs 54.4±3.1% at 30 min+1 h Recovery (CLRΔ9KR); expression over unstimulated). Those results suggest that after stimulation, both receptors CLR•RAMP2 and CLRΔ9KR•RAMP2 are internalised. Furthermore, those experiments show that HEK-CLRΔ9KR•RAMP2 express less receptors at the cell-surface than HEK-CLR•RAMP2 (**Fig. 5.18C**, 82.4±0.4% of CLRΔ9KR•RAMP2 over CLR•RAMP2). Altogether, transient ADM stimulation promotes internalisation of CLR•RAMP2 (about 40%), which coincide with the percentage of receptor degraded (about 30-40%), as seen in the previous experiment (see **Fig. 5.16**). Thus, all receptors internalised are degraded, which confirms the results of the CHX experiment (see **Fig. 5.3**).

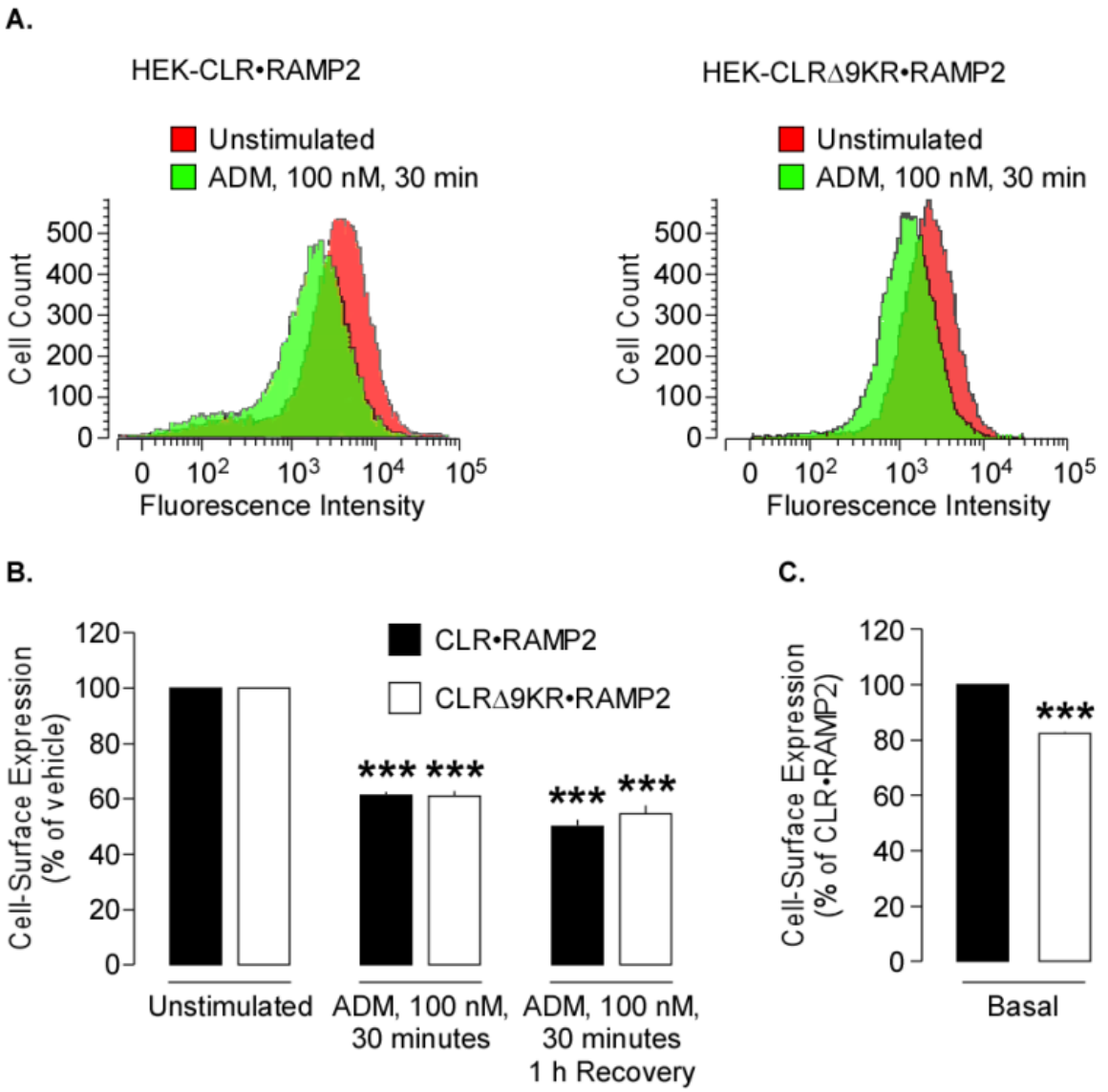

Figure 5.18 **Cell-surface expression and internalisation of CLR•RAMP2 and CLRΔ9KR•RAMP2 upon ADM stimulation.** HEK-CLR•RAMP2 and HEK-CLRΔ9KR•RAMP2 cells were incubated with myc antibody (30 min, 37°C), stimulated with ADM (100nM, 30 min) and incubated in agonist-free medium (0-1 h). Cells were then detached, suspended in ice-cold PBS and incubated (1 h, 4°C) with immunoreactive protein. Cells were then analysed using FACS flow cytometry method. (**A**) Examples of cell population stimulated with ADM or not are shown. (**B**) The mean fluorescence intensity of each condition (as indicated in the figure) was quantified and expressed as % of unstimulated cell population. Those results show a decrease of fluorescence intensity upon ADM stimulation compared to unstimulated population. (**C**) The cell-surface expression of both cell line were quantify and expressed as % of CLR•RAMP2 population. Those results show that in HEK-CLRΔ9KR•RAMP2 less receptors are expressed at the cell-surface than in HEK-CLR•RAMP2. n=4, * represent control vs stimulated where ***=p< 0.001.

5.7.3 ADM-Induced ERK Activation is Ubiquitin-Independent

It has been shown for IGF-1 receptor, that ubiquitination was involved in the activation of ERK (Vasilcanu et al., 2008). To determine the role of ubiquitin in the ADM-induced ERK activation, HEK-CLR•RAMP2 and HEK-CLR∆9KR•RAMP2 cells were stimulated with ADM (10 min), incubated in agonist-free medium (0-110 min) and levels of pERK1-2 and ERK2 determined by Western blotting. In unstimulated CLR•RAMP2 and CLR∆9KR•RAMP2 cells, levels of pERK1-2 were low (**Fig. 5.19**). ADM (10 min) caused a prompt increase in levels of pERK1-2 in both cell lines. However, the increase in CLR∆9KR•RAMP2 cells was reduced compared to CLR•RAMP2 cells, but not significantly for both pERK1 (**Fig. 5.19B**, 3.9±1.1 (CLR) and 2.7±0.4 (CLR∆9KR) for pERK1 and 3.9±0.7 (CLR) and 2.9±0.3 (CLR∆9KR) for pERK2; fold-increase at 10 min compare to basal). When expressed as % of maximal response they were no difference in the magnitude or duration of pERK1 and 2 levels in both cell lines (**Fig. 5.19D**, pERK1 51.5±9.6% (CLR) and 62.0±2.0% (CLR∆9KR); and **Fig. 5.19E**, pERK2 46.3±8.6% (CLR) and 54.7±6.7% (CLR∆9KR) at 110 min of maximal (10 min) response). Furthermore, the basal level of pERK was not affected by CLR∆9KR•RAMP2 (**Fig. 5.19C**, pERK1 1.0±0.05 and pERK2 1.1±0.1 fold increase over CLR•RAMP2). Thus, ADM induces similar level of phosphorylated ERK1 and 2, which suggests that ubiquitin is not involved in the ADM-induced ERK activation.

5.7.4 Kinetics of ADM-Induced Degradation of CLR•RAMP2 and CLR∆9KR•RAMP2

Ubiquitin of CLR does not seem to be involved in the degradation of CLR•RAMP2. However, it has been shown for the δ-opioid receptor, that ubiquitination of the receptor stimulates its degradation but is not essential (Henry et al., 2011; Hislop et al., 2009). To investigate this possibility, degradation of the receptor was looked for at an earlier time point.

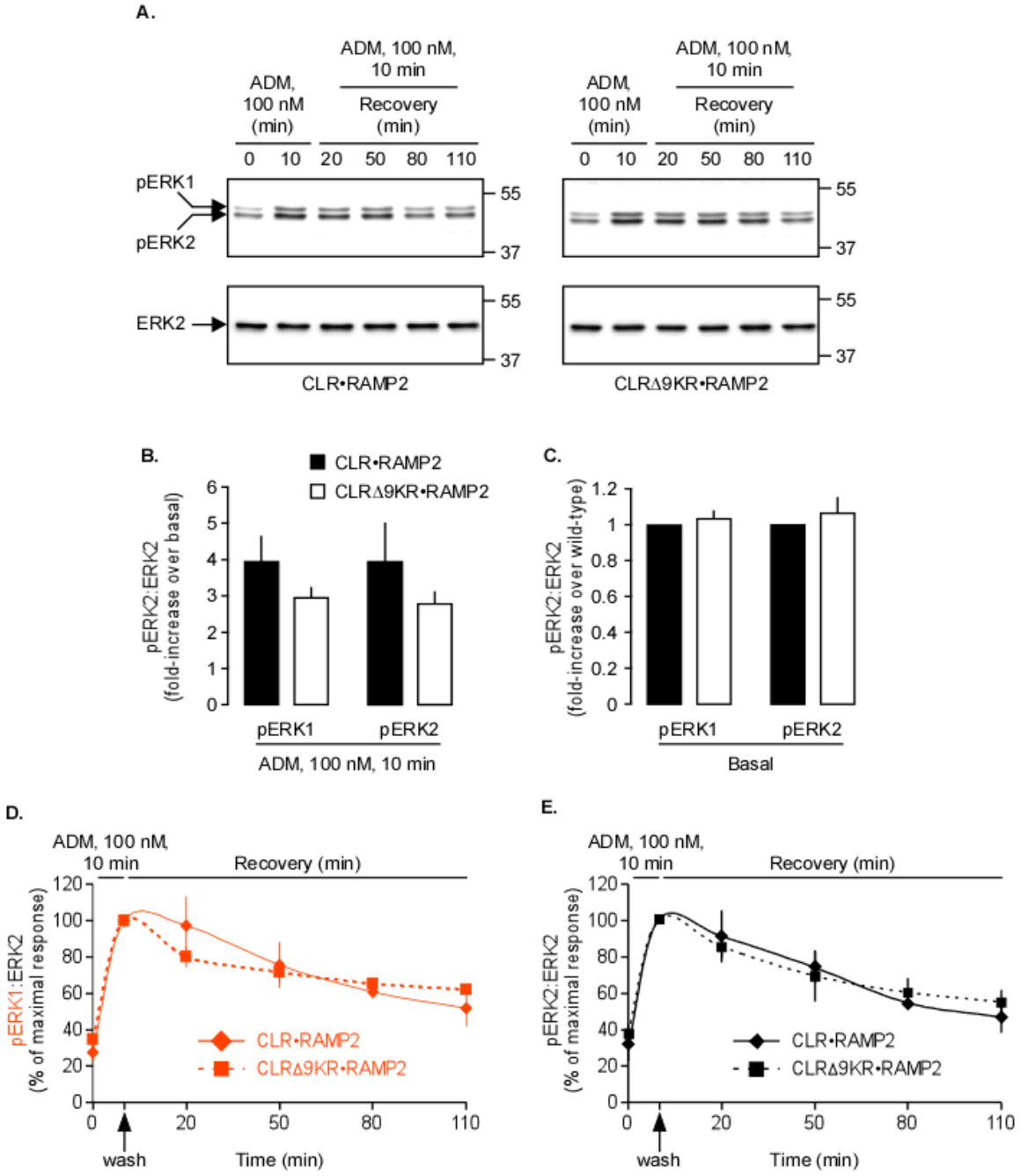

Figure 5.19 **Ubiquitination does not affect ADM-induced ERK activation.** (**A**) Serum-starved HEK-CLR•RAMP2 and HEK-CLRΔ9KR•RAMP2 cells stimulated with ADM (100 nM, 10 min), washed, incubated in ADM-free medium (0-110 min) and levels of pERK1-2 and ERK2 determined by Western blotting. Blots were quantified using ImageQuantTL. Representative blots are shown. (**B**) The maximal ADM-induced phosphorylation of ERK1 and 2, expressed in fold-increase over basal of pERK1:ERK2 and pERK2:ERK2, show no significant difference between both cell lines. (**C**) The effect of CLRΔ9KR•RAMP2 on the basal of pERK1-2, expressed in fold-increase over the basal, show no difference of pERK basal compared to CLR•RAMP2. The ADM-induced ERK activation, expressed as % maximal of response (10 min) of pERK1:ERK2 (**D**) and pERK2:ERK2 (**E**) are similar in both cell line. Thus, ADM induces similar level of ERK activation in both cell line, indicating that ubiquitin is not involved in ADM-induced ERK activation in HEK cells. n=3.

5.7.4.1 ADM Stimulation for 8 Hours

HEK-CLR•RAMP2 and HEK-CLRΔ9KR•RAMP2 cells were stimulated with ADM continuously (8 h). Levels of CLR, CLRΔ9KR, RAMP2 and TfR were determined by Western blotting (**Fig. 5.20**) and results express as % of expression compared to control. After 8 h stimulation, ADM induces in both cell line, almost complete degradation of CLR and CLRΔ9KR (**Fig. 5.20B**, 29.1±20.0% (CLR) and 12.5±8.9% (CLRΔ9KR) over control); and RAMP2 (**Fig. 5.20D**, 9.2±4.0% (CLR) and 26.6±2.6% (CLRΔ9KR) over control). Although, there were no significant differences between the degradation of CLR and CLRΔ9KR, the results show a significant difference in the degradation of RAMP2 between both cell lines, suggesting that the degradation of RAMP2 in the lysine-less mutant is slower than in the WT at 8 h. Altogether, these results show that ADM induces similar degradation profile in both cell lines, which suggests that ubiquitination is not involved in the degradation of CLR•RAMP2 at 8 h.

5.7.4.2 ADM Stimulation for 4 Hours

HEK-CLR•RAMP2 and HEK-CLRΔ9KR•RAMP2 cells were stimulated with ADM continuously (4 h). Levels of CLR, CLRΔ9KR, RAMP2 and TfR were determined by Western blotting (**Fig. 5.21**) and results express as % of expression compared to control. After 4 h stimulation, ADM induces significant degradation of CLR, whereas CLRΔ9KR is untouched (**Fig. 5.21B**, 64.2±3.5% (CLR•RAMP2) vs 109.5±10.3% (CLRΔ9KR•RAMP2) over control); and significant degradation of RAMP2 in both cell lines (**Fig. 5.21D**, 47.4±8.5% (CLR•RAMP2) and 85.9±4.9% (CLRΔ9KR•RAMP2) over control). However, ADM-induced degradation of CLR•RAMP2 is significantly higher than CLRΔ9KR•RAMP2, for both component of the receptor. These results show that ADM induces a greater degradation in the WT cell line than in the mutant, which suggests that ubiquitination is involved in the degradation of CLR•RAMP2 at 4 h. Altogether, the role of ubiquitination of CLR is involved in the rate of degradation of CLR, by accelerating the process.

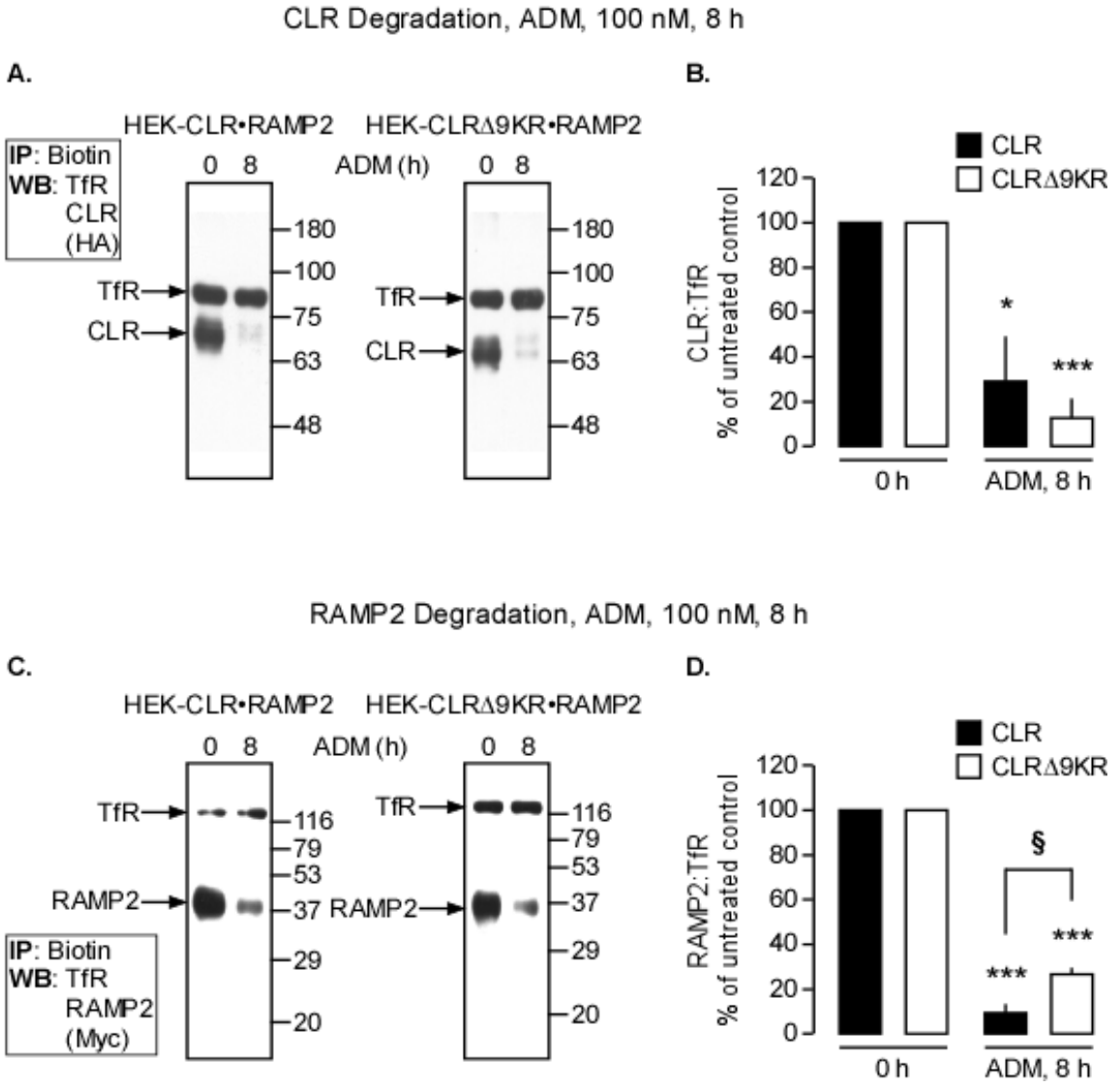

Figure 5.20 **Ubiquitination is not involved in ADM-induced degradation of CLR•RAMP2 at 8 h.** Cell-surface proteins of HEK-CLR•RAMP2 and HEK-CLRΔ9KR•RAMP2 cells were labelled with biotin. The cells were then stimulated with ADM (100 nM) continuously (8 h). Cells were lysed and biotinylated proteins isolated by immunoprecipitation with Neutravidin. Levels of CLR, CLRΔ9KR, RAMP2 and TfR in the isolated protein samples were then analysed by Western blotting. (**A**, **C**) Representative blots are shown. (**B**, **D**) Blots were quantified using ImageJ and ratios of CLR:TfR and RAMP2:TfR were calculated. The results were expressed as % of expression compared to the appropriate unstimulated control. (**A**, **B**) Both CLR and CLRΔ9KR are similarly degraded after ADM stimulation. Thus, ADM induces degradation of both CLR WT and mutant, which suggests that ubiquitin is not involved in the degradation of CLR at 8 h. (**C**, **D**) ADM induces degradation of RAMP2 in both cell lines, however RAMP2 in WT cell line was significantly more degraded that in mutant cell line. Thus, ADM induces a slower degradation of RAMP2 in the mutant cell line at 8 h, which suggests that ubiquitin is involved in the degradation process of RAMP2. n=3, *=$p<0.05$ and ***=$p<0.001$ compared to untreated cells, and §=$p<0.05$ compared to WT cell line at the same time point.

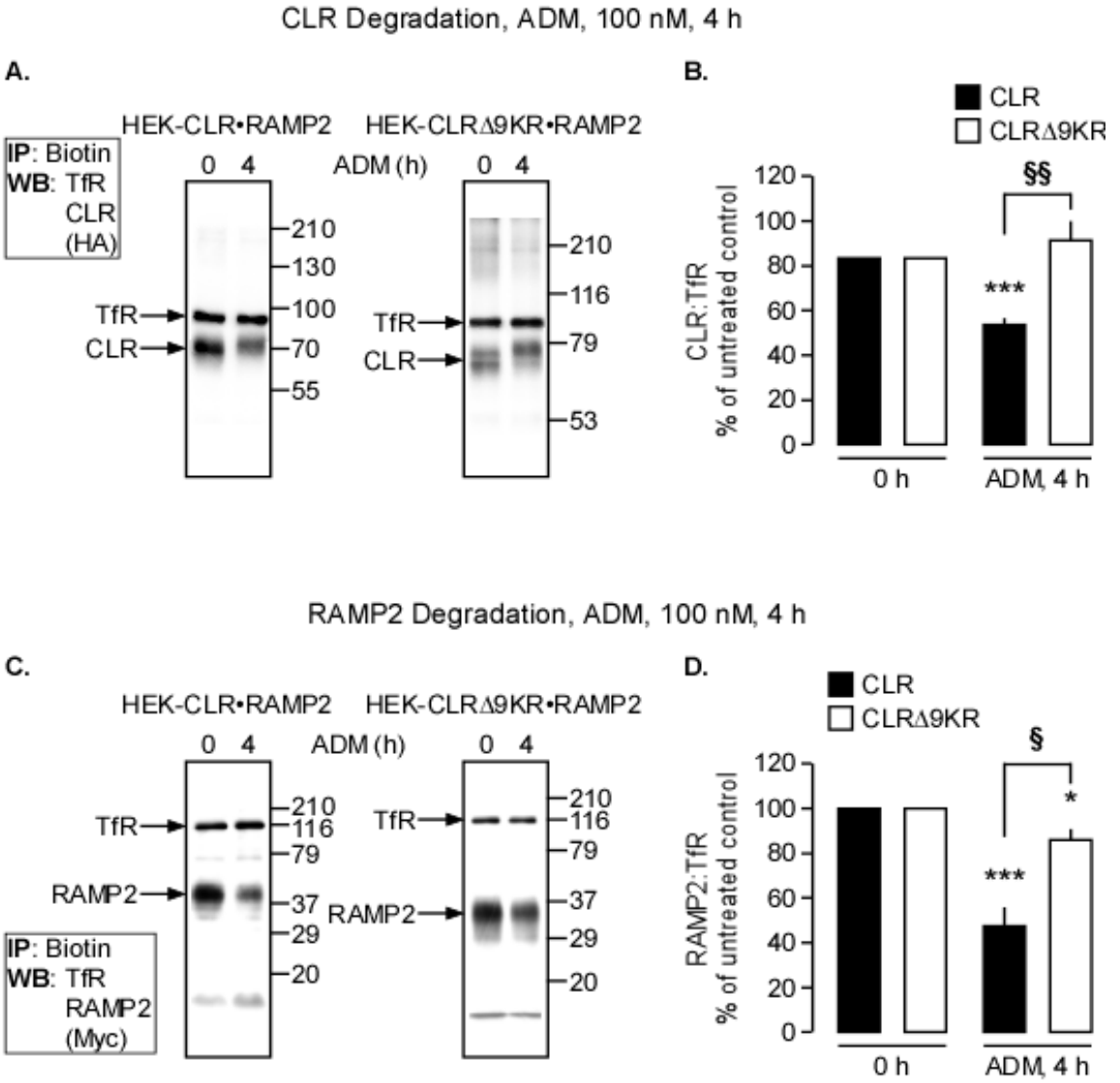

Figure 5.21 **Ubiquitination is involved in ADM-induced degradation CLR•RAMP2 at 4 h.** Cell-surface proteins of HEK-CLR•RAMP2 and HEK-CLRΔ9KR•RAMP2 cells were labelled with biotin. The cells were then stimulated with ADM (100 nM) continuously (4 h). Cells were lysed and biotinylated proteins isolated by immunoprecipitation with Neutravidin. Levels of CLR, CLRΔ9KR, RAMP2 and TfR in the isolated protein samples were then analysed by Western blotting. (**A**, **C**) Representative blots are shown. (**B**, **D**) Blots were quantified using ImageQuantRT and ratios of CLR:TfR and RAMP2:TfR were calculated. The results were expressed as % of expression compared to the appropriate unstimulated control. (**A**, **B**) ADM induces degradation of only CLR at 4 h, whereas CLRΔ9KR is untouched. This result suggests that ubiquitin is involved in the degradation of CLR at 4 h. (**C**, **D**) ADM induces degradation of RAMP2 in both cell lines, however RAMP2 in WT cell line was significantly more degraded that in mutant cell line. Thus, ADM induces a slower degradation of RAMP2 in the mutant cell line at 4 h, which suggests that ubiquitin is involved in the degradation process of RAMP2. n≥6, *=p<0.05 and ***=p<0.001 compared to untreated cells, and §§=p<0.01 compared to WT cell line at the same time point.

5.8 ADM-Induced Degradation is Partially Blocked by Lysosome or Proteasome Inhibitors

5.8.1 Effect of Lysosomal Protease Inhibitors and MG-132, Proteasome Inhibitor on ADM-Induced Degradation

GPCRs are generally degraded by proteolytic activities of the lysosome (Bouley et al., 2005; Cottrell et al., 2007; Jacob et al., 2005; Xia et al., 2008). However, some studies showed that the proteasome could also be involved in the degradation of GPCR (Chaturvedi et al., 2001; Cook et al., 2003). ADM induces CLR•RAMP2 trafficking to lysosomes. Therefore, it was anticipated that CLR•RAMP2 would be degraded by the lysosome. To investigate which proteolytic site is involved in the down-regulation of CLR•RAMP2, HEK-CLR•RAMP2 and HEK-CLRΔ9KR•RAMP2 cells were incubated with vehicle (control), a lysosomal protease inhibitors cocktail or a proteasome inhibitor, stimulated with ADM (16 h) and levels of CLR, CLRΔ9KR, RAMP2 and TfR determined by Western blotting (**Fig. 5.22** and **Fig. 5.23**). In vehicle-treated cells ADM induced degradation of CLR and CLRΔ9KR to a similar level as observed in the previous degradation experiment (see **5.7.2**) (**Fig. 5.22B**, 25.9±4.5% (CLR) and 23.5±8.7% (CLRΔ9KR) compared to untreated cells). In cells treated with lysosomal protease inhibitors, degradation of CLR was only partially prevented compared to vehicle-treated cells (**Fig. 5.22B**, 45.9±12.0% (CLR) and 44.6±13.3% (CLRΔ9KR) compared to untreated cells). Surprisingly, in cells treated with a proteasome inhibitor, MG-132 (Tsubuki et al., 1993), the degradation of CLR was also prevented. Moreover, MG-132 shows a higher significant effect on CLR, compared to CLRΔ9KR (**Fig. 5.22B**, 62.4±10.1% (CLR) versus 42.3±11.2% (CLRΔ9KR) compared to untreated cells), which suggests that CLR is degraded by the proteasome and that ubiquitin seems involved in this process.

Similar results were observed with RAMP2 (**Fig. 5.23**). ADM induces similar degradation of RAMP2 in vehicle-treated cells, in both cell lines (**Fig. 5.23B**, 24.6±4.3% (CLR) and 34.1±10.5% (CLRΔ9KR) compared to untreated cells). Incubation with lysosomal protease inhibitors, partially prevented the degradation of RAMP2 in both cell lines (**Fig. 5.23B**, 54.1±12.9% (CLR) and 45.2±9.5% (CLRΔ9KR) compared to untreated cells); and incubation with proteasome inhibitor also prevented the degradation of RAMP2. Likewise CLR, degradation of RAMP2 in WT cell line was significantly higher, than in mutant cell line (**Fig. 5.23B**, 78.2±5.4% (CLR) versus 51.8±5.3% (CLRΔ9KR) compared to untreated cells), suggesting again that RAMP2 is degraded by the proteasome and that ubiquitin is also involved in this process.

Altogether, these results suggest that ADM-induced degradation of CLR•RAMP2 require the proteolytic activity of both lysosome and proteasome. Moreover, the proteasomal activity seems to require ubiquitination of CLR.

5.8.2 Proteasomal Activity: Investigation of its Role in ADM-Induced Degradation of CLR•RAMP2

5.8.2.1 MG-132 does not Inhibit ADM-Induced Internalisation

The internalisation of certain cell-surface receptors has been found to be ubiquitin-dependent (Hicke, 1999; Marmor and Yarden, 2004; Strous and Govers, 1999). Moreover, it has been shown that MG-132 blocks the internalisation and thus the degradation of the β_2-adrenergic receptor (Shenoy et al., 2001). To determine if MG-132 affects the internalisation of CLR•RAMP2, HEK-CLR•RAMP2 and HEK-CLRΔ9KR•RAMP2 cells were incubated (30 min) with vehicle (DMSO) or MG-132. Cells were then stimulated with ADM (30 min) and CLR and CLRΔ9KR (RK11) localised by immunofluorescence and confocal microscopy (**Fig. 5.24**). In unstimulated cells, both CLR (**Fig. 5.24A**) and CLRΔ9KR (**Fig. 5.24B**) are localised at the cell-surface. Stimulation with ADM induces internalisation of CLR and CLRΔ9KR to intracellular vesicles in both vehicle- and MG-132-treated cells. Thus, ADM-induced internalisation of CLR•RAMP2 is not blocked by the proteasome inhibitor, which suggests that MG-132 does not affect the internalisation of the receptor.

5.8.2.2 Effect of Epoxomicin on ADM-Induced Degradation

To confirm the role of the proteasome in the ADM-induced degradation of CLR•RAMP2, another proteasome inhibitor was used. MG-132 has been shown to have some activity on other proteases, included lysosomal proteases (i.e. cathepsins) (Kisselev and Goldberg, 2001; Tawa et al., 1997). Therefore, to investigate the role of the proteasome in the ADM-induced degradation of CLR•RAMP2, HEK-CLR•RAMP2 cells were incubated with vehicle (DMSO) or another proteasome inhibitor, epoxomicin, which shows more specificity in the inhibition of the proteasome (Meng et al., 1999). Cells were stimulated with ADM (16 h) and levels of CLR, RAMP2 and TfR determined by Western blotting (**Fig. 5.25**). In vehicle-treated cells ADM induced degradation of CLR•RAMP2 to a similar level as observed in the previous degradation experiment (see **5.2.7**) (**Fig. 5.25B** and **Fig. 5.25D**, 17.1±7.2% (CLR) and 31.4±7.0% (RAMP2) compared to control). In cells treated with epoxomicin, ADM also induces the degradation of CLR•RAMP2 to a similar level as observed in vehicle-treated cells (**Fig. 5.25B** and **Fig. 5.25D**, 36.2±18.6% (CLR) and 30.6±5.1% (RAMP2) compared to control).

These results show that the proteasome inhibitor does not prevent ADM-induced degradation of CLR•RAMP2. Thus, ADM-induced degradation of CLR does not seem to require proteolytic activity of the proteasome and the effects of MG-132 observed may be not specific of the proteasome.

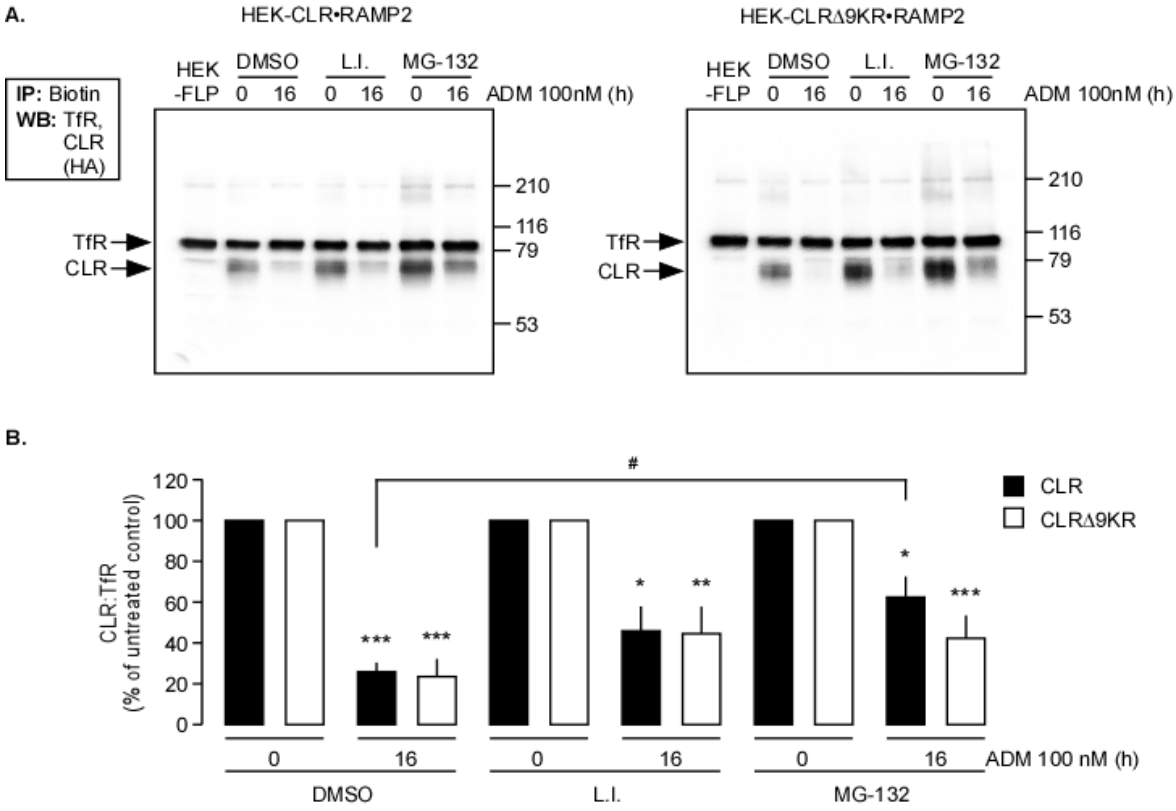

Figure 5.22 **ADM-induced degradation of CLR and CLRΔ9KR is partially prevented by inhibiting lysosomal and proteasomal proteolytic activities.** Cell-surface proteins of HEK-CLR•RAMP2 and HEK-CLRΔ9KR•RAMP2 cells were labelled with biotin. The cells were then incubated with vehicle, lysosomal protease inhibitors (L.I.): pepsatin A (10 μM), E-64d (10 μM) and Z-PAD (200 μM) or MG-132 (20 μM), stimulated with ADM (100 nM, 16 h). Cells were lysed and biotinylated proteins isolated by immunoprecipitation with Neutravidin. Levels of CLR, CLRΔ9KR and TfR in the isolated protein samples were then analysed by Western blotting. There were no signals for CLR and CLRΔ9KR in untransfected HEK-FLP cells, indicating specificity of the anti-CLR (HA) antibody. (**A**) Representative blots are shown. (**B**) Blots were quantified using ImageJ and ImageQuantTL, ratios of CLR:TfR calculated and results expressed as % of the appropriate unstimulated control. In vehicle-treated cells ADM-induced significant degradation of both CLR and CLRΔ9KR. Incubation with lysosomal protease inhibitors partially prevented degradation of receptors in both cell lines. By inhibiting the proteolytic activity of the proteasome, the degradation of CLR but not CLRΔ9KR, was significantly prevented. Thus, the ADM-induced degradation of CLR required both lysosomal and proteasomal activities, moreover ubiquitin seem to be involved in the proteasomal degradation. n≥5, *=p<0.05, **=p<0.01 and ***=p<0.001 compared to untreated cells, and #=p<0.05 compared to vehicle-treated cells at the same time point.

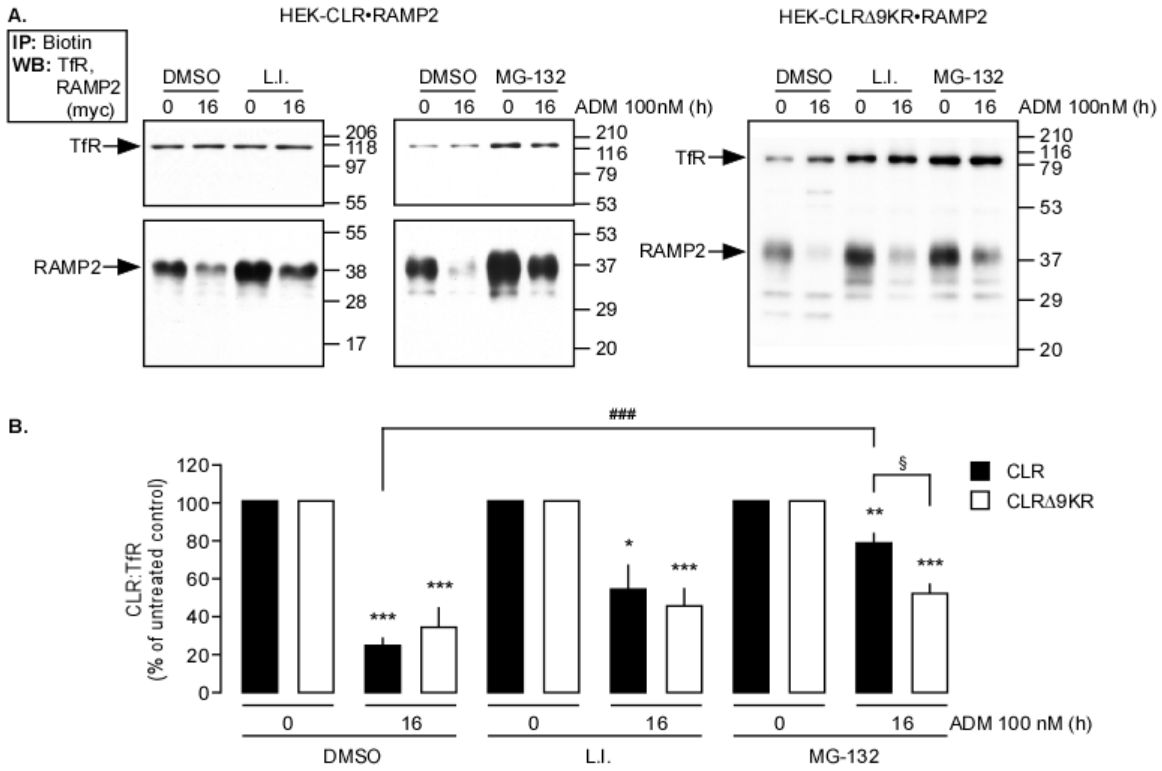

Figure 5.23 **ADM-induced degradation of CLR•RAMP2 and CLRΔ9KR•RAMP2 is partially prevented by inhibiting lysosomal and proteasomal proteolytic activities.** Cell-surface proteins of HEK-CLR•RAMP2 and HEK-CLRΔ9KR•RAMP2 cells were labelled with biotin. The cells were then incubated with vehicle, lysosomal protease inhibitors (L.I.): pepsatin A (10 μM), E-64d (10 μM) and Z-PAD (200 μM) or MG-132 (20 μM), stimulated with ADM (100 nM, 16 h). Cells were lysed and biotinylated proteins isolated by immunoprecipitation with Neutravidin. Levels of RAMP2 and TfR in the isolated protein samples were then analysed by Western blotting. (**A**) Representative blots are shown. (**B**) Blots were quantified using ImageJ and ImageQuantTL, ratios of RAMP2:TfR calculated and results expressed as % of the appropriate unstimulated control. In vehicle-treated cells ADM-induced significant degradation of RAMP2 in both cell lines. Incubation with lysosomal protease inhibitors partially prevented degradation in both cell lines. By inhibiting the proteolytic activity of the proteasome, the degradation of RAMP2 in WT but not in mutant cell line, was significantly prevented. Thus, the ADM-induced degradation of RAMP2 required both lysosomal and proteasomal activities, moreover ubiquitin seem to be involved in the proteasomal degradation of RAMP2. n≥5, *=p<0.05, **=p<0.01 and ***=p<0.001 compared to untreated cells, ###=p<0.001 compared to vehicle-treated cells at the same time point, and §=p<0.05 compared to WT cell line at the same time point.

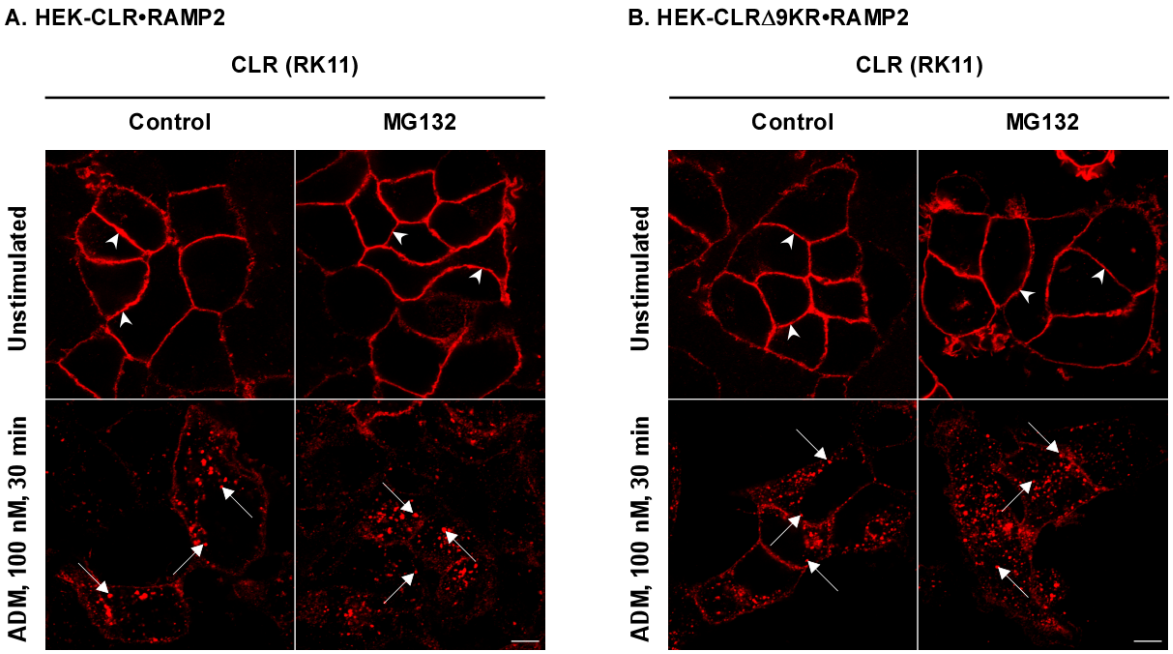

Figure 5.24 **CLR•RAMP2 and CLRΔ9KR•RAMP2 ADM-induced internalisation is not blocked by MG-132.** HEK-CLR•RAMP2 (**A**) and HEK-CLRΔ9KR•RAMP2 (**B**) cells were stimulated with ADM (100 nM, 0-30 min), immunoreactive proteins were detected by immunofluorescence and analysed by confocal microscopy. In unstimulated cells, CLR and CLRΔ9KR are present at the cell-surface (arrowheads). ADM induces internalisation of both CLR and CLRΔ9KR to localise in intracellular vesicles (arrows) in both vehicle- and MG-132-treated cells. Thus, ADM induces internalisation of CLR•RAMP2 and CLRΔ9KR•RAMP2 regardless the presence or not of MG-132, which suggests that the proteasomal activity is not involved in the internalisation of CLR•RAMP2. Scale bar = 10 μm.

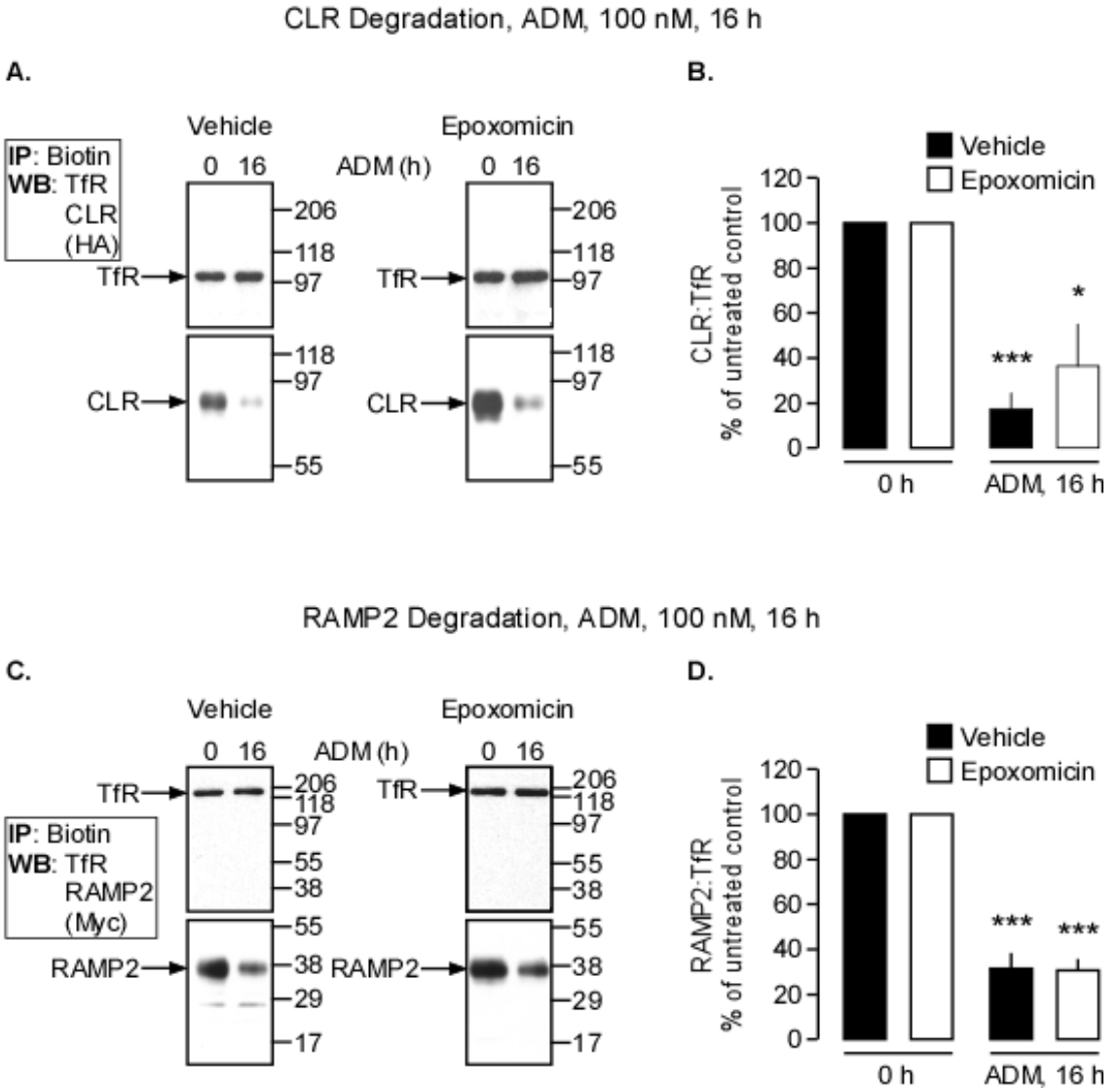

Figure 5.25 **ADM-induced degradation of CLR•RAMP2 is not prevented by epoxomicin.** Cell-surface proteins of HEK-CLR•RAMP2 cells were labelled with biotin. The cells were then incubated with vehicle or epoxomicin (5 µM), stimulated with ADM (100 nM, 16 h). Cells were lysed and biotinylated proteins isolated by immunoprecipitation with Neutravidin. Levels of CLR, RAMP2 and TfR in the isolated protein samples were then analysed by Western blotting. (**A**, **C**) Representative blots are shown. (**B**, **D**) Blots were quantified using ImageJ, ratios of CLR:TfR and RAMP2:TfR calculated and results expressed as % of the appropriate unstimulated control. In vehicle-treated cells, ADM induces significant degradation of CLR•RAMP2. Incubation of cells with epoxomicin, ADM also induces significant degradation of CLR•RAMP2 to a similar level observed in vehicle-treated cells. Thus, the ADM-induced degradation of CLR•RAMP2 is not prevented by epoxomicin. n=3, *=p<0.05 and ***=p<0.001 compared to untreated cells.

5.9 Expression and Trafficking of CLR•RAMP2 and CLRΔ9KR•RAMP2 in HMEC-1 Cells

ADM stimulation of HEK-CLR•RAMP2 promotes the degradation of the receptor and therefore, is not recycled back to the cell-surface. Moreover, ADM induces ubiquitination of CLR, which accelerates the rate of degradation of the receptor. However, HEK cells do not naturally express the receptor, which could suggest that the observed effects are due to artefact. Therefore, the need of another model is necessary. HMEC-1 cells are a human microvascular endothelial cell line that express both components of the receptor CLR and RAMP2 (unpublished data, G.S. Cottrell). However, the level of expression of CLR•RAMP2 is insufficient to allow biochemical analyses. Thus, HMEC-1 were transfected to facilitate biochemical analysis and to express both CLR•RAMP2 and CLRΔ9KR•RAMP2.

HMEC-1 cells were first transfected according to the protocol described in Materials and Methods (**Chap. 2.2.6**). However, this method leads to the cell death of HMEC-1 due to high sensitivity to the transfection reagent of these cells. The protocol was then optimised by varying the quantity of DNA transfected, the volume of transfection reagent as well as the number of cells plated. The optimal protocol was as follows: HMEC-1 cells were seeded 48 h prior transfection at $5x10^4$ cells per well in 12-well plate, the quantity of DNA was 1 µg per well and the volume of Lipofectamine was 1 µL per well (ratio 1:1). After 24 h, transfected HMEC-CLR•RAMP2 and -CLRΔ9KR•RAMP2 cells were stimulated with ADM (30 min or 4 h) and CLR and CLRΔ9KR (both RK11) simultaneously localised with EEA1 or LAMP1 by immunofluorescence and confocal microscopy (**Fig. 5.26**). In unstimulated cells, both CLR (**Fig. 5.26A** and **Fig. 5.26C**) and CLRΔ9KR (**Fig. 5.26B** and **Fig. 5.26D**) are localised at the cell-surface and EEA1 and LAMP1 are detected in intracellular vesicles. Stimulation with ADM induces internalisation of CLR and CLRΔ9KR to co-localise with EEA1- and LAMP1-positive vesicles. Thus, ADM causes trafficking of CLR•RAMP2 and CLRΔ9KR•RAMP2 to early endosome and lysosomes, which suggests that both receptor traffic in HMEC-1 as observed in HEK cells.

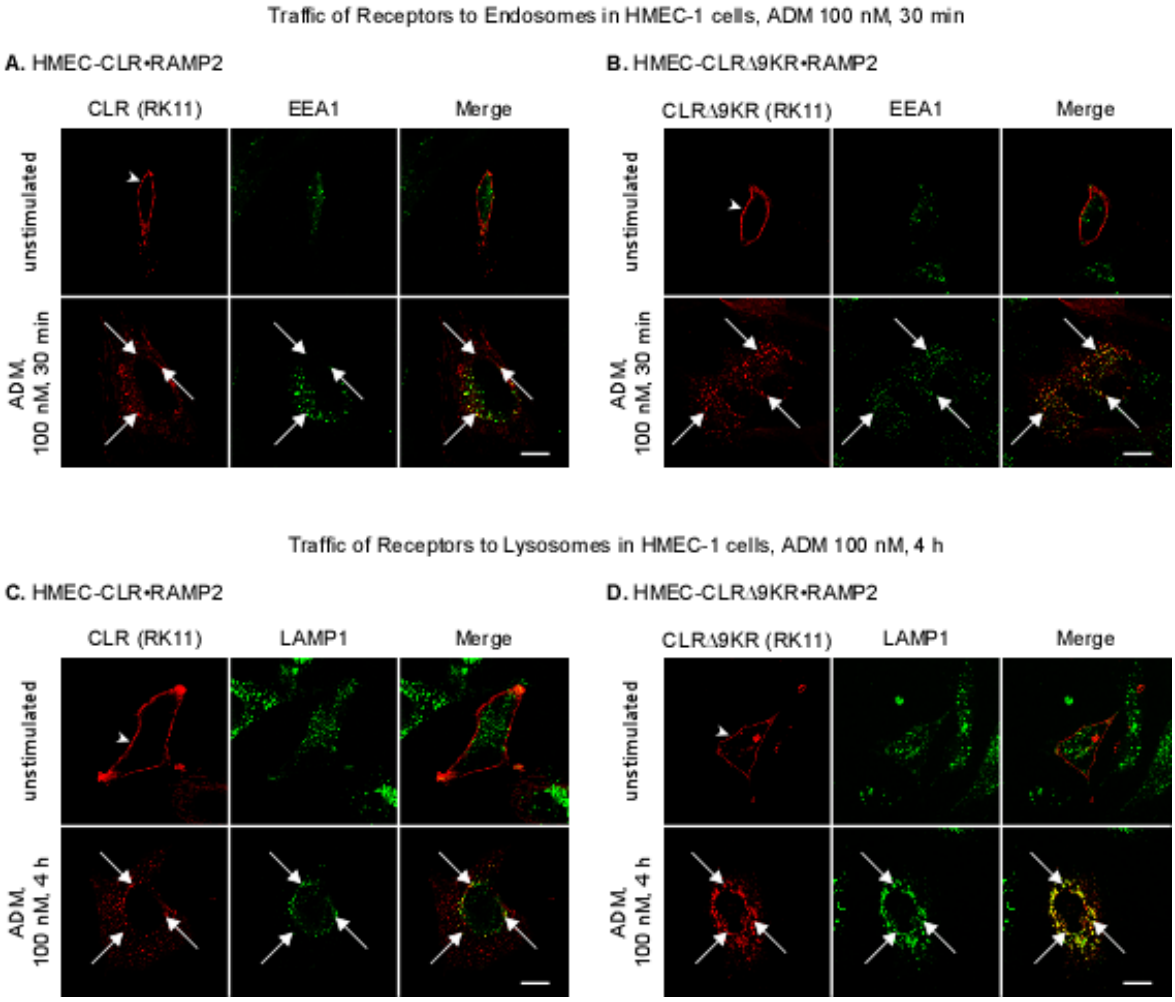

Figure 5.26 **CLR•RAMP2 and CLRΔ9KR•RAMP2 traffic to early endosomes and lysosomes upon ADM stimulation in HMEC-1 cells.** HMEC-CLR•RAMP2 (**A, C**) and HMEC-CLRΔ9KR•RAMP2 (**B, D**) cells were stimulated with ADM (100 nM, 0-4 h), immunoreactive proteins were detected by immunofluorescence and analysed by confocal microscopy. In unstimulated cells, CLR and CLRΔ9KR are present at the cell-surface (arrowheads), whereas (**A, B**) EEA1 and (**C, D**) LAMP1 are detected in intracellular vesicles. ADM induces internalisation of both CLR and CLRΔ9KR to co-localise with EEA1- or LAMP1-positive vesicles (arrows). Thus, ADM induces traffic of CLR•RAMP2 and CLRΔ9KR•RAMP2 to early endosomes and lysosomes, which suggests that both receptors traffic normally in HMEC-1. Scale bar = 10 µm.

5.10 Discussion

The receptor CLR•RAMP2 was stably transfected into HEK cells, in order to study its post-endocytic sorting. This cellular model has already been used for studying the traffic of CLR•RAMP2, where ADM stimulation induces internalisation of the receptor (Kuwasako et al., 2000). I also show by confocal microscopy that exposure to ADM induces a rapid internalisation of CLR•RAMP2 in HEK-cells. Studies have shown that ADM induces ERK1-2 activation in HMEC-1 (human microvascular endothelial cell line) and HUVEC (human umbilical vein endothelial cells) (Kim et al., 2003; Schwarz et al., 2006). I also show that ADM induces ERK1-2 activation in HEK-CLR•RAMP2, which suggests that the receptor is normally expressed and functional in HEK cells.

To investigate the post-endocytic sorting of CLR•RAMP2 I first examined the agonist-induced degradation of CLR•RAMP2 by using CHX to inhibit new protein synthesis and compared the results to CLR•RAMP1. It has been previously shown that following transient exposure to CGRP, it induces recycling of CLR•RAMP1 back to the cell-surface. However, in continued presence of CGRP, CLR•RAMP1 is trafficked to lysosomes for degradation via an ubiquitin-independent mechanism (Cottrell et al., 2007). Following transient and continuous stimulation with CGRP on HEK-CLR•RAMP1, I also show similar results, suggesting that CLR•RAMP1 does recycle back to the cell-surface. However, stimulation with ADM on HEK-CLR•RAMP2 induces degradation of CLR•RAMP2 following both transient and continuous stimulation. This result clearly shows a difference between agonist-induced degradation between CLR•RAMP1 and CLR•RAMP2 and confirm the suggestion made by another study, where it has been suggested that following a transient stimulation with ADM (30 min), CLR•RAMP2 is internalised and less than 10% of CLR•RAMP2 recycles back to cell-surface after 2 h (Kuwasako et al., 2000). However, in our study, I looked at a much longer recovery point (16 h) as it has been shown that CLR•RAMP1 recycles back to the cell-surface very slowly (at least 6 h) (Cottrell et al., 2007). In contrast to CLR•RAMP2, CLR•RAMP3, the other receptor for ADM, has been shown to internalise and recycle back to the cell-surface following agonist exposure (Bomberger et al., 2005). Thus, it appears that RAMPs play an important role in the post-endocytic sorting of CLR following agonist stimulation and can change the fate of CLR•RAMP complex.

The small regulatory protein ubiquitin has been involved in the degradation of many GPCRs (reviewed by (Hanyaloglu and von Zastrow, 2008; Marchese et al., 2008)). As I show that ADM stimulation induces CLR•RAMP2 degradation, I was interested to see if ubiquitination was involved in this process. Indeed, I show for the first time that ADM promotes ubiquitination of CLR, but not RAMP2. Interestingly, it has been shown that sustained stimulation of CGRP did not cause ubiquitination of either CLR nor RAMP1 (Cottrell et al., 2007). However, it is currently unknown if stimulation of CLR•RAMP3 by ADM induces or not

ubiquitination of CLR and/or RAMP3. It is interesting to note that I also observed a basal level of CLR ubiquitination, indicating that perhaps that CLR is constitutively ubiquitinated. This is not unusual as PAR1, that mediates thrombin sensitivity to cells is constitutively ubiquitinated (Wolfe et al., 2007). However, as oppose to PAR1, which is deubiquitinated following stimulation, ADM further enhanced the basal ubiquitination of CLR. Interestingly, ADM-induced ubiquitination is not rapid and probably does not occur at the cell-surface, compared to many other GPCRs (Hicke and Riezman, 1996; Jacob et al., 2005; Shenoy et al., 2001). I then believe that ubiquitination of CLR occurs between early endosomes and lysosomes, perhaps in the MVB or in late endosomes. It is interesting to see that the same receptor CLR is ubiquitinated upon ADM stimulation but not upon CGRP stimulation. Moreover, as I saw that CLR was constitutively ubiquitinated when associated with RAMP2, it suggests that association with RAMP1 or RAMP2 modify CLR ability to bind ubiquitin. It is then possible to imagine that the C-terminal tail of RAMP1 mask all the lysine residues and block any ubiquitination of CLR, while RAMP2 can allow it. However, it is unlikely as they both have short C-terminal tails (McLatchie et al., 1998). Further experiments are necessary to understand the mechanisms of CLR ubiquitination.

Ubiquitination has been shown to be involved in different process of the post-endocytic sorting of GPCRs, such as promoting (Hicke and Riezman, 1996) or blocking (Wolfe et al., 2007) internalisation, targeting to degradation (Shenoy et al., 2001) or increasing the rate of degradation (Hislop et al., 2009). To further understand the role of ADM-induced ubiquitination of CLR, I made a lysine-less mutant of CLR, where all intracellular facing lysine residues were replaced by arginine residues. I called this mutant CLRΔ9KR. This method that prevents covalent binding of ubiquitin to the receptor, has already been used in other studies to help understand the role of ubiquitination in GPCRs regulation (Shenoy et al., 2001; Tanowitz and Von Zastrow, 2002; Wolfe et al., 2007). I show that expression of CLRΔ9KR•RAMP2 did not affect its cellular localisation, internalisation and signalling, suggesting that the receptor was functional. But more importantly, I show that ADM did not induce ubiquitination of CLRΔ9KR. I first used immunofluorescence and confocal microscopy to examine if ADM-induced ubiquitination of CLR affect the trafficking of CLR•RAMP2 to endosomes and lysosomes compared to CLRΔ9KR•RAMP2. I show that ADM induced trafficking of CLR and RAMP2 to EEA1- and LAMP1-positive vesicles, presumably early endosomes and lysosomes respectively. This observation is supported by the study of Kuwasako *et al.* (Kuwasako et al., 2000), where CLR•RAMP2 co-localised with lysotracker (a marker for acidic vesicles) following stimulation with ADM. Interestingly, I show that CLRΔ9KR•RAMP2 also traffic to early endosomes and to lysosomes upon ADM stimulation, suggesting that constitutively ubiquitination of CLR is not involved in the internalisation of the receptor as opposed to PAR1 (Wolfe et al., 2007). This result was not surprising as ADM

further enhances ubiquitination of CLR, whereas thrombin induces deubiquitination leading to the internalisation of PAR1. However, the fact that CLRΔ9KR•RAMP2 traffic to lysosomes upon ADM stimulation was surprising but not uncommon. Indeed, the δOR is ubiquitinated after stimulation with the synthetic opioid peptide DADLE. The study by Tanowitz *et al.* showed that a lysine-less mutant still traffics to lysosomes to be degraded (Tanowitz and Von Zastrow, 2002), as oppose to β_2-AR, where a lysine deficient receptor blocks its traffic to lysosomes and therefore prevents its degradation (Shenoy et al., 2001). The fact that CLRΔ9KR•RAMP2 traffics to lysosomes might suggests that ubiquitination will not prevent the degradation of CLR•RAMP2 as it has been shown for δOR. As CLR is ubiquitinated, I chose to use a cell-surface biotinylation assay to monitor the degradation of CLR by lysosomal and proteasomal proteases, as CHX can affect the pool of free ubiquitin within the cell (Hanna et al., 2003). As suggested, I show that stimulation with ADM for 16 h did not show any differences in the degradation between CLR•RAMP2 or CLRΔ9KR•RAMP2, suggesting that ubiquitination was not involved in the degradation of CLR•RAMP2. It is interesting to note that in the first experiment looking at the degradation of CLR•RAMP2 with CHX, transient ADM stimulation promoted almost complete degradation of CLR. Whereas, biotin assays showed that transient ADM stimulation promotes only 20-30% of degradation. This difference can be explained by the fact that either CHX affects the degradation of CLR•RAMP2 or that the biotin assay is not as sensitive as the CHX degradation assay. Indeed, a recent study reported that CHX on its own induces internalisation and traffic to early endosomes of ErbB1 in HeLa cells (human cervical cancer cell line) (Oksvold et al., 2012). It is then possible than CHX also promotes internalisation of CLR•RAMP2 and further enhances its degradation. So, in order to confirm that transient ADM stimulation induces degradation of CLR•RAMP2, I decided to look at the internalisation of the receptor by a flow cytometry method. I showed that after transient ADM stimulation only 30-40% of the cell-surface receptors were internalised for both CLR•RAMP2 and CLRΔ9KR•RAMP2. These results show that the amount of receptor internalised coincide with the amount of receptors degraded after transient ADM stimulation. Therefore, all receptors internalised are degraded. Additionally, I showed that HEK-CLR•RAMP2 expressed about 20% more receptor at the cell-surface compared to HEK-CLRΔ9KR•RAMP2. Altogether, I showed that all the ADM-induced CLR•RAMP2 and CLRΔ9KR•RAMP2 receptors internalised are degraded and therefore that ubiquitin is not involved in the degradation of those receptors.

I also was interested to determine whether ubiquitination of CLR would modify ADM-induced signalling. Indeed, a study on the insulin-like growth factor 1 receptor (IGF1R) suggests that the role of ubiquitination of the receptor is important in mediating IGF1R signalling (Sehat et al., 2007). In contrast to IGF1R, where ERK activation was abolished when ubiquitination of IGF1R was prevented, I showed that CLRΔ9KR•RAMP2 had no effect on the duration or intensity of

ADM-induced ERK activation. However, even though it is not significant, I showed that the basal level of ERK activation in CLRΔ9KR•RAMP2 is lower compared to CLR•RAMP2. This could be explained by the fact that CLRΔ9KR•RAMP2 are less expressed at the cell-surface compared to CLR•RAMP2. Altogether, these results suggest that ubiquitination is not involved in ADM-induced ERK activation. However, it does not mean that ubiquitination is not involved in any CLR•RAMP2-mediated signalling.

The study carried out by Hislop *et al.* suggested that in fact ubiquitination of δOR was involved in the rate of degradation. They showed that after 3-5 h of stimulation with DADLE, lysine-less mutant receptor show a significant higher ability to bind radioactive δOR antagonist diprenorphine, suggesting that down-regulation of the lysine-less mutant receptor was slower than for the WT receptor (Hislop et al., 2009). I then decided to look at earlier time point of the degradation of CLR•RAMP2 and CLRΔ9KR•RAMP2. When both receptors were continuously stimulated for 8 h, no difference on the degradation was observed between the two receptors. However, when both receptors were continuously stimulated for 4 h, CLR•RAMP2 show a significant higher degradation amount than CLRΔ9KR•RAMP2. These results are similar of those obtained with δOR (Hislop et al., 2009) and suggest that CLR•RAMP2 undergo degradation more rapidly than CLRΔ9KR•RAMP2. Therefore, ubiquitination is involved in the rate of degradation of CLR•RAMP2, by accelerating the process.

I showed that CLR•RAMP2 traffics to lysosomes and it is known that lysosomal proteases degrade CLR when expressed with RAMP1 (Cottrell et al., 2007). Subsequently, I was expected that lysosomal enzymes would similarly degrade CLR•RAMP2. Indeed, I observed that the same protease inhibitor cocktail, which prevented degradation of CLR•RAMP1, was also able to partially prevent degradation of CLR•RAMP2. However, I was expecting to see the degradation of CLR•RAMP2 completely prevented, as it has been shown for CLR•RAMP1 (Cottrell et al., 2007). This result suggests that CLR•RAMP2 and CLR•RAMP1 are degraded by different lysosomal proteases. Another explanation is that CLR•RAMP2 degradation does not only take place in the lysosome. Indeed, when I inhibited the proteolytic activity of the proteasome, I also observed a reduction in ADM-induced degradation in both CLR•RAMP2 and CLRΔ9KR•RAMP2, even though the effects of MG-132 were more pronounced for CLR•RAMP2, suggesting a role of ubiquitination in the degradation of CLR•RAMP2. Although unexpected, the role of the proteasome in CLR•RAMP2 degradation is not without precedent. Indeed agonist-induced δOR degradation was prevented by different proteasome inhibitors, but not by lysosomal protease inhibitors (Chaturvedi et al., 2001). Similar results were also observed for the PTH receptor (Alonso et al., 2011) and the histamine H1 receptor (Hishinuma et al., 2010). The differences in the proteolytic degradation of CLR•RAMP1 and CLR•RAMP2 may be explained by the

differences in their ubiquitination state during their trafficking through the endocytic network or perhaps, a non-specific or non-direct effect of proteasomal inhibition with MG-132. Indeed, it has been shown that the internalisation of ErbB1 (Melikova et al., 2006) and β_2-AR (Shenoy et al., 2001) was blocked by MG-132. Although the latter does not apply to the agonist-induced trafficking of the δOR (Tanowitz and Von Zastrow, 2002) neither to CLR•RAMP2, as I showed that the internalisation of CLR•RAMP2 was not prevented by MG-132. Moreover, to confirm the implication of the proteasomal activity in ADM-induced degradation of CLR•RAMP2, I used another proteasomal inhibitor. Conversely to MG-132, the use of epoxomicin, which is believed to be more specific than MG-132 (Meng et al., 1999), did not prevent the degradation of CLR•RAMP2. These results strongly suggest that the effects observed with MG-132 are due to side effects. However, further experiments would be necessary to assess this hypothesis.

In order to confirm the post-endocytic sorting of CLR•RAMP2 observed in HEK cells, I aimed to repeat key experiments in HMEC-1, a more physiological model that endogenously express CLR•RAMP2. However, endogenous levels of CLR•RAMP2 are low, which makes biochemical assays difficult to analyse. Thus, I transfected HMEC-1 in order to overexpress CLR•RAMP2. Many studies with similar transfection procedures have shown that the transfection of HMEC-1 was not an issue (Faure et al., 2000; Zhu et al., 2003). Conversely, I found that HMEC-1 cells were sensitive to the transfection regent promoting the death of these cells. This result can be the consequence of a too large volume of transfection reagent. I then optimised the assay by changing the concentration of DNA, transfection reagent and number of cells. Although I succeeded to lower the toxicity of the assay, the rate of transfection remained poor. However, I managed to investigate the traffic of CLR•RAMP2 in HMEC-1. I show that CLR•RAMP2 traffic to endosomes and to lysosomes upon ADM stimulation, as observed in HEK cells. These primary data are really promising, suggesting that the study led in HEK cells are not due to artefacts.

5.11 Summary and Conclusion

Compared to CLR•RAMP1 and CLR•RAMP3, little is known about the post-endocytic sorting of CRL•RAMP2. Using HEK cells, stably expressing CLR•RAMP2, I investigated the regulation of the mechanisms of the ADM receptor. I first showed that, as oppose to CLR•RAMP1, transient stimulation of ADM causes degradation of CLR•RAMP2, which suggests that ADM receptors do not recycle to the cell-surface. As ubiquitin has been shown to be involved in the degradation of many GPCRs (reviewed in (Hanyaloglu and von Zastrow, 2008; Marchese et al., 2008)), I examined if CLR•RAMP2 was ubiquitinated upon ADM stimulation. I showed that CLR is constitutively ubiquitinated, which was further enhanced upon ADM stimulation. However, I did not observe any ubiquitination of RAMP2.

In order to elucidate the role of ADM-mediated ubiquitination of CLR, I made a lysine-less mutant of CLR, named CLRΔ9KR. I showed that ubiquitination of CLR did not affect the ADM-induced traffic to lysosome or the ERK signalling mediated by CLR•RAMP2. Although continuous stimulation of ADM induced degradation of both CLR•RAMP2 and CLRΔ9KR•RAMP2, I showed that ubiquitination of CLR was involved in the rate of degradation of the receptor. Indeed, I showed that at 4 h stimulation CLR WT was largely degraded, whereas CLRΔ9KR•RAMP2 was untouched.

I also used protease inhibitors of the lysosome and of the proteasome in order to investigate the proteolytic site of CLR•RAMP2. Surprisingly, I found that lysosomal proteases inhibitors did not fully prevent ADM-induced degradation of CLR•RAMP2. More surprisingly, was that MG-132, a proteasome inhibitor, significantly prevented the degradation of CLR•RAMP2. However, this effect is believed to be due to off target effects rather than proteasome-dependent degradation. Altogether, these results show that CLR•RAMP2 does not recycle back to the cell-surface after transient stimulation and therefore is degraded. Furthermore, ADM induces ubiquitination of CLR only, which is involved in the kinetics of down-regulation of CLR•RAMP2.

Chapter 6. General Discussion

6.1 Current Overview

This thesis aimed to better understand the molecular mechanisms of CGRP-induced ERK activation of CLR•RAMP1 and ADM-mediated post-endocytic sorting of CLR•RAMP2 using HEK cells as a model system.

CGRP is a neuropeptide implicated in the regulation of many biological functions, but it is mostly known for its vasodilator actions on the cardiovascular system. The mechanisms of action of CGRP are known to involve NO/endothelium-dependent mechanisms or cyclic adenosine monophosphate (cAMP)-mediated/endothelium-independent pathways (reviewed in (Brain and Grant, 2004)). Moreover, it is well documented that CGRP can promote activation of ERK in many cell types. However, the biological functions of CGRP-induced ERK activation remain poorly defined. Recently, CGRP-induced ERK activation has been linked with the induction of iNOS in trigeminal ganglion glial cells (Vause and Durham, 2009). iNOS has been shown to be upregulated in different pathologies including migraine, atherosclerosis and sepsis (Ginnan et al., 2008; Hauser et al., 2005; Olesen and Jansen-Olesen, 2000). The induction of iNOS is known to produce large amounts of NO (Nathan and Xie, 1994) and is potentially responsible for the hypotension observed in sepsis and migraine (Gupta, 2005; Neuhauser and Lempert, 2004; Wijdicks and Stevens, 1992). CGRP is similarly upregulated and secreted in migraine and sepsis (Goadsby et al., 1990; Zhou et al., 2001). In the cardiovascular system, CGRP has been shown to promote upregulation of iNOS and NO release in SMC pretreated with interleukin-1β (Schini-Kerth et al., 1994). As both CGRP and NO are important signalling molecules in the cardiovascular system, I aimed as a first step, to determine the exact mechanisms through which CGRP activates ERK1-2. Understanding these mechanisms would allow us to determine whether ERK activation is involved in CGRP-induced iNOS upregulation in SMC.

ADM and its receptors have been shown to be expressed in several tissues and organs, including the heart, blood vessels, kidneys, lungs, gastrointestinal tract, endocrine glands and brain (reviewed in (Hinson et al., 2000)). This wide distribution suggests many biological functions for ADM. In the cardiovascular system, ADM, similarly to CGRP, promotes vasodilation of blood vessels, (reviewed in (Hinson et al., 2000)), but also plays an important role in the regulation of the endothelial barrier. ADM has been shown to protect and maintain the endothelial barrier during sepsis (reviewed in (Temmesfeld-Wollbruck et al., 2007)). However, these mechanisms by which ADM protect and maintain the endothelial barrier remain poorly understood. Surprisingly, little is known about the post-endocytic sorting of ADM receptor, CLR•RAMP2. It has been shown that both CLR•RAMP1 and CLR•RAMP3 can recycle after transient stimulation (Bomberger et al., 2005; Cottrell et al., 2007). Moreover, it has been shown that ECE-1

regulates the recycling of CLR•RAMP1 by cleaving CGRP in endosomes (Padilla et al., 2007). As ADM is also cleaved by ECE-1, only at endosomal pH (unpublished data, G.S. Cottrell), I hypothesised that ECE-1 would similarly regulate CLR•RAMP2. To test this hypothesis I first examined the mechanisms of the post-endocytic sorting of CLR•RAMP2 using HEK cells as a model. I was especially interested to see whether CLR•RAMP2 recycles or is degraded following ADM stimulation. This study in HEK cells is a first step in the investigation of the molecular mechanisms controlling CLR•RAMP2 trafficking. Key experiments would need to be carried out in a more physiological model, such as HMEC-1 cells, to confirm my observations in HEK cells. It is important to study the post-endocytic sorting of CLR•RAMP2, as a better understanding of how receptors are trafficked may lead to the development of new therapies to treat disease.

6.2 CGRP-Induced ERK Activation and Future Direction

HEK cells are easy to manipulate and commonly used to study GPCRs-mediated ERK activation (e.g. (Cottrell et al., 2009; Della Rocca et al., 1997; Luttrell et al., 2001)). Moreover, they have already been used to study CGRP-induced ERK activation, showing that CGRP induces ERK phosphorylation in a concentration-dependent manner (Parameswaran et al., 2000). As expected, CGRP induces ERK activation in HEK-CLR•RAMP1 cells and I showed that CGRP-induced ERK activation is mainly activated through two major pathways: the $G\alpha_s$-mediated cAMP/PKA pathway and transactivation of ErbB1.

The cAMP/PKA pathway is commonly involved in GPCR-induced ERK activation (reviewed in (Goldsmith and Dhanasekaran, 2007; Rozengurt, 2007)). CLR•RAMP1 is known to couple a $G\alpha_s$ subunit in HEK cells and SK-N-MC cells (human neuroblastoma cell line that endogenously expresses CGRP receptor) (Aiyar et al., 1999; Van Valen et al., 1990), which leads to accumulation of cAMP. Indeed, I used H-89, a PKA inhibitor (Chijiwa et al., 1990) and showed that CGRP-induced ERK activation was reduced by about 50% (**Fig. 6.1**). This result confirms that CGRP promotes ERK activation through the cAMP/PKA pathway, possibly mediated by $G\alpha_s$ subunit. This result is consistent with similar observations in HEK cells, where CGRP-induced ERK activation was also blocked by H-89 (Parameswaran et al., 2000). Even though H-89 is commonly used to assess the role of PKA in different cellular systems (Chao and Hamilton, 2009; Lee and Linstedt, 2000; Murphy et al., 2010), H-89 has been found to inhibit kinases other than PKA (reviewed in (Lochner and Moolman, 2006)). Indeed, H-89 inhibits the p70 ribosomal protein S6 kinase 1, which is involved in protein synthesis and cell proliferation, and the mitogen- and stress-activated protein kinase-1 that mediates

activation of the cAMP response element-binding protein and activating transcription factor-1 (Davies et al., 2000). Therefore, I used two different concentrations of H-89 and obtained similar results. The lower concentration (10 μM) of H-89 gives a more specific inhibition of PKA. Thus, I can say with more certainty that CGRP activates ERK through PKA. However, it would be necessary to use other PKA inhibitors to verify that the same effect is observed on CGRP-induced ERK activation.

I show for the first time that CGRP induces transactivation of ErbB1 by using a specific ErbB1 inhibitor AG1478 (Osherov and Levitzki, 1994), which lead to about 40% inhibition of the total ERK activation (**Fig. 6.1**). This result is not uncommon, as many GPCRs have been shown to induce transactivation of ErbB1 (Daub et al., 1996; Eisinger and Ammer, 2008; Maudsley et al., 2000; Zajac et al., 2011). However, it is interesting to note that only a few $G\alpha_s$-mediated GPCRs have been described to promote ErbB1 transactivation, which are the EP_2 receptor, the GnRH receptor and the MC_2 receptor (Carbajal et al., 2011; Sales et al., 2004). ErbB1 transactivation has been reported to play an important role in cancer-related disorders (reviewed in (Fischer et al., 2003)), notably by promoting angiogenesis (de Jong et al., 1998; Schreiber et al., 1986). CGRP is also known to enhance tumour-associated angiogenesis (reviewed in (Majima et al., 2011)). However, the molecular mechanisms governing CGRP-mediated angiogenesis remain unknown. Future studies could be directed to investigate whether CGRP-induced ErbB1 transactivation plays a role in CGRP-mediated angiogenesis. This could lead to the identification of new drug targets and possibly to alternative therapies in cancer.

The tyrosine kinase Src is known to play an important role in GPCR-mediated ERK activation (reviewed in (McGarrigle and Huang, 2007)). Moreover, many studies reported that Src was involved in ErbB1 transactivation (Buteau et al., 2003; Daub et al., 1997; Eguchi et al., 1998), as well as in the cAMP/PKA pathway-mediated ERK activation (Obara et al., 2004; Schmitt and Stork, 2002). Interestingly, I showed by using PP2, a Src inhibitor, that CGRP-induced ERK activation was reduced (**Fig. 6.1**). Thus, Src is required for CGRP-induced ERK activation. However, further experiments are required to determine whether Src is involved in cAMP/PKA pathway, in ErbB1 transactivation pathway or both pathways.

The metalloprotease ECE-1 regulates the recycling and the endosomal ERK signalling of NK_1R (Cottrell et al., 2009; Roosterman et al., 2007). Surprisingly, even though ECE-1 also regulates the trafficking of CLR•RAMP1 (Padilla et al., 2007), inhibition of ECE-1 or preventing endosomal acidification, (both of which prevent CGRP degradation in endosomes) did not affect the magnitude or duration of CGRP-induced ERK signalling. One reason why perhaps ECE-1 does not regulate CGRP-induced ERK activation is that β-arrestin does not play a role in

CGRP-induced ERK activation. For example, the NK_1R-mediated endosomal ERK signalling have been showed to be dependent on β-arrestin (Cottrell et al., 2009). Indeed, β-arrestins, other than mediating GPCR desensitisation and internalisation, also facilitate mitogenic signalling due to their ability to act as a scaffold for signalling proteins (reviewed in (Luttrell and Gesty-Palmer, 2010)). Therefore, it is possible that ECE-1 does not regulate CGRP-induced ERK signalling because CGRP does not induce ERK activation through β-arrestin. To confirm this hypothesis, I used β-arrestin mutant to study CGRP-induced ERK activation. As expected, when I transfected HEK-CLR•RAMP1 with a dominant-negative β-arrestin1 P91G P121E mutant that cannot bind Src, the magnitude or duration of CGRP-induced ERK signalling was not affected. This result suggests that CGRP-ERK activation is not dependent on β-arrestin1, which confirms the results seen with ECE-1. However, CLR is a class B GPCR (that bind both β-arrestins) (Hilairet et al., 2001), it would then be interested to use a β-arrestin2 mutant to confirm these observations, such as the β-arrestin2 V54D, that act as a dominant negative (Ferguson et al., 1996). Altogether, these data suggest that CGRP does not activate ERK via a β-arrestin-dependent mechanism, nor does it use the endosome as a signalling platform to activate ERK.

GPCRs can also induce ERK activation through the PLC/PKC/Ca^{2+} pathway (reviewed in (Belcheva and Coscia, 2002; Goldsmith and Dhanasekaran, 2007; Rozengurt, 2007)) either through the coupling with a $G\alpha_q$ subunit or through $\beta\gamma$ subunits-dependent mechanism of the G protein. By using different inhibitors at different level of the signalling cascade, I show that CGRP-induced ERK activation is unlikely signalling through PLC/PKC/Ca^{2+} in HEK cells. It is a surprising result as CGRP has been shown to induce Ca^{2+} mobilisation through $G\alpha_{q/11}$-mediated activation of PLC-β1 in OHS-4 cells (human bone cell line) (Drissi et al., 1998). Moreover, CGRP has also been shown to induce Ca^{2+} mobilisation and cAMP production in HEK cells (Aiyar et al., 1999), suggesting that CLR•RAMP1 signals through both $G\alpha_s$ and $G\alpha_q$. Therefore, it would be interesting to confirm that CGRP induces Ca^{2+} mobilisation in HEK-CLR•RAMP1 and whether its mediated through the PLC/PKC/Ca^{2+} pathway. If CGRP do induce Ca^{2+} mobilisation in HEK-CLR•RAMP1, then it is possible that Ca^{2+} mobilisation is not involved in CGRP-induced ERK activation. Obviously, further experiments are required to confirm this hypothesis.

Altogether those results give a better understanding of the CGRP-induced ERK signalling in HEK cells (**Fig. 6.1**). The step forward to this study is to repeat the key experiments in a more physiological model such as the primary rat TA-SMC, in order to determine whether CGRP induces ERK activation that would lead to iNOS upregulation in these cells. With this aim to investigate the CGPR-induced ERK activation pathways in SMC, I managed to isolate and culture primary TA-SMC from rat thoracic artery. These cells express CLR•RAMP1 and I showed that

CGRP induces iNOS upregulation, as previously shown by an earlier study (Schini-Kerth et al., 1994). Although, they pretreated TA-SMC with IL-1β before stimulating them with CGRP. Despite the fact that CGRP induces iNOS upregulation, it is unknown whether iNOS promotes NO production. Therefore, the quantification of NO production is necessary to further assess the role of CGRP in iNOS expression/NO production. Primary data using the MEK inhibitor U0126 show that CGRP-induced iNOS expression is partially blocked. This promising result suggests that CGRP regulate the iNOS expression in SMC in an ERK-dependent manner. However, I was not able to take the study further as the primary TA-SMC seemed to lose the expression of CLR•RAMP1 and therefore were not responding to CGRP. Indeed, other studies reported similar loss of expression in SMC of other membrane proteins such as the α7 integrin (Yao et al., 1997) and the muscarinic acetylcholine receptor M2 (Hsieh and Farley, 2002) due to differentiation of these cells. Therefore, one way to overcome this issue would be to use exogenously expressed CLR and RAMP1 in TA-SMC, for example by using the lentivirus or adenovirus system. It would allow the ERK activation pathways in CGRP-induced iNOS upregulation to be investigated. Particularly, to determine whether CGRP induces iNOS through the cAMP/PKA pathway or through transactivation of ErbB1, by using pharmalogical inhibitors. The upregulation of iNOS is likely to require gene transcription, which can be promoted by transcription factor that can be activated by the translocation of pERK1-2 into the nucleus. Therefore, it is possible that only the cAMP/PKA pathway might be involved in the upregulation of iNOS as a study showed that the transactivation of ErbB1 does not lead to the translocation of pERK1-2 into the nucleus (Tilley et al., 2009). To further investigate CGRP-induced iNOS upregulation, it could be interesting to use knockdown, mutant or overexpression studies targeting key element of the ERK pathway. Determining the CGRP-induced iNOS upregulation mechanisms would help to better understand the relationship between CGRP and NO. These two components play an important role in the regulation of the blood pressure and understanding their regulation could potentially lead to the discovery of new drug target or alternative therapies in cardiovascular disease related.

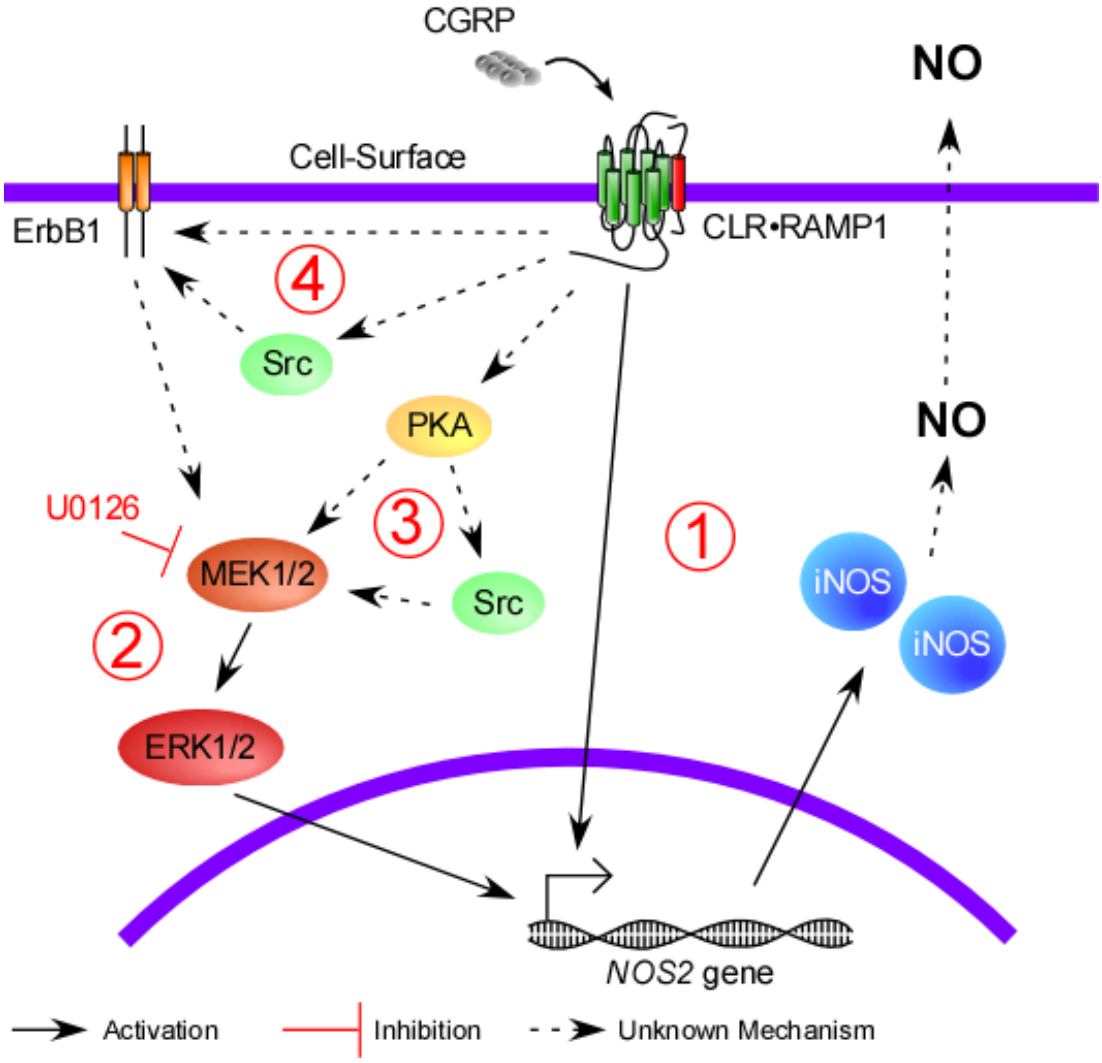

Figure 6.1 **General model of CGRP-induced iNOS upregulation.** (1) CGRP induces iNOS upregulation in primary rat TA-SMC. However, it is unknown whether CGRP-induced iNOS upregulation promotes NO formation. Therefore, the quantification of NO remains to be determine in CGRP-stimulated TA-SMC. (2) TA-SMC treated with the MEK inhibitor U0126, have shown that CGRP-induced iNOS upregulation is reduced, suggesting that upregulation of iNOS is ERK-dependent. As shown in HEK cells, CLR•RAMP1 promotes ERK signalling mainly through (3) the activation of the cAMP/PKA pathway or (4) the transactivation of ErbB1. The CGRP-induced ERK activation that promotes iNOS upregulation remains to be determined. Moreover, Src also has been shown to be involved in the CGRP-induced ERK activation. However, it is unknown whether Src is involved in the cAMP/PKA pathways or the ErbB1 transactivation.

6.3 The Post-Endocytic Sorting of CLR•RAMP2 and Future Direction

The receptor CLR•RAMP2 was stably transfected into HEK cells, in order to study its post-endocytic sorting. HEK cells are a common model used to study the molecular mechanisms regulating GPCRs (e.g (Luttrell et al., 2001; Roosterman et al., 2007)). Moreover, HEK cells have already been used for studying the traffic of CLR•RAMP2, where ADM stimulation induces internalisation of the receptor (Kuwasako et al., 2000). I also show by immunofluorescence and confocal microscopy that exposure to ADM induces a rapid internalisation of CLR•RAMP2 in HEK-cells. Moreover, I showed that ADM induces ERK1-2 activation in HEK-CLR•RAMP2, in accordance with other studies in HMEC-1 (human microvascular endothelial cell line) and HUVEC (human umbilical vein endothelial cells) (Kim et al., 2003; Schwarz et al., 2006). All together, these results suggest that CLR•RAMP2 is fully functional when expressed in HEK cells. Therefore, HEK-CLR•RAMP2 cells are a suitable model to study the post-endocytic sorting of CLR•RAMP2.

It is known that both CLR•RAMP1 and CLR•RAMP3 can recycle after transient stimulation (Bomberger et al., 2005; Cottrell et al., 2007). However, little is known about CRL•RAMP2 regulation. A study looking at the traffic of CRL•RAMP2 in HEK cells suggested that this receptor was degraded following transient stimulation with ADM (Kuwasako et al., 2000). By using CHX to inhibit newly synthesised proteins, I showed and confirmed that transient stimulation of ADM induces degradation of CRL•RAMP2 (**Fig. 6.2**). Therefore, as oppose to CLR•RAMP1 and CLR•RAMP3, CRL•RAMP2 does not recycle back to the cell-surface. It would be also interesting to see whether other agonists of CLR•RAMP2, such as ADM2 (Roh et al., 2004), also induce degradation of the receptor.

As ubiquitin has been involved in the degradation of many GPCRs (reviewed by (Hanyaloglu and von Zastrow, 2008; Marchese et al., 2008)), I investigated whether ADM promotes ubiquitination of CRL•RAMP2. However, it is known that continued stimulation with CGRP induces traffic and degradation to lysosomes of CLR•RAMP1, in an ubiquitin-independent mechanism (Cottrell et al., 2007). I then expected that CLR•RAMP2 would also be degraded in an ubiquitin-independent mechanism. Surprisingly, I show for the first time that CLR, but not RAMP2, is ubiquitinated in unstimulated cells, suggesting that CLR is constitutively ubiquitinated, which is further enhanced by ADM stimulation (**Fig. 6.2**). It is interesting to see that CLR is ubiquitinated upon ADM stimulation but not upon CGRP stimulation. Moreover, as I saw that CLR is constitutively ubiquitinated when associated with RAMP2, this suggests that association with RAMP1 or RAMP2 modify CLR ability to bind ubiquitin. These results could be explain by the fact that the C-terminal tail of RAMP1 physically covers all the intracellular facing

lysine residues of CLR and therefore block ubiquitination of the receptor. However, it is unlikely as RAMP1 and RAMP2 have short C-terminal tails (McLatchie et al., 1998), unless all the lysine residues of CLR form a "pocket" close to RAMP1. Thus, it would be interesting to investigate the difference of ubiquitination observed in CLR while associated with RAMP1 or RAMP2. For example, by "switching" the C-terminal tail of both RAMP1 and RAMP2, it would be interesting to see whether CGRP is able to induce ubiquitination of CLR or if ADM is still able to promote CLR ubiquitination. Other than the mechanisms of how ubiquitination occurs for CLR, I was first interested to understand what is the role of CLR ubiquitination in the regulation of CRL•RAMP2. Ubiquitination has been shown to be involved in different processes of the post-endocytic sorting of GPCRs, such as promoting or blocking internalisation (Hicke and Riezman, 1996; Wolfe et al., 2007), targeting to degradation (Shenoy et al., 2001) or increasing the rate of degradation (Hislop et al., 2009). I then undertook the construction of a CLR mutant named CLRΔ9KR, where all intracellular facing lysine residues were replaced by arginine residues. This method that prevents covalent binding of ubiquitin to the receptor, has already been used in other studies to help understand the role of ubiquitination in GPCRs regulation (Shenoy et al., 2001; Tanowitz and Von Zastrow, 2002; Wolfe et al., 2007). Once CLRΔ9KR•RAMP2 was stably express in HEK cells, I show that the receptor trafficked to early endosomes and lysosomes, as shown for CLR•RAMP2, suggesting that ubiquitin was not involved in neither the internalisation of the receptor nor its traffic to lysosomes. The fact that CLRΔ9KR•RAMP2 traffics to lysosomes suggests that the receptor is degraded, as it has been shown for the δOR lysine-less mutant (Tanowitz and Von Zastrow, 2002), as opposed to the lysine deficient β_2-AR receptor that was sequestered in endosomes and therefore not degraded (Shenoy et al., 2001). Indeed, as suggested I showed that stimulation with ADM for 16 h did not show any differences in the degradation of CLR•RAMP2 or CLRΔ9KR•RAMP2. The study carried out by Hislop *et al.*, showed that ubiquitin is involved in the rate of δOR degradation (Hislop et al., 2009), therefore I also looked at ADM-induced degradation of CLR•RAMP2 and CLRΔ9KR•RAMP2 at earlier time points. I showed, when both receptors were continuously stimulated for 4 h, CLR•RAMP2 is significantly degraded, whereas CLRΔ9KR•RAMP2 is untouched, suggesting that CLR•RAMP2 undergo degradation more rapidly than CLRΔ9KR•RAMP2 (**Fig. 6.2**). These results are similar of those obtained with δOR, where after 3-5 h of stimulation with DADLE, the lysine-less mutant show a significant higher ability to bind radioactive δOR antagonist diprenorphine, suggesting that the down-regulation of the lysine-less mutant was slower than for the WT receptor (Hislop et al., 2009). Altogether, these results suggest that the ubiquitination of CLR is involved in the rate of degradation of CLR•RAMP2.

In order to investigate the proteolytic site of CLR•RAMP2, I used inhibitors of lysosomal and proteasomal proteases (**Fig. 6.2**). Surprisingly, a lysosomal protease inhibitor cocktail that inhibits cysteine and aspartate proteases, which have been shown to completely block CGRP-induced CLR•RAMP1 degradation (Cottrell et al., 2007), only partially prevented ADM-induced CLR•RAMP2 degradation. This result suggests that CLR•RAMP2 could be degraded by other proteases such as serine, threonine or glutamic proteases. To investigate this eventuality, inhibitors targeting these proteases could be used to see whether ADM-induced CLR•RAMP2 degradation is prevented or not. Another, explanation is that CLR•RAMP2 is not degraded by the lysosome, which seems unlikely as I showed that CLR•RAMP2 traffic to lysosome. However, many studies have shown that δOR degradation is prevented by the proteasome inhibitor MG-132 (Chaturvedi et al., 2001; Tanowitz and Von Zastrow, 2002), suggesting that this receptor down-regulation is mediated by the proteasome. Interestingly, I also showed that CLR•RAMP2 degradation was significantly prevented by MG-132. This result could explain why the lysosome inhibitors did not fully blocked the degradation of CLR•RAMP2. However, in the aim to confirm these results I also used another proteasome inhibitor, epoxomicin, which did not prevent CLR•RAMP2 degradation, suggesting that the effects seen with MG-132 are due to off-target effects. Indeed, MG-132 has been found to inhibit certain cathepsins (e.g. B, L and K) found in lysosomes (Goulet et al., 2004; Guery et al., 2011; Longva et al., 2002). It is then possible than MG-132 prevents CLR•RAMP2 degradation through the inhibition of lysosomal proteases. Thus, using different cathepsins inhibitors would help to determine the site of down-regulation of ADM-induced CLR•RAMP2.

As already mentioned, HEK cells do not endogenously express CLR•RAMP2, therefore repeating key experiments in a more physiological relevant model, such as HMEC-1, is necessary. Primary data showed that HMEC-1 cells endogenously express CLR•RAMP2. However, endogenous levels of CLR•RAMP2 are low, which makes biochemical analysis impossible. Therefore, I decided to overexpress CLR•RAMP2 and CLRΔ9KR•RAMP2 in HMEC-1 cells. I used a cationic lipid-based transfection reagent to overexpress the receptor in HMEC-1 that has already been described to work in other studies (Faure et al., 2000; Zhu et al., 2003). However, I found that HMEC-1 cells were sensitive to the transfection regent and therefore promoted cell death. By modifying the protocol, I managed to lower the cell toxicity of the assay, however, the level of transfection was also negatively affected. Nevertheless, I showed that ADM promotes the trafficking of CLR•RAMP2 and CLRΔ9KR•RAMP2 to lysosomes in transfected HMEC-1 cells. These primary data are really promising, suggesting that observations made in HEK cells would also occur in endothelial cells. The next step would be to find alternative ways to overexpress CLR•RAMP2 and CLRΔ9KR•RAMP2 in HMEC-1, such as using a lentivirus or adenovirus system. Once HMEC-1 stably express

CLR•RAMP2 and CLRΔ9KR•RAMP2, it would be necessary to confirm that transient stimulation of ADM induces degradation of CLR•RAMP2 and that ADM promotes ubiquitination of CLR. This would allow us to confirm the results observed in HEK cells and would contribute to better characterise the post-endocytic regulation of CLR•RAMP2. Further ahead, as I show that the traffic or degradation is not driven by ubiquitin, it would be interesting to determine which system is responsible of CLR•RAMP2 traffic to lysosome. For example, the ESCRT machinery has been shown to regulate the traffic of many GPCRs, including CLR•RAMP1 (Gullapalli et al., 2006; Hasdemir et al., 2007; Marchese et al., 2003). Therefore, by using knockdown studies targeting components of the ESCRT machinery, the regulation of CLR•RAMP2 trafficking could be determined. Altogether, understanding the post-endocytic sorting of CLR•RAMP2 could lead to the discovery of new drug target and alternative therapies involved in cardiovascular disease related.

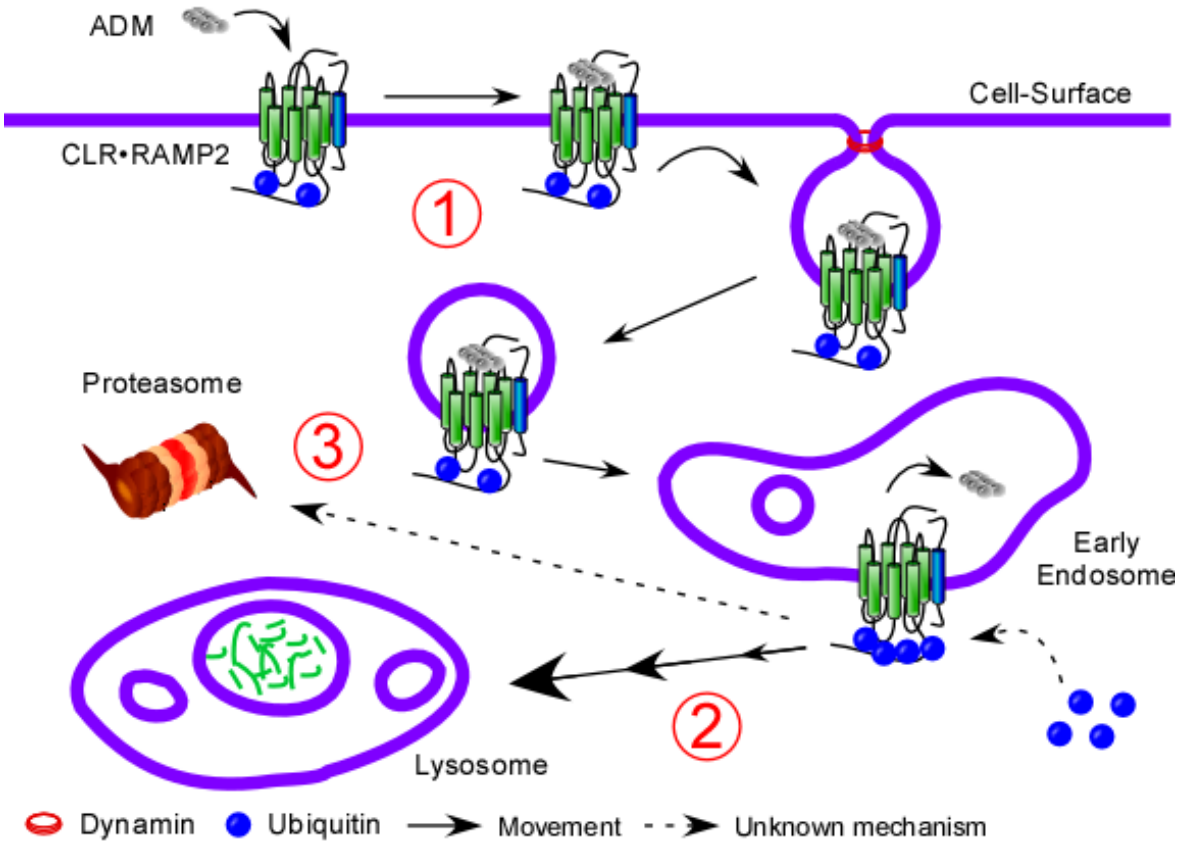

Figure 6.2 **General model of CLR•RAMP2 post-endocytic sorting.** (1) Transient ADM stimulation induces internalisation and trafficking to endosomes and lysosomes of CLR•RAMP2 to be degraded. CLR has been shown to be constitutively ubiquitinated, which is further enhanced by ADM stimulation. (2) ADM-induced ubiquitination of CLR observed occurs relatively late compared to other GPCRs. Therefore, CLR ubiquitination is thought to take place in endosomes, but further experiments are necessary to confirm this hypothesis. ADM-induced CLR ubiquitination has been shown to be involved in the rate of degradation of CLR•RAMP2, by accelerating the process. (3) The cocktail of lysosomal proteases inhibitors used in this study was not able to completely prevent the degradation of CLR•RAMP2. Moreover, a proteasome inhibitor also showed to partially prevent the degradation of CLR•RAMP2. These results suggest that CLR•RAMP2 is degraded by both lysosome and proteasome. Further experiments remain to determine whether other lysosomal proteases are involved in the degradation of CLR•RAMP2 or if the effect of the proteasome inhibitor observed are due to off-target effects.

Chapter 7. References

Adomeit, A., A. Graness, S. Gross, K. Seedorf, R. Wetzker, and C. Liebmann. 1999. Bradykinin B(2) receptor-mediated mitogen-activated protein kinase activation in COS-7 cells requires dual signaling via both protein kinase C pathway and epidermal growth factor receptor transactivation. *Mol Cell Biol*. 19:5289-5297.

Ahn, S., S. Maudsley, L.M. Luttrell, R.J. Lefkowitz, and Y. Daaka. 1999. Src-mediated tyrosine phosphorylation of dynamin is required for beta2-adrenergic receptor internalization and mitogen-activated protein kinase signaling. *J Biol Chem*. 274:1185-1188.

Ahn, S., S.K. Shenoy, H. Wei, and R.J. Lefkowitz. 2004. Differential kinetic and spatial patterns of beta-arrestin and G protein-mediated ERK activation by the angiotensin II receptor. *J Biol Chem*. 279:35518-35525.

Aiyar, N., J. Disa, J.M. Stadel, and P.G. Lysko. 1999. Calcitonin gene-related peptide receptor independently stimulates 3',5'-cyclic adenosine monophosphate and Ca2+ signaling pathways. *Mol Cell Biochem*. 197:179-185.

Aiyar, N., K. Rand, N.A. Elshourbagy, Z. Zeng, J.E. Adamou, D.J. Bergsma, and Y. Li. 1996. A cDNA encoding the calcitonin gene-related peptide type 1 receptor. *J Biol Chem*. 271:11325-11329.

Alonso, V., C.E. Magyar, B. Wang, A. Bisello, and P.A. Friedman. 2011. Ubiquitination-deubiquitination balance dictates ligand-stimulated PTHR sorting. *J Bone Miner Res*. 26:2923-2934.

Amara, S.G., J.L. Arriza, S.E. Leff, L.W. Swanson, R.M. Evans, and M.G. Rosenfeld. 1985. Expression in brain of a messenger RNA encoding a novel neuropeptide homologous to calcitonin gene-related peptide. *Science*. 229:1094-1097.

Amara, S.G., V. Jonas, M.G. Rosenfeld, E.S. Ong, and R.M. Evans. 1982. Alternative RNA processing in calcitonin gene expression generates mRNAs encoding different polypeptide products. *Nature*. 298:240-244.

Aoki, T., R. Nomura, and T. Fujimoto. 1999. Tyrosine phosphorylation of caveolin-1 in the endothelium. *Exp Cell Res*. 253:629-636.

Arai, H., and J.A. Escobedo. 1996. Angiotensin II type 1 receptor signals through Raf-1 by a protein kinase C-dependent, Ras-independent mechanism. *Mol Pharmacol*. 50:522-528.

Arrigo, A.P., K. Tanaka, A.L. Goldberg, and W.J. Welch. 1988. Identity of the 19S 'prosome' particle with the large multifunctional protease complex of mammalian cells (the proteasome). *Nature*. 331:192-194.

Attramadal, H., J.L. Arriza, C. Aoki, T.M. Dawson, J. Codina, M.M. Kwatra, S.H. Snyder, M.G. Caron, and R.J. Lefkowitz. 1992. Beta-arrestin2, a novel member of the arrestin/beta-arrestin gene family. *J Biol Chem*. 267:17882-17890.

Azmi, I., B. Davies, C. Dimaano, J. Payne, D. Eckert, M. Babst, and D.J. Katzmann. 2006. Recycling of ESCRTs by the AAA-ATPase Vps4 is regulated by a conserved VSL region in Vta1. *J Cell Biol*. 172:705-717.

Babst, M., G. Odorizzi, E.J. Estepa, and S.D. Emr. 2000. Mammalian tumor susceptibility gene 101 (TSG101) and the yeast homologue, Vps23p, both function in late endosomal trafficking. *Traffic*. 1:248-258.

Babst, M., B. Wendland, E.J. Estepa, and S.D. Emr. 1998. The Vps4p AAA ATPase regulates membrane association of a Vps protein complex required for normal endosome function. *EMBO J*. 17:2982-2993.

Bain, J., L. Plater, M. Elliott, N. Shpiro, C.J. Hastie, H. McLauchlan, I. Klevernic, J.S. Arthur, D.R. Alessi, and P. Cohen. 2007. The selectivity of protein kinase inhibitors: a further update. *Biochem J*. 408:297-315.

Bartlett, S.E., J. Enquist, F.W. Hopf, J.H. Lee, F. Gladher, V. Kharazia, M. Waldhoer, W.S. Mailliard, R. Armstrong, A. Bonci, and J.L. Whistler. 2005. Dopamine responsiveness is regulated by targeted sorting of D2 receptors. *Proc Natl Acad Sci U S A*. 102:11521-11526.

Belcheva, M.M., and C.J. Coscia. 2002. Diversity of G protein-coupled receptor signaling pathways to ERK/MAP kinase. *Neurosignals*. 11:34-44.

Benovic, J.L., H. Kuhn, I. Weyand, J. Codina, M.G. Caron, and R.J. Lefkowitz. 1987. Functional desensitization of the isolated beta-adrenergic receptor by the beta-adrenergic receptor kinase: potential role of an analog of the retinal protein arrestin (48-kDa protein). *Proc Natl Acad Sci U S A*. 84:8879-8882.

Benovic, J.L., F. Mayor, Jr., R.L. Somers, M.G. Caron, and R.J. Lefkowitz. 1986a. Light-dependent phosphorylation of rhodopsin by beta-adrenergic receptor kinase. *Nature*. 321:869-872.

Benovic, J.L., L.J. Pike, R.A. Cerione, C. Staniszewski, T. Yoshimasa, J. Codina, M.G. Caron, and R.J. Lefkowitz. 1985. Phosphorylation of the mammalian beta-adrenergic receptor by cyclic AMP-dependent protein kinase. Regulation of the rate of receptor phosphorylation and dephosphorylation by agonist occupancy and effects on coupling of the receptor to the stimulatory guanine nucleotide regulatory protein. *J Biol Chem*. 260:7094-7101.

Benovic, J.L., R.H. Strasser, M.G. Caron, and R.J. Lefkowitz. 1986b. Beta-adrenergic receptor kinase: identification of a novel protein kinase that phosphorylates the agonist-occupied form of the receptor. *Proc Natl Acad Sci U S A*. 83:2797-2801.

Berlin, I., K.M. Higginbotham, R.S. Dise, M.I. Sierra, and P.D. Nash. 2010. The deubiquitinating enzyme USP8 promotes trafficking and degradation of the chemokine receptor 4 at the sorting endosome. *J Biol Chem*. 285:37895-37908.

Bertelsen, L.S., K.E. Barrett, and S.J. Keely. 2004. Gs protein-coupled receptor agonists induce transactivation of the epidermal growth factor receptor in T84 cells: implications for epithelial secretory responses. *J Biol Chem*. 279:6271-6279.

Bishop, R., R. Martinez, K.D. Nakamura, and M.J. Weber. 1983. A tumor promoter stimulates phosphorylation on tyrosine. *Biochem Biophys Res Commun*. 115:536-543.

Blaukat, A., A. Barac, M.J. Cross, S. Offermanns, and I. Dikic. 2000. G protein-coupled receptor-mediated mitogen-activated protein kinase activation through cooperation of Galpha(q) and Galpha(i) signals. *Mol Cell Biol*. 20:6837-6848.

Bleasdale, J.E., N.R. Thakur, R.S. Gremban, G.L. Bundy, F.A. Fitzpatrick, R.J. Smith, and S. Bunting. 1990. Selective inhibition of receptor-coupled

phospholipase C-dependent processes in human platelets and polymorphonuclear neutrophils. *J Pharmacol Exp Ther*. 255:756-768.

Bomberger, J.M., N. Parameswaran, C.S. Hall, N. Aiyar, and W.S. Spielman. 2005. Novel function for receptor activity-modifying proteins (RAMPs) in post-endocytic receptor trafficking. *J Biol Chem*. 280:9297-9307.

Boulanger, Y., A. Khiat, Y. Chen, L. Senecal, Y. Tu, S. St-Pierre, and A. Fournier. 1995. Structure of human calcitonin gene-related peptide (hCGRP) and of its antagonist hCGRP 8-37 as determined by NMR and molecular modeling. *Pept Res*. 8:206-213.

Bouley, R., H.Y. Lin, M.K. Raychowdhury, V. Marshansky, D. Brown, and D.A. Ausiello. 2005. Downregulation of the vasopressin type 2 receptor after vasopressin-induced internalization: involvement of a lysosomal degradation pathway. *Am J Physiol Cell Physiol*. 288:C1390-1401.

Boulton, T.G., S.H. Nye, D.J. Robbins, N.Y. Ip, E. Radziejewska, S.D. Morgenbesser, R.A. DePinho, N. Panayotatos, M.H. Cobb, and G.D. Yancopoulos. 1991. ERKs: a family of protein-serine/threonine kinases that are activated and tyrosine phosphorylated in response to insulin and NGF. *Cell*. 65:663-675.

Boulton, T.G., G.D. Yancopoulos, J.S. Gregory, C. Slaughter, C. Moomaw, J. Hsu, and M.H. Cobb. 1990. An insulin-stimulated protein kinase similar to yeast kinases involved in cell cycle control. *Science*. 249:64-67.

Brain, S.D., and H. Cambridge. 1996. Calcitonin gene-related peptide: vasoactive effects and potential therapeutic role. *Gen Pharmacol*. 27:607-611.

Brain, S.D., and A.D. Grant. 2004. Vascular actions of calcitonin gene-related peptide and adrenomedullin. *Physiol Rev*. 84:903-934.

Brain, S.D., T.J. Williams, J.R. Tippins, H.R. Morris, and I. MacIntyre. 1985. Calcitonin gene-related peptide is a potent vasodilator. *Nature*. 313:54-56.

Brain, S.D., S. Wimalawansa, I. MacIntyre, and T.J. Williams. 1990. The demonstration of vasodilator activity of pancreatic amylin amide in the rabbit. *Am J Pathol*. 136:487-490.

Breeze, A.L., T.S. Harvey, R. Bazzo, and I.D. Campbell. 1991. Solution structure of human calcitonin gene-related peptide by 1H NMR and distance geometry with restrained molecular dynamics. *Biochemistry*. 30:575-582.

Breimer, L.H., I. MacIntyre, and M. Zaidi. 1988. Peptides from the calcitonin genes: molecular genetics, structure and function. *Biochem J*. 255:377-390.

Brell, B., B. Temmesfeld-Wollbruck, I. Altzschner, E. Frisch, B. Schmeck, A.C. Hocke, N. Suttorp, and S. Hippenstiel. 2005. Adrenomedullin reduces Staphylococcus aureus alpha-toxin-induced rat ileum microcirculatory damage. *Crit Care Med*. 33:819-826.

Brodsky, F.M., C.Y. Chen, C. Knuehl, M.C. Towler, and D.E. Wakeham. 2001. Biological basket weaving: formation and function of clathrin-coated vesicles. *Annu Rev Cell Dev Biol*. 17:517-568.

Brostrom, M.A., E.M. Reimann, D.A. Walsh, and E.G. Krebs. 1970. A cyclic 3',5'-amp-stimulated protein kinase from cardiac muscle. *Adv Enzyme Regul*. 8:191-203.

Bucci, C., P. Thomsen, P. Nicoziani, J. McCarthy, and B. van Deurs. 2000. Rab7: a key to lysosome biogenesis. *Molecular biology of the cell*. 11:467-480.

Buhlmann, N., K. Leuthauser, R. Muff, J.A. Fischer, and W. Born. 1999. A receptor activity modifying protein (RAMP)2-dependent adrenomedullin receptor is a

calcitonin gene-related peptide receptor when coexpressed with human RAMP1. *Endocrinology*. 140:2883-2890.

Buteau, J., S. Foisy, E. Joly, and M. Prentki. 2003. Glucagon-like peptide 1 induces pancreatic beta-cell proliferation via transactivation of the epidermal growth factor receptor. *Diabetes*. 52:124-132.

Cabrera-Vera, T.M., J. Vanhauwe, T.O. Thomas, M. Medkova, A. Preininger, M.R. Mazzoni, and H.E. Hamm. 2003. Insights into G protein structure, function, and regulation. *Endocr Rev*. 24:765-781.

Cady, R.J., J.R. Glenn, K.M. Smith, and P.L. Durham. 2011. Calcitonin gene-related peptide promotes cellular changes in trigeminal neurons and glia implicated in peripheral and central sensitization. *Mol Pain*. 7:94.

Callahan, J.W., R.D. Bagshaw, and D.J. Mahuran. 2009. The integral membrane of lysosomes: its proteins and their roles in disease. *J Proteomics*. 72:23-33.

Campbell, J.H., and G.R. Campbell. 1993. Culture techniques and their applications to studies of vascular smooth muscle. *Clinical science*. 85:501-513.

Camps, M., A. Carozzi, P. Schnabel, A. Scheer, P.J. Parker, and P. Gierschik. 1992. Isozyme-selective stimulation of phospholipase C-beta 2 by G protein beta gamma-subunits. *Nature*. 360:684-686.

Cao, T.T., H.W. Deacon, D. Reczek, A. Bretscher, and M. von Zastrow. 1999. A kinase-regulated PDZ-domain interaction controls endocytic sorting of the beta2-adrenergic receptor. *Nature*. 401:286-290.

Carbajal, L., A. Biswas, L.M. Niswander, H. Prizant, and S.R. Hammes. 2011. GPCR/EGFR cross talk is conserved in gonadal and adrenal steroidogenesis but is uniquely regulated by matrix metalloproteinases 2 and 9 in the ovary. *Mol Endocrinol*. 25:1055-1065.

Caron, K.M., and O. Smithies. 2001. Extreme hydrops fetalis and cardiovascular abnormalities in mice lacking a functional Adrenomedullin gene. *Proc Natl Acad Sci U S A*. 98:615-619.

Chabre, O., B.R. Conklin, H.Y. Lin, H.F. Lodish, E. Wilson, H.E. Ives, L. Catanzariti, B.A. Hemmings, and H.R. Bourne. 1992. A recombinant calcitonin receptor independently stimulates 3',5'-cyclic adenosine monophosphate and Ca2+/inositol phosphate signaling pathways. *Mol Endocrinol*. 6:551-556.

Chakraborty, M., D. Chatterjee, S. Kellokumpu, H. Rasmussen, and R. Baron. 1991. Cell cycle-dependent coupling of the calcitonin receptor to different G proteins. *Science*. 251:1078-1082.

Chance, W.T., A. Balasubramaniam, A. Stallion, and J.E. Fischer. 1993. Anorexia following the systemic injection of amylin. *Brain Res*. 607:185-188.

Chao, P.C., and K.L. Hamilton. 2009. Genistein stimulates electrogenic Cl-secretion via phosphodiesterase modulation in the mouse jejunum. *Am J Physiol Cell Physiol*. 297:C688-698.

Chattergoon, N.N., F.M. D'Souza, W. Deng, H. Chen, A.L. Hyman, P.J. Kadowitz, and J.R. Jeter, Jr. 2005. Antiproliferative effects of calcitonin gene-related peptide in aortic and pulmonary artery smooth muscle cells. *Am J Physiol Lung Cell Mol Physiol*. 288:L202-211.

Chaturvedi, K., P. Bandari, N. Chinen, and R.D. Howells. 2001. Proteasome involvement in agonist-induced down-regulation of mu and delta opioid receptors. *J Biol Chem*. 276:12345-12355.

Chijiwa, T., A. Mishima, M. Hagiwara, M. Sano, K. Hayashi, T. Inoue, K. Naito, T. Toshioka, and H. Hidaka. 1990. Inhibition of forskolin-induced neurite outgrowth and protein phosphorylation by a newly synthesized selective inhibitor of cyclic AMP-dependent protein kinase, N-[2-(p-bromocinnamylamino)ethyl]-5-isoquinolinesulfonamide (H-89), of PC12D pheochromocytoma cells. *J Biol Chem*. 265:5267-5272.

Chin, L.S., M.C. Raynor, X. Wei, H.Q. Chen, and L. Li. 2001. Hrs interacts with sorting nexin 1 and regulates degradation of epidermal growth factor receptor. *J Biol Chem*. 276:7069-7078.

Cho, E.Y., D.I. Cho, J.H. Park, H. Kurose, M.G. Caron, and K.M. Kim. 2007. Roles of protein kinase C and actin-binding protein 280 in the regulation of intracellular trafficking of dopamine D3 receptor. *Mol Endocrinol*. 21:2242-2254.

Choi, K.Y., B. Satterberg, D.M. Lyons, and E.A. Elion. 1994. Ste5 tethers multiple protein kinases in the MAP kinase cascade required for mating in S. cerevisiae. *Cell*. 78:499-512.

Christopoulos, A., G. Christopoulos, M. Morfis, M. Udawela, M. Laburthe, A. Couvineau, K. Kuwasako, N. Tilakaratne, and P.M. Sexton. 2003. Novel receptor partners and function of receptor activity-modifying proteins. *J Biol Chem*. 278:3293-3297.

Christopoulos, G., K.J. Perry, M. Morfis, N. Tilakaratne, Y. Gao, N.J. Fraser, M.J. Main, S.M. Foord, and P.M. Sexton. 1999. Multiple amylin receptors arise from receptor activity-modifying protein interaction with the calcitonin receptor gene product. *Mol Pharmacol*. 56:235-242.

Cianfrocca, R., L. Rosano, F. Spinella, V. Di Castro, P.G. Natali, and A. Bagnato. 2010. Beta-arrestin-1 mediates the endothelin-1-induced activation of Akt and integrin-linked kinase. *Can J Physiol Pharmacol*. 88:796-801.

Ciechanover, A., S. Elias, H. Heller, and A. Hershko. 1982. "Covalent affinity" purification of ubiquitin-activating enzyme. *J Biol Chem*. 257:2537-2542.

Claing, A., S.A. Laporte, M.G. Caron, and R.J. Lefkowitz. 2002. Endocytosis of G protein-coupled receptors: roles of G protein-coupled receptor kinases and beta-arrestin proteins. *Prog Neurobiol*. 66:61-79.

Collins, B.M., A.J. McCoy, H.M. Kent, P.R. Evans, and D.J. Owen. 2002. Molecular architecture and functional model of the endocytic AP2 complex. *Cell*. 109:523-535.

Collins, D.S., E.R. Unanue, and C.V. Harding. 1991. Reduction of disulfide bonds within lysosomes is a key step in antigen processing. *J Immunol*. 147:4054-4059.

Cong, M., S.J. Perry, L.A. Hu, P.I. Hanson, A. Claing, and R.J. Lefkowitz. 2001. Binding of the beta2 adrenergic receptor to N-ethylmaleimide-sensitive factor regulates receptor recycling. *J Biol Chem*. 276:45145-45152.

Conner, M., M.R. Hicks, T. Dafforn, T.J. Knowles, C. Ludwig, S. Staddon, M. Overduin, U.L. Gunther, J. Thome, M. Wheatley, D.R. Poyner, and A.C. Conner. 2008. Functional and biophysical analysis of the C-terminus of the CGRP-receptor; a family B GPCR. *Biochemistry*. 47:8434-8444.

Conner, S.D., and S.L. Schmid. 2003. Regulated portals of entry into the cell. *Nature*. 422:37-44.

Cook, L.B., C.C. Zhu, and P.M. Hinkle. 2003. Thyrotropin-releasing hormone receptor processing: role of ubiquitination and proteasomal degradation. *Mol Endocrinol*. 17:1777-1791.

Cook, S.J., and F. McCormick. 1993. Inhibition by cAMP of Ras-dependent activation of Raf. *Science*. 262:1069-1072.

Cooper, C.W., T.C. Peng, J.F. Obie, and S.C. Garner. 1980. Calcitonin-like immunoreactivity in rat and human pituitary glands: histochemical, in vitro, and in vivo studies. *Endocrinology*. 107:98-107.

Cooper, G.J., A.C. Willis, A. Clark, R.C. Turner, R.B. Sim, and K.B. Reid. 1987. Purification and characterization of a peptide from amyloid-rich pancreases of type 2 diabetic patients. *Proc Natl Acad Sci U S A*. 84:8628-8632.

Copp, D.H., E.C. Cameron, B.A. Cheney, A.G. Davidson, and K.G. Henze. 1962. Evidence for calcitonin--a new hormone from the parathyroid that lowers blood calcium. *Endocrinology*. 70:638-649.

Copp, D.H., and B. Cheney. 1962. Calcitonin-a hormone from the parathyroid which lowers the calcium-level of the blood. *Nature*. 193:381-382.

Corbit, K.C., D.A. Foster, and M.R. Rosner. 1999. Protein kinase Cdelta mediates neurogenic but not mitogenic activation of mitogen-activated protein kinase in neuronal cells. *Mol Cell Biol*. 19:4209-4218.

Corbit, K.C., N. Trakul, E.M. Eves, B. Diaz, M. Marshall, and M.R. Rosner. 2003. Activation of Raf-1 signaling by protein kinase C through a mechanism involving Raf kinase inhibitory protein. *J Biol Chem*. 278:13061-13068.

Cottrell, G.S., B. Padilla, S. Pikios, D. Roosterman, M. Steinhoff, E.F. Grady, and N.W. Bunnett. 2007. Post-endocytic sorting of calcitonin receptor-like receptor and receptor activity-modifying protein 1. *J Biol Chem*. 282:12260-12271.

Cottrell, G.S., B.E. Padilla, S. Amadesi, D.P. Poole, J.E. Murphy, M. Hardt, D. Roosterman, M. Steinhoff, and N.W. Bunnett. 2009. Endosomal endothelin-converting enzyme-1: a regulator of beta-arrestin-dependent ERK signaling. *J Biol Chem*. 284:22411-22425.

Cottrell, G.S., D. Roosterman, J.C. Marvizon, B. Song, E. Wick, S. Pikios, H. Wong, C. Berthelier, Y. Tang, C. Sternini, N.W. Bunnett, and E.F. Grady. 2005. Localization of calcitonin receptor-like receptor and receptor activity modifying protein 1 in enteric neurons, dorsal root ganglia, and the spinal cord of the rat. *J Comp Neurol*. 490:239-255.

Crossman, D.C., M.R. Dashwood, S.D. Brain, J. McEwan, and J.D. Pearson. 1990. Action of calcitonin gene-related peptide upon bovine vascular endothelial and smooth muscle cells grown in isolation and co-culture. *Br J Pharmacol*. 99:71-76.

Czyzyk, T.A., Y. Ning, M.S. Hsu, B. Peng, R.E. Mains, B.A. Eipper, and J.E. Pintar. 2005. Deletion of peptide amidation enzymatic activity leads to edema and embryonic lethality in the mouse. *Dev Biol*. 287:301-313.

Dackor, R.T., K. Fritz-Six, W.P. Dunworth, C.L. Gibbons, O. Smithies, and K.M. Caron. 2006. Hydrops fetalis, cardiovascular defects, and embryonic lethality in mice lacking the calcitonin receptor-like receptor gene. *Mol Cell Biol*. 26:2511-2518.

Dahlof, C. 2002. Integrating the triptans into clinical practice. *Curr Opin Neurol*. 15:317-322.

Damke, H., T. Baba, D.E. Warnock, and S.L. Schmid. 1994. Induction of mutant dynamin specifically blocks endocytic coated vesicle formation. *J Cell Biol*. 127:915-934.

Daub, H., C. Wallasch, A. Lankenau, A. Herrlich, and A. Ullrich. 1997. Signal characteristics of G protein-transactivated EGF receptor. *EMBO J*. 16:7032-7044.

Daub, H., F.U. Weiss, C. Wallasch, and A. Ullrich. 1996. Role of transactivation of the EGF receptor in signalling by G-protein-coupled receptors. *Nature*. 379:557-560.

Davies, S.P., H. Reddy, M. Caivano, and P. Cohen. 2000. Specificity and mechanism of action of some commonly used protein kinase inhibitors. *Biochem J*. 351:95-105.

De Duve, C., B.C. Pressman, R. Gianetto, R. Wattiaux, and F. Appelmans. 1955. Tissue fractionation studies. 6. Intracellular distribution patterns of enzymes in rat-liver tissue. *Biochem J*. 60:604-617.

de Gasparo, M., K.J. Catt, T. Inagami, J.W. Wright, and T. Unger. 2000. International union of pharmacology. XXIII. The angiotensin II receptors. *Pharmacol Rev*. 52:415-472.

de Jong, J.S., P.J. van Diest, P. van der Valk, and J.P. Baak. 1998. Expression of growth factors, growth-inhibiting factors, and their receptors in invasive breast cancer. II: Correlations with proliferation and angiogenesis. *J Pathol*. 184:53-57.

DeFea, K.A., Z.D. Vaughn, E.M. O'Bryan, D. Nishijima, O. Dery, and N.W. Bunnett. 2000a. The proliferative and antiapoptotic effects of substance P are facilitated by formation of a beta -arrestin-dependent scaffolding complex. *Proc Natl Acad Sci U S A*. 97:11086-11091.

DeFea, K.A., J. Zalevsky, M.S. Thoma, O. Dery, R.D. Mullins, and N.W. Bunnett. 2000b. beta-arrestin-dependent endocytosis of proteinase-activated receptor 2 is required for intracellular targeting of activated ERK1/2. *J Cell Biol*. 148:1267-1281.

Della Rocca, G.J., T. van Biesen, Y. Daaka, D.K. Luttrell, L.M. Luttrell, and R.J. Lefkowitz. 1997. Ras-dependent mitogen-activated protein kinase activation by G protein-coupled receptors. Convergence of Gi- and Gq-mediated pathways on calcium/calmodulin, Pyk2, and Src kinase. *J Biol Chem*. 272:19125-19132.

DeMartino, G.N., and A.L. Goldberg. 1979. Identification and partial purification of an ATP-stimulated alkaline protease in rat liver. *J Biol Chem*. 254:3712-3715.

Demaurex, N. 2002. pH Homeostasis of cellular organelles. *News Physiol Sci*. 17:1-5.

Derijard, B., M. Hibi, I.H. Wu, T. Barrett, B. Su, T. Deng, M. Karin, and R.J. Davis. 1994. JNK1: a protein kinase stimulated by UV light and Ha-Ras that binds and phosphorylates the c-Jun activation domain. *Cell*. 76:1025-1037.

Dhillon, A.S., C. Pollock, H. Steen, P.E. Shaw, H. Mischak, and W. Kolch. 2002. Cyclic AMP-dependent kinase regulates Raf-1 kinase mainly by phosphorylation of serine 259. *Mol Cell Biol*. 22:3237-3246.

Diener, H.C., P. Barbanti, C. Dahlof, U. Reuter, J. Habeck, and J. Podhorna. 2011. BI 44370 TA, an oral CGRP antagonist for the treatment of acute migraine attacks: results from a phase II study. *Cephalalgia : an international journal of headache*. 31:573-584.

Dikic, I., G. Tokiwa, S. Lev, S.A. Courtneidge, and J. Schlessinger. 1996. A role for Pyk2 and Src in linking G-protein-coupled receptors with MAP kinase activation. *Nature*. 383:547-550.

Doherty, G.J., and H.T. McMahon. 2009. Mechanisms of endocytosis. *Annu Rev Biochem*. 78:857-902.

Donnini, S., F. Finetti, R. Solito, E. Terzuoli, A. Sacchetti, L. Morbidelli, P. Patrignani, and M. Ziche. 2007. EP2 prostanoid receptor promotes squamous cell carcinoma growth through epidermal growth factor receptor transactivation and iNOS and ERK1/2 pathways. *FASEB J*. 21:2418-2430.

Doods, H. 2001. Development of CGRP antagonists for the treatment of migraine. *Curr Opin Investig Drugs*. 2:1261-1268.

Dores, M.R., B. Chen, H. Lin, U.J. Soh, M.M. Paing, W.A. Montagne, T. Meerloo, and J. Trejo. 2012. ALIX binds a YPX(3)L motif of the GPCR PAR1 and mediates ubiquitin-independent ESCRT-III/MVB sorting. *J Cell Biol*. 197:407-419.

Drissi, H., F. Lasmoles, V. Le Mellay, P.J. Marie, and M. Lieberherr. 1998. Activation of phospholipase C-beta1 via Galphaq/11 during calcium mobilization by calcitonin gene-related peptide. *J Biol Chem*. 273:20168-20174.

Dulon, S., C. Cande, N.W. Bunnett, M.D. Hollenberg, M. Chignard, and D. Pidard. 2003. Proteinase-activated receptor-2 and human lung epithelial cells: disarming by neutrophil serine proteinases. *Am J Respir Cell Mol Biol*. 28:339-346.

Edvinsson, L. 2001. Calcitonin gene-related peptide (CGRP) and the pathophysiology of headache: therapeutic implications. *CNS Drugs*. 15:745-753.

Edvinsson, L., T. Elsas, N. Suzuki, T. Shimizu, and T.J. Lee. 2001. Origin and Co-localization of nitric oxide synthase, CGRP, PACAP, and VIP in the cerebral circulation of the rat. *Microsc Res Tech*. 53:221-228.

Edvinsson, L., S. Gulbenkian, C.P. Barroso, M. Cunha e Sa, J.M. Polak, A. Mortensen, L. Jorgensen, and I. Jansen-Olesen. 1998. Innervation of the human middle meningeal artery: immunohistochemistry, ultrastructure, and role of endothelium for vasomotility. *Peptides*. 19:1213-1225.

Eguchi, S., K. Numaguchi, H. Iwasaki, T. Matsumoto, T. Yamakawa, H. Utsunomiya, E.D. Motley, H. Kawakatsu, K.M. Owada, Y. Hirata, F. Marumo, and T. Inagami. 1998. Calcium-dependent epidermal growth factor receptor transactivation mediates the angiotensin II-induced mitogen-activated protein kinase activation in vascular smooth muscle cells. *J Biol Chem*. 273:8890-8896.

Ehlenz, K., B. Koch, P. Preuss, B. Simon, I. Koop, and R.E. Lang. 1997. High levels of circulating adrenomedullin in severe illness: correlation with C-reactive protein and evidence against the adrenal medulla as site of origin. *Exp Clin Endocrinol Diabetes*. 105:156-162.

Eisinger, D.A., and H. Ammer. 2008. Delta-opioid receptors activate ERK/MAP kinase via integrin-stimulated receptor tyrosine kinases. *Cell Signal*. 20:2324-2331.

Enoki, S., T. Mitsukawa, J. Takemura, M. Nakazato, J. Aburaya, H. Toshimori, and S. Matsukara. 1992. Plasma islet amyloid polypeptide levels in obesity, impaired glucose tolerance and non-insulin-dependent diabetes mellitus. *Diabetes Res Clin Pract*. 15:97-102.

Enserink, J.M., A.E. Christensen, J. de Rooij, M. van Triest, F. Schwede, H.G. Genieser, S.O. Doskeland, J.L. Blank, and J.L. Bos. 2002. A novel Epac-specific cAMP analogue demonstrates independent regulation of Rap1 and ERK. *Nat Cell Biol*. 4:901-906.

Evans, B.N., M.I. Rosenblatt, L.O. Mnayer, K.R. Oliver, and I.M. Dickerson. 2000. CGRP-RCP, a novel protein required for signal transduction at calcitonin gene-related peptide and adrenomedullin receptors. *J Biol Chem*. 275:31438-31443.

Evaul, K., and S.R. Hammes. 2008. Cross-talk between G protein-coupled and epidermal growth factor receptors regulates gonadotropin-mediated steroidogenesis in Leydig cells. *J Biol Chem*. 283:27525-27533.

Fan, G.H., L.A. Lapierre, J.R. Goldenring, and A. Richmond. 2003. Differential regulation of CXCR2 trafficking by Rab GTPases. *Blood*. 101:2115-2124.

Faure, E., O. Equils, P.A. Sieling, L. Thomas, F.X. Zhang, C.J. Kirschning, N. Polentarutti, M. Muzio, and M. Arditi. 2000. Bacterial lipopolysaccharide activates NF-kappaB through toll-like receptor 4 (TLR-4) in cultured human dermal endothelial cells. Differential expression of TLR-4 and TLR-2 in endothelial cells. *J Biol Chem*. 275:11058-11063.

Faure, M., T.A. Voyno-Yasenetskaya, and H.R. Bourne. 1994. cAMP and beta gamma subunits of heterotrimeric G proteins stimulate the mitogen-activated protein kinase pathway in COS-7 cells. *J Biol Chem*. 269:7851-7854.

Favata, M.F., K.Y. Horiuchi, E.J. Manos, A.J. Daulerio, D.A. Stradley, W.S. Feeser, D.E. Van Dyk, W.J. Pitts, R.A. Earl, F. Hobbs, R.A. Copeland, R.L. Magolda, P.A. Scherle, and J.M. Trzaskos. 1998. Identification of a novel inhibitor of mitogen-activated protein kinase kinase. *J Biol Chem*. 273:18623-18632.

Fenteany, G., R.F. Standaert, W.S. Lane, S. Choi, E.J. Corey, and S.L. Schreiber. 1995. Inhibition of proteasome activities and subunit-specific amino-terminal threonine modification by lactacystin. *Science*. 268:726-731.

Ferguson, S.S. 2001. Evolving concepts in G protein-coupled receptor endocytosis: the role in receptor desensitization and signaling. *Pharmacol Rev*. 53:1-24.

Ferguson, S.S., W.E. Downey, A.M. Colapietro, L.S. Barak, L. Ménard, and M.G. Caron. 1996. Role of beta-arrestin in mediating agonist-promoted G protein-coupled receptor internalization. *Science*. 271:363-366.

Ferro, A., L.R. Queen, R.M. Priest, B. Xu, J.M. Ritter, L. Poston, and J.P. Ward. 1999. Activation of nitric oxide synthase by beta 2-adrenoceptors in human umbilical vein endothelium in vitro. *Br J Pharmacol*. 126:1872-1880.

Fineman, M., C. Weyer, D.G. Maggs, S. Strobel, and O.G. Kolterman. 2002a. The human amylin analog, pramlintide, reduces postprandial

hyperglucagonemia in patients with type 2 diabetes mellitus. *Horm Metab Res*. 34:504-508.

Fineman, M.S., J.E. Koda, L.Z. Shen, S.A. Strobel, D.G. Maggs, C. Weyer, and O.G. Kolterman. 2002b. The human amylin analog, pramlintide, corrects postprandial hyperglucagonemia in patients with type 1 diabetes. *Metabolism*. 51:636-641.

Fischer, J.A., P.H. Tobler, M. Kaufmann, W. Born, H. Henke, P.E. Cooper, S.M. Sagar, and J.B. Martin. 1981. Calcitonin: regional distribution of the hormone and its binding sites in the human brain and pituitary. *Proc Natl Acad Sci U S A*. 78:7801-7805.

Fischer, O.M., S. Hart, A. Gschwind, and A. Ullrich. 2003. EGFR signal transactivation in cancer cells. *Biochem Soc Trans*. 31:1203-1208.

Fluhmann, B., R. Muff, W. Hunziker, J.A. Fischer, and W. Born. 1995. A human orphan calcitonin receptor-like structure. *Biochem Biophys Res Commun*. 206:341-347.

Flynn, J.J., D.L. Margules, and C.W. Cooper. 1981. Presence of immunoreactive calcitonin in the hypothalamus and pituitary lobes of rats. *Brain Res Bull*. 6:547-549.

Force, T., J.V. Bonventre, M.R. Flannery, A.H. Gorn, M. Yamin, and S.R. Goldring. 1992. A cloned porcine renal calcitonin receptor couples to adenylyl cyclase and phospholipase C. *Am J Physiol*. 262:F1110-1115.

Fraser, N.J., A. Wise, J. Brown, L.M. McLatchie, M.J. Main, and S.M. Foord. 1999. The amino terminus of receptor activity modifying proteins is a critical determinant of glycosylation state and ligand binding of calcitonin receptor-like receptor. *Mol Pharmacol*. 55:1054-1059.

Fredriksson, R., M.C. Lagerstrom, L.G. Lundin, and H.B. Schioth. 2003. The G-protein-coupled receptors in the human genome form five main families. Phylogenetic analysis, paralogon groups, and fingerprints. *Mol Pharmacol*. 63:1256-1272.

Freed, W.J., M.J. Perlow, and R.J. Wyatt. 1979. Calcitonin: inhibitory effect on eating in rats. *Science*. 206:850-852.

Friedman, J., and L.G. Raisz. 1965. Thyrocalcitonin: inhibitor of bone resorption in tissue culture. *Science*. 150:1465-1467.

Frost, J.A., H. Steen, P. Shapiro, T. Lewis, N. Ahn, P.E. Shaw, and M.H. Cobb. 1997. Cross-cascade activation of ERKs and ternary complex factors by Rho family proteins. *EMBO J*. 16:6426-6438.

Gage, R.M., K.A. Kim, T.T. Cao, and M. von Zastrow. 2001. A transplantable sorting signal that is sufficient to mediate rapid recycling of G protein-coupled receptors. *J Biol Chem*. 276:44712-44720.

Gage, R.M., E.A. Matveeva, S.W. Whiteheart, and M. von Zastrow. 2005. Type I PDZ ligands are sufficient to promote rapid recycling of G Protein-coupled receptors independent of binding to N-ethylmaleimide-sensitive factor. *J Biol Chem*. 280:3305-3313.

Gagliardi, S., M. Rees, and C. Farina. 1999. Chemistry and structure activity relationships of bafilomycin A1, a potent and selective inhibitor of the vacuolar H+-ATPase. *Curr Med Chem*. 6:1197-1212.

Garland, A.M., E.F. Grady, M. Lovett, S.R. Vigna, M.M. Frucht, J.E. Krause, and N.W. Bunnett. 1996. Mechanisms of desensitization and resensitization of

G protein-coupled neurokinin1 and neurokinin2 receptors. *Mol Pharmacol*. 49:438-446.

Gedulin, B.R., T.J. Rink, and A.A. Young. 1997. Dose-response for glucagonostatic effect of amylin in rats. *Metabolism*. 46:67-70.

Gennari, C., and J.A. Fischer. 1985. Cardiovascular action of calcitonin gene-related peptide in humans. *Calcif Tissue Int*. 37:581-584.

Gill, G.N., and L.D. Garren. 1971. Role of the receptor in the mechanism of action of adenosine 3':5'-cyclic monophosphate. *Proc Natl Acad Sci U S A*. 68:786-790.

Gilman, A.G. 1984a. G proteins and dual control of adenylate cyclase. *Cell*. 36:577-579.

Gilman, A.G. 1984b. Guanine nucleotide-binding regulatory proteins and dual control of adenylate cyclase. *J Clin Invest*. 73:1-4.

Gilmore, T., and G.S. Martin. 1983. Phorbol ester and diacylglycerol induce protein phosphorylation at tyrosine. *Nature*. 306:487-490.

Ginnan, R., B.J. Guikema, K.E. Halligan, H.A. Singer, and D. Jourd'heuil. 2008. Regulation of smooth muscle by inducible nitric oxide synthase and NADPH oxidase in vascular proliferative diseases. *Free Radic Biol Med*. 44:1232-1245.

Giordano, F., S. Simoes, and G. Raposo. 2011. The ocular albinism type 1 (OA1) GPCR is ubiquitinated and its traffic requires endosomal sorting complex responsible for transport (ESCRT) function. *Proc Natl Acad Sci U S A*. 108:11906-11911.

Girgis, S.I., D.W. Macdonald, J.C. Stevenson, P.J. Bevis, C. Lynch, S.J. Wimalawansa, C.H. Self, H.R. Morris, and I. MacIntyre. 1985. Calcitonin gene-related peptide: potent vasodilator and major product of calcitonin gene. *Lancet*. 2:14-16.

Glickman, M.H., and A. Ciechanover. 2002. The ubiquitin-proteasome proteolytic pathway: destruction for the sake of construction. *Physiol Rev*. 82:373-428.

Goadsby, P.J., L. Edvinsson, and R. Ekman. 1990. Vasoactive peptide release in the extracerebral circulation of humans during migraine headache. *Ann Neurol*. 28:183-187.

Goldsmith, Z.G., and D.N. Dhanasekaran. 2007. G protein regulation of MAPK networks. *Oncogene*. 26:3122-3142.

Gong, K., Z. Li, M. Xu, J. Du, Z. Lv, and Y. Zhang. 2008. A novel protein kinase A-independent, beta-arrestin-1-dependent signaling pathway for p38 mitogen-activated protein kinase activation by beta2-adrenergic receptors. *J Biol Chem*. 283:29028-29036.

Goodman, O.B., Jr., J.G. Krupnick, F. Santini, V.V. Gurevich, R.B. Penn, A.W. Gagnon, J.H. Keen, and J.L. Benovic. 1996. Beta-arrestin acts as a clathrin adaptor in endocytosis of the beta2-adrenergic receptor. *Nature*. 383:447-450.

Gorvel, J.P., P. Chavrier, M. Zerial, and J. Gruenberg. 1991. rab5 controls early endosome fusion in vitro. *Cell*. 64:915-925.

Goulet, B., A. Baruch, N.S. Moon, M. Poirier, L.L. Sansregret, A. Erickson, M. Bogyo, and A. Nepveu. 2004. A cathepsin L isoform that is devoid of a signal peptide localizes to the nucleus in S phase and processes the CDP/Cux transcription factor. *Mol Cell*. 14:207-219.

Grafe, M., C. Bossaller, K. Graf, W. Auch-Schwelk, C.R. Baumgarten, A. Hildebrandt, and E. Fleck. 1993. Effect of angiotensin-converting-enzyme inhibition on bradykinin metabolism by vascular endothelial cells. *Am J Physiol*. 264:H1493-1497.

Grandage, V.L., T. Everington, D.C. Linch, and A. Khwaja. 2006. Go6976 is a potent inhibitor of the JAK 2 and FLT3 tyrosine kinases with significant activity in primary acute myeloid leukaemia cells. *Br J Haematol*. 135:303-316.

Graves, L.M., K.E. Bornfeldt, E.W. Raines, B.C. Potts, S.G. Macdonald, R. Ross, and E.G. Krebs. 1993. Protein kinase A antagonizes platelet-derived growth factor-induced signaling by mitogen-activated protein kinase in human arterial smooth muscle cells. *Proc Natl Acad Sci U S A*. 90:10300-10304.

Gray, D.W., and I. Marshall. 1992. Nitric oxide synthesis inhibitors attenuate calcitonin gene-related peptide endothelium-dependent vasorelaxation in rat aorta. *Eur J Pharmacol*. 212:37-42.

Gschwendt, M., S. Dieterich, J. Rennecke, W. Kittstein, H.J. Mueller, and F.J. Johannes. 1996. Inhibition of protein kinase C mu by various inhibitors. Differentiation from protein kinase c isoenzymes. *FEBS Lett*. 392:77-80.

Gschwind, A., S. Hart, O.M. Fischer, and A. Ullrich. 2003. TACE cleavage of proamphiregulin regulates GPCR-induced proliferation and motility of cancer cells. *EMBO J*. 22:2411-2421.

Guery, L., N. Benikhlef, T. Gautier, C. Paul, G. Jego, E. Dufour, A. Jacquel, R. Cally, B. Manoury, T. Vanden Berghe, P. Vandenabeele, N. Droin, and E. Solary. 2011. Fine-tuning nucleophosmin in macrophage differentiation and activation. *Blood*. 118:4694-4704.

Gullapalli, A., B.L. Wolfe, C.T. Griffin, T. Magnuson, and J. Trejo. 2006. An essential role for SNX1 in lysosomal sorting of protease-activated receptor-1: evidence for retromer-, Hrs-, and Tsg101-independent functions of sorting nexins. *Mol Biol Cell*. 17:1228-1238.

Guo, F.F., E. Kumahara, and D. Saffen. 2001. A CalDAG-GEFI/Rap1/B-Raf cassette couples M(1) muscarinic acetylcholine receptors to the activation of ERK1/2. *J Biol Chem*. 276:25568-25581.

Gupta, V.K. 2005. Recurrent syncope, hypotension, asthma, and migraine with aura: role of metoclopramide. *Headache*. 45:1413-1416.

Hafner, S., H.S. Adler, H. Mischak, P. Janosch, G. Heidecker, A. Wolfman, S. Pippig, M. Lohse, M. Ueffing, and W. Kolch. 1994. Mechanism of inhibition of Raf-1 by protein kinase A. *Mol Cell Biol*. 14:6696-6703.

Hamdy, R.C., and D.N. Daley. 2012. Oral calcitonin. *Int J Womens Health*. 4:471-479.

Hamm, H.E. 1998. The many faces of G protein signaling. *J Biol Chem*. 273:669-672.

Han, J., J.D. Lee, L. Bibbs, and R.J. Ulevitch. 1994. A MAP kinase targeted by endotoxin and hyperosmolarity in mammalian cells. *Science*. 265:808-811.

Han, N., D.Y. Zhang, T.B. Wang, P.X. Zhang, and B.G. Jiang. 2010. Calcitonin gene-related peptide induces proliferation and monocyte chemoattractant protein-1 expression via extracellular signal-regulated kinase activation in rat osteoblasts. *Chin Med J (Engl)*. 123:1748-1753.

Han, Z.Q., H.A. Coppock, D.M. Smith, S. Van Noorden, M.W. Makgoba, C.G. Nicholl, and S. Legon. 1997. The interaction of CGRP and adrenomedullin

with a receptor expressed in the rat pulmonary vascular endothelium. *J Mol Endocrinol*. 18:267-272.

Hanke, J.H., J.P. Gardner, R.L. Dow, P.S. Changelian, W.H. Brissette, E.J. Weringer, B.A. Pollok, and P.A. Connelly. 1996. Discovery of a novel, potent, and Src family-selective tyrosine kinase inhibitor. Study of Lck- and FynT-dependent T cell activation. *J Biol Chem*. 271:695-701.

Hanna, J., D.S. Leggett, and D. Finley. 2003. Ubiquitin depletion as a key mediator of toxicity by translational inhibitors. *Mol Cell Biol*. 23:9251-9261.

Hanson, P.I., R. Roth, Y. Lin, and J.E. Heuser. 2008. Plasma membrane deformation by circular arrays of ESCRT-III protein filaments. *J Cell Biol*. 180:389-402.

Hanyaloglu, A.C., and M. von Zastrow. 2008. Regulation of GPCRs by endocytic membrane trafficking and its potential implications. *Annu Rev Pharmacol Toxicol*. 48:537-568.

Harder, T., and K. Simons. 1997. Caveolae, DIGs, and the dynamics of sphingolipid-cholesterol microdomains. *Curr Opin Cell Biol*. 9:534-542.

Hardy, A.R., P.B. Conley, J. Luo, J.L. Benovic, A.W. Poole, and S.J. Mundell. 2005. P2Y1 and P2Y12 receptors for ADP desensitize by distinct kinase-dependent mechanisms. *Blood*. 105:3552-3560.

Harris, M.B., M.A. Blackstone, S.G. Sood, C. Li, J.M. Goolsby, V.J. Venema, B.E. Kemp, and R.C. Venema. 2004. Acute activation and phosphorylation of endothelial nitric oxide synthase by HMG-CoA reductase inhibitors. *Am J Physiol Heart Circ Physiol*. 287:H560-566.

Hasdemir, B., N.W. Bunnett, and G.S. Cottrell. 2007. Hepatocyte growth factor-regulated tyrosine kinase substrate (HRS) mediates post-endocytic trafficking of protease-activated receptor 2 and calcitonin receptor-like receptor. *J Biol Chem*. 282:29646-29657.

Hasdemir, B., J.E. Murphy, G.S. Cottrell, and N.W. Bunnett. 2009. Endosomal deubiquitinating enzymes control ubiquitination and down-regulation of protease-activated receptor 2. *J Biol Chem*. 284:28453-28466.

Hashimoto, H., S. Hyodo, M. Kawasaki, M. Shibata, T. Saito, H. Suzuki, H. Otsubo, T. Yokoyama, H. Fujihara, T. Higuchi, Y. Takei, and Y. Ueta. 2007. Adrenomedullin 2 (AM2)/intermedin is a more potent activator of hypothalamic oxytocin-secreting neurons than AM possibly through an unidentified receptor in rats. *Peptides*. 28:1104-1112.

Hauser, B., H. Bracht, M. Matejovic, P. Radermacher, and B. Venkatesh. 2005. Nitric oxide synthase inhibition in sepsis? Lessons learned from large-animal studies. *Anesth Analg*. 101:488-498.

Henley, J.R., E.W. Krueger, B.J. Oswald, and M.A. McNiven. 1998. Dynamin-mediated internalization of caveolae. *J Cell Biol*. 141:85-99.

Henry, A.G., I.J. White, M. Marsh, M. von Zastrow, and J.N. Hislop. 2011. The role of ubiquitination in lysosomal trafficking of delta-opioid receptors. *Traffic*. 12:170-184.

Hershenson, M.B., T.S. Chao, M.K. Abe, I. Gomes, M.D. Kelleher, J. Solway, and M.R. Rosner. 1995. Histamine antagonizes serotonin and growth factor-induced mitogen-activated protein kinase activation in bovine tracheal smooth muscle cells. *J Biol Chem*. 270:19908-19913.

Hershko, A., H. Heller, S. Elias, and A. Ciechanover. 1983. Components of ubiquitin-protein ligase system. Resolution, affinity purification, and role in protein breakdown. *J Biol Chem*. 258:8206-8214.

Heydorn, A., B.P. Sondergaard, B. Ersboll, B. Holst, F.C. Nielsen, C.R. Haft, J. Whistler, and T.W. Schwartz. 2004. A library of 7TM receptor C-terminal tails. Interactions with the proposed post-endocytic sorting proteins ERM-binding phosphoprotein 50 (EBP50), N-ethylmaleimide-sensitive factor (NSF), sorting nexin 1 (SNX1), and G protein-coupled receptor-associated sorting protein (GASP). *J Biol Chem*. 279:54291-54303.

Hibi, M., A. Lin, T. Smeal, A. Minden, and M. Karin. 1993. Identification of an oncoprotein- and UV-responsive protein kinase that binds and potentiates the c-Jun activation domain. *Genes Dev*. 7:2135-2148.

Hicke, L. 1999. Gettin' down with ubiquitin: turning off cell-surface receptors, transporters and channels. *Trends Cell Biol*. 9:107-112.

Hicke, L., and H. Riezman. 1996. Ubiquitination of a yeast plasma membrane receptor signals its ligand-stimulated endocytosis. *Cell*. 84:277-287.

Hilairet, S., C. Belanger, J. Bertrand, A. Laperriere, S.M. Foord, and M. Bouvier. 2001a. Agonist-promoted internalization of a ternary complex between calcitonin receptor-like receptor, receptor activity-modifying protein 1 (RAMP1), and beta-arrestin. *J Biol Chem*. 276:42182-42190.

Hilairet, S., S.M. Foord, F.H. Marshall, and M. Bouvier. 2001b. Protein-protein interaction and not glycosylation determines the binding selectivity of heterodimers between the calcitonin receptor-like receptor and the receptor activity-modifying proteins. *J Biol Chem*. 276:29575-29581.

Hillyard, C.J., C. Myers, G. Abeyasekera, J.C. Stevvensvenson, R.K. Craig, and I. MacIntyre. 1983. Katacalcin: a new plasma calcium-lowering hormone. *Lancet*. 1:846-848.

Hinshaw, J.E., and S.L. Schmid. 1995. Dynamin self-assembles into rings suggesting a mechanism for coated vesicle budding. *Nature*. 374:190-192.

Hinson, J.P., S. Kapas, and D.M. Smith. 2000. Adrenomedullin, a multifunctional regulatory peptide. *Endocr Rev*. 21:138-167.

Hippenstiel, S., M. Witzenrath, B. Schmeck, A. Hocke, M. Krisp, M. Krull, J. Seybold, W. Seeger, W. Rascher, H. Schutte, and N. Suttorp. 2002. Adrenomedullin reduces endothelial hyperpermeability. *Circ Res*. 91:618-625.

Hirata, Y., H. Hayakawa, Y. Suzuki, E. Suzuki, H. Ikenouchi, O. Kohmoto, K. Kimura, K. Kitamura, T. Eto, K. Kangawa, and et al. 1995. Mechanisms of adrenomedullin-induced vasodilation in the rat kidney. *Hypertension*. 25:790-795.

Hirata, Y., C. Mitaka, K. Sato, T. Nagura, Y. Tsunoda, K. Amaha, and F. Marumo. 1996. Increased circulating adrenomedullin, a novel vasodilatory peptide, in sepsis. *J Clin Endocrinol Metab*. 81:1449-1453.

Hirsch, P.F., G.F. Gauthier, and P.L. Munson. 1963. Thyroid Hypocalcemic Principle and Recurrent Laryngeal Nerve Injury as Factors Affecting the Response to Parathyroidectomy in Rats. *Endocrinology*. 73:244-252.

Hishinuma, S., H. Komazaki, H. Fukui, and M. Shoji. 2010. Ubiquitin/proteasome-dependent down-regulation following clathrin-mediated internalization of histamine H1-receptors in Chinese hamster ovary cells. *J Neurochem*. 113:990-1001.

Hislop, J.N., A.G. Henry, A. Marchese, and M. von Zastrow. 2009. Ubiquitination regulates proteolytic processing of G protein-coupled receptors after their sorting to lysosomes. *J Biol Chem*. 284:19361-19370.

Hislop, J.N., A. Marley, and M. Von Zastrow. 2004. Role of mammalian vacuolar protein-sorting proteins in endocytic trafficking of a non-ubiquitinated G protein-coupled receptor to lysosomes. *J Biol Chem*. 279:22522-22531.

Ho, S.N., H.D. Hunt, R.M. Horton, J.K. Pullen, and L.R. Pease. 1989. Site-directed mutagenesis by overlap extension using the polymerase chain reaction. *Gene*. 77:51-59.

Ho, T.W. 2009. Clinical profile of the novel oral CGRP receptor antagonist telcagepant for the acute treatment of migraine in phase 3 studies. *Journal of the Neurological Sciences*. 285:S149-S150.

Ho, T.W., M.D. Ferrari, D.W. Dodick, V. Galet, J. Kost, X. Fan, H. Leibensperger, S. Froman, C. Assaid, C. Lines, H. Koppen, and P.K. Winner. 2008a. Efficacy and tolerability of MK-0974 (telcagepant), a new oral antagonist of calcitonin gene-related peptide receptor, compared with zolmitriptan for acute migraine: a randomised, placebo-controlled, parallel-treatment trial. *Lancet*. 372:2115-2123.

Ho, T.W., L.K. Mannix, X. Fan, C. Assaid, C. Furtek, C.J. Jones, C.R. Lines, and A.M. Rapoport. 2008b. Randomized controlled trial of an oral CGRP receptor antagonist, MK-0974, in acute treatment of migraine. *Neurology*. 70:1304-1312.

Hocke, A.C., B. Temmesfeld-Wollbrueck, B. Schmeck, K. Berger, E.M. Frisch, M. Witzenrath, B. Brell, N. Suttorp, and S. Hippenstiel. 2006. Perturbation of endothelial junction proteins by Staphylococcus aureus alpha-toxin: inhibition of endothelial gap formation by adrenomedullin. *Histochem Cell Biol*. 126:305-316.

Hofmann, K., and L. Falquet. 2001. A ubiquitin-interacting motif conserved in components of the proteasomal and lysosomal protein degradation systems. *Trends Biochem Sci*. 26:347-350.

Hong, Y., D.L. Hay, R. Quirion, and D.R. Poyner. 2012. The pharmacology of adrenomedullin 2/intermedin. *Br J Pharmacol*. 166:110-120.

Hooper, N.M. 1993. Determination of Mammalian Membrane Protein Anchorage: Glycosyl-phosphatidylinositol (G-PI) or Transmembrane Polypeptide Anchor. *Biochemical Eduction*. 21:212-216.

Hoppener, J.W., P.H. Steenbergh, J. Zandberg, E. Bakker, P.L. Pearson, A.H. Geurts van Kessel, H.S. Jansz, and C.J. Lips. 1984. Localization of the polymorphic human calcitonin gene on chromosome 11. *Hum Genet*. 66:309-312.

Howard, T.L., D.R. Stauffer, C.R. Degnin, and S.M. Hollenberg. 2001. CHMP1 functions as a member of a newly defined family of vesicle trafficking proteins. *J Cell Sci*. 114:2395-2404.

Hsieh, J.T., and J.M. Farley. 2002. Characterization of contractile function and expression of muscarinic receptors, G proteins and adenylate cyclase in cultured tracheal smooth muscle of Swine. *J Biomed Sci*. 9:339-347.

Innamorati, G., H.M. Sadeghi, N.T. Tran, and M. Birnbaumer. 1998. A serine cluster prevents recycling of the V2 vasopressin receptor. *Proc Natl Acad Sci U S A*. 95:2222-2226.

Inoue, H., H. Nojima, and H. Okayama. 1990. High efficiency transformation of Escherichia coli with plasmids. *Gene*. 96:23-28.

Ishimitsu, T., M. Kojima, K. Kangawa, J. Hino, H. Matsuoka, K. Kitamura, T. Eto, and H. Matsuo. 1994. Genomic structure of human adrenomedullin gene. *Biochem Biophys Res Commun*. 203:631-639.

Iversen, H.K., and J. Olesen. 1996. Headache induced by a nitric oxide donor (nitroglycerin) responds to sumatriptan. A human model for development of migraine drugs. *Cephalalgia*. 16:412-418.

Jacob, C., G.S. Cottrell, D. Gehringer, F. Schmidlin, E.F. Grady, and N.W. Bunnett. 2005. c-Cbl mediates ubiquitination, degradation, and down-regulation of human protease-activated receptor 2. *J Biol Chem*. 280:16076-16087.

Jafri, F., H.M. El-Shewy, M.H. Lee, M. Kelly, D.K. Luttrell, and L.M. Luttrell. 2006. Constitutive ERK1/2 activation by a chimeric neurokinin 1 receptor-beta-arrestin1 fusion protein. Probing the composition and function of the G protein-coupled receptor "signalsome". *The Journal of biological chemistry*. 281:19346-19357.

Jaspard, E., L. Wei, and F. Alhenc-Gelas. 1993. Differences in the properties and enzymatic specificities of the two active sites of angiotensin I-converting enzyme (kininase II). Studies with bradykinin and other natural peptides. *J Biol Chem*. 268:9496-9503.

Johnson, G.D., T. Stevenson, and K. Ahn. 1999. Hydrolysis of peptide hormones by endothelin-converting enzyme-1. A comparison with neprilysin. *J Biol Chem*. 274:4053-4058.

Jonderko, G., T. Golab, and K. Jonderko. 1988. Effect of calcitonin on gastric emptying. *Digestion*. 40:191-196.

Jones, M.C. 2007. Therapies for diabetes: pramlintide and exenatide. *Am Fam Physician*. 75:1831-1835.

Kano, H., M. Kohno, K. Yasunari, K. Yokokawa, T. Horio, M. Ikeda, M. Minami, T. Hanehira, T. Takeda, and J. Yoshikawa. 1996. Adrenomedullin as a novel antiproliferative factor of vascular smooth muscle cells. *Journal of hypertension*. 14:209-213.

Katoh, K., H. Shibata, H. Suzuki, A. Nara, K. Ishidoh, E. Kominami, T. Yoshimori, and M. Maki. 2003. The ALG-2-interacting protein Alix associates with CHMP4b, a human homologue of yeast Snf7 that is involved in multivesicular body sorting. *J Biol Chem*. 278:39104-39113.

Katz, A., D. Wu, and M.I. Simon. 1992. Subunits beta gamma of heterotrimeric G protein activate beta 2 isoform of phospholipase C. *Nature*. 360:686-689.

Kawanami, Y., Y. Morimoto, H. Kim, T. Nakamura, K. Machida, T. Kido, E. Asonuma, K. Yatera, C. Yoshii, and M. Kido. 2009. Calcitonin gene-related peptide stimulates proliferation of alveolar epithelial cells. *Respir Res*. 10:8.

Kawase, T., K. Okuda, C.H. Wu, H. Yoshie, K. Hara, and D.M. Burns. 1999. Calcitonin gene-related peptide acts as a mitogen for human Gin-1 gingival fibroblasts by activating the MAP kinase signalling pathway. *J Periodontal Res*. 34:160-168.

Keen, J.H., M.C. Willingham, and I.H. Pastan. 1979. Clathrin-coated vesicles: isolation, dissociation and factor-dependent reassociation of clathrin baskets. *Cell*. 16:303-312.

Kennedy, M.B. 1995. Origin of PDZ (DHR, GLGF) domains. *Trends Biochem Sci*. 20:350.

Kim, W., S.O. Moon, M.J. Sung, S.H. Kim, S. Lee, J.N. So, and S.K. Park. 2003. Angiogenic role of adrenomedullin through activation of Akt, mitogen-activated protein kinase, and focal adhesion kinase in endothelial cells. *FASEB J*. 17:1937-1939.

Kim, Y.G., A.M. Lone, W.M. Nolte, and A. Saghatelian. 2012. Peptidomics approach to elucidate the proteolytic regulation of bioactive peptides. *Proc Natl Acad Sci U S A*. 109:8523-8527.

Kim, Y.M., and J.L. Benovic. 2002. Differential roles of arrestin-2 interaction with clathrin and adaptor protein 2 in G protein-coupled receptor trafficking. *J Biol Chem*. 277:30760-30768.

Kis, B., M.A. Deli, H. Kobayashi, C.S. Abraham, T. Yanagita, H. Kaiya, T. Isse, R. Nishi, S. Gotoh, K. Kangawa, A. Wada, J. Greenwood, M. Niwa, H. Yamashita, and Y. Ueta. 2001. Adrenomedullin regulates blood-brain barrier functions in vitro. *Neuroreport*. 12:4139-4142.

Kisselev, A.F., and A.L. Goldberg. 2001. Proteasome inhibitors: from research tools to drug candidates. *Chem Biol*. 8:739-758.

Kitamura, K., Y. Ichiki, M. Tanaka, M. Kawamoto, J. Emura, S. Sakakibara, K. Kangawa, H. Matsuo, and T. Eto. 1994. Immunoreactive adrenomedullin in human plasma. *FEBS Lett*. 341:288-290.

Kitamura, K., K. Kangawa, M. Kawamoto, Y. Ichiki, S. Nakamura, H. Matsuo, and T. Eto. 1993a. Adrenomedullin: a novel hypotensive peptide isolated from human pheochromocytoma. *Biochem Biophys Res Commun*. 192:553-560.

Kitamura, K., J. Sakata, K. Kangawa, M. Kojima, H. Matsuo, and T. Eto. 1993b. Cloning and characterization of cDNA encoding a precursor for human adrenomedullin. *Biochem Biophys Res Commun*. 194:720-725.

Kjeldgaard, M., J. Nyborg, and B.F. Clark. 1996. The GTP binding motif: variations on a theme. *FASEB J*. 10:1347-1368.

Kohno, T., E. Matsuda, H. Sasaki, and T. Sasaki. 2008. Protein-tyrosine kinase CAKbeta/PYK2 is activated by binding Ca2+/calmodulin to FERM F2 alpha2 helix and thus forming its dimer. *Biochem J*. 410:513-523.

Kolch, W., G. Heidecker, G. Kochs, R. Hummel, H. Vahidi, H. Mischak, G. Finkenzeller, D. Marme, and U.R. Rapp. 1993. Protein kinase C alpha activates RAF-1 by direct phosphorylation. *Nature*. 364:249-252.

Kolterman, O.G., A. Gottlieb, C. Moyses, and W. Colburn. 1995. Reduction of postprandial hyperglycemia in subjects with IDDM by intravenous infusion of AC137, a human amylin analogue. *Diabetes Care*. 18:1179-1182.

Kong, M.F., P. King, I.A. Macdonald, T.A. Stubbs, A.C. Perkins, P.E. Blackshaw, C. Moyses, and R.B. Tattersall. 1997. Infusion of pramlintide, a human amylin analogue, delays gastric emptying in men with IDDM. *Diabetologia*. 40:82-88.

Kraenzlin, M.E., J.L. Ch'ng, P.K. Mulderry, M.A. Ghatei, and S.R. Bloom. 1985. Infusion of a novel peptide, calcitonin gene-related peptide (CGRP) in man. Pharmacokinetics and effects on gastric acid secretion and on gastrointestinal hormones. *Regul Pept*. 10:189-197.

Krahn, D.D., B.A. Gosnell, A.S. Levine, and J.E. Morley. 1984. Effects of calcitonin gene-related peptide on food intake. *Peptides*. 5:861-864.

Krens, S.F., M. Corredor-Adamez, S. He, B.E. Snaar-Jagalska, and H.P. Spaink. 2008. ERK1 and ERK2 MAPK are key regulators of distinct gene sets in zebrafish embryogenesis. *BMC Genomics*. 9:196.

Kristiansen, K. 2004. Molecular mechanisms of ligand binding, signaling, and regulation within the superfamily of G-protein-coupled receptors: molecular modeling and mutagenesis approaches to receptor structure and function. *Pharmacol Ther*. 103:21-80.

Krueger, K.M., Y. Daaka, J.A. Pitcher, and R.J. Lefkowitz. 1997. The role of sequestration in G protein-coupled receptor resensitization. Regulation of beta2-adrenergic receptor dephosphorylation by vesicular acidification. *J Biol Chem*. 272:5-8.

Kuhn, H. 1978. Light-regulated binding of rhodopsin kinase and other proteins to cattle photoreceptor membranes. *Biochemistry*. 17:4389-4395.

Kurten, R.C., D.L. Cadena, and G.N. Gill. 1996. Enhanced degradation of EGF receptors by a sorting nexin, SNX1. *Science*. 272:1008-1010.

Kuwasako, K., Y. Shimekake, M. Masuda, K. Nakahara, T. Yoshida, M. Kitaura, K. Kitamura, T. Eto, and T. Sakata. 2000. Visualization of the calcitonin receptor-like receptor and its receptor activity-modifying proteins during internalization and recycling. *J Biol Chem*. 275:29602-29609.

Kyriakis, J.M., P. Banerjee, E. Nikolakaki, T. Dai, E.A. Rubie, M.F. Ahmad, J. Avruch, and J.R. Woodgett. 1994. The stress-activated protein kinase subfamily of c-Jun kinases. *Nature*. 369:156-160.

Lang, M.G., R. Paterno, F.M. Faraci, and D.D. Heistad. 1997. Mechanisms of adrenomedullin-induced dilatation of cerebral arterioles. *Stroke*. 28:181-185.

Laporte, S.A., R.H. Oakley, J. Zhang, J.A. Holt, S.S. Ferguson, M.G. Caron, and L.S. Barak. 1999. The beta2-adrenergic receptor/betaarrestin complex recruits the clathrin adaptor AP-2 during endocytosis. *Proc Natl Acad Sci U S A*. 96:3712-3717.

Laroche-Joubert, N., S. Marsy, S. Michelet, M. Imbert-Teboul, and A. Doucet. 2002. Protein kinase A-independent activation of ERK and H,K-ATPase by cAMP in native kidney cells: role of Epac I. *J Biol Chem*. 277:18598-18604.

Lee, J.C., J.T. Laydon, P.C. McDonnell, T.F. Gallagher, S. Kumar, D. Green, D. McNulty, M.J. Blumenthal, J.R. Heys, S.W. Landvatter, and et al. 1994. A protein kinase involved in the regulation of inflammatory cytokine biosynthesis. *Nature*. 372:739-746.

Lee, T.H., and A.D. Linstedt. 2000. Potential role for protein kinases in regulation of bidirectional endoplasmic reticulum-to-Golgi transport revealed by protein kinase inhibitor H89. *Mol Biol Cell*. 11:2577-2590.

Lee, Y.H., and P.J. Sinko. 2000. Oral delivery of salmon calcitonin. *Adv Drug Deliv Rev*. 42:225-238.

Lefkowitz, R.J., and S.K. Shenoy. 2005. Transduction of receptor signals by beta-arrestins. *Science*. 308:512-517.

Lev, S., H. Moreno, R. Martinez, P. Canoll, E. Peles, J.M. Musacchio, G.D. Plowman, B. Rudy, and J. Schlessinger. 1995. Protein tyrosine kinase PYK2 involved in Ca(2+)-induced regulation of ion channel and MAP kinase functions. *Nature*. 376:737-745.

Levine, A.S., and J.E. Morley. 1981. Reduction of feeding in rats by calcitonin. *Brain Res*. 222:187-191.

Li, J.G., J.L. Benovic, and L.Y. Liu-Chen. 2000. Mechanisms of agonist-induced down-regulation of the human kappa-opioid receptor: internalization is required for down-regulation. *Molecular pharmacology*. 58:795-801.

Li, S., R. Seitz, and M.P. Lisanti. 1996. Phosphorylation of caveolin by src tyrosine kinases. The alpha-isoform of caveolin is selectively phosphorylated by v-Src in vivo. *J Biol Chem*. 271:3863-3868.

Lin, H.Y., T.L. Harris, M.S. Flannery, A. Aruffo, E.H. Kaji, A. Gorn, L.F. Kolakowski, Jr., M. Yamin, H.F. Lodish, and S.R. Goldring. 1991. Expression cloning and characterization of a porcine renal calcitonin receptor. *Trans Assoc Am Physicians*. 104:265-272.

Linseman, D.A., C.W. Benjamin, and D.A. Jones. 1995. Convergence of angiotensin II and platelet-derived growth factor receptor signaling cascades in vascular smooth muscle cells. *J Biol Chem*. 270:12563-12568.

Lloyd, T.E., R. Atkinson, M.N. Wu, Y. Zhou, G. Pennetta, and H.J. Bellen. 2002. Hrs regulates endosome membrane invagination and tyrosine kinase receptor signaling in Drosophila. *Cell*. 108:261-269.

Lochner, A., and J.A. Moolman. 2006. The many faces of H89: a review. *Cardiovasc Drug Rev*. 24:261-274.

Lohse, M.J., J.L. Benovic, J. Codina, M.G. Caron, and R.J. Lefkowitz. 1990. beta-Arrestin: a protein that regulates beta-adrenergic receptor function. *Science*. 248:1547-1550.

Longva, K.E., F.D. Blystad, E. Stang, A.M. Larsen, L.E. Johannessen, and I.H. Madshus. 2002. Ubiquitination and proteasomal activity is required for transport of the EGF receptor to inner membranes of multivesicular bodies. *J Cell Biol*. 156:843-854.

Lorenz, K., M.J. Lohse, and U. Quitterer. 2003. Protein kinase C switches the Raf kinase inhibitor from Raf-1 to GRK-2. *Nature*. 426:574-579.

Lorenzo, A., B. Razzaboni, G.C. Weir, and B.A. Yankner. 1994. Pancreatic islet cell toxicity of amylin associated with type-2 diabetes mellitus. *Nature*. 368:756-760.

Lu, Q., L.W. Hope, M. Brasch, C. Reinhard, and S.N. Cohen. 2003. TSG101 interaction with HRS mediates endosomal trafficking and receptor down-regulation. *Proc Natl Acad Sci U S A*. 100:7626-7631.

Luebke, A.E., G.P. Dahl, B.A. Roos, and I.M. Dickerson. 1996. Identification of a protein that confers calcitonin gene-related peptide responsiveness to oocytes by using a cystic fibrosis transmembrane conductance regulator assay. *Proc Natl Acad Sci U S A*. 93:3455-3460.

Luo, G., L. Chen, C.M. Conway, R. Denton, D. Keavy, L. Signor, W. Kostich, K.A. Lentz, K.S. Santone, R. Schartman, M. Browning, G. Tong, J.G. Houston, G.M. Dubowchik, and J.E. Macor. 2012a. Discovery of (5S,6S,9R)-5-amino-6-(2,3-difluorophenyl)-6,7,8,9-tetrahydro-5H-cyclohepta[b]pyri din-9-yl 4-(2-oxo-2,3-dihydro-1H-imidazo[4,5-b]pyridin-1-yl)piperidine-1-carboxylate (BMS-927711): an oral calcitonin gene-related peptide (CGRP) antagonist in clinical trials for treating migraine. *Journal of medicinal chemistry*. 55:10644-10651.

Luo, G.L., L. Chen, C.M. Conway, R. Denton, D. Keavy, M. Gulianello, Y. Huang, W. Kostich, K.A. Lentz, S.E. Mercer, R. Schartman, L. Signor, M. Browning, J.E. Macor, and G.M. Dubowchik. 2012b. Discovery of BMS-846372, a

Potent and Orally Active Human CGRP Receptor Antagonist for the Treatment of Migraine. *Acs Med Chem Lett*. 3:337-341.

Luttrell, L.M. 2003. 'Location, location, location': activation and targeting of MAP kinases by G protein-coupled receptors. *J Mol Endocrinol*. 30:117-126.

Luttrell, L.M., S.S. Ferguson, Y. Daaka, W.E. Miller, S. Maudsley, G.J. Della Rocca, F. Lin, H. Kawakatsu, K. Owada, D.K. Luttrell, M.G. Caron, and R.J. Lefkowitz. 1999. Beta-arrestin-dependent formation of beta2 adrenergic receptor-Src protein kinase complexes. *Science*. 283:655-661.

Luttrell, L.M., and D. Gesty-Palmer. 2010. Beyond desensitization: physiological relevance of arrestin-dependent signaling. *Pharmacol Rev*. 62:305-330.

Luttrell, L.M., F.L. Roudabush, E.W. Choy, W.E. Miller, M.E. Field, K.L. Pierce, and R.J. Lefkowitz. 2001. Activation and targeting of extracellular signal-regulated kinases by beta-arrestin scaffolds. *Proc Natl Acad Sci U S A*. 98:2449-2454.

Lutz, T.A., E. Del Prete, and E. Scharrer. 1994. Reduction of food intake in rats by intraperitoneal injection of low doses of amylin. *Physiol Behav*. 55:891-895.

Lynch, B., and E.T. Kaiser. 1988. Biological properties of two models of calcitonin gene related peptide with idealized amphiphilic alpha-helices of different lengths. *Biochemistry*. 27:7600-7607.

Ma, W., J.G. Chabot, K.J. Powell, K. Jhamandas, I.M. Dickerson, and R. Quirion. 2003. Localization and modulation of calcitonin gene-related peptide-receptor component protein-immunoreactive cells in the rat central and peripheral nervous systems. *Neuroscience*. 120:677-694.

Maggi, C.A. 1995. Tachykinins and calcitonin gene-related peptide (CGRP) as co-transmitters released from peripheral endings of sensory nerves. *Prog Neurobiol*. 45:1-98.

Main, M.J., J. Brown, S. Brown, N.J. Fraser, and S.M. Foord. 1998. The CGRP receptor can couple via pertussis toxin sensitive and insensitive G proteins. *FEBS Lett*. 441:6-10.

Majima, M., M. Toda, Y. Ito, T. Ohno, T. Mishima, T. Suzuki, K. Hosono, and I. Hayashi. 2011. Roles of calcitonin gene-related peptide in ehancement of angiogenesis. *Inflammation and Regeneration*. 23:146-150.

Marchese, A., and J.L. Benovic. 2001. Agonist-promoted ubiquitination of the G protein-coupled receptor CXCR4 mediates lysosomal sorting. *J Biol Chem*. 276:45509-45512.

Marchese, A., M.M. Paing, B.R. Temple, and J. Trejo. 2008. G protein-coupled receptor sorting to endosomes and lysosomes. *Annu Rev Pharmacol Toxicol*. 48:601-629.

Marchese, A., C. Raiborg, F. Santini, J.H. Keen, H. Stenmark, and J.L. Benovic. 2003. The E3 ubiquitin ligase AIP4 mediates ubiquitination and sorting of the G protein-coupled receptor CXCR4. *Dev Cell*. 5:709-722.

Marmor, M.D., and Y. Yarden. 2004. Role of protein ubiquitylation in regulating endocytosis of receptor tyrosine kinases. *Oncogene*. 23:2057-2070.

Martinez, A., C. Weaver, J. Lopez, S.J. Bhathena, T.H. Elsasser, M.J. Miller, T.W. Moody, E.J. Unsworth, and F. Cuttitta. 1996. Regulation of insulin secretion and blood glucose metabolism by adrenomedullin. *Endocrinology*. 137:2626-2632.

Martinez, V., F. Cuttitta, and Y. Tache. 1997. Central action of adrenomedullin to inhibit gastric emptying in rats. *Endocrinology*. 138:3749-3755.

Martiny-Baron, G., M.G. Kazanietz, H. Mischak, P.M. Blumberg, G. Kochs, H. Hug, D. Marme, and C. Schachtele. 1993. Selective inhibition of protein kinase C isozymes by the indolocarbazole Go 6976. *J Biol Chem*. 268:9194-9197.

Mastick, C.C., M.J. Brady, and A.R. Saltiel. 1995. Insulin stimulates the tyrosine phosphorylation of caveolin. *J Cell Biol*. 129:1523-1531.

Maudsley, S., K.L. Pierce, A.M. Zamah, W.E. Miller, S. Ahn, Y. Daaka, R.J. Lefkowitz, and L.M. Luttrell. 2000. The beta(2)-adrenergic receptor mediates extracellular signal-regulated kinase activation via assembly of a multi-receptor complex with the epidermal growth factor receptor. *J Biol Chem*. 275:9572-9580.

Mayle, K.M., A.M. Le, and D.T. Kamei. 2012. The intracellular trafficking pathway of transferrin. *Biochim Biophys Acta*. 1820:264-281.

McCole, D.F., S.J. Keely, R.J. Coffey, and K.E. Barrett. 2002. Transactivation of the epidermal growth factor receptor in colonic epithelial cells by carbachol requires extracellular release of transforming growth factor-alpha. *J Biol Chem*. 277:42603-42612.

McDonald, P.H., C.W. Chow, W.E. Miller, S.A. Laporte, M.E. Field, F.T. Lin, R.J. Davis, and R.J. Lefkowitz. 2000. Beta-arrestin 2: a receptor-regulated MAPK scaffold for the activation of JNK3. *Science*. 290:1574-1577.

McGarrigle, D., and X.Y. Huang. 2007. GPCRs Signaling Directly Through Src-Family Kinases. *Sci STKE*. 2007:pe35.

McLatchie, L.M., N.J. Fraser, M.J. Main, A. Wise, J. Brown, N. Thompson, R. Solari, M.G. Lee, and S.M. Foord. 1998. RAMPs regulate the transport and ligand specificity of the calcitonin-receptor-like receptor. *Nature*. 393:333-339.

McMillan, P.J., W.M. Hooker, and L.J. Deptos. 1974. Distribution of calcitonin-containing cells in the human thyroid. *Am J Anat*. 140:73-79.

Melikova, M.S., K.A. Kondratov, and E.S. Kornilova. 2006. Two different stages of epidermal growth factor (EGF) receptor endocytosis are sensitive to free ubiquitin depletion produced by proteasome inhibitor MG132. *Cell Biol Int*. 30:31-43.

Mellman, I. 1996. Endocytosis and molecular sorting. *Annu Rev Cell Dev Biol*. 12:575-625.

Meng, L., R. Mohan, B.H. Kwok, M. Elofsson, N. Sin, and C.M. Crews. 1999. Epoxomicin, a potent and selective proteasome inhibitor, exhibits in vivo antiinflammatory activity. *Proc Natl Acad Sci U S A*. 96:10403-10408.

Meresse, S., J.P. Gorvel, and P. Chavrier. 1995. The rab7 GTPase resides on a vesicular compartment connected to lysosomes. *Journal of cell science*. 108 (Pt 11):3349-3358.

Meyer, J.S., and W. Abdel-Bari. 1968. Granules and thyrocalcitonin-like activity in medullary carcinoma of the thyroid gland. *N Engl J Med*. 278:523-529.

Miller, J.L., and E.A. Dratz. 1984. Phosphorylation at sites near rhodopsin's carboxyl-terminus regulates light initiated cGMP hydrolysis. *Vision research*. 24:1509-1521.

Miret, J.J., L. Rakhilina, L. Silverman, and B. Oehlen. 2002. Functional expression of heteromeric calcitonin gene-related peptide and adrenomedullin receptors in yeast. *J Biol Chem*. 277:6881-6887.

Mischak, H., T. Seitz, P. Janosch, M. Eulitz, H. Steen, M. Schellerer, A. Philipp, and W. Kolch. 1996. Negative regulation of Raf-1 by phosphorylation of serine 621. *Mol Cell Biol*. 16:5409-5418.

Mittra, S., and J.P. Bourreau. 2006. Gs and Gi coupling of adrenomedullin in adult rat ventricular myocytes. *Am J Physiol Heart Circ Physiol*. 290:H1842-1847.

Moore, C.X., and G.J. Cooper. 1991. Co-secretion of amylin and insulin from cultured islet beta-cells: modulation by nutrient secretagogues, islet hormones and hypoglycemic agents. *Biochem Biophys Res Commun*. 179:1-9.

Morales, C.R., Q. Zhao, and S. Lefrancois. 1999. Biogenesis of lysosomes by endocytic flow of plasma membrane. *Biocell*. 23:149-160.

Morley, J.E., J.F. Flood, M. Horowitz, P.M. Morley, and M.J. Walter. 1994. Modulation of food intake by peripherally administered amylin. *Am J Physiol*. 267:R178-184.

Muff, R., N. Buhlmann, J.A. Fischer, and W. Born. 1999. An amylin receptor is revealed following co-transfection of a calcitonin receptor with receptor activity modifying proteins-1 or -3. *Endocrinology*. 140:2924-2927.

Mundell, S.J., J. Luo, J.L. Benovic, P.B. Conley, and A.W. Poole. 2006. Distinct clathrin-coated pits sort different G protein-coupled receptor cargo. *Traffic*. 7:1420-1431.

Murasawa, S., Y. Mori, Y. Nozawa, H. Masaki, K. Maruyama, Y. Tsutsumi, Y. Moriguchi, Y. Shibasaki, Y. Tanaka, T. Iwasaka, M. Inada, and H. Matsubara. 1998. Role of calcium-sensitive tyrosine kinase Pyk2/CAKbeta/RAFTK in angiotensin II induced Ras/ERK signaling. *Hypertension*. 32:668-675.

Murphy, J.E., B.E. Padilla, B. Hasdemir, G.S. Cottrell, and N.W. Bunnett. 2009. Endosomes: a legitimate platform for the signaling train. *Proc Natl Acad Sci U S A*. 106:17615-17622.

Murphy, S., S. Martin, and R.G. Parton. 2010. Quantitative analysis of lipid droplet fusion: inefficient steady state fusion but rapid stimulation by chemical fusogens. *PLoS One*. 5:e15030.

Murphy, T.C., and W.K. Samson. 1995. The novel vasoactive hormone, adrenomedullin, inhibits water drinking in the rat. *Endocrinology*. 136:2459-2463.

Nagai, K., H. Ino, H. Yamamoto, H. Nakagawa, M. Yamano, M. Tohyama, S. Shiosaka, Y. Shiotani, S. Inagaki, and S. Kitoh. 1987. Lesions in the Lateral Part of the Dorsal Parabrachial Nucleus Caused Hyperphagia and Obesity. *J Clin Biochem Nutr*. 3:103-112.

Naghashpour, M., M.I. Rosenblatt, I.M. Dickerson, and G.P. Dahl. 1997. Inhibitory effect of calcitonin gene-related peptide on myometrial contractility is diminished at parturition. *Endocrinology*. 138:4207-4214.

Nakamura, K.D., R. Martinez, and M.J. Weber. 1983. Tyrosine phosphorylation of specific proteins after mitogen stimulation of chicken embryo fibroblasts. *Mol Cell Biol*. 3:380-390.

Nathan, C., and Q.W. Xie. 1994. Regulation of biosynthesis of nitric oxide. *J Biol Chem*. 269:13725-13728.

Nekrasova, T., C. Shive, Y. Gao, K. Kawamura, R. Guardia, G. Landreth, and T.G. Forsthuber. 2005. ERK1-deficient mice show normal T cell effector function

and are highly susceptible to experimental autoimmune encephalomyelitis. *J Immunol*. 175:2374-2380.

Nelson, M.T., Y. Huang, J.E. Brayden, J. Hescheler, and N.B. Standen. 1990. Arterial dilations in response to calcitonin gene-related peptide involve activation of K+ channels. *Nature*. 344:770-773.

Neuhauser, H., and T. Lempert. 2004. Vertigo and dizziness related to migraine: a diagnostic challenge. *Cephalalgia*. 24:83-91.

Nijman, S.M., M.P. Luna-Vargas, A. Velds, T.R. Brummelkamp, A.M. Dirac, T.K. Sixma, and R. Bernards. 2005. A genomic and functional inventory of deubiquitinating enzymes. *Cell*. 123:773-786.

Nikitenko, L.L., N. Blucher, S.B. Fox, R. Bicknell, D.M. Smith, and M.C. Rees. 2006. Adrenomedullin and CGRP interact with endogenous calcitonin-receptor-like receptor in endothelial cells and induce its desensitisation by different mechanisms. *J Cell Sci*. 119:910-922.

Nishimatsu, H., E. Suzuki, D. Nagata, N. Moriyama, H. Satonaka, K. Walsh, M. Sata, K. Kangawa, H. Matsuo, A. Goto, T. Kitamura, and Y. Hirata. 2001. Adrenomedullin induces endothelium-dependent vasorelaxation via the phosphatidylinositol 3-kinase/Akt-dependent pathway in rat aorta. *Circ Res*. 89:63-70.

Niu, P., T. Shindo, H. Iwata, S. Iimuro, N. Takeda, Y. Zhang, A. Ebihara, Y. Suematsu, K. Kangawa, Y. Hirata, and R. Nagai. 2004. Protective effects of endogenous adrenomedullin on cardiac hypertrophy, fibrosis, and renal damage. *Circulation*. 109:1789-1794.

Njuki, F., C.G. Nicholl, A. Howard, J.C. Mak, P.J. Barnes, S.I. Girgis, and S. Legon. 1993. A new calcitonin-receptor-like sequence in rat pulmonary blood vessels. *Clin Sci (Lond)*. 85:385-388.

Noma, T., A. Lemaire, S.V. Naga Prasad, L. Barki-Harrington, D.G. Tilley, J. Chen, P. Le Corvoisier, J.D. Violin, H. Wei, R.J. Lefkowitz, and H.A. Rockman. 2007. Beta-arrestin-mediated beta1-adrenergic receptor transactivation of the EGFR confers cardioprotection. *J Clin Invest*. 117:2445-2458.

Nomura, R., and T. Fujimoto. 1999. Tyrosine-phosphorylated caveolin-1: immunolocalization and molecular characterization. *Mol Biol Cell*. 10:975-986.

Numaga, T., M. Nishida, S. Kiyonaka, K. Kato, M. Katano, E. Mori, T. Kurosaki, R. Inoue, M. Hikida, J.W. Putney, and Y. Mori. 2010. Ca2+ influx and protein scaffolding via TRPC3 sustain PKC beta and ERK activation in B cells. *Journal of Cell Science*. 123:927-938.

Nystedt, S., K. Emilsson, C. Wahlestedt, and J. Sundelin. 1994. Molecular cloning of a potential proteinase activated receptor. *Proc Natl Acad Sci U S A*. 91:9208-9212.

O'Gorman, S., D.T. Fox, and G.M. Wahl. 1991. Recombinase-mediated gene activation and site-specific integration in mammalian cells. *Science*. 251:1351-1355.

Oakley, R.H., S.A. Laporte, J.A. Holt, L.S. Barak, and M.G. Caron. 1999. Association of beta-arrestin with G protein-coupled receptors during clathrin-mediated endocytosis dictates the profile of receptor resensitization. *J Biol Chem*. 274:32248-32257.

Oakley, R.H., S.A. Laporte, J.A. Holt, L.S. Barak, and M.G. Caron. 2001. Molecular determinants underlying the formation of stable intracellular G

protein-coupled receptor-beta-arrestin complexes after receptor endocytosis*. *J Biol Chem*. 276:19452-19460.

Oakley, R.H., S.A. Laporte, J.A. Holt, M.G. Caron, and L.S. Barak. 2000. Differential affinities of visual arrestin, beta arrestin1, and beta arrestin2 for G protein-coupled receptors delineate two major classes of receptors. *J Biol Chem*. 275:17201-17210.

Obara, Y., K. Labudda, T.J. Dillon, and P.J. Stork. 2004. PKA phosphorylation of Src mediates Rap1 activation in NGF and cAMP signaling in PC12 cells. *J Cell Sci*. 117:6085-6094.

Obrig, T.G., W.J. Culp, W.L. McKeehan, and B. Hardesty. 1971. The mechanism by which cycloheximide and related glutarimide antibiotics inhibit peptide synthesis on reticulocyte ribosomes. *J Biol Chem*. 246:174-181.

Ogawa, Y., Y. Takai, Y. Kawahara, S. Kimura, and Y. Nishizuka. 1981. A new possible regulatory system for protein phosphorylation in human peripheral lymphocytes. I. Characterization of a calcium-activated, phospholipid-dependent protein kinase. *J Immunol*. 127:1369-1374.

Oh, P., D.P. McIntosh, and J.E. Schnitzer. 1998. Dynamin at the neck of caveolae mediates their budding to form transport vesicles by GTP-driven fission from the plasma membrane of endothelium. *J Cell Biol*. 141:101-114.

Ohno, H., J. Stewart, M.C. Fournier, H. Bosshart, I. Rhee, S. Miyatake, T. Saito, A. Gallusser, T. Kirchhausen, and J.S. Bonifacino. 1995. Interaction of tyrosine-based sorting signals with clathrin-associated proteins. *Science*. 269:1872-1875.

Ohtsu, H., P.J. Dempsey, and S. Eguchi. 2006. ADAMs as mediators of EGF receptor transactivation by G protein-coupled receptors. *Am J Physiol Cell Physiol*. 291:C1-10.

Okamoto, H., O. Ito, R.J. Roman, and A.G. Hudetz. 1998. Role of inducible nitric oxide synthase and cyclooxygenase-2 in endotoxin-induced cerebral hyperemia. *Stroke*. 29:1209-1218.

Oksvold, M.P., N.M. Pedersen, L. Forfang, and E.B. Smeland. 2012. Effect of cycloheximide on epidermal growth factor receptor trafficking and signaling. *FEBS Lett*. 586:3575-3581.

Olesen, J., H.C. Diener, I.W. Husstedt, P.J. Goadsby, D. Hall, U. Meier, S. Pollentier, and L.M. Lesko. 2004. Calcitonin gene-related peptide receptor antagonist BIBN 4096 BS for the acute treatment of migraine. *N Engl J Med*. 350:1104-1110.

Olesen, J., and I. Jansen-Olesen. 2000. Nitric oxide mechanisms in migraine. *Pathol Biol (Paris)*. 48:648-657.

Orsini, M.J., and J.L. Benovic. 1998. Characterization of dominant negative arrestins that inhibit beta2-adrenergic receptor internalization by distinct mechanisms. *J Biol Chem*. 273:34616-34622.

Osherov, N., and A. Levitzki. 1994. Epidermal-growth-factor-dependent activation of the src-family kinases. *Eur J Biochem*. 225:1047-1053.

Overgaard, K., M.A. Hansen, S.B. Jensen, and C. Christiansen. 1992. Effect of salcatonin given intranasally on bone mass and fracture rates in established osteoporosis: a dose-response study. *BMJ*. 305:556-561.

Padilla, B.E., G.S. Cottrell, D. Roosterman, S. Pikios, L. Muller, M. Steinhoff, and N.W. Bunnett. 2007. Endothelin-converting enzyme-1 regulates endosomal

sorting of calcitonin receptor-like receptor and beta-arrestins. *J Cell Biol*. 179:981-997.

Pages, G., S. Guerin, D. Grall, F. Bonino, A. Smith, F. Anjuere, P. Auberger, and J. Pouyssegur. 1999. Defective thymocyte maturation in p44 MAP kinase (Erk 1) knockout mice. *Science*. 286:1374-1377.

Pai, R., B. Soreghan, I.L. Szabo, M. Pavelka, D. Baatar, and A.S. Tarnawski. 2002. Prostaglandin E2 transactivates EGF receptor: a novel mechanism for promoting colon cancer growth and gastrointestinal hypertrophy. *Nat Med*. 8:289-293.

Panigone, S., M. Hsieh, M. Fu, L. Persani, and M. Conti. 2008. Luteinizing hormone signaling in preovulatory follicles involves early activation of the epidermal growth factor receptor pathway. *Mol Endocrinol*. 22:924-936.

Parameswaran, N., J. Disa, W.S. Spielman, D.P. Brooks, P. Nambi, and N. Aiyar. 2000a. Activation of multiple mitogen-activated protein kinases by recombinant calcitonin gene-related peptide receptor. *European journal of pharmacology*. 389:125-130.

Parameswaran, N., J. Disa, W.S. Spielman, D.P. Brooks, P. Nambi, and N. Aiyar. 2000b. Activation of multiple mitogen-activated protein kinases by recombinant calcitonin gene-related peptide receptor. *Eur J Pharmacol*. 389:125-130.

Parekh, A.B., and J.W. Putney, Jr. 2005. Store-operated calcium channels. *Physiol Rev*. 85:757-810.

Parent, J.L., P. Labrecque, M.J. Orsini, and J.L. Benovic. 1999. Internalization of the TXA2 receptor alpha and beta isoforms. Role of the differentially spliced cooh terminus in agonist-promoted receptor internalization. *J Biol Chem*. 274:8941-8948.

Passariello, N., D. Giugliano, S. Sgambato, R. Torella, and F. D'Onofrio. 1981. Calcitonin, a diabetogenic hormone? *J Clin Endocrinol Metab*. 53:318-323.

Patel, S., A.R. Lyons, and D.J. Hosking. 1993. Drugs used in the treatment of metabolic bone disease. Clinical pharmacology and therapeutic use. *Drugs*. 46:594-617.

Pearse, B.M. 1975. Coated vesicles from pig brain: purification and biochemical characterization. *J Mol Biol*. 97:93-98.

Pearson, G., F. Robinson, T. Beers Gibson, B.E. Xu, M. Karandikar, K. Berman, and M.H. Cobb. 2001. Mitogen-activated protein (MAP) kinase pathways: regulation and physiological functions. *Endocr Rev*. 22:153-183.

Pearson, G.W., S. Earnest, and M.H. Cobb. 2006. Cyclic AMP selectively uncouples mitogen-activated protein kinase cascades from activating signals. *Mol Cell Biol*. 26:3039-3047.

Pelzer, C., I. Kassner, K. Matentzoglu, R.K. Singh, H.P. Wollscheid, M. Scheffner, G. Schmidtke, and M. Groettrup. 2007. UBE1L2, a novel E1 enzyme specific for ubiquitin. *The Journal of biological chemistry*. 282:23010-23014.

Perlow, M.J., W.J. Freed, J.S. Carman, and R.J. Wyatt. 1980. Calcitonin reduces feeding in man, monkey and rat. *Pharmacol Biochem Behav*. 12:609-612.

Permert, J., J. Larsson, G.T. Westermark, M.K. Herrington, L. Christmanson, P.M. Pour, P. Westermark, and T.E. Adrian. 1994. Islet amyloid polypeptide in patients with pancreatic cancer and diabetes. *N Engl J Med*. 330:313-318.

Perriere, G., and M. Gouy. 1996. WWW-query: an on-line retrieval system for biological sequence banks. *Biochimie*. 78:364-369.

Petaja-Repo, U.E., M. Hogue, S. Bhalla, A. Laperriere, J.P. Morello, and M. Bouvier. 2002. Ligands act as pharmacological chaperones and increase the efficiency of delta opioid receptor maturation. *EMBO J*. 21:1628-1637.

Petaja-Repo, U.E., M. Hogue, A. Laperriere, S. Bhalla, P. Walker, and M. Bouvier. 2001. Newly synthesized human delta opioid receptors retained in the endoplasmic reticulum are retrotranslocated to the cytosol, deglycosylated, ubiquitinated, and degraded by the proteasome. *J Biol Chem*. 276:4416-4423.

Pierce, K.L., A. Tohgo, S. Ahn, M.E. Field, L.M. Luttrell, and R.J. Lefkowitz. 2001. Epidermal growth factor (EGF) receptor-dependent ERK activation by G protein-coupled receptors: a co-culture system for identifying intermediates upstream and downstream of heparin-binding EGF shedding. *J Biol Chem*. 276:23155-23160.

Piiper, A., I. Dikic, M.P. Lutz, J. Leser, B. Kronenberger, R. Elez, H. Cramer, W. Muller-Esterl, and S. Zeuzem. 2002. Cyclic AMP induces transactivation of the receptors for epidermal growth factor and nerve growth factor, thereby modulating activation of MAP kinase, Akt, and neurite outgrowth in PC12 cells. *J Biol Chem*. 277:43623-43630.

Piiper, A., M.P. Lutz, H. Cramer, R. Elez, B. Kronenberger, I. Dikic, W. Muller-Esterl, and S. Zeuzem. 2003. Protein kinase A mediates cAMP-induced tyrosine phosphorylation of the epidermal growth factor receptor. *Biochem Biophys Res Commun*. 301:848-854.

Pippig, S., S. Andexinger, and M.J. Lohse. 1995. Sequestration and recycling of beta 2-adrenergic receptors permit receptor resensitization. *Mol Pharmacol*. 47:666-676.

Pitcher, J.A., E.S. Payne, C. Csortos, A.A. DePaoli-Roach, and R.J. Lefkowitz. 1995. The G-protein-coupled receptor phosphatase: a protein phosphatase type 2A with a distinct subcellular distribution and substrate specificity. *Proc Natl Acad Sci U S A*. 92:8343-8347.

Ponting, C.P. 1996. Novel domains in NADPH oxidase subunits, sorting nexins, and PtdIns 3-kinases: binding partners of SH3 domains? *Protein Sci*. 5:2353-2357.

Poyner, D.R., D.P. Andrew, D. Brown, C. Bose, and M.R. Hanley. 1992. Pharmacological characterization of a receptor for calcitonin gene-related peptide on rat, L6 myocytes. *Br J Pharmacol*. 105:441-447.

Prado, M.A., B. Evans-Bain, K.R. Oliver, and I.M. Dickerson. 2001. The role of the CGRP-receptor component protein (RCP) in adrenomedullin receptor signal transduction. *Peptides*. 22:1773-1781.

Premont, R.T., and R.R. Gainetdinov. 2007. Physiological roles of G protein-coupled receptor kinases and arrestins. *Annu Rev Physiol*. 69:511-534.

Prenzel, N., E. Zwick, H. Daub, M. Leserer, R. Abraham, C. Wallasch, and A. Ullrich. 1999. EGF receptor transactivation by G-protein-coupled receptors requires metalloproteinase cleavage of proHB-EGF. *Nature*. 402:884-888.

Przepiorka, D., S.B. Baylin, O.W. McBride, J.R. Testa, A. de Bustros, and B.D. Nelkin. 1984. The human calcitonin gene is located on the short arm of chromosome 11. *Biochem Biophys Res Commun*. 120:493-499.

Putney, J.W., Jr. 1986. A model for receptor-regulated calcium entry. *Cell Calcium*. 7:1-12.

Raisz, L.G., and I. Niemann. 1967. Early effects of parathyroid hormone and thyrocalcitonin on bone in organ culture. *Nature*. 214:486-487.

Rao, G.N., P. Delafontaine, and M.S. Runge. 1995. Thrombin stimulates phosphorylation of insulin-like growth factor-1 receptor, insulin receptor substrate-1, and phospholipase C-gamma 1 in rat aortic smooth muscle cells. *J Biol Chem*. 270:27871-27875.

Raposo, G., I. Dunia, C. Delavier-Klutchko, S. Kaveri, A.D. Strosberg, and E.L. Benedetti. 1989. Internalization of beta-adrenergic receptor in A431 cells involves non-coated vesicles. *Eur J Cell Biol*. 50:340-352.

Rawlings, N.D., A.J. Barrett, and A. Bateman. 2012. MEROPS: the database of proteolytic enzymes, their substrates and inhibitors. *Nucleic Acids Res*. 40:D343-350.

Raybould, H.E., E. Kolve, and Y. Tache. 1988. Central nervous system action of calcitonin gene-related peptide to inhibit gastric emptying in the conscious rat. *Peptides*. 9:735-737.

Rhee, S.G. 2001. Regulation of phosphoinositide-specific phospholipase C. *Annu Rev Biochem*. 70:281-312.

Roberts, A.N., B. Leighton, J.A. Todd, D. Cockburn, P.N. Schofield, R. Sutton, S. Holt, Y. Boyd, A.J. Day, E.A. Foot, and et al. 1989. Molecular and functional characterization of amylin, a peptide associated with type 2 diabetes mellitus. *Proc Natl Acad Sci U S A*. 86:9662-9666.

Robinson, M.J., and M.H. Cobb. 1997. Mitogen-activated protein kinase pathways. *Curr Opin Cell Biol*. 9:180-186.

Robinson, M.S., and J.S. Bonifacino. 2001. Adaptor-related proteins. *Curr Opin Cell Biol*. 13:444-453.

Rock, K.L., C. Gramm, L. Rothstein, K. Clark, R. Stein, L. Dick, D. Hwang, and A.L. Goldberg. 1994. Inhibitors of the proteasome block the degradation of most cell proteins and the generation of peptides presented on MHC class I molecules. *Cell*. 78:761-771.

Roettger, B.F., R.U. Rentsch, D. Pinon, E. Holicky, E. Hadac, J.M. Larkin, and L.J. Miller. 1995. Dual pathways of internalization of the cholecystokinin receptor. *J Cell Biol*. 128:1029-1041.

Roh, J., C.L. Chang, A. Bhalla, C. Klein, and S.Y. Hsu. 2004. Intermedin is a calcitonin/calcitonin gene-related peptide family peptide acting through the calcitonin receptor-like receptor/receptor activity-modifying protein receptor complexes. *J Biol Chem*. 279:7264-7274.

Roosterman, D., G.S. Cottrell, B.E. Padilla, L. Muller, C.B. Eckman, N.W. Bunnett, and M. Steinhoff. 2007. Endothelin-converting enzyme 1 degrades neuropeptides in endosomes to control receptor recycling. *Proc Natl Acad Sci U S A*. 104:11838-11843.

Rosenblatt, M.I., G.P. Dahl, and I.M. Dickerson. 2000. Characterization and localization of the rabbit ocular calcitonin gene-related peptide (CGRP)-receptor component protein (RCP). *Invest Ophthalmol Vis Sci*. 41:1159-1167.

Rosenfeld, M.G., J.J. Mermod, S.G. Amara, L.W. Swanson, P.E. Sawchenko, J. Rivier, W.W. Vale, and R.M. Evans. 1983. Production of a novel neuropeptide encoded by the calcitonin gene via tissue-specific RNA processing. *Nature*. 304:129-135.

Rossomando, A.J., D.M. Payne, M.J. Weber, and T.W. Sturgill. 1989. Evidence that pp42, a major tyrosine kinase target protein, is a mitogen-activated serine/threonine protein kinase. *Proc Natl Acad Sci U S A*. 86:6940-6943.

Roth, T.F., and K.R. Porter. 1964. Yolk Protein Uptake in the Oocyte of the Mosquito Aedes Aegypti. L. *J Cell Biol*. 20:313-332.

Rothberg, K.G., J.E. Heuser, W.C. Donzell, Y.S. Ying, J.R. Glenney, and R.G. Anderson. 1992. Caveolin, a protein component of caveolae membrane coats. *Cell*. 68:673-682.

Rouse, J., P. Cohen, S. Trigon, M. Morange, A. Alonso-Llamazares, D. Zamanillo, T. Hunt, and A.R. Nebreda. 1994. A novel kinase cascade triggered by stress and heat shock that stimulates MAPKAP kinase-2 and phosphorylation of the small heat shock proteins. *Cell*. 78:1027-1037.

Rozengurt, E. 2007. Mitogenic signaling pathways induced by G protein-coupled receptors. *J Cell Physiol*. 213:589-602.

Sakata, J., T. Shimokubo, K. Kitamura, S. Nakamura, K. Kangawa, H. Matsuo, and T. Eto. 1993. Molecular cloning and biological activities of rat adrenomedullin, a hypotensive peptide. *Biochem Biophys Res Commun*. 195:921-927.

Sales, K.J., S. Maudsley, and H.N. Jabbour. 2004. Elevated prostaglandin EP2 receptor in endometrial adenocarcinoma cells promotes vascular endothelial growth factor expression via cyclic 3',5'-adenosine monophosphate-mediated transactivation of the epidermal growth factor receptor and extracellular signal-regulated kinase 1/2 signaling pathways. *Mol Endocrinol*. 18:1533-1545.

Samson, W.K. 1998. Proadrenomedullin-derived peptides. *Front Neuroendocrinol*. 19:100-127.

Santiskulvong, C., and E. Rozengurt. 2007. Protein kinase Calpha mediates feedback inhibition of EGF receptor transactivation induced by Gq-coupled receptor agonists. *Cell Signal*. 19:1348-1357.

Schafer, B., A. Gschwind, and A. Ullrich. 2004a. Multiple G-protein-coupled receptor signals converge on the epidermal growth factor receptor to promote migration and invasion. *Oncogene*. 23:991-999.

Schafer, B., B. Marg, A. Gschwind, and A. Ullrich. 2004b. Distinct ADAM metalloproteinases regulate G protein-coupled receptor-induced cell proliferation and survival. *J Biol Chem*. 279:47929-47938.

Scheuring, S., R.A. Rohricht, B. Schoning-Burkhardt, A. Beyer, S. Muller, H.F. Abts, and K. Kohrer. 2001. Mammalian cells express two VPS4 proteins both of which are involved in intracellular protein trafficking. *J Mol Biol*. 312:469-480.

Schini-Kerth, V.B., B. Fisslthaler, and R. Busse. 1994. CGRP enhances induction of NO synthase in vascular smooth muscle cells via a cAMP-dependent mechanism. *Am J Physiol*. 267:H2483-2490.

Schlegel, A., P. Arvan, and M.P. Lisanti. 2001. Caveolin-1 binding to endoplasmic reticulum membranes and entry into the regulated secretory pathway are regulated by serine phosphorylation. Protein sorting at the level of the endoplasmic reticulum. *J Biol Chem*. 276:4398-4408.

Schmid, H.P., O. Akhayat, C. Martins De Sa, F. Puvion, K. Koehler, and K. Scherrer. 1984. The prosome: an ubiquitous morphologically distinct RNP

particle associated with repressed mRNPs and containing specific ScRNA and a characteristic set of proteins. *EMBO J*. 3:29-34.

Schmidlin, F., O. Dery, K.O. DeFea, L. Slice, S. Patierno, C. Sternini, E.F. Grady, and N.W. Bunnett. 2001. Dynamin and Rab5a-dependent trafficking and signaling of the neurokinin 1 receptor. *The Journal of biological chemistry*. 276:25427-25437.

Schmitt, J.M., and P.J. Stork. 2000. beta 2-adrenergic receptor activates extracellular signal-regulated kinases (ERKs) via the small G protein rap1 and the serine/threonine kinase B-Raf. *J Biol Chem*. 275:25342-25350.

Schmitt, J.M., and P.J. Stork. 2001. Cyclic AMP-mediated inhibition of cell growth requires the small G protein Rap1. *Mol Cell Biol*. 21:3671-3683.

Schmitt, J.M., and P.J. Stork. 2002. Galpha and Gbeta gamma require distinct Src-dependent pathways to activate Rap1 and Ras. *J Biol Chem*. 277:43024-43032.

Schnitzer, J.E., P. Oh, and D.P. McIntosh. 1996. Role of GTP hydrolysis in fission of caveolae directly from plasma membranes. *Science*. 274:239-242.

Schonwasser, D.C., R.M. Marais, C.J. Marshall, and P.J. Parker. 1998. Activation of the mitogen-activated protein kinase/extracellular signal-regulated kinase pathway by conventional, novel, and atypical protein kinase C isotypes. *Mol Cell Biol*. 18:790-798.

Schreiber, A.B., M.E. Winkler, and R. Derynck. 1986. Transforming growth factor-alpha: a more potent angiogenic mediator than epidermal growth factor. *Science*. 232:1250-1253.

Schuldt, C., and P.M. Kloetzel. 1985. Analysis of cytoplasmic 19 S ring-type particles in Drosophila which contain hsp 23 at normal growth temperature. *Dev Biol*. 110:65-74.

Schwarz, N., D. Renshaw, S. Kapas, and J.P. Hinson. 2006. Adrenomedullin increases the expression of calcitonin-like receptor and receptor activity modifying protein 2 mRNA in human microvascular endothelial cells. *J Endocrinol*. 190:505-514.

Seachrist, J.L., P.H. Anborgh, and S.S. Ferguson. 2000. beta 2-adrenergic receptor internalization, endosomal sorting, and plasma membrane recycling are regulated by rab GTPases. *The Journal of biological chemistry*. 275:27221-27228.

Seachrist, J.L., S.A. Laporte, L.B. Dale, A.V. Babwah, M.G. Caron, P.H. Anborgh, and S.S. Ferguson. 2002. Rab5 association with the angiotensin II type 1A receptor promotes Rab5 GTP binding and vesicular fusion. *J Biol Chem*. 277:679-685.

Seemuller, E., A. Lupas, D. Stock, J. Lowe, R. Huber, and W. Baumeister. 1995. Proteasome from Thermoplasma acidophilum: a threonine protease. *Science*. 268:579-582.

Seger, R., and E.G. Krebs. 1995. The MAPK signaling cascade. *FASEB J*. 9:726-735.

Sehat, B., S. Andersson, R. Vasilcanu, L. Girnita, and O. Larsson. 2007. Role of ubiquitination in IGF-1 receptor signaling and degradation. *PLoS One*. 2:e340.

Sellers, L.A., J. Simon, T.S. Lundahl, D.J. Cousens, P.P. Humphrey, and E.A. Barnard. 2001. Adenosine nucleotides acting at the human P2Y1 receptor

stimulate mitogen-activated protein kinases and induce apoptosis. *J Biol Chem*. 276:16379-16390.

Shah, B.H., J.A. Olivares-Reyes, and K.J. Catt. 2005. The protein kinase C inhibitor Go6976 [12-(2-cyanoethyl)-6,7,12,13-tetrahydro-13-methyl-5-oxo-5H-indolo(2,3-a)pyrrolo(3 ,4-c)-carbazole] potentiates agonist-induced mitogen-activated protein kinase activation through tyrosine phosphorylation of the epidermal growth factor receptor. *Mol Pharmacol*. 67:184-194.

Shajahan, A.N., B.K. Timblin, R. Sandoval, C. Tiruppathi, A.B. Malik, and R.D. Minshall. 2004. Role of Src-induced dynamin-2 phosphorylation in caveolae-mediated endocytosis in endothelial cells. *J Biol Chem*. 279:20392-20400.

Shenoy, S.K., M.T. Drake, C.D. Nelson, D.A. Houtz, K. Xiao, S. Madabushi, E. Reiter, R.T. Premont, O. Lichtarge, and R.J. Lefkowitz. 2006. beta-arrestin-dependent, G protein-independent ERK1/2 activation by the beta2 adrenergic receptor. *J Biol Chem*. 281:1261-1273.

Shenoy, S.K., and R.J. Lefkowitz. 2003. Trafficking patterns of beta-arrestin and G protein-coupled receptors determined by the kinetics of beta-arrestin deubiquitination. *J Biol Chem*. 278:14498-14506.

Shenoy, S.K., P.H. McDonald, T.A. Kohout, and R.J. Lefkowitz. 2001. Regulation of receptor fate by ubiquitination of activated beta 2-adrenergic receptor and beta-arrestin. *Science*. 294:1307-1313.

Shimada, S., S. Shiosaka, P.C. Emson, C.J. Hillyard, S. Girgis, I. MacIntyre, and M. Tohyama. 1985. Calcitonin gene-related peptidergic projection from the parabrachial area to the forebrain and diencephalon in the rat: an immunohistochemical analysis. *Neuroscience*. 16:607-616.

Sibley, D.R., R.H. Strasser, J.L. Benovic, K. Daniel, and R.J. Lefkowitz. 1986. Phosphorylation/dephosphorylation of the beta-adrenergic receptor regulates its functional coupling to adenylate cyclase and subcellular distribution. *Proc Natl Acad Sci U S A*. 83:9408-9412.

Simonin, F., P. Karcher, J.J. Boeuf, A. Matifas, and B.L. Kieffer. 2004. Identification of a novel family of G protein-coupled receptor associated sorting proteins. *J Neurochem*. 89:766-775.

Skalli, O., M.F. Pelte, M.C. Peclet, G. Gabbiani, P. Gugliotta, G. Bussolati, M. Ravazzola, and L. Orci. 1989. Alpha-smooth muscle actin, a differentiation marker of smooth muscle cells, is present in microfilamentous bundles of pericytes. *J Histochem Cytochem*. 37:315-321.

Skeggs, L.T., Jr., J.R. Kahn, and N.P. Shumway. 1956. The preparation and function of the hypertensin-converting enzyme. *J Exp Med*. 103:295-299.

Smillie, S.J., and S.D. Brain. 2011. Calcitonin gene-related peptide (CGRP) and its role in hypertension. *Neuropeptides*. 45:93-104.

Smith, P.K., R.I. Krohn, G.T. Hermanson, A.K. Mallia, F.H. Gartner, M.D. Provenzano, E.K. Fujimoto, N.M. Goeke, B.J. Olson, and D.C. Klenk. 1985. Measurement of protein using bicinchoninic acid. *Anal Biochem*. 150:76-85.

Smrcka, A.V., J.R. Hepler, K.O. Brown, and P.C. Sternweis. 1991. Regulation of polyphosphoinositide-specific phospholipase C activity by purified Gq. *Science*. 251:804-807.

Sohlemann, P., M. Hekman, M. Puzicha, C. Buchen, and M.J. Lohse. 1995. Binding of purified recombinant beta-arrestin to guanine-nucleotide-binding-protein-coupled receptors. *Eur J Biochem*. 232:464-472.

Sonnichsen, B., S. De Renzis, E. Nielsen, J. Rietdorf, and M. Zerial. 2000. Distinct membrane domains on endosomes in the recycling pathway visualized by multicolor imaging of Rab4, Rab5, and Rab11. *The Journal of cell biology*. 149:901-914.

Stack, J.H., D.B. DeWald, K. Takegawa, and S.D. Emr. 1995. Vesicle-mediated protein transport: regulatory interactions between the Vps15 protein kinase and the Vps34 PtdIns 3-kinase essential for protein sorting to the vacuole in yeast. *J Cell Biol*. 129:321-334.

Stadel, J.M., P. Nambi, R.G. Shorr, D.F. Sawyer, M.G. Caron, and R.J. Lefkowitz. 1983. Catecholamine-induced desensitization of turkey erythrocyte adenylate cyclase is associated with phosphorylation of the beta-adrenergic receptor. *Proc Natl Acad Sci U S A*. 80:3173-3177.

Steenbergh, P.H., J.W. Hoppener, J. Zandberg, C.J. Lips, and H.S. Jansz. 1985. A second human calcitonin/CGRP gene. *FEBS Lett*. 183:403-407.

Stewart, J.R., and C.A. O'Brian. 2005. Protein kinase C-{alpha} mediates epidermal growth factor receptor transactivation in human prostate cancer cells. *Mol Cancer Ther*. 4:726-732.

Strasser, R.H., D.R. Sibley, and R.J. Lefkowitz. 1986. A novel catecholamine-activated adenosine cyclic 3',5'-phosphate independent pathway for beta-adrenergic receptor phosphorylation in wild-type and mutant S49 lymphoma cells: mechanism of homologous desensitization of adenylate cyclase. *Biochemistry*. 25:1371-1377.

Strous, G.J., and R. Govers. 1999. The ubiquitin-proteasome system and endocytosis. *J Cell Sci*. 112 (Pt 10):1417-1423.

Su, Y., M. Chakraborty, M.H. Nathanson, and R. Baron. 1992. Differential effects of the 3',5'-cyclic adenosine monophosphate and protein kinase C pathways on the response of isolated rat osteoclasts to calcitonin. *Endocrinology*. 131:1497-1502.

Sugo, S., N. Minamino, K. Kangawa, K. Miyamoto, K. Kitamura, J. Sakata, T. Eto, and H. Matsuo. 1994. Endothelial cells actively synthesize and secrete adrenomedullin. *Biochem Biophys Res Commun*. 201:1160-1166.

Sugo, S., N. Minamino, H. Shoji, K. Kangawa, K. Kitamura, T. Eto, and H. Matsuo. 1995. Interleukin-1, tumor necrosis factor and lipopolysaccharide additively stimulate production of adrenomedullin in vascular smooth muscle cells. *Biochem Biophys Res Commun*. 207:25-32.

Tache, Y., M. Gunion, M. Lauffenberger, and Y. Goto. 1984. Inhibition of gastric acid secretion by intracerebral injection of calcitonin gene related peptide in rats. *Life Sci*. 35:871-878.

Takahashi, K., R. Morimoto, T. Hirose, F. Satoh, and K. Totsune. 2011. Adrenomedullin 2/intermedin in the hypothalamo-pituitary-adrenal axis. *J Mol Neurosci*. 43:182-192.

Takei, Y., K. Inoue, M. Ogoshi, T. Kawahara, H. Bannai, and S. Miyano. 2004. Identification of novel adrenomedullin in mammals: a potent cardiovascular and renal regulator. *FEBS Lett*. 556:53-58.

Tanowitz, M., and M. Von Zastrow. 2002. Ubiquitination-independent trafficking of G protein-coupled receptors to lysosomes. *J Biol Chem*. 277:50219-50222.

Tao, M., M.L. Salas, and F. Lipmann. 1970. Mechanism of activation by adenosine 3':5'-cyclic monophosphate of a protein phosphokinase from rabbit reticulocytes. *Proc Natl Acad Sci U S A*. 67:408-414.

Tawa, N.E., Jr., R. Odessey, and A.L. Goldberg. 1997. Inhibitors of the proteasome reduce the accelerated proteolysis in atrophying rat skeletal muscles. *J Clin Invest*. 100:197-203.

Taylor, G.M., K. Meeran, D. O'Shea, D.M. Smith, M.A. Ghatei, and S.R. Bloom. 1996. Adrenomedullin inhibits feeding in the rat by a mechanism involving calcitonin gene-related peptide receptors. *Endocrinology*. 137:3260-3264.

Taylor, M.M., S.L. Bagley, and W.K. Samson. 2005. Intermedin/adrenomedullin-2 acts within central nervous system to elevate blood pressure and inhibit food and water intake. *Am J Physiol Regul Integr Comp Physiol*. 288:R919-927.

Taylor, M.M., and W.K. Samson. 2005. Stress hormone secretion is altered by central administration of intermedin/adrenomedullin-2. *Brain Res*. 1045:199-205.

Taylor, S.J., H.Z. Chae, S.G. Rhee, and J.H. Exton. 1991. Activation of the beta 1 isozyme of phospholipase C by alpha subunits of the Gq class of G proteins. *Nature*. 350:516-518.

Taylor, S.J., J.A. Smith, and J.H. Exton. 1990. Purification from bovine liver membranes of a guanine nucleotide-dependent activator of phosphoinositide-specific phospholipase C. Immunologic identification as a novel G-protein alpha subunit. *J Biol Chem*. 265:17150-17156.

Temmesfeld-Wollbruck, B., A.C. Hocke, N. Suttorp, and S. Hippenstiel. 2007. Adrenomedullin and endothelial barrier function. *Thromb Haemost*. 98:944-951.

Tepper, S.J., and C. Cleves. 2009. Telcagepant, a calcitonin gene-related peptide antagonist for the treatment of migraine. *Curr Opin Investig Drugs*. 10:711-720.

Tepper, S.J., A.M. Rapoport, and F.D. Sheftell. 2002. Mechanisms of action of the 5-HT1B/1D receptor agonists. *Arch Neurol*. 59:1084-1088.

Terata, K., H. Miura, Y. Liu, F. Loberiza, and D.D. Gutterman. 2000. Human coronary arteriolar dilation to adrenomedullin: role of nitric oxide and K(+) channels. *Am J Physiol Heart Circ Physiol*. 279:H2620-2626.

Tilley, D.G., I.M. Kim, P.A. Patel, J.D. Violin, and H.A. Rockman. 2009. beta-Arrestin mediates beta1-adrenergic receptor-epidermal growth factor receptor interaction and downstream signaling. *J Biol Chem*. 284:20375-20386.

Tohgo, A., K.L. Pierce, E.W. Choy, R.J. Lefkowitz, and L.M. Luttrell. 2002. beta-Arrestin scaffolding of the ERK cascade enhances cytosolic ERK activity but inhibits ERK-mediated transcription following angiotensin AT1a receptor stimulation. *J Biol Chem*. 277:9429-9436.

Trump, B.F., P.J. Goldblatt, and R.E. Stowell. 1962. An electron microscopic study of early cytoplasmic alterations in hepatic parenchymal cells of mouse liver during necrosis in vitro (autolysis). *Lab Invest*. 11:986-1015.

Tsao, P., and M. von Zastrow. 2000a. Downregulation of G protein-coupled receptors. *Curr Opin Neurobiol*. 10:365-369.

Tsao, P.I., and M. von Zastrow. 2000b. Type-specific sorting of G protein-coupled receptors after endocytosis. *J Biol Chem*. 275:11130-11140.

Tsubuki, S., H. Kawasaki, Y. Saito, N. Miyashita, M. Inomata, and S. Kawashima. 1993. Purification and characterization of a Z-Leu-Leu-Leu-MCA degrading protease expected to regulate neurite formation: a novel catalytic activity in proteasome. *Biochem Bioph Res Co*. 196:1195-1201.

Tuvim, M.J., R. Adachi, S. Hoffenberg, and B.F. Dickey. 2001. Traffic control: Rab GTPases and the regulation of interorganellar transport. *News in physiological sciences : an international journal of physiology produced jointly by the International Union of Physiological Sciences and the American Physiological Society*. 16:56-61.

Ueda, Y., S. Hirai, S. Osada, A. Suzuki, K. Mizuno, and S. Ohno. 1996. Protein kinase C activates the MEK-ERK pathway in a manner independent of Ras and dependent on Raf. *J Biol Chem*. 271:23512-23519.

Umekawa, K., H. Hasegawa, Y. Tsutsumi, K. Sato, Y. Matsumura, and N. Ohashi. 2000. Pharmacological characterization of a novel sulfonylureid-pyrazole derivative, SM-19712, a potent nonpeptidic inhibitor of endothelin converting enzyme. *Jpn J Pharmacol*. 84:7-15.

Uzan, B., A. Villemin, J.M. Garel, and M. Cressent. 2008. Adrenomedullin is anti-apoptotic in osteoblasts through CGRP1 receptors and MEK-ERK pathway. *J Cell Physiol*. 215:122-128.

Vallotton, M.B., W. Dolci, C. Gerber-Wicht, and J.A. Fischer. 1989. Action of calcitonin gene-related peptide on rat aortic smooth muscle. *Eur J Pharmacol*. 166:219-222.

van der Sluijs, P., M. Hull, P. Webster, P. Male, B. Goud, and I. Mellman. 1992. The small GTP-binding protein rab4 controls an early sorting event on the endocytic pathway. *Cell*. 70:729-740.

van Rossum, D., U.K. Hanisch, and R. Quirion. 1997. Neuroanatomical localization, pharmacological characterization and functions of CGRP, related peptides and their receptors. *Neurosci Biobehav Rev*. 21:649-678.

Van Valen, F., G. Piechot, and H. Jurgens. 1990. Calcitonin gene-related peptide (CGRP) receptors are linked to cyclic adenosine monophosphate production in SK-N-MC human neuroblastoma cells. *Neurosci Lett*. 119:195-198.

Vasilcanu, R., D. Vasilcanu, B. Sehat, S. Yin, A. Girnita, M. Axelson, and L. Girnita. 2008. Insulin-like growth factor type-I receptor-dependent phosphorylation of extracellular signal-regulated kinase 1/2 but not Akt (protein kinase B) can be induced by picropodophyllin. *Mol Pharmacol*. 73:930-939.

Vause, C.V., and P.L. Durham. 2009. CGRP stimulation of iNOS and NO release from trigeminal ganglion glial cells involves mitogen-activated protein kinase pathways. *J Neurochem*. 110:811-821.

Villalon, C.M., and J. Olesen. 2009. The role of CGRP in the pathophysiology of migraine and efficacy of CGRP receptor antagonists as acute antimigraine drugs. *Pharmacol Ther*. 124:309-323.

Vito, P., L. Pellegrini, C. Guiet, and L. D'Adamio. 1999. Cloning of AIP1, a novel protein that associates with the apoptosis-linked gene ALG-2 in a Ca2+-dependent reaction. *J Biol Chem*. 274:1533-1540.

Vossler, M.R., H. Yao, R.D. York, M.G. Pan, C.S. Rim, and P.J. Stork. 1997. cAMP activates MAP kinase and Elk-1 through a B-Raf- and Rap1-dependent pathway. *Cell*. 89:73-82.

Vu, T.K., D.T. Hung, V.I. Wheaton, and S.R. Coughlin. 1991. Molecular cloning of a functional thrombin receptor reveals a novel proteolytic mechanism of receptor activation. *Cell*. 64:1057-1068.

Wan, Y., and X.Y. Huang. 1998. Analysis of the Gs/mitogen-activated protein kinase pathway in mutant S49 cells. *J Biol Chem*. 273:14533-14537.

Wang, Y., Y. Zhou, K. Szabo, C.R. Haft, and J. Trejo. 2002. Down-regulation of protease-activated receptor-1 is regulated by sorting nexin 1. *Mol Biol Cell*. 13:1965-1976.

Wang, Z., T.J. Dillon, V. Pokala, S. Mishra, K. Labudda, B. Hunter, and P.J. Stork. 2006. Rap1-mediated activation of extracellular signal-regulated kinases by cyclic AMP is dependent on the mode of Rap1 activation. *Mol Cell Biol*. 26:2130-2145.

Wang, Z., W. Ma, J.G. Chabot, and R. Quirion. 2009. Cell-type specific activation of p38 and ERK mediates calcitonin gene-related peptide involvement in tolerance to morphine-induced analgesia. *FASEB J*. 23:2576-2586.

Warshawsky, H., D. Goltzman, M.F. Rouleau, and J.J. Bergeron. 1980. Direct in vivo demonstration by radioautography of specific binding sites for calcitonin in skeletal and renal tissues of the rat. *J Cell Biol*. 85:682-694.

Webb, B.L., S.J. Hirst, and M.A. Giembycz. 2000. Protein kinase C isoenzymes: a review of their structure, regulation and role in regulating airways smooth muscle tone and mitogenesis. *Br J Pharmacol*. 130:1433-1452.

Weissman, J.T., J.N. Ma, A. Essex, Y. Gao, and E.S. Burstein. 2004. G-protein-coupled receptor-mediated activation of rap GTPases: characterization of a novel Galphai regulated pathway. *Oncogene*. 23:241-249.

Weissmann, G. 1964. Lysosomes. *Blood*. 24:594-606.

Westermark, P., C. Wernstedt, E. Wilander, D.W. Hayden, T.D. O'Brien, and K.H. Johnson. 1987. Amyloid fibrils in human insulinoma and islets of Langerhans of the diabetic cat are derived from a neuropeptide-like protein also present in normal islet cells. *Proc Natl Acad Sci U S A*. 84:3881-3885.

Whistler, J.L., J. Enquist, A. Marley, J. Fong, F. Gladher, P. Tsuruda, S.R. Murray, and M. Von Zastrow. 2002. Modulation of postendocytic sorting of G protein-coupled receptors. *Science*. 297:615-620.

Wijdicks, E.F., and M. Stevens. 1992. The role of hypotension in septic encephalopathy following surgical procedures. *Arch Neurol*. 49:653-656.

Wilden, U., S.W. Hall, and H. Kuhn. 1986. Phosphodiesterase activation by photoexcited rhodopsin is quenched when rhodopsin is phosphorylated and binds the intrinsic 48-kDa protein of rod outer segments. *Proceedings of the National Academy of Sciences of the United States of America*. 83:1174-1178.

Wilk, S., and M. Orlowski. 1983. Evidence that pituitary cation-sensitive neutral endopeptidase is a multicatalytic protease complex. *J Neurochem*. 40:842-849.

Williams, R.L., and S. Urbe. 2007. The emerging shape of the ESCRT machinery. *Nat Rev Mol Cell Biol*. 8:355-368.

Wisskirchen, F.M., D.W. Gray, and I. Marshall. 1999. Receptors mediating CGRP-induced relaxation in the rat isolated thoracic aorta and porcine isolated coronary artery differentiated by h(alpha) CGRP(8-37). *Br J Pharmacol*. 128:283-292.

Withers, D.J., H.A. Coppock, T. Seufferlein, D.M. Smith, S.R. Bloom, and E. Rozengurt. 1996. Adrenomedullin stimulates DNA synthesis and cell proliferation via elevation of cAMP in Swiss 3T3 cells. *FEBS Lett*. 378:83-87.

Wolfe, B.L., A. Marchese, and J. Trejo. 2007. Ubiquitination differentially regulates clathrin-dependent internalization of protease-activated receptor-1. *J Cell Biol*. 177:905-916.

Wolfe, H.J., K.E. Melvin, S.J. Cervi-Skinner, A.A. Saadi, J.F. Juliar, C.E. Jackson, and A.H. Tashjian, Jr. 1973. C-cell hyperplasia preceding medullary thyroid carcinoma. *N Engl J Med*. 289:437-441.

Wu, J., P. Dent, T. Jelinek, A. Wolfman, M.J. Weber, and T.W. Sturgill. 1993. Inhibition of the EGF-activated MAP kinase signaling pathway by adenosine 3',5'-monophosphate. *Science*. 262:1065-1069.

Xia, S., X.P. Dun, P.S. Hu, S. Kjaer, K. Zheng, Y. Qian, C. Solen, T. Xu, B. Fredholm, T. Hokfelt, and Z.Q. Xu. 2008. Postendocytotic traffic of the galanin R1 receptor: a lysosomal signal motif on the cytoplasmic terminus. *Proc Natl Acad Sci U S A*. 105:5609-5613.

Xu, S., J. Fu, J. Chen, P. Xiao, T. Lan, K. Le, F. Cheng, L. He, X. Shen, H. Huang, and P. Liu. 2009. Development of an optimized protocol for primary culture of smooth muscle cells from rat thoracic aortas. *Cytotechnology*. 61:65-72.

Yamada, E. 1955. The fine structure of the gall bladder epithelium of the mouse. *J Biophys Biochem Cytol*. 1:445-458.

Yao, C.C., J. Breuss, R. Pytela, and R.H. Kramer. 1997. Functional expression of the alpha 7 integrin receptor in differentiated smooth muscle cells. *Journal of cell science*. 110 (Pt 13):1477-1487.

Yao, Y., W. Li, J. Wu, U.A. Germann, M.S. Su, K. Kuida, and D.M. Boucher. 2003. Extracellular signal-regulated kinase 2 is necessary for mesoderm differentiation. *Proc Natl Acad Sci U S A*. 100:12759-12764.

Yasuda, J., A.J. Whitmarsh, J. Cavanagh, M. Sharma, and R.J. Davis. 1999. The JIP group of mitogen-activated protein kinase scaffold proteins. *Mol Cell Biol*. 19:7245-7254.

Young, A.A., B. Gedulin, W. Vine, A. Percy, and T.J. Rink. 1995. Gastric emptying is accelerated in diabetic BB rats and is slowed by subcutaneous injections of amylin. *Diabetologia*. 38:642-648.

Yu, X.J., C.Y. Li, K.Y. Wang, and H.Y. Dai. 2006. Calcitonin gene-related peptide regulates the expression of vascular endothelial growth factor in human HaCaT keratinocytes by activation of ERK1/2 MAPK. *Regul Pept*. 137:134-139.

Zajac, M., J. Law, D.D. Cvetkovic, M. Pampillo, L. McColl, C. Pape, G.M. Di Guglielmo, L.M. Postovit, A.V. Babwah, and M. Bhattacharya. 2011. GPR54 (KISS1R) transactivates EGFR to promote breast cancer cell invasiveness. *PLoS One*. 6:e21599.

Zeng, L., S.V. Webster, and P.M. Newton. 2012. The biology of protein kinase C. *Adv Exp Med Biol*. 740:639-661.

Zerial, M., and H. McBride. 2001. Rab proteins as membrane organizers. *Nature reviews. Molecular cell biology*. 2:107-117.

Zheng, M., S.J. Zhang, W.Z. Zhu, B. Ziman, B.K. Kobilka, and R.P. Xiao. 2000. beta 2-adrenergic receptor-induced p38 MAPK activation is mediated by

protein kinase A rather than by Gi or gbeta gamma in adult mouse cardiomyocytes. *J Biol Chem*. 275:40635-40640.

Zhou, M., A.J. Arthur, Z.F. Ba, I.H. Chaudry, and P. Wang. 2001. The small intestine plays an important role in upregulating CGRP during sepsis. *Am J Physiol Regul Integr Comp Physiol*. 280:R382-388.

Zhu, K., M.A. Amin, M.J. Kim, K.J. Katschke, C.C. Park, and A.E. Koch. 2003. A novel function for a glucose analog of blood group H antigen as a mediator of leukocyte-endothelial adhesion via intracellular adhesion molecule 1. *J Biol Chem*. 278:21869-21877.

Zwick, E., H. Daub, N. Aoki, Y. Yamaguchi-Aoki, I. Tinhofer, K. Maly, and A. Ullrich. 1997. Critical role of calcium- dependent epidermal growth factor receptor transactivation in PC12 cell membrane depolarization and bradykinin signaling. *J Biol Chem*. 272:24767-24770.

Appendix I:

Reagent, Chemicals, Peptides, Inhibitors and Other Consumables

Chemicals

Product	Supplier	Cat. number
Ammonium persulphate (APS): $(NH_4)_2S_2O_8$	Sigma-Aldrich	A3678
Bromophenol blue sodium salt: $C_{19}H_{10}Br_4O_5S$	Sigma-Aldrich	B5525
Butan-2-ol: $CH_3(CH_2)_3OH$	BDH	100616J
Calcium chloride (1 M): $CaCl_2$	Sigma-Aldrich	21114
Chloroform: $CHCl_3$	Sigma-Aldrich	C2432
Dimethyl sulphoxide (DMSO): $(CH_3)_2SO$	Sigma-Aldrich	D2650
Diethyl pyrocarbonate (DEPC): $O(COOC_2H_5)_2$	Sigma-Aldrich	D5758
Ethanol: C_2H_6O (Molecular Biology Grade)	Sigma-Aldrich	E7023
Ethanol: C_2H_6O	Sigma-Aldrich	32221
Ethylenediaminetetraacetic acid (EDTA): $C_{10}H_{14}N_2Na_2O_8$	Sigma-Aldrich	E5134
Ethylene glycotetraacetic acid (EGTA): $C_{14}H_{24}N_2O_{10}$	Sigma-Aldrich	E4378
Glacial acetic acid: $C_2H_4O_2$	BDH	27013
Glycerol: $C_3H_8O_3$	Sigma-Aldrich	G6279
Glycine: NH_2CH_2COOH	Sigma-Aldrich	G7403

4-(2-Hydroxyethyl)piperazine-1-ethanesulfonic acid (HEPES): $C_8H_{18}N_2O_4S$	Sigma-Aldrich	H3375
Hydrochloric acid: HCl	Fisher Scientific	J/4310/15
Magnesium chloride: $MgCl_2$	Fisher Scientific	M/0550/53
Manganese chloride: $MnCl_2$	Sigma-Aldrich	M3634
2-*mercaptoethanol:* C_2H_6SO	Sigma-Aldrich	M6250
Methanol: CH_3OH	Sigma-Aldrich	34860
Nonidet P-40 (NP-40): $C_{18}H_{30}O_3$	BDH	560092L
Paraformaldehyde (PFA): $OH(CH_2O)_nH$ (n=8-100)	Sigma-Aldrich	P6148
1,4-Piperazinediethanesulfonic acid (PIPES): $C_8H_{18}N_2O_6S_2$	Sigma-Aldrich	P6757
1-Phenylazo-2-naphthol-6,8-disulfonic acid disodium salt (Orange G): $C_{16}H_{10}N_2Na_2O_7S_2$	Sigma-Aldrich	O3756
Potassium dihydrogen orthophosphate: KH_2PO_4	BDH	436053H
Potassium chloride: KCl	Sigma-Aldrich	P9333
2-propanol: C_3H_8O	Sigma-Aldrich	I9516
Saponin from Quillaja Bark	Sigma-Aldrich	S4521
Sodium Chloride: NaCl	Sigma-Aldrich	433209
Sodium dodecyl sulphate (SDS): $NaC_{12}H_{25}SO_4$	Sigma-Aldrich	L6026
Sodium fluoride: NaF	BDH	102464T
Sodium hydroxide: NaOH	Fisher Scientific	J/7800/15
Sodium orthovanadate: Na_3VO_4	Sigma-Aldrich	S6508
Sodium phosphate dibasic: HNa_2O_4P	Sigma-Aldrich	S3264

Sodium pyrophosphate tetrabasic: $Na_4P_2O_7$	Sigma-Aldrich	S9515
Tetramethylethylenediamine (TEMED): $(CH_3)_2NCH_2CH_2N(CH_3)_2$	Sigma-Aldrich	T9281
Triton™-X-100: $C_{14}H_{22}O(C_2H_4O)_n$ (n=9-10)	Sigma-Aldrich	X100
Trizma® base (Tris/HCl): $NH_2C(CH_2OH)_3$•HCl	Sigma-Aldrich	T6066
Tween® 20: $C_{58}H_{114}O_{26}$	Sigma-Aldrich	P7949
Xylene cyanol FF: $C_{25}H_{27}N_2NaO_6S_2$	Sigma-Aldrich	X4126

Table I.1 **List of chemicals.** All chemicals were store according to the manufacturer's guidelines.

Peptides

Stock of peptides	Diluent	Stock	Supplier	Cat. number
rat ADM	DDW*	1 mM	Bachem	H-2934
rat CGRP	DDW	1 mM	Bachem	H-2265

Table I.2 **List of peptides.** All peptides were stored in -80°C. *DDW = Distilled deionised water.

Bacteria Consumable

Antibiotics	Supplier	Cat. number
Ampicillin	Sigma-Aldrich	A9518
Lysogeny Broth (LB) Broth, tablets	Sigma-Aldrich	L7275
Tryptone (EZMix™): Pancreatic digest of casein	Sigma-Aldrich	T2559
Yeast extract (EZMix™)	Sigma-Aldrich	Y1626

Table I.3 **List of bacteria consumable.** Ampicillin was stored at 4°C. All the other consumables were stored at RT.

Cell Culture Consumables

Media	Supplier	Cat. number
Dulbecco's Modified Eagles medium (DMEM): L-glutamine, high glucose, sodium pyruvate, phenol red	Invitrogen	41966-029
DMEM: no L-glutamine, high glucose, no sodium pyruvate, no phenol red	Invitrogen	31053-028
Ad. DMEM: no L-glutamine, non-essential amino acids (NEAA), high glucose, sodium pyruvate, phenol red	Invitrogen	12491-023
MCDB 131: no L-glutamine, low glucose, sodium pyruvate, phenol red	Invitrogen	10372-019
Opti-MEM® Reduced-Serum Medium: L-glutamine, phenol red	Invitrogen	31985-062
Serum and supplements	**Supplier**	**Cat. number**
Heat Inactivated Foetal Bovine Serum (HIFBS) Certified	Invitrogen	10082-147
L-glutamine: 100x	Invitrogen	25030-123
Bovine serum albumin (BSA): protease free, heat shock process	Fisher Scientific	BPE9703-100
Epidermal Growth Factor (EGF): from mouse, tested for cell culture	VWR	734-1304
Hydrocortisone (HCORT): suitable for cell culture	Sigma-Aldrich	H0888
MEM NEAA: 100x	Invitrogen	11140-035
Antibiotics	**Supplier**	**Cat. number**
Hygromycin B	Invitrogen	10687-010
Zeocin™	Invitrogen	R250-01
Penicillin-Streptomycin (P/S)	Invitrogen	15070-063
Amphotericin B preparation (Fungizone™)	Sigma-Aldrich	A 2942

Other consumables	Supplier	Cat. number
Dulbecco's Phosphate-Buffered Saline (PBS): no calcium no magnesium	Invitrogen	14190-169
Dulbecco's PBS: calcium and magnesium (PBSCM)	Invitrogen	14040-174
0.05% Trypsin-EDTA: phenol red	Invitrogen	25300-096
BD™ Poly-D-Lysine: synthetic	BD Bioscience	734-1102
Gelatin: from porcine skin	Sigma-Aldrich	G1890
Cell Surface protein Isolation kit: includes EZ-Link Sulfo-NHS-SS-Biotin, NeutrAvidin Agarose	Pierce	89881
Lipofectamine® 2000 Transfection Reagent	Invitrogen	11668-019

Table I.4 **List of Cell Culture Consumables.** All consumables were stored according to the manufacturer's guidelines.

Protein Analysis Consumables

Product	Supplier	Cat. number
40 % (w:v) Acrylamide/Bis Solution, ratio 37.5:1	Bio-Rad	161-0149
BCA Protein Assay Reagent (bicinchoninic acid)	Pierce	23225
Bovine Serum Albumin (BSA)	Fisher	BPE9702-
Enhanced chemiluminescence kit (ECL)	Geneflow	K1-0170
Horse Serum	Invitrogen	16050-122
Milk powder	Local store	N/A
Polyvinylidene fluoride (PVDF) membrane	Millipore	IPVH00010
Protease inhibitor cocktail	Roche	1183617000
Extra thick blot paper	Biorad	170-3965

Table I.5 **Consumable for Western Blotting.** All consumables were stored according to the manufacturer's guidelines.

Inhibitors

Stock of inhibitors	Diluent	Stock	Supplier	Cat. number
AG1478	DMSO	1 mM	Calbiochem	658548
Bafilomycin A_1	DMSO	1 mM	Acros Organic	328120001
Cycloheximide (CHX)	Ethanol	140 mM	Sigma-Aldrich	C7698
E-64d	DMSO	10 mM	Enzo Life Science	BML-PI107
Epoxomicin	DMSO	5 mM	Enzo Life Science	BML-PI127
Gö6976	DMSO	10 mM	Calbiochem	365250
Gö6983	DMSO	10 mM	Tocris	2285
H-89	DMSO	50 mM	Enzo Life Science	BML-EI196
MG-132	DMSO	20 mM	Enzo Life Science	BML-PI102
Pepstatin A	DMSO	10 mM	Enzo Life Scicence	ALX-260-085
PP2	DMSO	10 mM	Enzo Life Science	BML-EI297
SM-19712	DDW	10 mM	Sigma-Aldrich	S3445
U-0126	DMSO	10 mM	Enzo Life Science	BML-EI282
U-73122	DMSO	100 mM	Enzo Life Science	BML-ST391
Z-Phe-Ala-diazomethylketone (Z-PAD)	DMSO	200 mM	Bachem	N-1040

Table I.6 **List of inhibitors.** All inhibitors were used at a single concentration (except for H-89, **see 3.6**) according to previously published findings. All inhibitors were stored at -80°C.

Appendix II:

Preparation of Buffers and Other Solutions

Biochemical Buffers

Phosphate buffered saline (PBS)

Component	Quantity per liter	Working solution
NaCl	80 g	136.9 mM
KCl	2 g	2.7 mM
HNa_2PO_4	14.4 g	10.1 mM
KH_2PO_4	2.4 g	1.8 mM

Table II.1 **Composition of 10x PBS.** Components were dissolved in DDW. *To make 1x solution, 10x PBS was diluted in DDW*

PBS-Tween® 20 (PBS-T)

PBS-T was composed of 1x PBS supplemented with Tween® 20 (0.1 % (v:v)). Stored at RT.

Blocking Buffer for Western Blotting

Blocking Buffer was composed of 1x PBS-T, BSA (2% (w:v)) and/or Milk powder (5% (w:v)). Blocking buffer was made fresh before each WB.

Blocking Solution for Immunocytochemistry

Blocking solution was composed of 1x PBS containing normal horse serum (2% (v:v)) and saponin (0.1% (w:v)). The solution was stored at -20°C.

Fixation solution: 4% PFA

For solution (100mL) of PFA (4% (w:v)), DDW (~70 mL) was heated (~60°C) and PFA (4 g) and 10x PBS (10 mL) were added. NaOH (10 M) was then added (2-3 drops) and swirl until the PFA has dissolved. The solution was allowed to cool

at RT and the pH was adjusted to 7.4. Then the volume was adjusted to 100 mL. The solution was then filtered through 0.2 µm filter, aliquoted (10 mL) in centrifuge tube and stored at -20°C.

Lysis Buffer

Solution of Na_3VO_4 (100 mM) was prepared separately in DDW, aliquoted in microcentrifuge tube (1 mL) and stored at -20°C. Before use, aliquot were heated (100°C).

Component	Quantity/Volume per 500 mL	Working solution
Tris/HCl	3.02 g	50 mM
NaF	0.21 g	10 mM
Na_3VO_4 (100 mM)	500 µL	0.1 mM
Triton-X-100	500 µL	0.1% (v:v)
Protease inhibitors*	1 tablet/10 mL	-

Table II.2 **Composition of Lysis Buffer.** Components were dissolved in DDW. The pH was adjusted to 7.4. *Protease inhibitors (Roche, 11836170001) were used according to the manufacturer's guidelines.

Radio-Immunoprecipitation Assay (RIPA) Buffer

Component	Quantity/Volume per 500 mL	Working solution
Tris/HCl	3.02 g	50mM
NaF	0.21 g	10 mM
NaCl	4.38 g	150 mM
$Na_4P_2O_7$	2.23 g	10 mM
EGTA	0.19 g	1 mM
Na_3VO_4 (100 mM)	500 µL	0.1 mM
NP-40	2.5 mL	0.5% (v:v)

Table II.3 **Composition of RIPA Buffer.** Components were dissolved in DDW. The pH was adjusted to 7.4.

SDS-Loading Buffer

Component	5x buffer
Tris/HCl	250 mM
Bromophenol blue	0.001% (w/v)
SDS	10% (w/v)
Glycerol	50% (v:v)

Table II.4 **Composition of SDS-Loading Buffer.** Components were dissolved in DDW. The pH was adjusted to 6.8. The solution was aliquoted (875 µL) in microcentrifuge tubes and stored at -20°C. Before use, *2-mercaptoethanol (125 µL) was added to the aliquot (final working solution 12.5 % (v:v)) and kept at -20°c after use.*

Running Buffer

Component	Quantity per liter	Working solution
Tris/HCl	30.3 g	25 mM
Glycine	188 g	192 mM

Table II.5 **Composition of 10x Running Buffer.** Components were dissolved in DDW. The pH was adjusted to 8.3. To make 1x solution, 10x running buffer was diluted in DDW, supplemented with SDS 10% (w:v) (10 mL) to make a final working solution of 0.1% (w:v) SDS.

Transfer Buffer

Component	Quantity per liter	Working solution
Tris/HCl	116 g	25 mM
Glycine	58 g	192 mM
SDS	7.4 g	1.3 mM

Table II.6 **Composition of 20x Transfer Buffer.** Components were dissolved in DDW. The pH was adjusted to 8.3. To make 1x solution, 20x transfer buffer was diluted in DDW, supplemented with methanol (200 mL/liter) to make a final working solution of 20% (v:v) methanol.

Stripping Buffer

Component	Quantity per liter	Working solution
Tris/HCl	7.6 g	62.7 mM
SDS	20.0 g	2% (w:v)

Table II.7 **Composition of 1x Stripping Buffer.** Components were dissolved in DDW. The pH was adjusted to 6.8. Just before use, 2-mercaptoethanol (140µL) was added in stripping buffer (20 mL) to make a final working solution at 0.7% (v:v) of 2-mercaptoethanol.

Bacterial Buffer and Culture Broth

Super Optimal Broth (SOB) Medium

Solution of KCl (250 mM) and $MgCl_2$ (2 M) were prepared separately in DDW and autoclaved (105 kPa, 30 min, 121°C).

Component	Quantity/Volume per liter	Working solution
Tryptone	20 g	2% (w:v)
Yeast extract	5 g	0.5% (w:v)
NaCl	0.5 g	8.56 mM
KCl (250 mM)	10 mL	2.5 mM

Table II.8 **Composition of SOB medium.** The components were dissolved in DDW. The pH was adjusted to 7 and autoclaved (105 kPa, 30 min, 121°C). Just before use, MgCl2 (5 mL) was added to the solution for a final concentration of 10 mM

LB Broth

LB was supplied as tablets. One tablet was diluted in 50 mL of DDW according to the manufacturer's guideline. LB broth was then autoclaved (105 kPa, 30 min, 121°C). LB broth was store at room temperature (RT).

Preparation of LB-agar

Bacteria were grown on a solid surface referred to as LB-agar plate: 1.5 % (w:v) of agar (BDH, 33004) was added to LB broth, autoclaved (105 kPa, 30 min, 121°C) and left to cool (~50-55°C) before adding appropriate antibiotics. LB-Agar (20 mL) was added to a 100 mm dish and left set at room temperature (RT). Plates were then dried upside down in an incubator (30 min, 37°C) and then stored at 4°C.

Transformation Buffer (TB)

Component	Quantity/Volume per liter	Working solution
PIPES	3.02 g	10 mM
KCl	11.18 g	150 mM
$CaCl_2$ (1 M)	10 mL	10 mM

Table II.9 **Composition of TB buffer.** The components were dissolved in DDW. The pH was adjusted to 6.7. Then $MnCl_2$ (35 mM) was added and the buffer was sterilised by filtration through 0.45 µm filter. Buffer was stored at 4°C.

Molecular Biology Buffers

DEPC-H_2O

DEPC (0.01% (w:v)) was dissolved in DDW, incubated on the bench (overnight, RT) and then autoclaved (105 kPa, 30 min, 121°C). DEPC-H_2O was store at RT.

Tris-Acetate EDTA (TAE) Buffer

Solution of EDTA (0.5 M) was prepared separately. EDTA will not go completely into solution until the pH is around 8. Once completely dissolve the pH was adjusted to 8.

Component	Quantity/Volume per liter	Working solution
Tris/HCl	242 g	40 mM
Glacial acetic acid	57.1 mL	
EDTA (0.5 M, pH 8)	100 mL	1 mM

Table II.10 **Preparation of 50x TAE buffer.** The components were dissolved in DDW. To make 1x solution, 50x TAE was diluted in DDW.

DNA Loading Buffer

Component	6x buffer
Bromophenol blue	0.25% (w:v)
Xylene cyanol FF	0.25% (w/v)
Orange G	0.25% (w/v)
Glycerol	30% (v:v)

Table II.11 **DNA Loading Buffer preparation.** The components were dissolved in DDW. The buffer was stored at 4°C.